The CD8-Mediated Optimisation of the

Antigen Specific T-cell Response

--oOo--

A thesis submitted in requirement of

Cardiff University

For the degree of Doctor of Philosophy

--oOo--

Tamsin Dockree

--oOo--

2017

Angela Kay Williams

1949 – 2008

Who believed that anything is possible.

Abstract

$CD8^+$ T-cells target infected and dysregulated cells for deletion. Failure of this response can result in persistent challenge, such as cancer or chronic infection. $CD8^+$ T-cells recognize peptides in the context of major histocompatibility complex class I (MHCI) molecules on the surface of host cells. The detection of T-cell antigens involves the binding of two receptors (TCR and CD8) to a single ligand (pMHCI). Individual TCRs cross-react with $>10^6$ different peptide antigens to ensure coverage of all possible pMHCI. As a result of this high level of T-cell crossreactivity the TCR/pMHCI interaction is usually suboptimal and significant scope exists in optimization for therapeutic benefit. The CD8 coreceptor enhances T-cell sensitivity through several mechanisms and has a potent ability to tune the antigen specific T-cell response. The pMHCI/CD8 interaction is characterised by very weak affinity. Increasing the strength of the pMHCI/CD8 interaction by 15-fold has been shown to result in complete loss of antigen specificity. In this thesis, I have shown that loss of antigen specificity occurs at a defined pMHCI/CD8 threshold (K_D ~ 27 μM). This finding suggests that there is scope to increase the strength of the pMHCI/CD8 interaction for therapeutic benefit without non-specific CD8 T-cell activation. I demonstrated that increasing the strength of the pMHCI/CD8 interaction by engineering a point mutation into cell surface CD8 can result in improved T-cell antigen sensitivity. I have further classified the means by which CD8 can control T-cell crossreactivity and how altering the strength of the pMHCI/CD8 interaction can alter the focus of the TCR. And finally, I demonstrated that the level of CD8 expressed at the surface can have a dramatic effect on T-cell activation. Overall, I have demonstrated that cell surface CD8 can be engineered to enhance the therapeutic efficacy of adoptive T-cell transfer irrespective of antigen specificity.

Acknowledgements

I was supported by a Clinical Research Training Fellowship, awarded to me by the Wellcome Trust, which has made this thesis possible.

My sincerest thanks go to my excellent supervisors; Prof. Linda Wooldridge, Prof. David Price, Dr. John Bridgeman, and Prof. Mick Bailey. Firstly to Prof. Wooldridge, whose support, advice, enthusiasm and meticulous attention to detail have been invaluable; deepest thanks, Linda. Thanks also to Prof. Price for your helpful suggestions, and willingness to do battle with the 'Big, Bad Admin'; Prof. Mick Bailey, for passing on your excitement and enthusiasm for both scientific research and real ale; and Dr. John Bridgman for your help and guidance in the lab, and for your unending patience and support.

Massive thanks too to all the members of the Wooldridge Group and Price group for much help and support along the way, most notably, Dr. Mat Clement for guidance and tolerance whilst teaching, and Dr. Emma Grant for much appreciated advice whilst writing.

This journey would have been impossible without my friends and family. To my long-suffering husband, Paul, thank you for your love and understanding which has made all things possible. Without you, I am nothing. To my son Jacob, thanks for waiting; I promise that there will now be more time for rugby and mountain biking. Thanks also to my wonderful friends who have put up with my flakiness and ranting as this journey reached its end, most particularly to all those Jingles.

Finally, this thesis is dedicated to my wonderful and inspirational mother, Angie Williams. She changed the world for me, because she believed that I could change the world.

Abbreviations

A2	A*0201
Ab	Antibody
ACT	Adoptive Cell Transfer
AEBSF	4-(2-Aminoethyl)Benzenesulfonyl Fluoride Hydrochloride
AICD	Activation-Induced Cell Death
AP-1	Activation Protein-1
APC	Antigen Presenting Cell
APC	Allophycocyanin
B35	B*3501
B8	B*0801
BCR	B-Cell Receptor
BSA	Bovine Serum Albumen
BTN	Butyrophilin
BV	Brilliant Violet
CAR	Chimeric Antigen Receptor
CD	Cluster of Differentiation (e.g. CD8)
cDNA	Complementary DNA

CDR	Complementarity-Determining Region
CK	Cellkines
CMV	Cytomegalovirus
CPL	Combinatorial Peptide Library
cPPT	Central Polypurine tract
CRAC	Calcium Release Activated Calcium Channels
cSMAC	Central SMAC
CTL	Cytotoxic T-Lymphocyte
CTLA-4	Cytotoxic T-Lymphocyte Antigen 4
D-	Diversity Region
dH_2O	Distilled water
DAG	Di-Acylglycerol
DC	Dendritic Cell
DMEM	Dulbecco Modified Eagle's Medium
DMSO	Dimethyl Sulfoxide
DN	$CD4^-/CD8^-$, Double Negative
DNA	Deoxyribonucleic Acid
DNA-PK	DNA-dependent Protein Kinase complex
DP	$CD4^+/CD8^+$, Double Positive

DRiP	Defective Ribosomal Product
DRIP	Degraded Ribosomal Product
dSMAC	Distal SMAC
DTT	Di-Thio-3-Etinol *or* Dithiothreitol
EBV	Epstein Barr Virus
EDC	1-Ethyl-3-(3-Dimethylaminpropyl)Carbodimide Hydrochloride
EDTA	Ethylenediaminetetraacetic acid
EF-1α	Elongation Factor-1-α
ELISA	Enzyme Linked Immunosorbant Assay
ER	Endoplasmic Reticulum
FACS	Fluorescence-activated cell sorting
Fas	Fas *aka* CD95, APO-1
FasL	Fas Ligand, CD95 Ligand, CD95L
FBS	Foetal Bovine Serum
FITC	Fluorescein Isothiocyanate
FPLC	Fast Protein Liquid Chromatography
GF	Gel Filtration
GLuc	Gaussia Luciferase

GT	Gene Transfer
H1	Histone
HBSS	Hank's Balanced Salt Solution (Hank's Salt)
HEK	Human Embryonic Kidney
HEPES	4-(2-Hydroxyethyl)Piperazine-1-Ethanesulfonic Acid
HF	High Fidelity
HIV	Human Immunodeficiency Virus
HLA	Human Leucocyte Antigen
hTERT	Human Tlomerase Reverse Transcriptase
ICOS	Inducible T-cell Co-Stimulator
ICS	Intracellular Staining
IE	Ion Exchange
IEL	Intra-Epithelial Lymphocyte
IFNγ	Interferon γ
Ig	Immunoglobulin
IK	Immunological Kinapse
IL	Interleukin
IL-2	Interleukin-2
IL-2Rα	IL-2 Receptor α

iNKT	Natural Killer T-cells
iNOS	Inducible Nitrous Oxide Synthase
IP_3	Inositol 1.4.5-triPhosphate
IPTG	Isopropyl-1-Thio-ß-D-Galactopyranoside
IRES	Internal Ribosome Entry Site
IS	Immunological Synapse
ITAM	Immunoreceptor Tyrosine-based Activation Motif
ITIM	Immunoreceptor Tyrosine-based Inhibitory Motif
J-	Joining Region
K_D	Dissociation Constant
K_{off}	Off-rate
K_{on}	On-rate
KS	Kinetic Segregation
-L	Ligand
LAT	Linker of Activated T-cells
LB	Lysogeny Broth
Lck	$p56^{lck}$
LTR	Long terminal Repeat sequence
LV	Lentivirus / Lentiviridae

mAb	Monoclonal Antibody
MACS	Magnetic activated cell sorting
MAIT	Mucosal-Associated Invariant T-cells
MC	Micro cluster
MES	2-N-Morpholinoethanesulfonic Acid
MHC	Major Histocompatibility Complex
MHCI	MHC class I
MHCII	MHC class II
MIP	Macrophage Inflammatory Proteins
MIP1β	Macrophage Inflammatory Protein-1-β
MOPS	3-(N-Morpholino)Propanesulfonic Acid
mRNA	Messenger RNA
MWCO	Molecular Weight Cut Off
NFAT	Nuclear Factor of Activated T-cells
NHS	Sulfo-*N*-Hydroxysuccinimide
OD	Optical Density (absorbance)
OD_{600}	Optical Density at 600 nm wavelength
ORF	Open reading Frame
PAGE	Polyacrylamide Gel Electrophoresis

PAMP	Pattern-Associated Molecular Pattern
PB	Pacific Blue
PBMC	Peripheral Blood Mononuclear Cells
PBS	Phosphate buffered saline
PBS (2)	Primer Binding site
PCR	Polymerase Chain Reaction
PD-1	Programmed Death 1
PD-L1	Programmed Death Ligand 1 *aka* B7H1
PD-L2	Programmed Death Ligand 2 *aka* B7-DC
PE	Phycoerythrin
PerCP	Peridinin chlorophyll
PFA	Paraformaldehyde
PFN	Perforin
PHA	Phytohaemagglutinin
PI	phosphatidylinositol
PIP_2	Phosphatidylinositol 4,5-bisphosphat *or* $PtdIns(4,5)P_2$
PKC	Protein Kinase C
PKCθ	Protein Kinase C-θ

PLC	Peptide Loading Complex
PLC	Phospholipase C
pMHC	peptide-MHC
PPR	Pattern Recognition Receptor
pSMAC	Peripheral SMAC
pTα	pre-TCR
-R	Receptor
RAG	Recombinase Activating Gene
rCD2	Rat CD2
RNA	Ribonucleic Acid
Ros	Reactive Oxygen Species
rpm	Revolutions per minute
RPMI-1640	Roswell Park Memorial Institute 1640
RRE	*rev* Response Element
RSV	Respiratory Syncytiovirus
RV	Retrovirus
S1P1	Sphingosine 1-Phosphate Receptor 1
SDM	Site Directed Mutagenesis
SDS	Sodium Doecyl Sulphate

SHP-2	SH-domain containing tyrosine Phosphatase-2
SLEC	Short-Lived Effector Cells
SMAC	Super-Molecular Activation Cluster
SOB	Super Optimal Broth
SOC	Super Optimal Broth with Catabolyte repression
SP	Single Positive
SPR	Surface Plasmon Resonance
StrepHRP	Streptavidin Horseradish Peroxidase
$t_{½}$	Half life
TAE	Tris-Acetate-EDTA
TAP	Transporter Associated Processing
T_C	Cytotoxic T-cell
T_{CM}	Central Memory T-cell
TCR	T-cell Receptor
TDT	Terminal Deoxynucleaotidal Transferase
TE	Tris-EDTA
T_{Eff}	Effector T-cell
T_{FH}	Follicular Helper T-cell
T_H	Helper T-cell

TIL	Tumour Infiltrating Lymphocyte
TLR	Toll-Like Receptor
T_M	Memory T-cell
T_N	Naïve T-cell
TNF	Tumour Necrosis Factor
TNFR	TNF Receptor
T_{Reg}	Regulatory T-cell
tRNA	Transfer RNA
V-	Variable Region
ViViD	Violet Fixable Fluorescin Amine Dye
WHV	Woodchuck Hepatitis Virus
WPRE	WHV Post-transcriptional Regulatory Element
ZAP-70	CD3ζ-Associated Protein-70
α-GalCer	α-Galactosylceramide
ß2m	ß2-Microglobulin

Table of Contents

Table of Figures

Chapter 1

Chapter 2

Chapter 3

Chapter 4

Chapter 5

Chapter 6

Table of Tables

Chapter 1

Introduction

1.1 The Immune System

1.1.1 Overview of the Immune System

The function of the immune system is to protect the host against damage; either in the form of infectious agent challenge or by dysregulation of self cells e.g. neoplasia. The immune system can be split into two parts, the innate and the adaptive systems, which are characterised by the speed of the response, and the specificity of targeting.

All multicellular organisms have some form of innate (or natural) immunity (Fearon and Locksley, 1996). The more sophisticated adaptive, or acquired, response is found only in vertebrates, having evolved 400 million years ago, and involves a highly specific (targeted) response to challenges, which is increased with subsequent exposure owing to its capacity for 'immunological memory'. The level of response changes throughout the host's life as new pathogens are encountered. The different ways in which pathogens are recognised and responded to forms the main difference between the two systems. In order to mount an immune response, the host's immune systems must first recognise a challenge, which in turn results in effector function activation to control or eliminate the infection. This response must be regulated i.e. kept under control to ensure damage to self does not occur, and, in the case of the adaptive immune response, remembered, so that a greater and more rapid response may be mounted upon repeated challenge.

1.1.2 The Innate System

The innate immune system utilises germ-line encoded proteins, that recognise molecular patterns which are common to microbial pathogens (pathogen-associated molecular patterns; PAMPs) via pattern recognition receptors (PRRs) (Medzhitov and Janeway, 1998), of which toll-like receptors (TLRs) are vitally important (Moser and Leo, 2010). The response is elicited immediately upon engagement of these receptors, and the response is the same upon repeated exposure to the pathogen. Activation of PRRs by PAMPs can elicit responses such as phagocytosis (by macrophages, neutrophils and monocytes), synthesis of anti-microbial peptides (via eosinophils and basophils), and natural killer cell migration and activation, and complement release. The innate immune response may thus be considered to be the first line of defence against harmful agents.

1.1.3 Adaptive Immunity

The adaptive immune system is highly specialised, acquired, develops through the lifetime of the host, and is capable of recognising and responding to challenges presented by pathogens with rapid mutation rates, which have evolved to evade the innate response (Moser and Leo, 2010). One hallmark of the adaptive response is its capacity for immunological memory, whereby response is both quicker and greater upon repeated challenge (Vischer et al., 1967, Klaus, 1978). It is organised around lymphocytes, which express a vast array of unique antigen-specific receptors. Lymphocytes develop in two distinctly different anatomical locations; the thymus and the bone marrow (Boehm, 2011), giving rise to two different lineages (T- and B-cells, respectively). The adaptive immune system may therefore

be further sub-divided in to the humoral (B-lymphocytes) and cell-mediated (T-lymphocytes) responses.

1.1.4 B-lymphocytes

The humoral response, named from the ancient medical term ‘humors' (Nutton, 2005), recognises antigen via the B-cell receptor (BCR), a membrane-bound immunoglobulin (Ig), which upon activation, causes B-cells to terminally differentiate into plasma cells, and secrete antibody (Ab), an immunoglobulin of the same specificity as the B-cell receptor, into the extra-cellular space (Hardy and Hayakawa, 2001, McHeyzer-Williams and Ahmed, 1999, Shapiro-Shelef and Calame, 2005). Antibodies bind pathogens and toxins, in some cases marking them for phagocytosis or complement destruction by the innate immune system (Cohen, 1991, Savill et al., 1993, Kerr et al., 1972). Antibodies can also recruit other cells of the immune system to the site of infection, facilitating destruction and removal by T-cells (Cohen et al., 1985, Kerr et al., 1972).

1.1.5 T-lymphocytes

T-cells are responsible for the cellular immune response, or ‘cell mediated Immunity’. T-cells are thymically derived from a common progenitor cell, and express a unique T-cell receptor (TCR) at their cell surface. In response to challenge, a single T-cell may proliferate thus giving rise to a clonal population of T-cells, all expressing the appropriate TCR, in a process termed, ‘clonal expansion’ (Denizot et al., 1986). There are several different functional subsets of T-cell, and a degree of plasticity can exist between some of these T-cell subsets (Table 1.1).

	Type	Phenotype (cell surface)	Effector molecules
CD4	Naïve	αβTCR, CD3, CD4, CCR7, CD45RA, CD62L^{HI}, IL-7R(CD127)	-
	Helper, TH1	αβTCR, CD3, CD4, IL-12R, IFNγR, CXCR3	IFNγ, IL-2, LTα
	Helper, TH2	αβTCR, CD3, CD4, IL-4R, IL-33R, CCR4, IL-17RB, CRTH2	IL-4, IL-5, IL-10, IL-13
	Helper, TH9	αβTCR, CD3, CD4,	IL-9, IL-10
	Helper, TH17	αβTCR, CD3, CD4, CD161, IL-23R, CCR6, IL-1R,	IL-17A, IL-17F, IL-21, IL-22, CCL20
	Helper, TH22	αβTCR, CD3, CD4, CCR10	IL-22
	Helper, TFH	αβTCR, CD3, CD4, CXCR5, SLAM, OX40L, CD40L, ICOS, IL-21R, PD1	IL-21
	Natural Treg	αβTCR, CD3, CD4, CD25, CTLA4, GITR	IL-10, TGFβ, IL-35
	Inducible Treg	αβTCR, CD3, CD4, CD25, CTLA4, GITR	IL-10, TGFβ
	Central memory	αβTCR, CD3, CD4, CCR7^{HI}, CD44, CD62L^{HI}, IL-7R(CD127), IL-15R	IL-2, CD40L, (IL-4, IFNY, IL-17A)
	Effector memory	αβTCR, CD3, CD4, CD62^{LO}, CD44, IL-7R(CD127), IL-15R, CCR7^{LO}	Inflammatory cytokines^{+++}
CD8	Naïve	αβTCR, CD3, CD8AB, CCR7, CD45RA, CD62L^{HI}, IL-7R(CD127)	-
	Cytotoxic effector	αβTCR, CD3, CD8αβ,	Perforin, Granzyme, IFNγ
	Central memory	αβTCR, CD3, CD8αβ, CCR7^{HI}, CD44, CD62L^{HI}, IL-7R(CD127), IL-15R	IL-2, CD40L, (IL-4, IFNY, IL-17A)
	Effector memory	αβTCR, CD3, CD8αβ, CD62^{LO}, CD44, IL-7R(CD127), IL-15R, CCR7^{LO}	Inflammatory cytokines^{+++}
	Exhausted	CD3, CD8αβ, PD1, TIM3, 1B11, LAG3	-
others	Γδ	γδTCR, CD3	IFNγ, IL-17A, IL-17F, IL-22
	NKT	Vα24Jα17-αβTCR, CD3, NK1.1, SLAMF1, TGFβR	IL-4, IFNγ, IL-17A
	MAIT	Vα7.2Jα19-αβTCR, CD3, NK1.1, SLAMF1, TGFβR	IL-4, IFNγ, IL-17A
	IEL	AβTCR or γδTCR, CD3, CD8αα, B220	IL-10, TGFβ
	Anergic	αβTCR, CD3, CTLA	GRAIL, CBL-B, ITCH, NEDD4

Table 1:1 T-cell subsets (Martinez, 2010).

The TCR may be comprised of either α and ß (αß TCR), or, γ and δ (γδ TCR) sub-units, giving rise to an αßTCR or a γδTCR, the αßTCR usually being the more abundant. During thymic maturation, αß T-cells become committed to expressing either the CD4 or the CD8 co-receptor.

1.1.6 CD8$^+$ T-cells

Occasionally referred to as cytotoxic T-cells (T_c) due to their function, CD8$^+$ T-cells recognise intracellular challenge in the context of target cell surface expressed peptide-major histocompatibility complexes class I (pMHCI), which are constitutively expressed on most nucleated mammalian cells. pMHCI are comprised of small peptide fragments (8-14 amino acids in length) presented in the context of major histocompatibility complex class I molecules (MHCI) (Davis and Bjorkman, 1988, Bjorkman et al., 1987b, Bjorkman et al., 1987a). Naïve CD8$^+$ T-cells are capable of recognising this challenge if their specific TCR can bind the target pMHCI, triggering expansion, however differentiation into an effector phenotype is required to elicit cytotoxicity (Trifari et al., 2013, Pennock et al., 2013). Effector CD8$^+$ T-cells bring about target cell death by secretion of perforin and granzymes (Trapani and Smyth, 2002, Trapani, 2012). This thesis is concerned mostly with CD8$^+$ T-cells, thus their function will be discussed in further detail later.

1.1.7 CD4+ T-cells

CD4$^+$ T-cells recognise antigen presented via MHCII, which are only expressed on professional antigen presenting cells (dendritic cells, macrophages and B-cells), and present slightly longer peptide fragments, typically 15-24 amino acid length, of

extracellular origin. $CD4^+$ T-cells may be further sub-divided into regulatory T-cells (T_{Reg}), which may be natural (generated in the thymus and committed to this function) or inducible (differentiate into this phenotype from naïve $CD4^+$ T-cells), or helper T-cells (T_H), of which there are several further subsets. Both subsets of T_{Reg} cells are responsible for promotion of tolerance and immunosuppression by both contact-dependant and contact-independent means, although there exists slight differences in their phenotypes and effector function (Table 1.1). The first described further differentiation of T-cells sub-sets from that fixed by their thymic ontogeny was of naïve $CD4^+$ T-cells into T_H1 and T_H2 (Sad and Mosmann, 1994, Mosmann and Sad, 1996). Further sub-sets of helper T-cells have since been described; T_H9, T_H17, T_H22 and follicular helper T-cells (T_{FH}) (Bluestone et al., 2009). Broadly speaking T_H1 cells promote cell-mediated immunity to intracellular challenges. They secrete IFNγ and induce macrophage activation by up-regulation of inducible nitrous oxide synthase (iNOS). T_H2 cells promote humoral immunity; they stimulate antibody release and eosinophil activation (thus are also important in parasitic disease). They have also been implicated in many $CD4^+$ T-cell mediated allergic conditions, e.g. asthma (Ray and Cohn, 1999). T_H9 cells are involved in clearance of parasitic disease, particularly gastro-intestinal nematodes, and have been implicated in allergic disease and are characterised by their potent production of IL-9 (Kaplan, 2013). T_H17 cells promote immunity against fungi and bacteria and are found mainly at mucosal surfaces (Annunziato et al., 2007). They are anti-inflammatory and, again, have been implicated in CD4+ T-cell mediated autoimmune disease (Park et al., 2005). T_H22 cells have only recently been classified and whether they are a true independent subset remains unclear, however this phenotype is found in inflammatory skin disease (Eyerich et al., 2009, Fujita, 2013). T_{FH} cells are found in lymphoid follicles and promote germinal centre immune responses. They provide help for B-cell class switching (Crotty, 2014). Plasticity, or

the potential to alter phenotype from one to another, exists between the T_H subsets and also inducible T_{Reg} cells, especially in the case of the T_H17 and T_{FH} subsets (Zhou et al., 2009, Bluestone et al., 2009, O'Shea and Paul, 2010, Murphy and Stockinger, 2010). Experimentally some authors have demonstrated that cells possess the ability to induce phenotype change, however it has been argued whether true plasticity and the ability of these cells to switch phenotype as required exists *in vivo* or whether there is merely normal differentiation down a terminal pathway (Hirahara et al., 2013).

1.1.8 γδ T-cells

The function of γδ T-cells is less clearly understood, however they are found enriched at epithelial surfaces and appear to have some characteristics of both innate and acquired immunity (Wencker et al., 2014). γδ T-cells are, like αß T-cells, differentiated in the thymus from a common lymphoid progenitor, with their TCR being formed by a similar re-arrangement process to the αß TCR. Indeed the TCRδ gene locus is embedded within the TCRα gene locus (Vantourout and Hayday, 2013), and recent work has identified a TCR comprised of a variant δ chain combined with the VJα, paired with the ß chain (Pellicci et al., 2014).

γδ T-cells make up 2-5% of circulating T-cells in man, however some individuals have considerably more than this as their resting normal, and in the context of some immunological challenge this can increase to over 50%, suggesting that they are capable of undergoing expansion in the face of challenge similarly to αß T-cells. Abundance of γδ T-cells also varies greatly across species, with, for example, farmyard ungulates having 70-80% of their $CD3^+$ population being $γδ^+$ (Baldwin and Telfer, 2015).

There is a small variation of Vδ arrangements, of which Vδ1, Vδ2 and Vδ3 are the most common (Adams et al., 2015). Vδ1 γδ T-cells have been shown to recognise certain lipids such as supfatide and α-Galactosylceramide (α-GalCer), in the context of CD1d (Uldrich et al., 2013). Other ligands recently identified include other CD1 ligands, phosphatate activating Vδ9 TCRs, and members of the butyrophilin family, BTN3A activating Vγ9Vδ2 TCR. Whilst the structure of a γδ TCR complexed with CD1d-αGalCer has recently been solved (Uldrich et al., 2013), the exact role and function of γδ T-cells remains uncertain.

1.1.9 Other T-cell subsets

In addition to the well-characterised $CD4^+$ and $CD8^+$ αβ T-cells, there are other subsets which are less well characterised. Intraepithelial lymphocytes (IELs) are found only in the intestinal mucosa (Sheridan and Lefrancois, 2011, Sheridan and Lefrancois, 2010). They may express either an αβ or a γδ TCR. They express CD8αα and are thought to have a regulatory function (Leishman et al., 2001). Natural Killer T-cells (NKT cells) express an αβ TCR, but no co-receptor. They are CD1d restricted, and do not recognise Major Histocompatibility Complex (MHC). They have been shown to have both anti-inflammatory and pro-inflammatory functions, but their exact role is as yet uncertain. Mucosal associated invariant T-cells (MAIT cells) express an αβ TCR with an invariant α-chain, and no associated co-receptor (Sheridan and Lefrancois, 2011). MAIT cells are MR1 restricted, but are otherwise similar to NKT cells, and both may be considered innate-like T-cells (Bennett et al., 2015).

1.2 Surface Molecule Interactions of T-cells

1.2.1 The T-cell Receptor (TCR)

The TCR is a heterodimer which consists of an alpha (α-) and a beta (ß-) chain, and associates at the cell surface with CD3, which in turn is made up of the sub-units CD3-gamma (CD3γ), CD3-delta (CD3δ), CD3-epsilon (CD3ε) and CD3-zeta (CD3ζ) (Figure 1.1). The αβTCR recognizes small antigenic peptide fragments presented in the context of MHC molecules at the cell surface; and is therefore responsible for the specificity of T-cell activation. Both αß and γδ T-cells are thymically derived, and their TCRs are formed by RAG-mediated V(D)J recombination (discussed in more detail in section 1.5.2). αß T-cells are frequently described in the literature as 'conventional' T-cells, although this largely seems to be because more is known about their function, and, in man at least, they are usually more frequent.

The TCR is generated through somatic re-arrangement (including mutation on recombination) of a limited number of genes, giving rise to a vast repertoire of recognition receptors (n = 10^{18})(Mason, 1998, Arstila TP, 1999). Of this potential repertoire diversity, it has been shown that the actual number of different TCRs which may be present in the blood at any given time is a minimum of 25 x 10^6, with the maximum number being dictated by the number of α-chains available (Arstila TP, 1999). Artsilla *et al* found that in naïve T cells, they were able to demonstrate 10^6 ß-chain possibilities, and 25 α-chains, however this reduces to 1-2 x 10^5 ß-chains and a single α-chain in the memory pool. Other authors have shown different estimates of TCR diversity; Nikolich-Žugich *et al* calculated 2.5 x 10^7 TCR clonotypes in man (Nikolich-Zugich et al., 2004), and demonstrated more variety in the alpha chain.

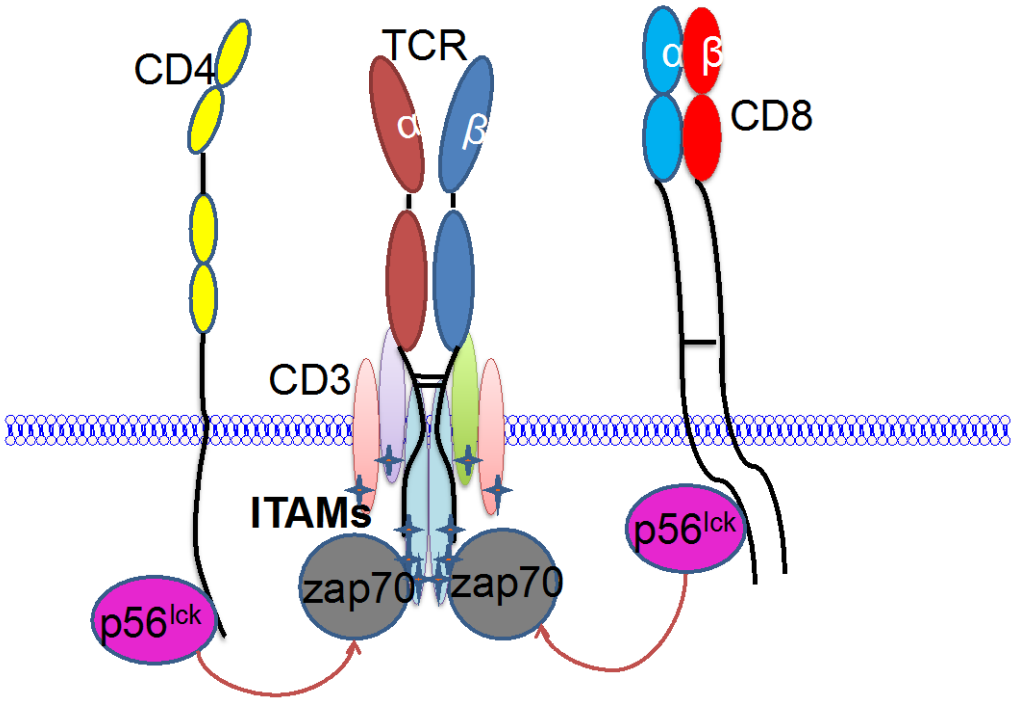

Figure 1.1: The TCR/CD3 complex.
The heterodimeric αβTCR can only be expressed at the cell surface in association with the six sub-units that comprise the CD3 complex. There are ten ITAMs within the cytoplasmic tails of the CD3 sub-units, which must be phosphorylated by kinases such as lck in order to initiate TCR triggering. An essential function of the co-receptor, be it CD4 or CD8, is thought to be to recruit these kinases to the CD3 complex facilitating triggering.

It is estimated that there are around 10^{12} T-cells in the adult host's blood (in man) at any one time, although the number of different specific TCRs and the frequency of repetition is uncertain. In the mouse, it has been shown that there are less TCRs available in the blood, as would be expected owing to the smaller circulating volume and thus smaller number of T-cells circulating, and this has been shown to be in the region of 1-2 x 10^6 (Armanda Casrouge, 2000).

1.2.2 The γδTCR

The γδTCR is derived by somatic recombination of the γ and δ gene loci in the thymus, in an identical manner to the αβTCR. As has already been discussed, less is known about the structure and function of the γδTCR, although it is known that they are not co-receptor dependent, or MHC-restricted. The recent discovery of a TCR comprised of a pairing of part a δ-chain with an αβTCR, the δ/αβTCR (Pellicci et al., 2014) may suggest the existence of other combinations.

1.2.3 Major Histocompatibility Complex (MHC)

MHC genes are highly diverse. Indeed they are one of the most polymorphic genes expressed (Okamura et al., 1997), with over 12,500 MHCI alleles and over 4,600 MHCII alleles having thus far been identified in man (Robinson et al., 2015). They are also co-dominant and polygenic, i.e. all genotypes present are concurrently expressed. There are two different classes of MHC molecules: MHC class I (MHCI) and MHC class II (MHCII) (Neefjes et al., 2011, Amadou et al., 1999, Maenaka and Jones, 1999). MHCI molecules are expressed on the surface of most nucleated cells within the body (Maenaka and Jones, 1999, Shatz, 2009, Corriveau et al., 1998, Joly

et al., 1991), and they present small (8-14 amino acids in length), linear peptide fragments, which have been processed from intracellular proteins (Okamura et al., 1997, Amadou et al., 1999, Maenaka and Jones, 1999, Praveen et al., 2010, Germain, 1994). TCRs capable of recognising these peptide-MHCI complexes (pMHCI) are co-expressed at the cell surface with the co-receptor molecule CD8 (Germain, 1994). These $CD8^+$ T-cells recognise and result in death of infected or damaged and dysfunctional cells, i.e. they are necessary for the control of intracellular challenges (Harty et al., 2000). Nucleated cells may express up to 10^6 MHCI on their cell surface (Yewdell et al., 2003), although some cell populations express far less, and certain diseases or conditions such as neoplasia, may result in down-regulation leading to potential immune system evasion.

In contrast, MHCII molecules are predominantly expressed by professional antigen presenting cells (APCs) and the peptide fragments presented are slightly larger (>13 amino acid length) and processed from extracellular proteins (Cella et al., 1997, Germain, 1994, Cresswell, 1994). The cell surface co-receptor found on T-cells that co-engages with pMHCII complexes is CD4. Whilst the majority of αβTCRs are restricted to either MHCI or MHCII (Van Laethem et al., 2012), there are exceptions that are capable of recognising antigens presented in the context of both; however, their specificity is determined by their co-receptor phenotype (Pearce et al., 2004, Matechak et al., 1996).

1.2.4 MHC structure

MHCI comprises two glycoprotein chains, an α chain which is associated with β_2-microgloubulin (β_2m). The α-chain (or 'heavy chain') consists of three domains (α1, α2 and α3), and spans the cell membrane. The smaller and non-polymorphic β_2m

sub-unit is associated with the heavy chain, but is not anchored to the cell membrane. The peptide is presented in a closed-ended peptide-binding groove, formed by the α1 and α2 domains. The MHCII glycoprotein comprises an α and ß chain, which both consist of two domains, and both span the cell membrane. The peptide-binding groove is open ended, facilitating the presentation of larger peptides (Figure 1.2). MHCs are hugely polymorphic, with each MHC able to present a range of different peptides in its peptide-binding groove. Whilst not all of the thousands, or in some cases millions, of possible peptides which may be presented exist in nature (Wooldridge et al., 2012), a great many do, giving rise to the vast array of peptides which are presented to the immune system at the cell surface. It is estimated that there are of the order of 10^{15} different pMHCs expressed in the human host (Wooldridge et al., 2012). It has already been stated that a single cell may express up to 10^{6} MHCI at its cell surface (Yewdell et al., 2003), and whilst some of these may present the same peptides, the vast majority will differ, creating a very complex environment at the cell surface for the immune system to survey in order to identify anomalous cells. The potential number of different peptide possibilities can be mathematically calculated (>10^{15} (Wooldridge et al., 2012)). Each individual will express 6 different MHCI (two HLA-A, two HLA-B, and two HLA-C) on the surface of their cells, and up to 6 different MHCII (two HLA-DR, two HLA-DQ and two HLA-DP) giving rise to their individual tissue type, or MHC restriction (Sewell, 2012); HLA (Human Leucocyte Antigen) being the specific human MHC. This restriction is genetically pre-determined, however the TCRs that recognise them are selected during development in the thymus

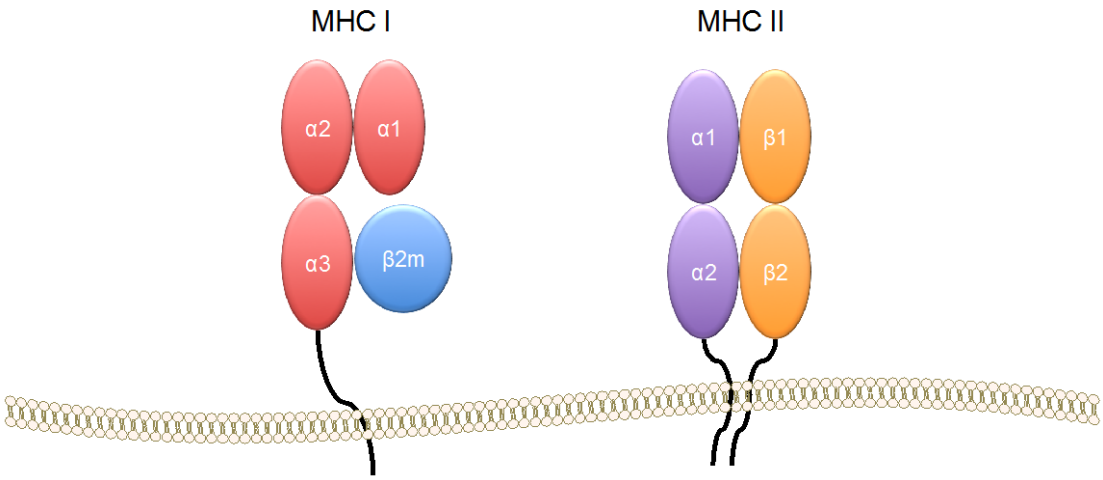

Figure 1.2: MHC class I and MHC class II
MHCI molecules are expressed on most nucleated cells. They comprise two polypeptide chains; a single 'heavy chain' made up of a cytoplasmic domain, a trans-membrane domain, and three extracellular domains (α1, α2 and α3), associated with the much shorter, single-domained and non-polymorphic ß2m. The peptide-binding groove is formed between the α1 and α2 domains at the membrane distal part of MHCI, and is highly variable between MHCI alleles.
MHCII are expressed only on professional APCs (dendritic cells, macrophages and B-cells). They also are comprised of two polypeptide chains, α and ß, however here they are similarly sized and each comprise of a cytoplasmic domain, a trans-membrane domain and two extracellular domains (α1 and α2, and ß1 and ß2 respectively). Despite the differences thus far described, there are similarities to MHCI, the peptide is presented in a binding groove at the membrane distal part of the molecule, in this case between the α1 and ß1 sub-units. Again, this region varies between MHCII alleles.

1.2.5 Antigen Processing and Presentation by MHCI

As has been previously mentioned, this thesis focuses on $CD8^+$ T-cells, which are MHCI-restricted. MHCI are expressed on most nucleated mammalian cells. MHC are polygenic, therefore the individual host can express up to 6 different MHCI alleles, capable of presenting a multitude of different small peptide fragments on the cell surface (Germain, 1994, Janeway CA Jr, 2001). For the most part, these peptide fragments are of intracellular origin, derived from the cell's own translational machinery, allowing the immune system to scan the proteins present inside that cell, thus facilitating immune surveillance. There does however exist evidence of extracellular peptides being processed and presented in this manner in a process termed cross-presentation (Harding and Song, 1994, Cao et al., 2002, Accapezzato et al., 2005).

Protein is degraded in the cytosol via the ubiquitin proteasome pathway, a process conserved in the eukaryotic cell from yeast to mammal. Proteins in the cytosol are flagged for degradation and polyubiquitinated, which in turn allows binding of the proteasomal 19S regulatory cap (Adams, 2003), resulting in denaturation of the protein, allowing it to feed into the proteasomal core where enzyme degradation occurs (Gaczynska et al., 1993, Rock et al., 1994). The peptide fragments generated during this process are then transported into the endoplasmic reticulum via the Transporter Associated Processing (TAP) complex where it binds to the newly synthesised MHCI molecules. Chaperone proteins such as calnexin, tapasin, calreticulin and ERp57 associate with the MHCI forming the Peptide Loading Complex (PLC), which in turn facilitates the loading of peptides into the peptide-binding groove. Tapasin also has a role in peptide editing, allowing a range of peptides to be presented at the cell surface (Praveen et al., 2010). Vesicles containing the newly formed pMHCI may then traffic to the cell surface (Figure 1.3

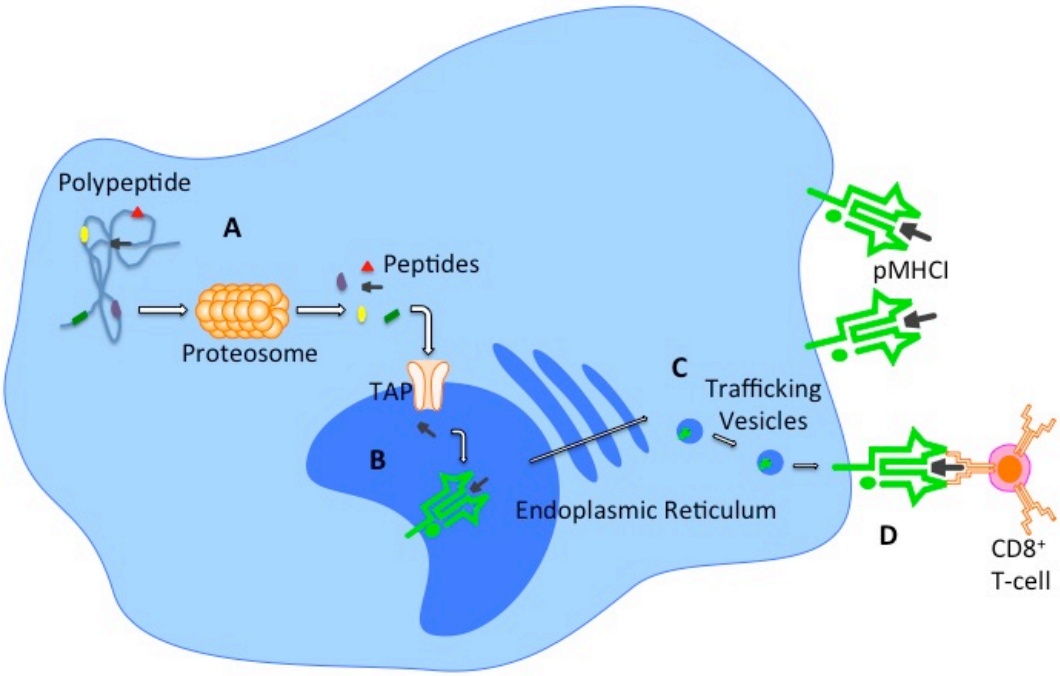

Figure 1.3: Antigen Presentation by MHCI
Proteins in the cytosol are denatured and are thus able to feed into the core of the proteasome where they are degraded by enzymes (**A**). The resultant peptide fragments enter the endoplasmic reticulum (ER) via the Transporter Associated Processing (TAP) complex. Chaperone protein and the immature MHCI form the peptide-loading complex (PLC), loading the peptide onto the peptide-binding groove (**B**). ß2m associates, and the fully formed pMHCI move through the ER and traffics to the cell membrane via vesicles (**C**). The pMHCI are expressed on the cell surface, where they may be recognised by specific $CD8^+$ T-cells (**D**).

It should also be noted that viral antigens are presented on the cell surface very rapidly after infection, far faster than the half-life of the viral peptide would permit, and even several hours before functional viral proteins are first detected in the cell (Neefjes et al., 2011, Vyas et al., 2008, Schubert et al., 2000). This anomaly is because of degraded ribosomal products (DRiPs) within the cell (Schubert et al., 2000, Berglund et al., 2007). These DRiPs are protein fragments resultant from anomalous protein synthesis (e.g. deletions, insertions or mutations in translation etc.), which are rapidly degraded to prevent the formation of protein aggregates within the cytosol that would otherwise be damaging to the cell (Neefjes et al., 2011).

MHCI molecules are unstable in the absence of peptide, meaning that all MHCI at the cell surface are pMHCI complexes. The peptide is bound as the MHC forms in the endoplasmic reticulum (ER) and is trafficked to the surface in this form. There is however evidence that high concentrations of peptide in the surrounding fluids can allow the bound peptide to be 'exchanged' and this has been utilized in experimental design (Praveen et al., 2010).

1.2.6 TCR recognition of MHC

The αßTCR is highly variable and exhibits overall structural similarity to immunoglobulins (Ig). Disulphide bonds link the α- and ß-chains of the TCR, and each chain contains a constant region (membrane proximal) and a variable region (membrane distal). It is this distal variable region that allows for recognition of different MHC-presented antigenic peptides (Wucherpfennig et al., 2010, Rudolph et al., 2006). The variable regions of the α-and ß-chain, Vα and Vß respectively, mediate recognition of the peptide-binding platform of pMHCI. This peptide-binding

region of the TCR is formed by 3 complementarity-determining loops (CDR1, CDR2 and CDR3), the latter of which makes contact with the peptide, with CDR1 and CDR2 making contact with the MHC. The orientation of the TCR is such that the Vα domain sits over the N-terminus of the peptide, with the Vß domain overlies the C-terminus of the peptide (Bjorkman et al., 1987a, Hennecke et al., 2000). TCR binding of the pMHC is diverse, however, in general, the TCR engages with the α and ß chains orientated diagonally across the compound surface created by the peptide and the flanking α helices of the MHC (Ferber et al., 2012). It is thought that this rotation could be to facilitate the binding of the co-receptors CD4 or CD8 to the invariant region of the MHC (Wucherpfennig et al., 2010), however there can be considerable variation (35°) in the degree of rotation (Ferber et al., 2012). In addition to the diversity of the TCR repertoire, each TCR is highly cross-reactive, recognising between 10^2 and 10^8 different peptides (Mason, 1998, Wooldridge et al., 2010b, Wooldridge et al., 2012).

1.2.7 The co-receptors: CD4 and CD8

T-cells that possess TCRs that recognise MHCI express the CD8 co-receptor on their surface, whereas TCRs that recognise MHCII are found on T-cells that express CD4, a restriction imposed on the T-cell during thymic ontogeny (Van Laethem et al., 2012). These two molecules, whilst similar in function, are structurally quite different (Leahy, 1995). CD4 is a single chain glycoprotein consisting of four domains, whereas CD8 exists as a dimer of two chains linked by a disulphide bond. In its co-receptor form, CD8 exists as a heterodimer, comprising two different chains; α and ß. CD8 can also form a homodimer of two α chains, CD8αα, which is found largely on other cell lineages such as dendritic cells (DCs), IELs and γδ T-cells (Konkel et al., 2011, Maldonado-Lopez et al., 1999, Sato et al., 1993). In contrast,

CD8αß is expressed only on double positive (DP)($CD4^+CD8^+$) thymocyes and MHCI-restricted, mature αß T-cells.

The TCR recognises and engages pMHC, causing the CD3 sub-units to initiate the cascade of signalling events within the T-cell, leading to cell activation. In most cases the co-receptors (CD4 or CD8) are required to enhance early intracellular signalling in order for this to occur. Once the TCR has engaged pMHC, the co-receptor molecules localise to the TCR-pMHC contact region, and bind to the invariant region of the MHC, a distinctly separate location to the TCR binding platform, which acts to stabilise the TCR/pMHC interaction (1.4). Some authors argue, that whilst CD8 has been shown to stabilise this interaction, CD4, which binds with a much weaker affinity, does not, acting only to recruit kinases to the signalling complex intracellularly (Artyomov et al., 2010).

1.2.8 The CD8 Co-receptor

CD4 and CD8 were initially identified as phenotypic markers based on MHC restriction, however once it had been shown that antibody blockade of these molecules results in failure of T-cell activation, their function in T-cell activation was realised (Miceli and Parnes, 1993, Daniels and Jameson, 2000, Miceli and Parnes, 1991). CD8 binds the same pMHCI molecule as the TCR, and acts to stabilise the TCR/pMHCI complex (Borger et al., 2014). This in turn facilitates TCR triggering thus in some cases increasing the specific sensitivity of the T-cell by over a million fold (Holler and Kranz, 2003). Evidence that CD8 binds the same pMHC simultaneously to the TCR, and has an important role in facilitating the T cells

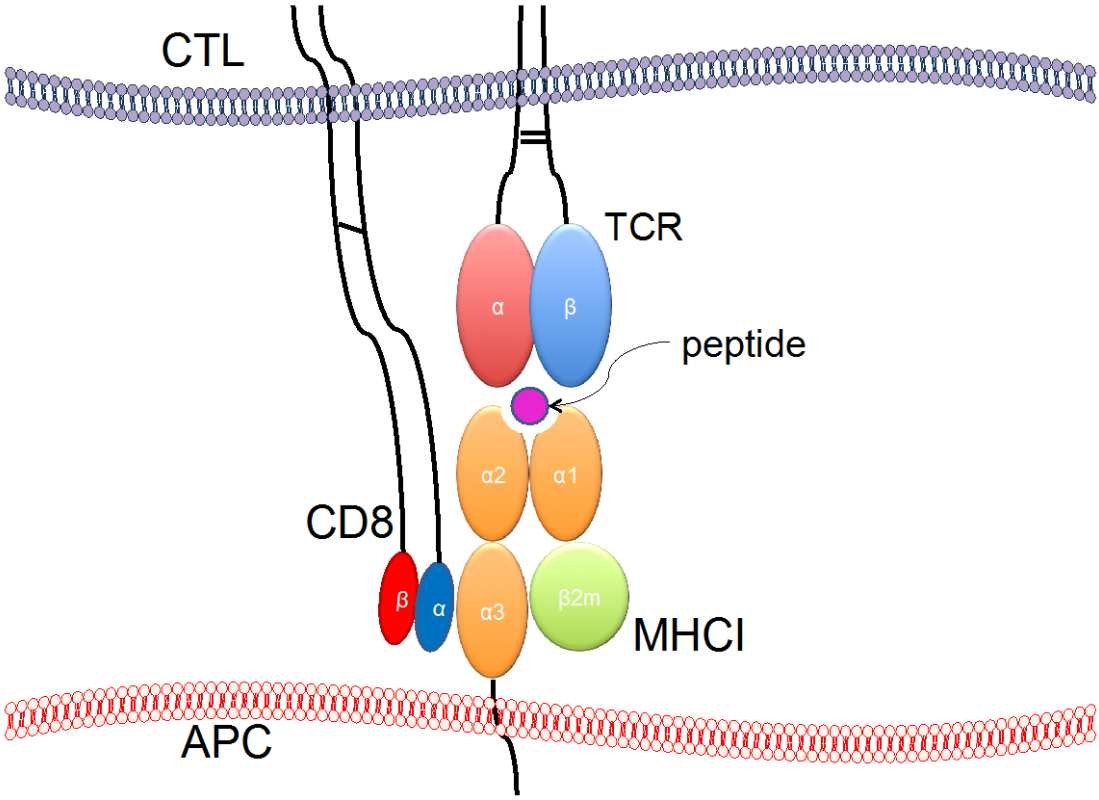

Figure 1.4: The Tri-partite structure.
At the cell: cell interface, TCR signalling usually requires formation of a triple structure; TCR/pMHCI/CD8. The highly variable and specific TCR binds the peptide-binding platform of the pMHCI complex, having contacts with both the peptide, which is held in the peptide binding groove, and the variable regions of the polymorphic MHCI (α1 and α2 domain). The CD8 co-receptor is non-polymorphic and binds the invariant region of the MHCI, making contacts largely with the α3 domain.

response led to the use of the term ‘co-receptor’ (Janeway, 1992, Miceli et al., 1991, Meuer et al., 1982).

1.2.9 Structure of CD8

CD8 is expressed on the cell surface either as a homodimer (CD8αα) or a heterodimer (CD8αß) (Norment and Littman, 1988). The heterodimer is constitutively expressed on $CD8^+$ T-cells and double positive thymocyes. Both dimers may serve as a co-receptor, albeit with a limited capacity in the case of CD8αα (Zamoyska, 1994, Van Laethem et al., 2007). Each chain of the dimer comprises four regions; a short cytoplasmic tail, the trans-membrane domain, and longer glycosylated ‘stalk’ region which is rich in serine, threonine and proline residues to allow the immunoglobulin- like head to reach the invariant region of the target MHCI (Zamoyska, 1994). A di-sulphide bond in the stalk-region links the two sub-units of the CD8 dimer. The stalk, or ‘hinge’, region comprises 50 residues in the case of CD8α and 30 residues in the case of CD8ß (Delves and Roitt, 1998) i.e. CD8ß is shorter. The ‘head’ is a globular glycoprotein, formed from the 113 N-terminal amino acids, which shares homology with the variable region of immunoglobulin (Ig), and binds the constant region of the MHCI. Some authors have suggested further di-sulphide linkage between cysteine residues in the α and ß chain in this membrane distal region of the dimer (Cole et al., 2012) others, however report this C36 as un-paired (Delves and Roitt, 1998), and that the corresponding cysteine (C31) in CD8ß is replaced with isoleucine (Chang et al., 2005).

The role of the cytoplasmic tail region has been heavily implicated in facilitating co-receptor function. It is believed that palmitoylation of the free cysteine residue in the cytoplasmic tail of CD8ß allows for partition into lipid rafts, and recruitment of

the receptors therein, which are important for stronger and sustained signal transduction (Arcaro et al., 2001, Arcaro et al., 2000). This explanation goes someway to explain why CD8αβ can serve as a better co-receptor for the TCR than CD8αα (Zamoyska, 1994, Cheroutre and Lambolez, 2008). A regulatory role has been ascribed to CD8αα by some authors, hypothesising that CD8αα acts to sequester lck thus inhibiting signalling (Cheroutre and Lambolez, 2008). Indeed, there exists some evidence of some cell populations transiently up-regulating CD8αα in order to suppress or temporarily dampen signalling (Cheroutre and Lambolez, 2008).

Cells expressing CD8αβ recognise antigen at lower concentrations than similar cells expressing CD8αα (Arcaro et al., 2000), however, given that similar pMHCI-binding affinities have been demonstrated between murine CD8αα and CD8αβ and it is likely that the same is true in man (Garcia et al., 1996, Kern et al., 1999), it follows that differences in co-receptor function are likely to be due to other features of the heterodimer, rather than differences in affinity for the MHCI, thus differences are likely to be intracellular. The cytoplasmic tail of CD8α binds the kinase $p56^{lck}$ (lck) via two vicinal cysteine residues and a common zinc ion (Zn^{2+}) (Davis and Berg, 2009), thus upon MHCI engagement by CD8, it is recruited to the CD3 complex in the region of CD3ε (Beddoe et al., 2009, Kjer-Nielsen et al., 2003), where it can act to bring about phosphorylation of the ITAMs. Whilst the triple structure is maintained, being stabilised by CD8, phosphorylation of all ITAMs can continue, allowing further phosphorylation by CD3ζ-associated protein 70 (ZAP70), and downstream signalling, which will be discussed in more depth in later sections.

It has been suggested that because the homodimer CD8αα may bind two lck molecules, there exists steric hindrance of this interaction inhibiting phosphorylation, thus the heterodimer, recruiting a single lck at a time, may recruit lck more effectively, although little evidence exists for this theory (Gascoigne et

al., 2011, Cheroutre and Lambolez, 2008). Whilst this argument may have some merit, Arcaro *et al* demonstrated enhanced antigen recognition in the presence of CD8αß, as compared to both CD8αα and CD8αß where the cytoplasmic tail of the ß-chain were lacking (Arcaro et al., 2000), suggesting that the cytoplasmic tail of CD8ß is important to co-receptor function. The cytoplasmic tail of CD8ß is thought to promote effective lck binding (Bosselut et al., 2000)

1.2.10 The pMHCI/CD8 Interaction

Human CD8 is largely non-polymorphic in nature and binds to the invariant region of the MHCI, making contact primarily with the α3 domain of the MHCI heavy chain, but also to a lesser extent with the α2 domain of MHCI and $ß_2m$ (Norment and Littman, 1988, Cole et al., 2007, Chang et al., 2005, Xu et al., 2001). Polymorphisms have been identified in the CD8α gene, although not expressed at the cell surface as they result in either failed expression (de la Calle-Martin et al., 2001), or a secretory form (Giblin et al., 1989, Norment et al., 1989), thus they do not affect MHCI contact and interaction. Variation in the CD8ß gene is seen only in the trans membrane and cytoplasmic region (DiSanto et al., 1993, Thakral et al., 2013, Thakral et al., 2008), and these splice variants will be discussed in more detail in the final discussion, and in Appendix E.

The crystal structure of human MHCI in complex with CD8αß is thus far unsolved. If, however, solved structures of the murine CD8αα and H2-K^b and human CD8αα and HLA-A*0201(Gao et al., 1997a, Kern et al., 1998) are compared it is observed that CD8αα binds MHCI in a similar manner in both the mouse and in man, thus our assumptions as to the spatial relationships of CD8αß and MHCI are based upon these structures, and that of the murine CD8αß (Shore et al., 2008). Gao *et al*

demonstrated that CD8αα binds to MHCI asymmetrically, with the subunits binding in what can be considered the *proximal* and *distal* positions, relative to the cell membrane, with one sub unit occupying around 70% of the contact residues (Gao et al., 1997a, Chang et al., 2006). Residues 51-55 of the CD8α form the main contact with residues 223-229 α3 domain of the MHCI heavy chain. The structure of CD8αα has been demonstrated to contain flexible loops (complementarity determining region (CDR)-like) which clamp to bind a finger-like projection of the α3 heavy chain (Gao et al., 1997a). The resulting conformational changes are limited to the α3 domain of the pMHCI and do not extend to the peptide binding platform. Murine CD8αα, whilst binding in similar locations, has been shown to have more contact points with the MHCI, a feature which likely explains the higher binding affinity of the murine system as compared with man (Purbhoo et al., 2001, Wooldridge et al., 2010a).

Gao *et al* predicted from the structure of human CD8αα complexed with pMHCI that the CD8ß would occupy the position of the CD8α-2 subunit (Gao et al., 1997a). However, Wang *et al* solved the structure of murine CD8αß complexed with H-2D^{d} and demonstrated that the CD8ß subunit was membrane-proximal; the position occupied CD8α-1 subunit (Wang et al., 2009). It has been argued that both may be true, that CD8αß may bind in either orientation (Chang et al., 2006), however to date there is little structural evidence for this.

1.2.11 The CD4 Co-receptor

CD4^{+} T-cells are MHCII-restricted. CD4 is the co-receptor to the TCR/pMHCII interaction. The structure of CD4 is markedly different to that of CD8. CD4 is a monomer comprised of four extracellular immunoglobulin-related domains (D1-D4),

a hydrophobic trans membrane domain, and a cytoplasmic tail. The cytoplasmic tail is highly basic, and contains 3 serine residues, which may be phosphorylated (Pitcher et al., 1999) and motifs which facilitate association with Lck in a zinc-dependent manner, similarly to those residues found on the cytoplasmic tail of CD8 (Kappes, 2007b). CD4 binds the conserved region of the MHCII, with the N-terminal Ig-like domains having contacts with the α2 and ß2 subunits (Wang et al., 2001, Li et al., 2013). As with pMHCI/CD8, there are no induced conformational changes to the peptide-binding platform when CD4 binds the pMHCII. Studies suggest that the affinity of the pMHCII/CD4 interaction is even weaker than that of the pMHCI/CD8 interaction. Xiong *et al* suggested a dissociation constant (K_D) of greater than 200 μM for the murine system (Xiong et al., 2001), however more recent studies demonstrate that this is incorrect, that it is not possible to detect CD4 binding of MHCII in solution, and demonstrating a far weaker association (>2.5 mM) (Jonsson et al., 2016).

1.2.12 Co-receptor Function of CD8

Early studies examining the apparent ability of CD8 to enhance T-cell antigen sensitivity proposed a role for CD8 as an accessory molecule, binding the pMHCI independently of TCR. It was postulated that CD8 at the cell surface increased effector: target adhesion thus allowing the T-cell to respond to lower levels of antigen. It has since been shown that CD8 binds the same pMHCI at the same time as the TCR in what was first termed the 'co-receptor model' by Charles Janeway (Janeway, 1992). In the case of all but the strongest TCR/pMHCI interactions, this co-engagement of CD8 is essential for TCR triggering and subsequent T-cell activation. High affinity TCR/pMHCI interactions, which do not absolutely require CD8 engagement in order to facilitate T-cell activation, are said to be CD8-

independent (Laugel et al., 2011), however some authors have demonstrated that full cytotoxic function of the $CD8^+$ T-cell is not possible without CD8 engagement (Knall et al., 1995). It has also been shown that if pMHCI/CD8 affinity is super-enhanced, TCR engagement is not required to achieve triggering (Wooldridge et al., 2010a), however, owing to the non-polymorphic nature of CD8, this is an experimental rather than a physiologically normal phenomenon. This would suggest that for the majority of antigens, both receptors are required to simultaneously engage the pMHCI in order to initiate activation. The relative kinetics of these interactions would suggest that the TCR docks first and when CD8 co-engages TCR triggering is initiated. Recent mathematical modelling would suggest that this ordering is not essential; if the TCR/pMHCI interaction exhibits more rapid kinetics and a weaker interaction then the reverse may be true, and likewise if the pMHCI/CD8 interaction strength is increased (Szomolay et al., 2013).

1.2.13 Kinetics of TCR/pMHCI/CD8 tri-molecular complex

The interaction kinetics of cell surface receptors can be analysed by producing soluble versions of these receptors and collecting measurements using surface plasmon resonance (SPR) techniques, for example using BIAcore instrumentation. This typically involves the immobilization of a ligand to the surface of a SPR chip and flowing over soluble receptor at multiple concentrations, allowing detection of binding in real time and calculation of interaction kinetic parameters. It has been shown that the TCR binds the pMHCI complex with moderate affinity, usually K_D = 1-90 μM (Irving et al., 2012). This varies between different TCRs, and between different peptide ligands 'seen' by the same TCR. Stronger agonists with a K_D of 1-5 μM and 'super-agonists' (K_D<1 μM) are able to trigger a TCR response without the need for CD8 engagement and can be referred to as 'CD8 independent' (Irving et

al., 2012, Purbhoo et al., 2004). The half life ($t_{½}$) of this interaction is ~10 s, however it has recently been suggested that on-rate (K_{on}) for TCR/pMHC binding is faster than that of the off-rate (K_{off}), thus the same TCR can immediately re-bind pMHC, facilitating stable complex formation (Irving et al., 2012).

The CD8/pMHC interaction is characterised by low affinity (K_D ~90-220 μM), significantly lower than that of the TCR/pMHC interaction (Wyer et al., 1999). The kinetics of this interaction are extremely rapid, characterised by a K_{off} in the region of 18 s^{-1}. It has been demonstrated that if the strength of the pMHC/CD8 interaction is increased sufficiently, the TCR is effectively bypassed, resulting in T-cell activation irrelevant of the preference of the TCR or the nature of the presented peptide ligand (Wooldridge et al., 2010a).

1.2.14 TCR Signalling; recognition of pMHCI

In vivo, cells are constantly interacting with each other, and thus TCRs and pMHC come into contact with each other, forming short-lived connections. These are termed immunological kinapses (IK) when they are fleeting, and immunological synapses (IS) when they persist for longer (Fooksman et al., 2010). A single APC will likely express many different pMHC, presenting an array of antigenic peptide fragments. There may be considered to be 3 phases to signalling; during the first phase, early signals are initiated though the transient immunological kinapse. Aggregation of these kinapses leads to small protein clusters forming the more stable and organised immunological synapse (phase 2) (Billadeau, 2010). TCRs are up-regulated and recruited to the site, resulting in many TCR clusters forming in an IS. Many of the surface molecules on T cells and APCs separate themselves into distinct clusters or supramolecular activation clusters (SMACs) (Monks et al., 1998).

The cell surface molecules are organised into a 'bull's-eye' pattern, with a central cluster of TCR/pMHC (cSMAC) and a peripheral region packed with adhesion molecules (pSMAC) (Anton van der Merwe et al., 2000). It can take many signalling events within the same cell to induce activation. The IS has been traditionally thought to be required for sustained TCR triggering, however subsequent literature suggests that cSMAC formation is not required (Alarcon et al., 2011). For T-cell activation to occur a second signal is also required. This is received from co-stimulatory molecules, such as CD28 (Lichtenfels et al., 2012). The distal SMAC (dSMAC) is rich in CD45 and other accessory molecules, and also is the site of formation of TCR microclusters (MCs), which contain large amounts of CD28 bound to CD80, its primary ligand, initiating the co-stimulatory signal (Yokosuka et al., 2008). TCR MCs are constantly forming here in the dSMAC and then migrating to the cSMAC, thus perpetuating the IS (Fooksman et al., 2010). The organisation of the surface molecules into the regions that make up the IS is dependent of the actin filament cytoskeleton (Grakoui et al., 1999).

1.2.15 CD3

The TCR α and ß sub-units can only be expressed at the cell surface in association with the CD3 sub-units, γ, δ and ε (Weiss and Stobo, 1984). The CD3 sub-units have long cytoplasmic tails, are involved in early signalling events once the TCR has engaged cognate pMHCI, communicating the signal across the plasma membrane. All six sub-units (γ, δ, 2 ε, and 2 ζ) span the surface membrane, and contain Immunoreceptor tyrosine-based activation motifs (ITAMs): one in the case of the γ, δ, and ε sub-units, and three in the case of CD3ζ. These are conserved sequence motifs common to the cytoplasmic region of molecules within the immunoglobulin superfamily, with the form YXXLX(7-12)YXXL (Fooksman et al., 2010), i.e. each ITAM

has two aliphatic and two tyrosine residues (Wucherpfennig et al., 2010). Upon peptide recognition, these common motifs become phosphorylated by lck, thus propagating the signal through the cell membrane and amplifying the signals from the TCR. This is essential for signal propagation, as has been demonstrated by mutation of tyrosine residues abrogating signal transduction (Sunder-Plassmann et al., 1997). There is enrichment of the complex with ZAP70, however both tyrosines must be phosphorylated before ZAP70 can bind (Janes et al., 2000). Complete phosphorylation of these motifs is necessary for T cell activation. It has been suggested that premature phosphorylation (i.e. without TCR engagement) is prevented by the insertion of the CD3ε tyrosines into the hydrophobic core of the plasma membrane (Aivazian and Stern, 2000), although other authors argue that the CD3 ITAMs are in a constant flux of phosphorylation and de-phosphorylation and that triggering is prevented in the resting cell by de-phosphorylation occurring at a greater rate than phosphorylation (Davis and van der Merwe, 2006). Lck is largely associated with the co-receptors CD4 and CD8, and as such the dominant role of the CD4 and CD8 co-receptors is to recruit lck to the pMHCI/TCR/CD3 complex (Artyomov et al., 2010, Kappes, 2007a), although some sources argue that it is the lck which recruits the co-receptors to the complex (van der Merwe and Cordoba, 2011, Gao and Jakobsen, 2000).

It has been demonstrated that the cytoplasmic tail of CD3ζ is, when associated with lipid, folded in such a way as to prevent phosphorylation, thus the association of these tails with the hydrophobic, lipid-rich membrane prevents phosphorylation, in what has been termed the ‘conformational change model’, or ‘ITAM sequestration’. In aqueous solution lck phosphorylation is favoured. It has been postulated that TCR engagement facilitates conformational changes in the internal sub-units, releasing the cytoplasmic tails from the membrane and thus facilitating phosphorylation by lck (Aivazian and Stern, 2000). What triggers this release, or how it comes about is

unclear. It has been suggested that TCR aggregation and an associated multimerisation of receptors may play a role, as has the effects of the mechanical force of the TCR binding the pMHCI. This hypothesis has not thus far been tested; it remains to be explained how the formation of the tri-partite complex results in the phosphorylation events that take place in the intracellular regions of the CD3 complex ('TCR triggering'), and other authors have demonstrated that in vivo ITAMs are largely and constitutively phosphorylated (Chakraborty and Weiss, 2014, van Oers et al., 1993). Another theory, the kinetic segregation model (KS), suggests that the IS promotes and facilitates the formation of a pro-signalling environment. Segregation of phosphatases such as CD45 from the IS allows for phosphorylation by lck, thus triggering downstream signalling (van der Merwe and Davis, 2003, Davis and van der Merwe, 2006). Whilst these theories have been put forward as alternative explanations, they may not be mutually exclusive.

1.2.16 The Kinetic Segregation Model

Davis and Van der Merwe propose an alternative model for the initiation of cell signalling, summarised in Figure 1.5, which is based around the spatial re-organisation of signalling proteins (Davis and van der Merwe, 2006). Proteins are very abundant in the cell membrane, making up around 20 - 25% by mass of the cells surface membrane (Cooper, 2000, Nicolson, 2014). These proteins are wide varying and diverse, and perform many different functions, and include proteins involved in

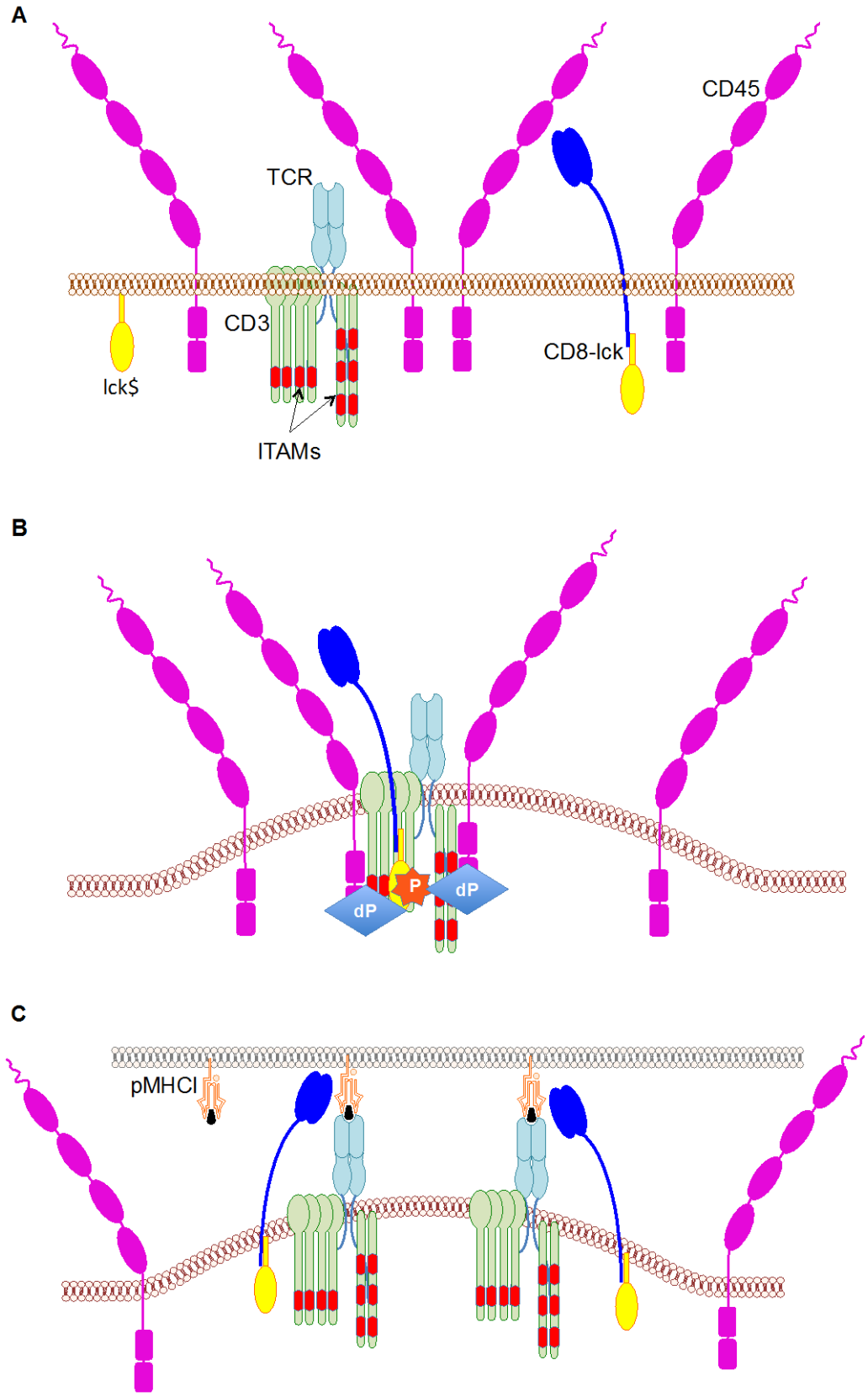
A
CD45
TCR
CD3
CD8-lck
lck$
ITAMs
B
P
dP
dP
C
pMHCI

Figure 1.5: Kinetic Segregation model
(Davis and van der Merwe, 2006)
At the cell surface large, de-phosphorylating CD45, phosphorylating kinases such as lck and TCR/CD3 complexes are present in approximately 4:2:1 ratios (**A**). Phosphorylation of the TCR/CD3 complex iTAMs are is a state of constant flux, with constant phosphorylation (**P**) by lck being in turn countered by constant de-phosphorylation (**dP**) by CD45. In the resting T-cell, phosphorylation of the CD3 ITAMs occurs randomly, however the relative numbers of lck is approximately half of that of CD45, thus net de-phosphorylation is greater and the TCR cannot trigger (**B**). CD45 is appreciably larger than the TCR/pMHCI, thus when an APC is held is close contact with the T-cell by this interaction, CD45 is excluded, thus net phosphorylation occurs facilitating TCR triggering (**C**).

cell: cell interactions and signalling. Proportionally, phospho-kinases such as lck make up about twice as many of these proteins as the TCR, and phosphatases, primarily CD45, up to twice as many again (Davis and van der Merwe, 2006). In addition, diffusion and thus protein movement within the cell membrane is very rapid, constantly shifting, meaning that by random bumping of intracellular proteins is frequent (Nicolson, 2014, Singer and Nicolson, 1972, Nicolson, 1976). There is a large super-family of membrane proteins with cytoplasmic tails bearing tyrosine motifs. The TCR-CD3 complex possesses 10 ITAMS, which are constantly being phosphorylated by lck and de-phosphorylated by CD45, however, the ratio of Lck: CD45 is such that overall de-phosphorylation is favoured, thus triggering is suppressed in the resting cell.

CD45 is a large, rigid molecule whose prominence from the cell surface is significantly larger than the gap afforded by the TCR/pMHCI interaction. When the IS is formed, CD45 is excluded by this narrow gap, and is unable to move back in, meaning that de-phosphorylation cannot occur. This model would suggest that the role of the co-receptor is likely to recruit lck, and that the absence of CD45 facilitates signalling, i.e. dephosphorylation is prevented by steric exclusion, CD45 being too large to enter the IS when TCR is bound to presented pMHCI. TCRs which have not engaged pMHC, because of their small size and rapid diffusion are able to leave the IS. Whilst they are likely to have become phosphorylated whilst in the IS, the authors postulate that they are able to exit and become de-phosphorylated before downstream signalling occurs.

They have demonstrated that truncation of the CD45 molecule suppresses signalling, presumably by allowing this molecule to enter the IS and de-phosphorylate the ITAMS. Similarly, enlarging the intracellular gap by increasing the size of the TCR/pMHC complex, thus allowing phosphatase in to the IS also affords signalling.

1.3 T-cell Signalling

1.3.1 T-cell signalling Pathways

Activated ZAP70 phosphorylates the linker of activated T cells (LAT) and lymphocyte cytosolic protein 2 (SLP-76) (Smith-Garvin et al., 2009). These substrates of ZAP70 function as scaffold (adaptor) proteins and aggregates of scaffold proteins form microclusters within the IS. LAT is a membrane protein which, when it interacts with Lck, becomes palmitoylated and interacts with the cholesterol and sphingolipid rich lipids rafts. The lipid rafts are the platform for later signalling events within the cell, leading to transcription and thus effector function (Pang et al., 2007). Lipid rafts are micro domains within the cell membrane, spanning ~20 nm, which are used to bring proteins necessary for signal transduction together in this highly specialised domain, once they have undergone post-translational addition of lipids by processes such as palmitoylation (Nicolson, 2014). CD45 is excluded from lipid rafts, probably because it would act to inhibit phosphorylation. This is further evidenced by its likely role in the regulation of lck activity (Chichili et al., 2012).

Following tyrosine phosphorylation of kinases, there follows activation of phospholipase C (PLC), calcineurin and Ras, which in turn leads to the transcriptional activation of the IL-2 gene. PLC causes breakdown of the membrane protein PIP_2 (Phosphatidylinositol 4,5-bisphosphate) into diacylglycerol (DAG) and inositol 1.4.5-triphosphate (IP_3). DAG remains membrane-bound and activates protein kinase C-θ (PKCθ), leading to activation of the transcription factor NF_KB. DAG also activates RasGRP, causing a kinase cascade, ultimately resulting in activation of the Fos component of the transcription factor Activation Protein-1 (AP-1) (Smith-Garvin et al., 2009). IP_3 is released into the cytosol of which in turn binds

the IP_3 receptors on the endoplasmic reticulum (ER) causing release into the cytosol of the Ca^{2+} stored therein (Robert et al., 2011). The resulting depletion in ER stored calcium causes opening of calcium release activated calcium channels (CRAC channels) in the plasma membrane, allowing further Ca^{2+} to flood the cell. Increase intracellular calcium causes activation of the phosphatase calcineurin, which itself activates nuclear factor of activated T cells (NFAT), another transcription factor. NF_kB, AP-1 and NFAT all induce nuclear events, such as transcription of the IL-2 gene, causing effector activity and proliferation of the T-cell (Figure 1.6).

In a secondary pathway, activation of the PLC pathway by TCR engagement causes an influx of free cytosolic calcium ($[Ca^{2+}]$) and activation of protein kinase C (PKC). This phosphatidylinositol (PI) pathway causes transcriptional events and thus IL-2 production. Activation of the T cell without engagement of this secondary PI pathway have been observed (Sussman et al., 1988). Calcineurin release is also regulated by $[Ca^{2+}]$ flux, with the phosphatise activity of this molecule contributing to transcription factor activation and therefore nuclear events.

1.3.2 Down-regulation of cell surface TCR upon Activation

Following TCR engagement of pMHCI, cell surface TCRs are down regulated. This cycling of the TCR is considered by some to be a crucial part of T-cell activation, involving internalisation of the TCR following engagement (Itoh et al., 1999, Valitutti et al., 1996b). This remains to be proven, however, and indeed others argue that non-engaged TCRs are also internalised (San Jose et al., 2000). It is known that the TCR/CD3 complex is very stable and is constantly being internalised and recycled in the normal resting T-cell (Valitutti et al., 1997, Cai et al., 1997, Liu et al., 2000). It is also known that internalisation and recycling of surface molecules

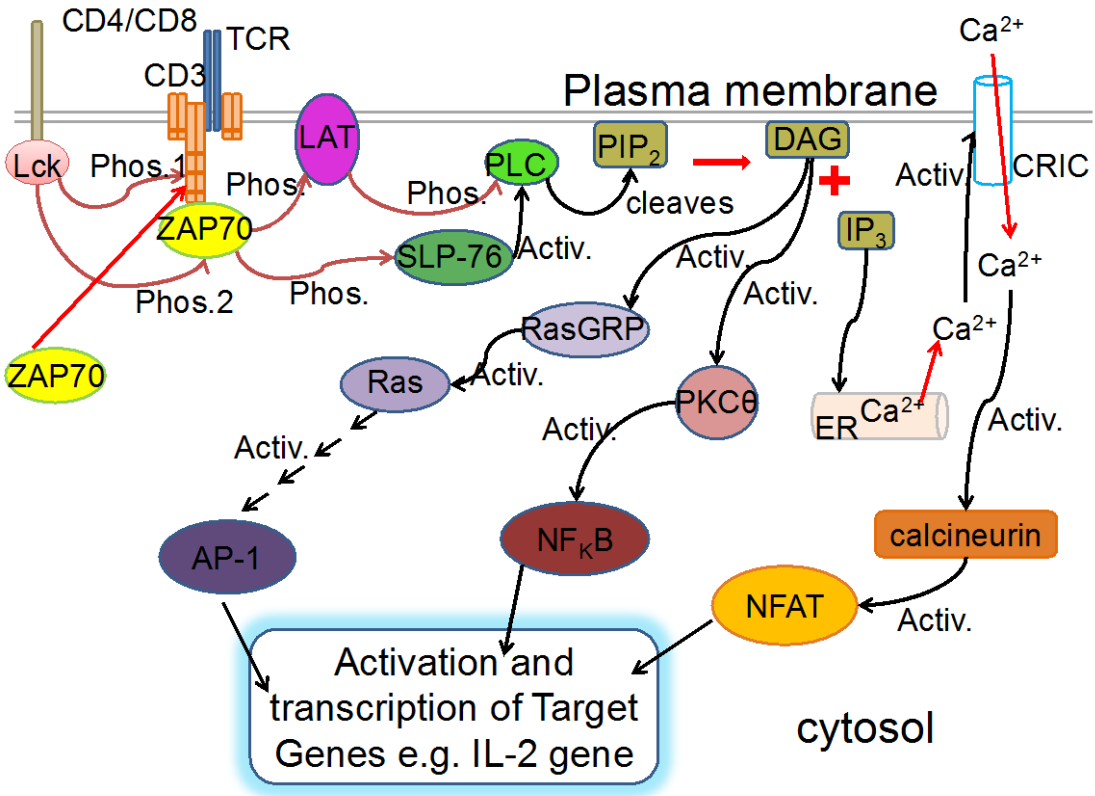

Figure 1.6: Signalling pathways following TCR triggering.
Following phosphorylation of CD3 ITAMs, activated ZAP70 causes further downstream phosphorylation of LAT and PLC within the lipid rafts. This causes activation of the Ras, calcineurin and NFκB pathways, and a net influx of calcium, resulting in transcriptional activation of the IL-2 gene, which in turn results in activation of other effector pathways and the initiation of a positive feedback loop causing further signal amplification.

is a feature common to cell membrane receptors, mediated via a tyrosine-based motif (Pandey, 2009). Liu *et al* demonstrated that the stable TCR/CD3 complex is constantly being internalised and recycled in resting cells, however, following T-cell activation, recycling to the cell surface is blocked resulting in down-modulation of TCR and associated CD3 (Liu et al., 2000). This study would suggest that there is no increase in the rate of internalisation following activation, but that recycling is blocked following the activation process, possibly by transcriptional inhibition of expression, thus involving TCRs which were internalised as part of an on-going process and may or may not have individually themselves been part of triggering (Liu et al., 2000).

1.3.3 $CD8^+$ T-cell Activation

T-cells express large numbers of TCRs at the cell surface. In most cases this is the same TCR formed of identical α and ß subunits. Allelic exclusion favours only a single Vα and Vß recombination, however it is possible for a cell to produce more than one of either chain, allowing for the expression of 2 or more different TCRs at the cell surface (Matis et al., 1988, Hardardottir et al., 1995). In this instance, one of the TCRs will dominate, making up the majority of the TCRs at the cell surface. In contrast, an APC may express up to 6 different MHCI alleles at the cell surface, which can present a multitude of different peptides. This vast array of different pMHCIs is constantly being scanned, but the huge number of different possible combinations means that only a tiny proportion of these are the same. Indeed it is possible, given the plethora of different peptides presented in the context of MHCI by the APC, that some pMHCI may be unique events. A single pMHCI can trigger up to ~200 TCRs at the cell surface (Valitutti et al., 1995) meaning that a low number

of pMHCIs can achieve high TCR occupancy leading to a sustained and amplified signal.

During an infectious challenge APCs engage and prime T-cells in the accessory lymphoid organs such as the lymph nodes and spleen. Naïve T-cells are present in low numbers in the host, too low to effectively rise to infectious challenge. Additionally, they are incapable of effector function such as inducing target cytolysis or IFNγ production. Therefore specialised APC such as DCs present pMHCI to naive T-cells in the accessory lymphoid tissue, initiating proliferation and differentiation. This activation of naïve T-cells induces intense proliferation giving rise to a large pool of effector T-cells. The vast majority of these are 'short-lived effector cells' (SLEC) which die off once the challenge has been cleared. Approximately 5% are memory T-cells, and remain in the circulation in case of a repeat challenge. The replicative drive of the memory population is much slower and thus burnout is not achieved, or rather is delayed, allowing these cells to remain. It has been shown that a single naïve T-cell may divide to give rise to both effector and memory subsets (Stemberger et al., 2007, Gerlach et al., 2010) although other authors have argued that this is not the case, that the eventual phenotype of the naïve T-cell is pre-programmed before the antigenic challenge (Beuneu et al., 2010). In the instance of different antigenic challenge (viral, bacterial, parasite, dysregulated cell etc.) different innate populations producing different cytokines are present adding increased complexity.

1.3.4 Co-stimulation of T-cells; A Three signal Process

In order for a naïve T-cell to become fully activated, the signal generated by the TCR/pMHCI interaction is insufficient; a second 'co-stimulatory' signal is required (Figure 1.7).

This signal, termed 'signal 2', the TCR/pMHCI interaction being 'signal 1', is delivered only when the T-cell encounters pMHCI presented by a 'professional' APC (Bretscher, 1999, Pardigon et al., 1998). The professional APC possesses at its surface B7.1 (CD80) and B7.2 (CD86), which are ligands to CD28. CD28 is the only receptor to B7.1 and B7.2 which is expressed on naïve T-cells. Following engagement of the TCR to the pMHCI, the APC and the T-cell are held in close proximity, enabling CD28 to engage with its ligand. The 'close contacts' are essential for CD28 engagement, thus the specificity of the interaction is generated by the TCR/pMHCI interaction, with the non-specific CD28-B7.1/2 interaction only occurring after the TCR/pMHCI complex has formed. Whilst signal 1 is insufficient for full activation, it has been demonstrated that if the close contacts may be formed by another means, such as by exclusion of CD45, then signal 2 may be sufficient to bring about T-cell activation (Chang et al., 2016), an observation which may account for the observed loss of specificity of the TCR when the pMHCI/ CD8 interaction affinity is super-enhanced (Wooldridge et al., 2010a, Dockree et al., 2017). In the absence of signal 2, the T-cell becomes anergic (Yamamoto et al., 2007, Appleman and Boussiotis, 2003). It has been postulated that the requirement for two signals exists in order to differentiate between self- and non-self stimulation, i.e. weak self-stimulation is required for maintenance of the naïve population, whereas full and robust activation is necessitated in the face of challenge (Bretscher, 1999), however it should be remembered that the strength of the TCR/pMHCI interaction has a quantitative effect on the T-cell response, and

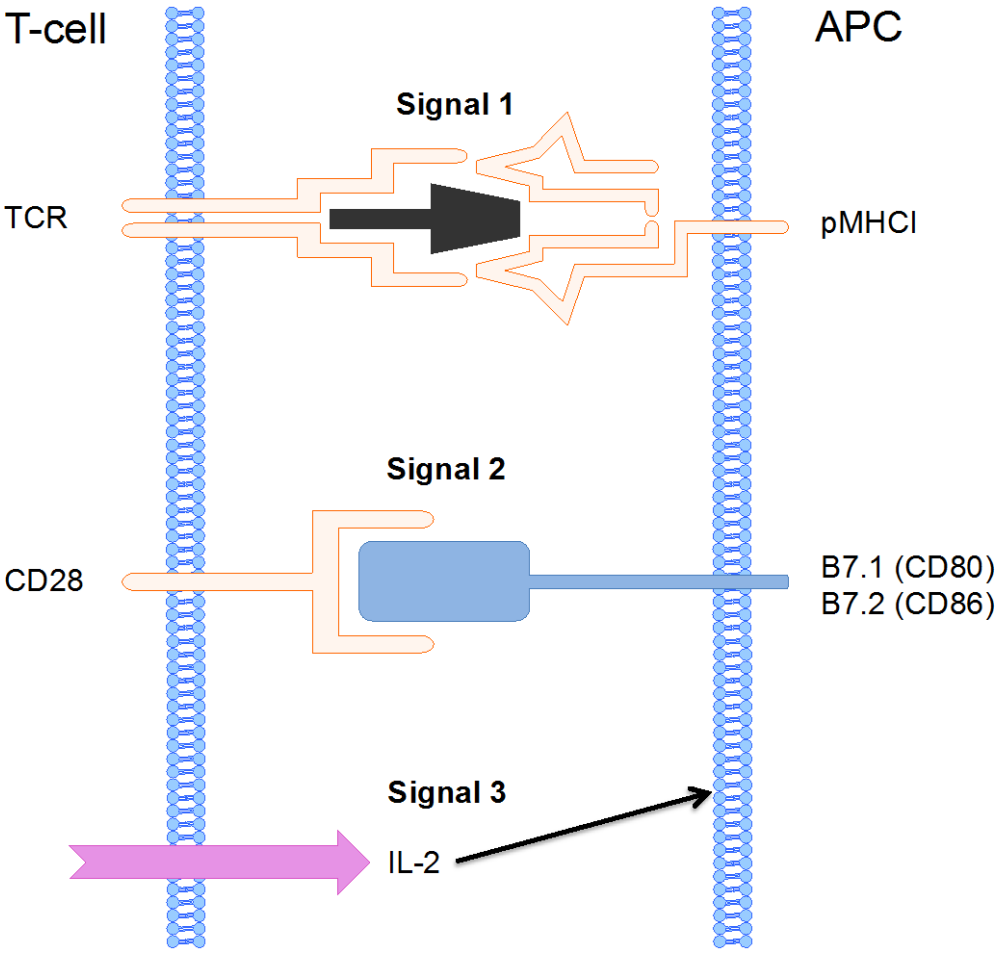

Figure 1.7: Co-stimulatory signals.

Activation of naïve T-cell requires both stimulation through the TCR (signal 1) and co-stimulatory pathways (signal 2). The effect of these signals is to drive IL-3 release, resulting in positive feedback (signal 3).

some authors have suggested that T-cell activation may still occur in the absence of signal 2 if signal 1 is particularly strong (Sharpe and Freeman, 2002, Yamamoto et al., 2007).

Only professional APCs possess on their surface B7.2 and may be induced to up-regulate B7.1 following engagement (Chen and Flies, 2013), thus professional APC are absolutely required to initiate the immune response. These are usually encountered in the draining lymph nodes or associated lymphoid tissue rather than the local environment, however following activation the activated T-cells migrate to target tissue where clonally expanded effector T-cells target anomalous or infected cells for deletion. In order for professional APCs to present antigenic peptide in the context of MHCI in the secondary lymphoid tissue, these peptides must have been internalised at the site of the challenge, however the criteria for presentation of exogenous peptide by MHCI have not been fully realised.

A third signal is provided to the $CD8^+$ T-cell by the APC in the form of cytokine release. Following TCR engagement and co-stimulation, the APC releases pro-inflammatory cytokines such as IL-2. In the absence of this third signal, the T-cell may fail to develop full effector functions, and a memory pool is not generated (Curtsinger and Mescher, 2010, Mescher et al., 2006). Inactivated naïve T-cells do not express IL-2 nor its receptors, thus initiation of signalling is considered to take place in the order which is described; 1) TCR engagement, 2) Co-stimulatory signal transmission, 3) IL-2 mediated signalling. Further IL-2 may be supplied by T_H1-cells, in the event that insufficient is produced by the APC(Chen and Flies, 2013). The anergy resulting from the absence of signal 2 may be reversed or 'rescued', by IL-2 (Appleman and Boussiotis, 2003).

Knowledge of the 3 signals required to induce T-cell activation is utilised by researchers; Dynabeads™ are impregnated with CD3 and CD28, and may be used in IL-2 enriched culture media to expand T-cells *in vitro* (Trickett and Kwan, 2003).

1.3.5 Other Co-stimulatory and Co-inhibitory Molecules

Whilst the only receptor to B7.1/2 expressed by naïve T-cells is CD28, effector T-cell may also express Cytotoxic T-lymphocyte Antigen 4 (CTLA-4). Following priming of the naïve T-cell, CTLA-4, which is accumulated in lysosomes, is trafficked to the cell surface at the APC close contact zone (Saito and Yamasaki, 2003). When CTLA-4 engages B7.1/2, the signal generated is inhibitory. The inhibitory signal generated results in down-regulated endocytosis and thus expression of CD28 at the cell surface. This in turn reduces the activation signal that the CD28-B7.1/2 interaction induces, whilst the inhibitory signal generated by The CTLA-4-B7.1/2 interaction persists, in a negative feedback process. CTLA-4 accumulates in the cSMAC, and has been shown to physically exclude CD28 from this region, further dampening the T-cell response (Yokosuka et al., 2010).

Programmed Death 1 (PD-1) has been shown to have an inhibitory response on T-cell activation, following engagement with its ligand PD-L1 (B7-H1) (Riley, 2009). It has an additional ligand, PD-L2 (B7-DC), which is only present on professional APCs, whereas PD-L1 is widely expressed, and has also been found to engage B7-1 (Butte et al., 2007). PD-1 engagement results in recruitment of SH-domain containing tyrosine phosphatase-2 (SHP-2), and as a consequence, down-regulation of PI3 activity, as well as inhibiting phosphorylation of the CD3 and ZAP70, and inhibiting phosphorylation of other TCR signalling components (Chen and Flies, 2013, Saito and Yamasaki, 2003, Riella et al., 2012).

PD-1 has a vital role in regulation of the T-cell response and in maintaining peripheral tolerance. It inhibits alloreactive responses, and it has been shown that PD-1 up-regulation in transplanted tissue is associated with a favourable prognosis in graft survival. The PD-1 pathway has been usurped by pathogens and neoplastic processes resulting in chronic infection and tumour survival (Carreno et al., 2006). In cancer immunology, tumours with high levels of PD-1L are associated with a less favourable prognosis for the host (Wang et al., 2017, Muenst et al., 2014).

The ligands to these inhibitory receptors are collectively known as the B7 ligand family, and there is crossover between ligands and receptors. There are further B7 homologues which have been found, many of which have unknown receptors, thus their effects are uncertain (Sharpe and Freeman, 2002). In addition to those described above, the receptor Inducible Co-stimulator (ICOS) has an unique B7-like receptor, B7RP-1 (ICOSL, B7-H2). ICOS is the third member of the CD28 superfamily (after CD28 and CTLA-4), and is rapidly up-regulated following TCR engagement. Its effect is stimulatory, however rather than promoting expansion like CD28, its main effect is to induce differentiation to an effector phenotype and upon regulation of cytokine production (Sharpe and Freeman, 2002). Its effects on proliferation are mild, and whilst it can promote IL-2 release in the low levels, this is insufficient to that which is required for a fully robust response.

The combine effects of these co-stimulatory and co-inhibitory pathways are shown in Figure 1.8.

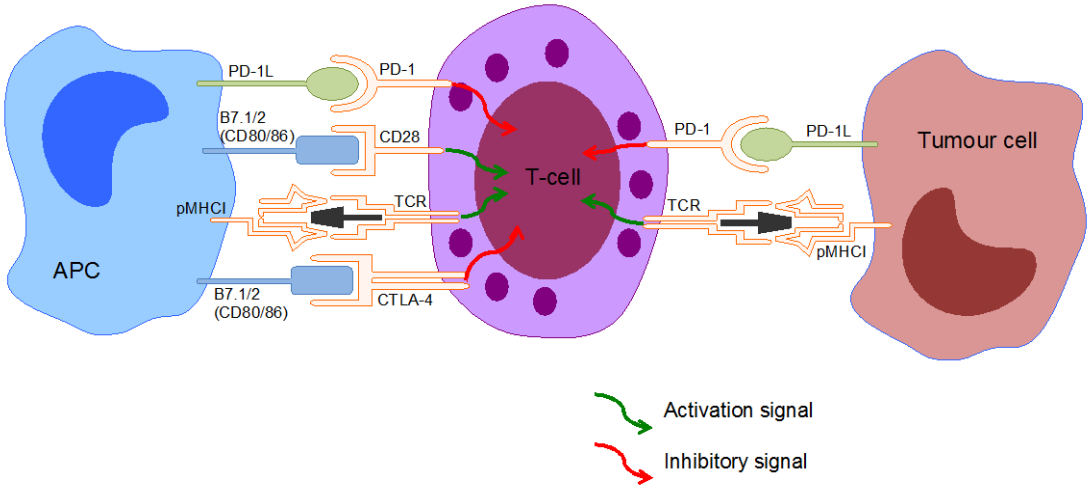

Figure 1.8: Co-stimulatory and Co-inhibitory Pathways in T-cell Activation. Additionally to the TCR/pMHCI/CD8 interaction, the T-cell receives signals from other concurrent molecular interactions with the APC (professional APC or tumour). These interactions may be stimulatory or inhibitory. Early co-signals provided by the APC are stimulatory, and necessary for complete activation. Inhibitory signals are necessary to damp down and control the T-cell response. Tumour cells may hijack these pathways in order to evade the immune system.

1.4 T-cell Activation

1.4.1 Activated Antigen-specific T-cells

Upon activation, the naïve T-cells become activated antigen-specific T-cells. Naive T-cells become committed to clonal expansion within 2-14 hours of antigen exposure, and are committed to expansion and differentiation without the need for further antigenic stimulation (van Stipdonk et al., 2001). This is thought to alleviate the need for prolonged confinement to peripheral lymphoid tissue, releasing the effector cells to the periphery. They expand and differentiate, acquiring the abilities to kill and to produce cytokines. The expansion is rapid, with a single naïve T-cell being capable of undergoing several divisions in the first few days, giving rise to a several-thousand-fold expansion (Kaech et al., 2002, Badovinac and Harty, 2006). They also undergo phenotypic changes, expressing different cell-surface molecules, which have different roles in T-cell biology corresponding to their new differentiated function. The expanded effector cell population is heterogenous and contains both $CD4^+$ T helper (T_H) cells and cytotoxic $CD8^+$ T-cells. Because MHCI are expressed on most cells throughout the body, infected cells will present the target antigen in the context of their MHCI, and thus mark themselves for deletion by the effector $CD8^+$ T-cells. These effector T-cells are capable of producing IFN-γ, tumour necrosis factor (TNF) and IL-2, and of deleting infected cells via cytolysis.

A typical viral challenge will be cleared in a few days following this expansion, and there follows a contracture of the active effector population, with over 90% of these cells dying as the cells become exhausted. The remaining population are memory T-cells that are capable of undergoing slow divisions over the life of the host. These cells are phenotypically different again, and are able to respond rapidly in the case of a second challenge. The exact origin of the memory population is not yet fully understood. It remains uncertain whether memory T-cells arise from the effector

pool, or whether they originate via a separate lineage. Some authors have presented data which suggest that the memory pool are a daughter population, directly descended from the effector T-cells (Jacob and Baltimore, 1999), however other authors have demonstrated the reverse, outlining a 'central' memory population which differentiates separate from effector cells (Iezzi et al., 2001). The memory cells persist following the exhaustion and deletion of the effector population, and may generate a more rapid and robust response in the event of secondary challenge.

$CD8^+$ T-cell expansion is dependent on repeated antigen exposure, however the MHCI receptor required for this is ubiquitous within the host, which may be a reason why $CD8^+$ T-cell expansion is more rapid that that observed with $CD4^+$ T-cells (Kaech et al., 2002).

1.4.2 Extracellular feedback: the role of IL-2

For extracellular feedback via cytokines to occur the cytokine must be present in the extracellular fluid, however the responding cell must also have up-regulated the specific cytokine receptor. Upon T-cell activation, IL-2 is produced and secreted by the activated T-cell (Boyman and Sprent, 2012). In addition to this, T-cell activation also causes up-regulation of the alpha subunit of the IL-2 receptor, IL-2Rα, to be mobilized to the cell surface (Boyman and Sprent, 2012, Busse et al., 2010). This results in positive feedback, increased activation, and thus further amplification of the signal (Busse et al., 2010). Signals via the IL-2 receptor also result in down-regulation of the receptor, causing negative feedback (Popmihajlov and Smith, 2008). The effector population contracts and reduces, despite the antigen levels remaining high for longer periods (Mitchell et al., 2010). Effector population contraction is thought to be important to avoid excessive immunopathology during

prolonged antigenic challenge (Mitchell et al., 2010, Sheridan and Lefrancois, 2011). The extent of cell death (and the size of the initial expansion) will determine the size of the memory population (Sheridan and Lefrancois, 2011, Obar and Lefrancois, 2010).

1.4.3 The role of Tumour Necrosis Factor (TNF)

A role in memory pool formation has been suggested for the TNF receptor (TNFR) and other similar receptors (the TNFR family) and their ligands (e.g. CD27 and CD154 (CD40L)). It has been shown that CD154 knock-out mice have greatly increased $CD8^+$ effector cell death and a reduced resultant memory population (Whitmire and Ahmed, 2000). There is no effect on the initial clonal expansion suggesting that CD154 interactions may regulate memory formation by interfering with effector population contracture. Both Fas (CD95) and TNFR1 cause little effect on effector cell death, suggesting that other pathways influence apoptosis of the effector T-cells (Zimmermann et al., 1996). It is very likely that multiple mechanisms contribute and overlap causing contraction, since disruption to no single pathway has thus far been shown to inhibit Activation Induce cell death (AICD).

1.4.4 Down-regulation and the switch to memory Phenotype

It has been shown that the cytolytic activity of a common pool of effector T-cells directly affects the resultant memory cell population, namely that the more targeted cytolysis which a CD8+ T-cell has induced, the less likely it is to develop into a memory cell (Schluns and Lefrancois, 2003). This would suggest that memory

cell development is dependent not on the naive cells pre-cursor, but on the extent of granule-mediated cytolysis which the T-cell has induced (Opferman et al., 2001). It is, however, unclear whether this is a direct effect (perforin ultimately causing cytolysis of the parent cell) or indirect due to increased antigen exposure when target killing is reduced.

The role of IFN-γ in down-regulation of the effector T-cell population and in AICD regulation is even less well understood, although it has been suggested that this may be achieved by regulation of controlling the expression of death factors, death receptors, or survival receptors such as the interleukin-15 receptor (IL-15R) (Badovinac et al., 2000).

1.4.5 The Importance of T-cell memory

As has already been discussed, memory T-cells exist in low numbers following a challenge, dividing slowly, providing the host with the ability to respond more rapidly in the event of a recurrence of challenge (Sheridan and Lefrancois, 2011, Ariotti et al., 2012). Upon stimulation with specific antigen a naïve T-cell undergoes rapid and robust proliferation and differentiation (Figure 1.9). The resultant effector pool phenotype continues to respond to the challenge, however memory cells may be generated in as little as a day following antigenic stimulation (Arens and Schoenberger, 2010). It may be argued that memory is not essential to the host given that for the memory pool to exist requires the infectious agent having been encountered and successfully controlled previously. This is however taking an over-simplified view. The outcome of infectious challenge, both in terms of mortality and morbidity are very often dose-dependent. In addition, other factors such as

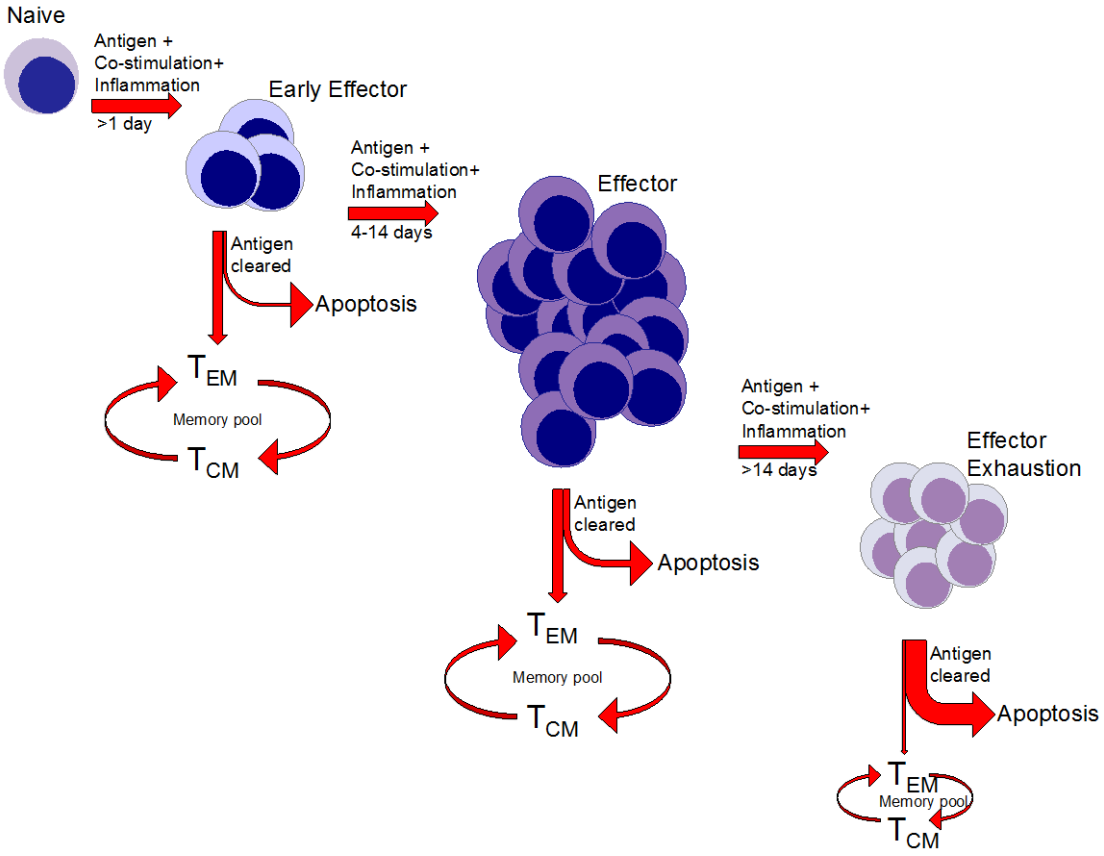

Adapted from (Arens and Schoenberger, 2010)

Figure 1.9: Upon stimulation, a naïve T-cell undergoes expansion and proliferation
On stimulation with specific antigen, the naïve T-cell undergoes proliferation and differentiation into an effector phenotype. Early clearance of the challenge (>24h) allows for generation of a memory pool. Elimination of challenge causes apoptosis of the effector pool, whilst the memory phenotype persists in the case of repeated challenge. Effector function of effector cells increases up to day 14, and then begins to tail off as the effector pool becomes exhausted. Following prolonged infection, the effector pool is unable to sustain rapid proliferation and much of this exhausted population undergoes apoptosis.

concurrent disease and/or the general health status of the host will also play an important role. In addition, prompt and effective clearance of challenge will result in a lesser degree or morbidity and so is evidently beneficial to the host. Memory $CD8^+$ T-cells demonstrate a clear survival advantage to the host when compared to naïve T-cells, especially at higher doses (Badovinac and Harty, 2006, Kaech et al., 2002). These facts are utilised for patient advantage when developing vaccination strategies, enabling us to provide immunity to patients without them having to physically encounter the disease. This fact has enabled us to provide preventative medicine for diseases with a naturally high mortality rate and to protect those who would otherwise be more susceptible e.g. infants, the elderly and the immunocompromised. In addition, vaccination of a high percentage of the population will provide so-called 'herd immunity', protecting the small percentage who cannot themselves be vaccinated with a degree of protection by reducing the endemic levels of the challenge.

Memory $CD8^+$ T-cells are phenotypically different from both naïve T-cells and effector T-cells, however they are capable of rapidly elaborating their responses in terms of cytokine production and target killing, and of robust proliferation generating a clonal expansion of secondary effector cells. These will expand, respond to challenge before and either undergo activation induced cell death (AICD) or leave a memory pool once again, in the same manner as the primary insult. The response time of the memory population is very much faster, thus the challenge is cleared more quickly. The memory T-cells are present in the periphery, meaning that the antigenic challenge may be detected by the immune system very rapidly in the target tissue, rather than be required to be presented by professional APC in accessory lymph nodes. This also means that the infection may be less severe or widespread before a response is elicited. In addition the memory T-cells tend to be

found in greater numbers in the tissues where the infectious challenge may be encountered (Ariotti et al., 2012, Mackay and Gebhardt, 2013).

1.4.6 Target Killing by $CD8^+$ T-cells

There are two main cytotoxic pathways in $CD8^+$ T-cells: Ca^{2+}-dependent perforin/Granzyme-mediated apoptosis, and Ca^{2+}-independent Fas ligand/Fas-mediated apoptosis, both of which are initiated via TCR signalling. $CD8^+$ T-cells possess excretory cytolytic granules within their cytosol. These lysosomes are comprised of an electron dense core surrounded by several vesicles, within which are stored lytic proteins in inactive form. Upon activation, these lysosomes are directed towards the cell surface by migrating along the cell's microtubular apparatus and are polarised close to the IS, where their contents may be exocytosed into the synaptic cleft (Trapani, 2012). The two proteins, perforin and granzyme, may act in cohort or alone to bring about target cell lysis (Peters et al., 1991).

1.4.7 Perforin

Perforin is stored within the lysosome as a monomer, and is released into the extracellular space as such, where it inserts into the target cells membrane. The target receptor facilitating this is currently un-identified, and it appears likely that one is not required, with perforin monomers inserting into the target membrane without the presence of any specific partner protein. Once integrated into the target cell membrane, the perforin molecules coalesce to form polymers, excluding the lipid bilayer, thus forming pores within the membrane of approximately 16 nm diameter (Podack et al., 1985). This in turn causes an uncontrolled influx of Ca^{2+},

resulting in the osmotic collapse of the cell. These pores may also act as a conduit for other killing proteins such as granzymes (Lowin et al., 1995). Bystander cells may be protected from perforin activity by the presence of proteoglycans and lipoproteins in their cell membranes (Lowin et al., 1995). In addition the release of perforin into the tightly controlled environment of the synaptic cleft may offer some protection, however it remains uncertain how the $CD8^+$ T-cell itself avoids lysis. Müller and Tschopp demonstrated evidence that The $CD8^+$ T-cell was able to block perforin entry (Muller and Tschopp, 1994), however these findings have not proven to be repeatable (Trapani, 2012).

1.4.8 Granzymes

Granzymes were first described by Jürg Tschopp in 1987 (Masson and Tschopp, 1987). Five have to date been described in man (A, B, K, H, and M), all of which can be found in $CD8^+$ T-cells (Bovenschen and Kummer, 2010, Grossman et al., 2003). Further gene loci (C, D, E, F, G L, and N) have been identified in the mouse (but not in man), however most of these (all but C) are 'orphaned'; the gene locus has been identified but the granzyme itself has not been isolated in the host (Grossman et al., 2003). Granzymes A and B have been the most studied. Granzyme A was initially thought to act extracellularly by inducing IL-6 and IL-8 production and cleaving matrix proteins (Barry and Bleackley, 2002), and whilst these remain important modes of action, more recently intracellular targets have been identified. Granzymes are capable of entering the cytoplasm in a receptor dependent fashion (receptor-mediated endocytosis), but it is likely that the main mode of entry is via pores created by perforin polymers (Catalfamo and Henkart, 2003). Heparan sulphate proteoglycans and the mannose-6-phosphate receptor have been identified as likely receptors for granzymes. They were initially first thought to be receptors

for perforin monomer insertion too (Veugelers et al., 2006), but it has since been shown that perforin inserts without receptor protein assistance. Once inside the cell, granzymes are capable of mediating apoptosis in the target cell via both caspase-dependent and caspase-independent mechanisms. Of the human granzymes, granzyme B is the most studied and is responsible for rapid induction of caspase-dependent apoptosis. Human granzyme B-mediated apoptosis is in part mediated by the target cells' mitochondria. Mitochondrial changes are induced by granzyme B by causing cleavage of the BH3-only pro-apoptotic protein, Bid. The truncated Bid migrates to the mitochondria alongside Bax and/or Bak, where it causes mitochondrial outer-membrane permeablisation and release of other pro-apoptotic proteins, including cytochrome c, which is crucial for the formation of apoptosomes and the activation of caspase-9, which in turn cleaves other caspases downstream. Granzyme B may also cleave Mcl-1, a member of the anti-apoptotic family Bcl-2, which in turn also causes cytochrome c release. Other caspases such as effector caspase 3 and initiator caspase 8 are also processed by granzyme B. Several other granzyme B substrates have been reported, however these interactions have not been as rigorously tested.

Other granzymes have been less well studied. Granzymes H and K are so-called 'orphan-granzymes', owing to the fact that their substrate is as yet unidentified (Bots and Medema, 2006), although some authors have hinted that their mode of action is caspase independent and similar to that of granzyme A (Johnson et al., 2003). Granzyme M-induced cell death is rapid and independent of both caspase and the mitochondria (Kelly et al., 2004). It induces large vacuole formation within the target cells which may be suggestive of induced autophagy, although the exact mechanism is still unclear (Bots and Medema, 2006).

1.4.9 Fas-mediated cytotoxicity:

Target cells express on their surface Fas molecules, which is also known as CD95 or Apo-1. Fas is a member of the TNFR superfamily, and is expressed in a variety of different cell types, both immune and non-immune. It possesses an intracellular 'death' domain, which can initiate caspase-dependent apoptosis upon binding to its ligand (Chinnaiyan et al., 1995, Cleveland and Ihle, 1995, Accapezzato et al., 2005). TCR signaling induces up-regulation of Fas ligand (CD95L) to the cell surface in a Ca^{2+}-independent manner (Waring and Mullbacher, 1999). These molecules are enriched in lipid rafts, thus are recruited to the immunological synapse during TCR/ pMHCI complex formation and are held in tight junction with the target cell allowing for Fas activation. Fas ligand is also expressed within the endocytosed cytolytic granules (He et al., 2010, He and Ostergaard, 2007). Fas-mediated apoptosis may also be involved in homeostasis and cell proliferation among other populations (Cleveland and Ihle, 1995).

1.5 Development of T-cells

1.5.1 Thymic development of T-cells

In order to provide protection against all possible pathogens that a host may encounter in its lifetime the T-cell repertoire is required to be as diverse as possible. In addition it must remain unresponsive to normal healthy self-tissue and retain a robust response to dysregulated self. To this end T-cells are developed and then undergo a rigorous selection and maturation process in the thymus during development, from which less than 5% emerge. Lymphoid progenitors develop from stem cells in the bone marrow and migrate to the thymus. They begin their maturation in the sub-capsular cortex, migrating deeper into the medulla as they

mature into thymocytes (Figure 1.10). Initial maturation into functional T-cells is antigen-independent. First they develop their specific T-cell cell-surface markers such as the TCR, CD3, CD4, CD8, and CD2. Initially, the immature cells begin to express CD2, followed by the adhesion molecule, CD44. At this stage they have not yet re-arranged their TCR genes, nor do they express other phenotypic cell surface molecules and are $CD4^-$ $CD8^-$ double negative, or DN1. DN2 cells then express CD25-Rα and begin to re-arrange the ß chain of the TCR genes. Once productive re-arrangement of the ß chain has occurred, this is expressed, alongside the CD3 molecule, with a surrogate α-chain, pTα. Signalling via this receptor causes the cessation of ß-chain re-arrangement and a brief period of proliferation. During this proliferative period, the cells become $CD4^+$ $CD8^+$ double positive (DP) and lose their cell surface CD25. They re-express RAG-1 and RAG-2 in order to re-arrange the α-chain, which will continue until the cell either undergoes positive selection, or dies. The DP TCR^+ thymocytes have now migrated to the cortico-medullary junction, where they undergo positive and negative selection. Cells that are unable to recognise self-MHC within 3-4 days remain in the thymic cortex and die by neglect. The positively selected DP thymocytes migrate to the medulla where they undergo negative selection. APCs presenting self-peptide in the context of either MHCI or MHCII interact with the DP thymocytes; those that recognise self-antigen strongly receive a strong signal for apoptosis, thus are selected for deletion. The co-receptor molecules are essential at this stage, and once a T-cell has recognised either MHCI or MHCII, the DP thymocyte is then committed to become either $CD4^+$ or $CD8^+$, and the redundant co-receptor is then lost. In the absence of either co-receptor, the resultant T-cell repertoire is skewed in favour of the other T-cell phenotype, and if both are absent thymic selection results in T-cells that recognise non-MHC ligands

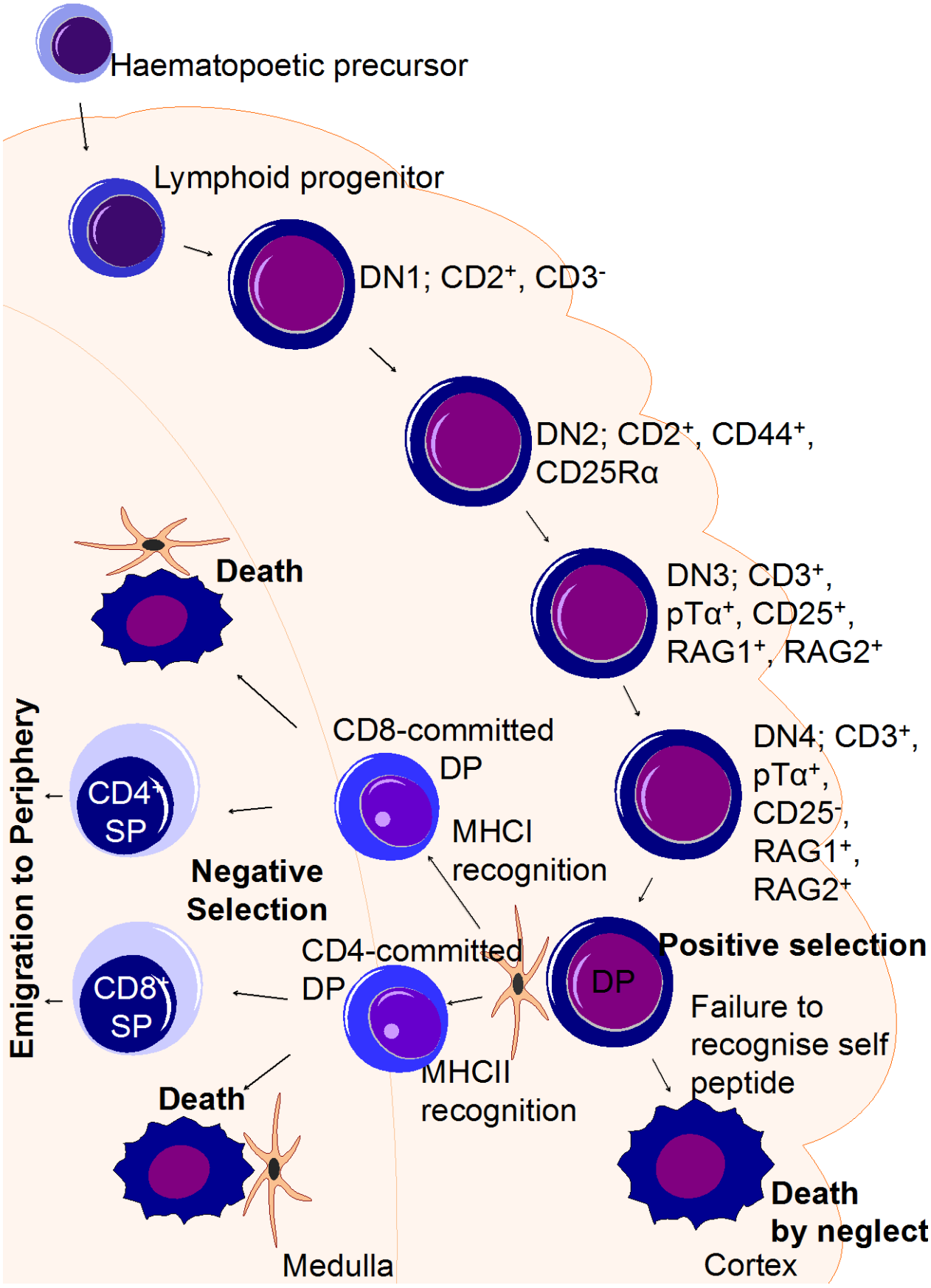
Haematopoetic precursor
Lymphoid progenitor
DN1; CD2+, CD3-
DN2; CD2+, CD44+, CD25Rα
DN3; CD3+, pTα+, CD25+, RAG1+, RAG2+
DN4; CD3+, pTα+, CD25-, RAG1+, RAG2+
Positive selection
DP
Failure to recognise self peptide
Death by neglect
Cortex
MHCII recognition
CD4-committed DP
CD4+ SP
CD8+ SP
Death
Medulla
MHCI recognition
CD8-committed DP
Negative Selection
Death
Emigration to Periphery

Figure 1.10: Thymic Ontogeny
Double negative (DN) thymocytes progress through four distinctly separate phenotypes in the thymic cortex. They undergo RAG (recombination-activating gene) re-arrangement of the TCR ß-chain and generate a preTCR with pre-α-chain (pTα) in order to undergo expansion. The α-chain is then re-arranged by a similar process. The immature double positive (DP) thymocytes that fail to recognise self-MHC die by neglect. MHC-restriction is imposed at this stage. The co-receptor committed thymocytes migrate to the medulla, where those that recognise MHC too strongly are marked for deletion. The single positive (SP) thymocytes migrate to the periphery where they circulate as naïve T-cells.

(Van Laethem et al., 2007, Trobridge et al., 2001). It should be noted that both positive and negative selection are directed under self-antigen. Positive selection ensures that self-MHC are recognised, negative selection ensures that self-recognition is not strong enough to trigger autoimmunity. No pathogenic antigen has been encountered, relying on the promiscuity of the TCR to recognise foreign peptides with much greater affinity.

1.5.2 VDJ Rearrangement

The TCR repertoire is highly diverse. Unlike MHC, this is achieved by recombination, rather than polymorphism, however, in contrast to antibody generation, there is no somatic hypermutation. This allows the selection of appropriate and robust TCRs during thymic selection. This process is ligand-independent and thus the selection process in the thymus is essential to ensure only appropriate (neither auto-reactive, nor non-functional) TCRs enter the periphery. Only around 5% of those TCRs originally generated recognise self-MHC at an appropriate level and are matured following positive and negative selection in the thymus. In order to achieve this huge range of potential TCRs, known as the primary repertoire, from which the final repertoire is selected, the thymocytes undergo a series of re-arrangement events of the α and ß chains of the TCR. This 'somatic recombination' of the Variable (V), Diversity (D, only present in some loci), and Joining (J), gene segments, known as VDJ recombination, are mediated by VDJ recombinase enzymes such as Recombinase Activating Genes 1 and 2 (RAG1 and RAG2) (Schatz and Ji, 2011). The enzymes cleave and recombine the V, D and J segments at specific sites, where the double stranded DNA is repaired by the enzyme DNA-dependent protein kinase complex (DNA-PK), before recruiting a further enzyme, terminal deoxynucleotidal transferase (TDT). This enzyme then randomly adds nucleotides to the DNA ends,

giving rise to junctional and thus TCR diversity. This process is summarised in Table 1.2 and Figure 1.11.

As has previously been discussed, the ß-chain is first re-arranged. The newly re-arranged ß-chain is expressed with the pre-existing α-chain, which acts as a surrogate α-chain in order to form the pre-T receptor (pTα). This allows for activation through the pTα, which causes the ß-rearrangement to stop once a viable chain has been produced, and instigating proliferation before α-chain re-arrangement, which occurs in a similar manner. There is no signal to stop α-chain re-arrangement, rather if recognition of self-MHC has not happened within 3-4 days, death by neglect occurs.

Whilst most TCR chain transcripts arise from fully rearranged gene loci, some germ line transcripts have been identified (Abbey and O'Neill, 2008).

V(D)J recombination is essential for the development of the adaptive immune system in most vertebrate hosts, and gives rise to an extraordinarily diverse array of antigen receptors. It must be noted that occasional genome instability and lymphoid malignancies can arise.

1.5.3 T-cell Maturation

Around 5% of the initial lymphoid progenitor cells emerge as single positive (SP) thymocytes having successfully undergone positive and negative selection. In order to achieve functional competency they must still undergo a final stage of T-cell maturation; a series of steps is required in order for them to be competent naïve T-cells capable of participating in an immune response.

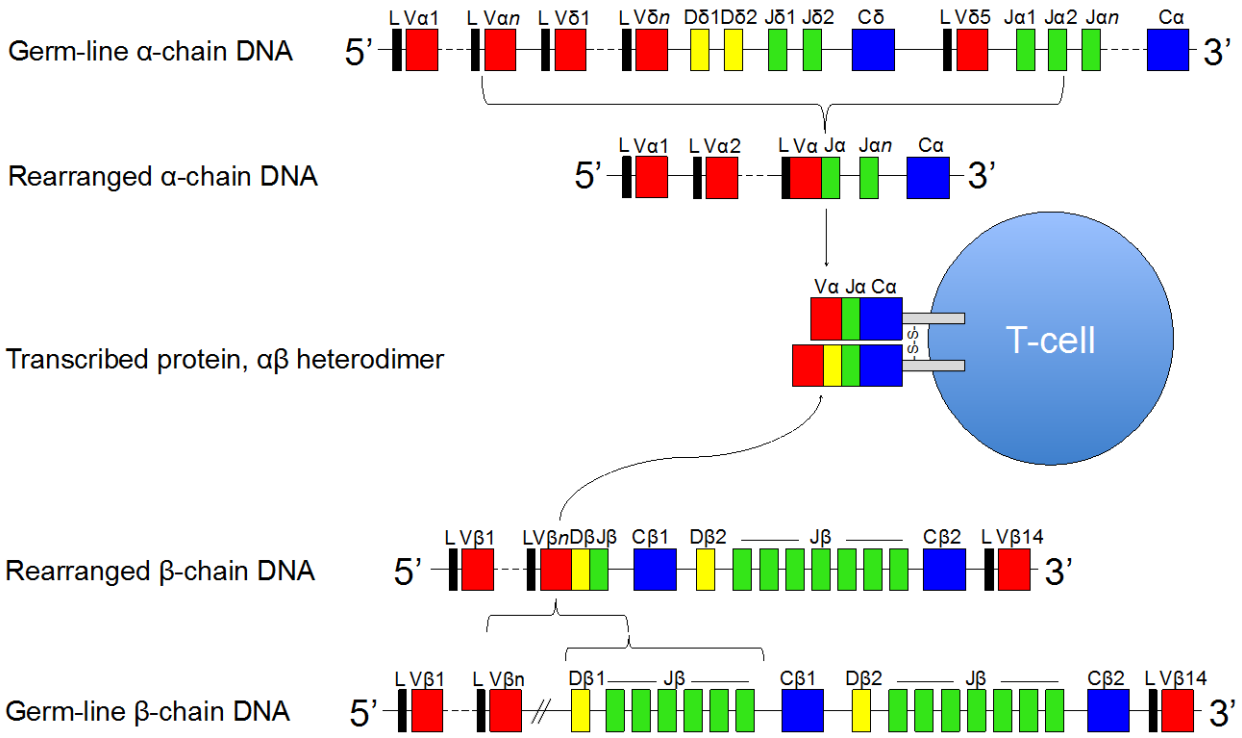

Figure 1.11: V(D)J re-arrangement of TCR α and ß loci to generate novel TCR

The ß-chain is re-arranged first during thymic generation. Firstly the Dß1 may combine with one of six Jß, or Dß2 may combine with one of seven Jß. The DJ is then re-combined with a Vß. The resultant locus is transcribed from the leader sequence (L) and any additional material is spliced out, giving rise to an mRNA transcript, L $V_ßD_ßJ_ßC_ß$. Splicing out is under the enzymes RAG1 and RAG2, and the repair is by DNA-PK and TDT. A preTCR, pTα, is expressed through pairing with the germ line ß-chain. Stimulation through the pTα initiates thymocyte expansion prior to α-chain rearrangement.

Stage	Process	Features
1	Synapsis	Binding the enzyme to the conserved sequences
2	Cutting	Precise double-stranded breaks at the nucleotide preceding and following the recognition sequences
3	Trimming	Nucleotide deletions from the coding regions
4	Addition	Nucleotide insertions
5	Repair	Polymerisation
6	Joining	Ligation

Table 1.2: The stages of the V(D)J recombination reaction

Firstly, they must be capable of proliferation and expansion when antigen stimulated through the TCR. 'Semi-mature' lymphocytes are still susceptible to programmed apoptosis when stimulated through the TCR (Kishimoto and Sprent, 1997). MHCI up-regulation by these cells has been shown to be a useful indicator of competency to divide (Hogquist et al., 2015). Down-regulation of CD69 and up-regulation of CD62L and S1P1 is seen with tissue egress, and by this stage the maturing thymocytes are acquiring resistance to death receptor signalling. Thymic egress is noted after approximately 4 days of maturation in the medulla, and is via the blood vessels rather than lymphatics, although why this should be so remains uncertain.

Once in the periphery, the thymocytes gain the ability to produce cytokines, and may respond to antigen presented by APCs as mature naïve T-cells. Naïve T-cells are thought to survive and persist owing to weak stimulation via contact with self-ligands presented in the context of MHC, and by anti-apoptotic signals from low levels of the cytokine IL-7 (Surh and Sprent, 2008, Kishimoto and Sprent, 1997). This weak stimulation of the TCR by self-peptides may also enhance sensitivity to foreign antigens.

1.6 Cancer Immunology

1.6.1 Cancer Immunology Overview

Despite improved understanding and earlier detection of pathology, cancer remains a massive global health issue, and a leading cause of death worldwide. With many cancers remaining refractory to traditional treatment approaches, and world-wide cancer mortalities increasing by several million each year, researchers have

increasingly looked for novel approaches to treatment, including harnessing and/or augmenting the natural ability of the immune system to target cancer.

Cancer immunotherapy has yielded many positive results for patients with late stage cancers, traditionally considered to be untreatable. The expanded T-cell may be infused back into the patient in high numbers following *ex vivo* expansion in a process called Adoptive Cell Transfer (ACT). In addition to this, greater understanding in the field of cancer immunology has enabled us as researchers and clinicians to better understand to pathology and behaviour of tumours, and the ways in which they evade the immune system, and in doing so devise novel ways of treating them and/or optimising our treatments.

1.6.2 T-cells and Cancer

$CD8^+$ T-cells have a pivotal role in anti-tumour immunity. $CD8^+$ T-cells recognise and target infected and dysregulated cells for deletion, indeed this is a key role of the immune system, thus cancer itself may be considered to be a disease resulting from failure of the immune system to do so (Swann and Smyth, 2007, Finn, 2012). $CD8^+$ T-cells do exist which recognise cancer antigens, however cancer is observed and persists in the host (Topalian et al., 1987, Kawakami et al., 1994, Hicklin et al., 1999, Jager et al., 1998). Researchers have recognised the potential power of the cytotoxic $CD8^+$ T-cell to eliminate cancer for many years, yet in order to harness this power for the benefit of the host, one must first appreciate reasons why the immune system may have initially failed to clear this disease.

Firstly, we must consider the possibility that the cancer we observe in the host is the cancer that has already evaded the immune system. It is possible, indeed likely, that many cancers are recognised and eliminated by the immune system before they

reach a level that is detectable in the host. Anti-cancer T-cells are identified in individuals with no previous history of cancer (Vella et al., 2009, Boon and van der Bruggen, 1996), and many cancers are observed at increased rates in immunocompromised patients (Kubica and Brewer, 2012, Schulz, 2009), although it is recognised that there are multiple reasons as to why this should be so.

Demonstrably, cancers do successfully evade the immune system, persist, and become deleterious to the host, and researchers have devoted much time to understanding why this should be so; if one could create an environment where the immune system had the greater advantage, then the prognosis is likely to be more favourable. It is well recognised that established tumours employ multiple strategies in order to evade the immune system (Costello et al., 1999, Igney and Krammer, 2002, Topfer et al., 2011, Seliger, 2005). Tumours are capable of down-regulating MHCI, thus reducing the available target ligands that may be recognised by anti-cancer T-cells, and also of creating a hostile microenvironment, which inhibits, discourages, or fails to provide help to these cells. Not only are tumour cells and the surrounding environment abnormal, but the bloods vessels which supply tumours are too; they may grow abnormally, flow abnormally, or even change direction of flow readily, thus normal mechanisms by which T-cells which are potentially protective to the host are cut off once the tumour is established. The larger and more established the tumour becomes, the more alien and hostile the microenvironment within, and thus the more difficult it becomes for the immune system to infiltrate, thus traditionally oncologists have considered early recognition, intervention and treatment to be the key to treating cancer. However many cancer immunologists believe that harnessing the power of the $CD8^+$ T-cell and other anti-cancer immune response could hold the key to future cancer therapies.

1.6.3 Tumour Immune Surveillance

There exists strong supporting evidence that the immune system plays a pivotal role in controlling neoplastic processes in the host. Cancer exists in immunocompetant hosts, suggesting a failure of immune surveillance. The immune system may act to control and shape the tumours behaviour, for example by targeting and deleting cells which break free from the tumour, thus delaying the spread of malignancy.

T-cells are likely to have a key role in tumour immune surveillance. RAG deficient mice, which lack both B- and T-cells, and NK cells, have been used in models to demonstrate the importance of these populations. It has been demonstrated that mice lacking IFNγ, IFNγ receptors, and perforin fail to suppress malignancies (Kaplan et al., 1998, Shankaran et al., 2001, Smyth et al., 2000, Street et al., 2002). Increased rates of cancer have been reported in human hosts with either congenital or acquired immunodeficiency (Penn and Starzl, 1973, Mayor et al., 2017, Chapman et al., 2013, Boshoff and Weiss, 2002). This is particularly true of viral-driven malignancies.

Additionally, it has been demonstrated that tumours derived from immunocompromised hosts are of increased immunogenicity, even when transplanted into an immunocompetant host, suggesting that the immune system plays a role in shaping the behaviour of the tumour (Kaplan et al., 1998).

The 'immunoediting' hypothesis was first suggested in 2002 (Dunn et al., 2002), and described 3 possible outcomes for the cancer host; elimination of the tumour, the establishment of equilibrium between the tumour and the host's immune system, and tumour escape from immune control (Arum et al., 2010). In a malignant process, these three stages are progressive; initially the host's immune system is capable of identifying, targeting and deleting neoplastic cells, however this

progresses to a state of equilibrium where growth is contained however the cancer cells are not fully eliminated. During this phase, however, the malignant cells undergo changes in gene expression and mutations, possibly due to the mounting selectional pressure from the immune response, and are increasingly able to evade the immune response. This results in uncontrolled proliferation of the malignancy, or immune escape.

1.6.4 Immune Evasion and Tumour Escape

Cancer cells employ numerous mechanisms to evade the immune system. Broadly, these involve evading recognition by the immune system, induction of immune tolerance, or resistance to cytotoxic mechanisms employed by the immune system. The tumour antigen self may be lost or expression reduced, therefore this is less available in the cytosol for proteasomic degradation and so loading and expression in the context of MHCI (Yee and Greenberg, 2002). The intracellular machinery required for antigen processing and presentation (the proteasome, tapesin and TAP, MHCI and ß2M) may be compromised in cancer cells, resulting in failure of antigen expression at the surface of the cell (Tertipis et al., 2015, Bicknell et al., 1994, Bubenik, 2004). Proteasome aberrations result in a lack of peptide for loading and presentation. TAP deficits disallow peptide entry to the ER. MHCI are unable to exist without ß2M.

Tumour cells may release cytokines which can induce T-cell death, or disrupt the T-cell's signalling pathways e.g. chemokine ligand 12 (CXCLI2), Transforming growth factor ß (TGFß), IL-10, receptor binding cancer antigen (RCAS1). CXCL12 promotes neovascularisation and is associated with a poor prognosis (Salmaggi et al., 2004). In the early phase of immunosurveillance and pre-malignancy, TGFß is suppressive of

the tumour, anti-inflammatory and promotes homeostasis, however once the tumour has entered the malignant and proliferative stage the tumour's TGFß signalling pathways become inactive. Now, paradoxically, TGFß actively aids in tumour spread and growth, and facilities metastasis (Massague, 2008, Jakowlew, 2006).

Additionally, the tumour may protect itself from apoptosis by the up-regulation of a mutated form of FasL, which inhibits this pathway, or molecules such as FLICE (FADD-like interleukin-1ß-converting enzyme)-like inhibitory protein (FLIP), and protein inhibitor-9 (PI9), which can protect from granzyme degradation and promote resistance to death receptors (Kataoka et al., 1998, Hahne et al., 1996, Soriano et al., 2012).

Tumours can up-regulate PD-L1, thus utilising the T-cells own inhibitory mechanisms to dampen down the T-cell response (Juneja et al., 2017). It has been shown that high levels of PD-L1 are associated with a less favourable outcome for the host (Zhao et al., 2017). If the tumour possesses professional APC properties, it can also down-regulate B7.1 and B7.2 expression on the tumour surface can be reduced or absent, resulting in T-cell anergy (de Charette et al., 2016) (Figure 1.8).

Indeolamine 2,3 dioxygenase (IDO, INDO) can be overproduced by tumour cells, or by local DCs, which can the activity of $CD8^+$ T-cells and promote the activity of T_{regs} (Uyttenhove et al., 2003, Moon et al., 2015).

DCs in the draining lymph nodes can be incompletely activated, thus inducing tolerance rather than robust activation of $CD8^+$ T-cells (Cuenca et al., 2003).

1.6.5 Cancer Immunotherapy

Cancer immunotherapy is the use of the host's own immune system to treat cancer. Strategies act to counter ways in which the cancer cells evade and edit the immune system, or exploit the cell surface molecules expressed by cancer cells that may be recognised by the immune system. Broadly, strategies may be divided into active or passive approaches. Active approaches either prime the host's own immune system to target the cancer cells (e.g. cancer vaccines), or involve the infusion of immune cells into the patient which will target the cancer (Adoptive cell transfer, ACT). The other approach aims to target the mechanisms employed by the tumour to evade the existing immune response with the use of antibodies or cytokines.

Several monoclonal antibodies (mAb) are currently in therapeutic use for the treatment of both solid and haematological tumours, with many more currently under development or trial (Corraliza-Gorjon et al., 2017).

Pro-inflammatory cytokines have been successfully used to treat cancer. Currently in use are IL-2 and IFNs (Antony and Dudek, 2010, Parker et al., 2016). Down-regulation of MHCI by the tumour has the effect that T-cells fail to recognise the tumour, thus effectively rendering the adoptive arm of the immune system ineffective. Innate NK cells are still able to target the tumour, however in the absence of MHC they become anergic. Pro-inflammatory cytokines have been demonstrated to be effective at rescuing this response (Ardolino et al., 2014, Ardolino et al., 2015).

1.6.6 Monoclonal Antibody Therapy

Antibodies have long been considered a possible therapeutic agent, and the creation of the first hybridoma in 1975 has facilitated the manufacture of mAbs. The first mAbs were murine in origin and therefore immunogenic, however as technologies advanced, chimaeric, humanised and then fully human mAbs were created. mAbs may trigger cytotoxic destruction of tumour cells by NKs (antibody-dependant cell-cytotoxicity (ADCC)), phagocytosis of tumour cells by macrophages (antibody-dependant cell-phagocytosis (ADCP)), facilitate complement targeting of the tumour (complement-dependent cytotoxicity (CDC)), block ligands and receptors at the tumour cell surface, or bind tumour antigens to induce apoptosis.

Most mAbs target immune checkpoints rather than the tumour itself, acting to arrest the tumours immune evasion mechanisms, thus re-programming and rescuing the immune system's anti-tumour response.

There are currently over 50 mAbs in therapeutic use (Ayyar et al., 2016), with 20 specifically licensed for solid tumours, 13 for haematological tumours (correct as of 2017 (Corraliza-Gorjon et al., 2017)). Many are bi-specific or multi-specific, listed as targeting 21 different antigens (Corraliza-Gorjon et al., 2017). Many more are under development or currently in therapeutic trials (Corraliza-Gorjon et al., 2017, Ayyar et al., 2016). Currently there is a large focus upon modulating immune function and redirecting T-cell responses. mAbs targeting the B7-CD28 superfamilies have proven to be extremely effective at reducing the tumours ability to evade the host's T-cells (Ni and Dong, 2017, Corraliza-Gorjon et al., 2017, Assal et al., 2015). Blockade of the PD-1 or PD-L1 interaction, which is frequently utilised by the tumour to limit the host T-cell response, has yielded positive results, at least in the short term, for several aggressive and metastatic cancers (Balar and Weber, 2017, Sunshine and Taube, 2015, Homet Moreno and Ribas, 2015, Mahoney et al., 2015, Wang and Wu,

2017, Ni and Dong, 2017). Another molecule successfully targeted is CTLA-4 (Assal et al., 2015, Mocellin and Nitti, 2013, Wolchok and Saenger, 2008).

As with many anti-cancer treatments, the tumour can become resistant to therapy (Wang and Wu, 2017, Sharma et al., 2017), and side-effects have been reported (Wolchok and Saenger, 2008, Naidoo et al., 2015, Naidoo et al., 2016, Kahler et al., 2016, Baldo, 2013), however overall the response to such therapies, particularly in late stage disease which has traditionally considered to be refractory to treatment has been extremely encouraging, and further B7-CD28 superfamily targets are currently under trial (Assal et al., 2015).

1.6.7 Adoptive Cell Transfer and Gene Therapy

ACT involves the expansion of anti-tumour cell populations, and the re-infusion back into the patient. Expansions may be of directly *ex vivo* cells, or cells which have been modified in some way to improve their efficacy. Modifications may be the creation of a chimaeric antigen receptor (CAR) in order to introduce a *de novo* receptor. Usually this is created using the internal machinery from an existing receptor of the cell, fused with the external receptor to a desired ligand, thus the resulting receptor is fused of two parts (chimaera). Alternatively, the cells own receptors can be modified in order to enhance the cell's response; these are said to be 'engager-modified'.

Different immune cell populations have been considered for ACT cancer therapies, however, the focus of this thesis is $CD8^+$ T-cells, and so these approaches will be discussed in greater depth.

NK cells are part of the innate response, and are considered to be the host's 'first line of defence' against cancer. Mixed results have been reported, with earliest trials eliciting disappointing responses, however improvements have been seen in recent studies (Davis et al., 2015, Rezvani and Rouce, 2015, Besser et al., 2013).

Most other approaches have utilised lymphocytes, mostly T-cell, however B-cell ACT has also been trialled (Besser, 2013). B-cells may act as APCs, Ab producing cells, and as immune effectors cells, so have their place in cancer treatment where they can augment the T-cell response, or directly target the cancer.

Tumour infiltrating lymphocytes (TILs) have also been used for ACT (Goff et al., 2010, Kvistborg et al., 2012, Rosenberg et al., 1986, Topalian et al., 1987). TILs are derived from solid tumours, and comprise of a mixed cell population; all lymphocytes found in the tumour – $CD8^+$, $CD4^+$, B-cells and γδ T-cells. Owing to the nature of the acquisition of these cells, one cannot be certain which target the cancer, provide help, are incidental, or may even hinder the response, and it is also possible that some important populations are 'grown out' or lost in the expansion process, however extremely positive responses have been reported in some trials, with some patients achieving lengthy remissions (Geukes Foppen et al., 2015). Additionally, this sampling technique has been used to then prime and select clones for expansion, or to select TCRs for gene transfer. Owing to the nature of the techniques required for this, i.e. the use of a whole solid tumour from which to obtain the TILs, target cancers are limited to those which may be easily biopsied, with skin cancers such as melanoma being ideal candidates. TILs were one of the first conceived ACTs to treat cancer, with a murine model being pioneered in 1986 (Rosenberg et al., 1986). Clinical trials using this technique had begun the following year (Topalian et al., 1987, Rosenberg et al., 1988).

Many ACT therapies for cancer utilises the cytotoxic properties of $CD8^+$ T-cells to directly target the tumour cells. Initial trials using a clonally expanded population of T-cells that recognise anti-cancer antigens showed were encouraging. Remission (partial or complete) rates of 50% or more have been reported for metastatic melanoma patients (Besser et al., 2010, Dudley et al., 2008, Khammari et al., 2009). Increasingly, genetically modified T-cells have been considered. Strategies utilised include the creation of CARs in order to target ligands not naturally recognised by T-cells (Bridgeman et al., 2010b). CARs are created by the hinging of a single chain variable fragment (scFv) specific for the antigen of choice, to the cytoplasmic elements of either CD3 or CD28, thus linking the specificity of the antibody from the scFv is derived to the signalling machinery of the cell. The scFv is a fusion protein, created of the variable heavy (V_H) and light (V_L) of the specific immunoglobulin (Ig). The removal of the constant regions maintains the specificity of the Ig, whilst generating a small protein for the extracellular part of the CAR. An example of this is the creation of a CAR recognising CD19, thus targeting B-cells, which has been successfully used to treat lymphoma (Klebanoff et al., 2014, Ramos et al., 2014, Lipowska-Bhalla et al., 2012).

Another modification strategy employed to enhance ACT is to enhance of the TCR for the cancer ligand. It has already been discussed that the affinity with which some anti-cancer TCRs recognise tumour antigen may be sub-optimal, thus the resulting antigen-specific T-cell response to the tumour can be less than adequate, therefore efforts to enhance the TCR/pMHCI interaction be beneficial to the patient. It has been discussed that some cancer antigens are of a not dissimilar order to some pathogenic TCRs, however it has been suggested that the 'ideal' affinity for TCR/ pMHCI interactions is 10 μM (Zhong et al., 2013). Few anti-cancer TCRs of this affinity are recorded, with most falling short, thus scope for enhancement exists, and TCR gene therapy is increasingly important.

Recently, media attention has been given to reports of the use of donor T-cells to treat two babies with acute and refractory leukaemia. The T-cells in question were described as 'off the shelf', for use in un-matched donors, and had been gene-edited using TALENs, and engineered to express CARs. The initial research appears to be flawed, in that the patients had also received chemotherapy, however, this may represent a new strategy in the future (Qasim et al., 2017).

1.6.8 Principles of TCR Gene Therapy

An effective anti-cancer TCR should maintains its specificity for the tumour, recognise the target with sufficient affinity to initiate a robust response against the target cell. The T-cell itself must be capable of evading the tumours inherent suppression mechanisms, countering the tumour's immune editing and reversing the immune tolerance of the tumour that occurs in the metastatic patient. The TCR itself should be specific to the tumour antigen, without promiscuous recognition of autoreactive or allo-antigens, thus rigorous screening of the TCR is required to avoid auto- and allo-reactivity, which could be deleterious to the patient. Ideal antigens are tumour-specific and expressed only on the tumour such as onco-antigens, mutated antigens or neo-antigens, or related to viruses that may drive some tumour.

Using multimer technology, T-cells that recognise known onco-antigens may be isolated from *ex vivo* PBMC for clonal expansion (Wooldridge et al., 2009), whereupon their ability to lyse target cells either pulsed targets, or tumour lines) can be tested *in vitro*. Following identification of a high-affinity clone, the TCR can be clonotyped, the α- and ß-chain sequenced, and cloned into a retroviral vector, enabling the manufacture of retroviral particles for transduction into T-cells.

Mutations to enhance the affinity of the TCR for the pMHCI can be introduced for testing (Robbins et al., 2008). As has been previously stated, the ideal affinity for these TCRs has been suggested as around 10 μM. Above this affinity, further increase has minimal effect on the avidity of the T-cell. It has also been demonstrated that very high affinity TCRs recognise the TCR contribution to the TCR binding platform such that the peptide presented becomes less relevant, and autoreactivity ensues
(Cole et al., 2014).

Retroviral particles can only infect actively dividing cells, thus *ex vivo* T-cells must be induced to proliferate with the use of Dynabeads™, which induce T-cell proliferation by providing signals 1 and 2 with anti-CD3 and anti-CD28 antibodies (Brimnes et al., 2012). T-cells can then be enriched for the transduced populations for rigorous testing, before they can be considered for adoptive transfer (Tan et al., 2015). Testing involves testing the efficacy of the transduced lines; response to targets and if possible tumour lines, and for antigen-driven proliferation, and also for autoreactivity and alloreactivity with the use of combinatorial peptide library screening (Wooldridge et al., 2012).

1.6.9 The lentiviral Vector Gene Delivery System

Lentiviridae are members of the family Retroviridae, characterised by a long incubation period ('lenti', Latin for 'slow'). Examples of such are Human Immunodeficiency Virus (HIV) and Feline Immunodeficiency Virus (FIV). Retroviruses are capable of inserting viral DNA (or RNA) into the host cell DNA in significant quantities, and replicating themselves by utilising the replication system of the host cell. However lentiviridae are unique amongst retroviridae in that they can infect non-dividing (quiescent) cells. For this reason lentiviral vectors (LVs) are commonly

used tools in research for Gene Transfer (GT) (Klimatcheva et al., 1999). In addition, they have been widely used in clinical trials (196 trials at the time of publishing, 7.5% of trialled systems) (ABEDIA, 2017) (Figure 1.12). LVs may stably integrate expression vector inserts into host DNA; expression is prolonged and phenotype is maintained (Wanisch and Yanez-Munoz, 2009). They are also relatively well tolerated and of lower toxicity compared to other delivery systems, and may be utilised to deliver up to 8kb of transgenic DNA (Matrai et al., 2010).

Earlier LV delivery systems have the potential to revert to pathogenic retrovirus (Klimatcheva et al., 1999, Matrai et al., 2010). In order to overcome this, the lentiviral system utilised in this thesis is a replication-deficient HIV-1 derivative, grown in human embryonic kidney (HEK293T) packaging cells, with four distinct 3rd generation lentiviral plasmids; a transfer plasmid, two packaging plasmids and an envelope plasmid. These plasmids contain genes encoding only the relevant structural proteins, and the enzymes involved in lentiviral infection and DNA integration of the host; *pol*, *gag*, and *rev*. These enzymes are separately expressed by two different packaging plasmids, thus increasing the safety of the system by vastly increasing the number of random recombination/mutation events required to revert to a wild type virus. Of these essential viral genes, pol encodes for reverse transcriptase and other essential translation enzymes, gag encodes the capsid, and rev encodes a structural protein that serves to bind the viral mRNA, facilitating export from the nucleus and thus protein transcription.

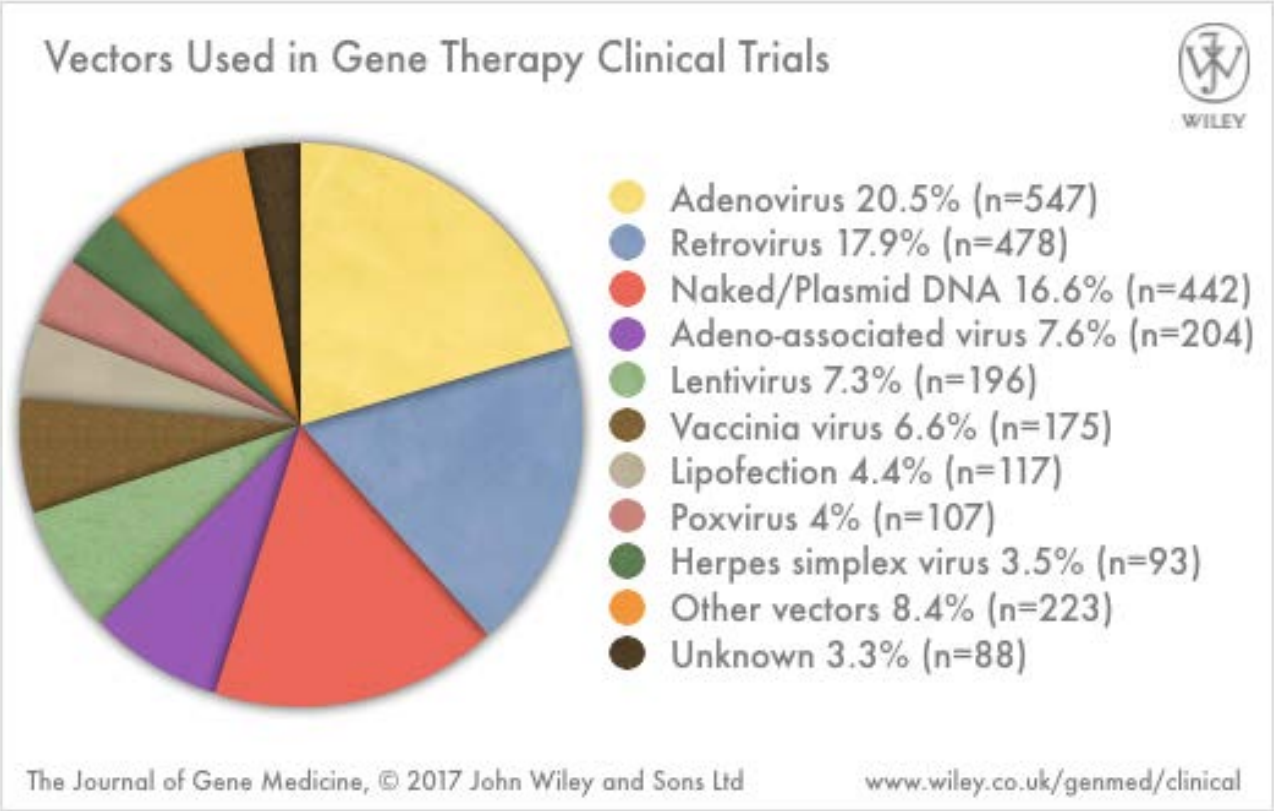

Figure 1.12: Viral vectors used in clinical trials
Taken from the Gene Therapy Clinical Trials Database (ABEDIA, 2017).

1.6.10 Lentiviral Plasmids

The lentiviral expression vector: Transgene expression is mediated by elongation factor-1α (EF-1α). The virion particles contain DNA encoding only for the designated transgene, and the ψ packaging signal, preceded by the primer binding site (PBS), where reverse transcription starts. Long terminal repeat sequences (LTR) are found at either end of the genes encoding for lentiviral function (3' and 5' LTRs). In order to enhance safety and reduce the potential for insertional mutagenesis, these have been mutated to an alternate open reading frame (ORF), and mutations inserted to eliminate endogenous enhancer activity of the transfer vector. In addition to the transgene and the ψ sequence (lentiviral machinery), the vector also incorporates the Woodchuck hepatitis virus (WHV) post-transcriptional regulatory element
(WPRE) and the central polypurine tract (cPPT) (Barry et al., 2001). The WPRE is situated immediately downstream of the transgene and acts to enhance expression (Higashimoto et al., 2007, Schambach et al., 2006). The cPPT acts to enhance transduction by enhancing nuclear import, thus facilitating better insertion (Van Maele et al., 2003). The *rev* response element (RRE) binds the mRNA, promoting nuclear export and translation (Barry et al., 2001).

The lentiviral packaging plasmids The *rev* enzyme is encoded in a separate plasmid, pRSVrev. This enzyme is derived from respiratory syncytiovirus (RSV) rather than HIV in order to further enhance the safety of the system. The other two enzymes necessary for lentiviral generation, *pol* and *gag* are encoded in the pMLDg/ pRRE plasmid, which also encodes for the RRE.

The envelope plasmid: The third packaging plasmid is pVSV-G which encodes for the viral envelope.

The expression plasmid, pELN, encodes the inserted transgene expression cassette, and additional promoter sequences.

1.6.11 Summary

As one might expect, the responses have been variable, depending on the trial, the strategy, and the nature of the target cancer. Due to the massive variability in both host and pathology, direct comparison of these approaches is extremely difficult, and it seems likely that, rather than a 'cure for cancer', a targeted approach to each tumour is necessary. These trials have largely been conducted on patients with large, aggressive and seemingly intractable cancers, thus any response should be considered a positive sign, yet many studies report some degree of response in most patients, with a percentage achieving complete remission (Rosenberg and Dudley, 2009, Rosenberg et al., 2008, Rosenberg et al., 1986, Dudley and Rosenberg, 2003, Hinrichs and Rosenberg, 2014, Kvistborg et al., 2012, June, 2007, Besser, 2013, Perica et al., 2015).

This exciting field of research represents the shape of the future in targeted cancer treatment. Whilst it is recognised that poor sub-optimal TCR/pMHCI affinity is not necessarily the reason why tumours escape the immune system and persist in the host, the success of some attempts to create enhanced affinity TCRs, suggests that this is an important feature for at least some cancers. One downfall to this approach is the need to be targeted to both ligand and specific MHCI. Moreover, the timescale required to create such a 'designer TCR' can be lengthy; at a recent workshop considering TCR gene therapy, Adaptimune suggested 2 – 2.5 years, from bench to bedside. This thesis considers the possibility that the non-polymorphic CD8 molecule may be considered as a novel way of enhancing the TCR response to cancer ligand.

1.7 Aims of this Thesis

1.7.1 *Hypothesis*

Co-receptor mediated optimisation of the antigen specific T-cell response may be achieved by either tuning the strength of the pMHCI/CD8 interaction, or altering the level of CD8 expressed at the cell surface.

1.7.2 Aims

Specifically, I intend to:

1) Define the optimal pMHCI/CD8 interaction strength required which affords enhanced T-cell immunity by introducing point mutations into MHC at the CD8 binding site in order to examine this response.
2) Design and optimise a system for the stable transduction of CD8αß and a known TCR into immortalised and primary cell systems.
3) Define the effect of introducing point mutations into the α chain of CD8, specifically examining the kinetics of this interaction *in vitro*, and the effect on the T-cell response *in vivo*.
4) Examine the T-cell response of altering the splice variant expressed on the cytoplasmic tail of the CD8ß chain.

Define the effect of altering cell surface CD8 expression levels on pMHCI recognition, and subsequent $CD8^+$ T-cell activation.

Chapter 2

Materials and Methods

2.1 Mammalian Cell Culture

2.1.1 Cell Culture Media

The following cell culture media were used:

R10: Roswell Park memorial Institute 1640 media (RPMI-1640) (Life Technologies, ThermoFisher Scientific, U.K.) supplemented with 10% heat inactivated foetal bovine serum (FBS) (Life Technologies, ThermoFisher Scientific, U.K.), 2 mM L-glutamine (Life Technologies, ThermoFisher Scientific, Paisley, U.K.), 100 IU/ml penicillin and 100 µg/ml streptomycin (Life Technologies, ThermoFisher Scientific, Paisley, U.K.).

R0 (PSG): RPMI-1640 supplemented with 2 mM L-glutamine, 100 IU/ml penicillin and 100 µg/ml streptomycin.

R2: RPMI-1640 supplemented with 2% heat inactivated FBS, 2 mM L-glutamine, 100 IU/ml penicillin and 100 µg/ml streptomycin.

R20: RPMI-1640 supplemented with 20% heat inactivated FBS, 2 mM L-glutamine, 100 IU/ml penicillin and 100 µg/ml streptomycin.

CK media: R10 supplemented with 2.5% Cellkines (Helvetica Healthcare, Geneva), 200 IU/ml IL-2 (Proleukin®, aldesleukin, Novartis, U.K.) and 25 ng/ml IL-15 (PeproTech, London, U.K.).

T-cell media: R10 supplemented with 200 IU/ml IL-2 and 25 ng/ml IL-15.

D10: Dulbecco modified Eagle's medium (DMEM) (Life Technologies, ThermoFisher Scientific, U.K.) supplemented with 10% heat inactivated FBS, 2 mM L-glutamine, 100 IU/ml penicillin and 100 µg/ml streptomycin.

D0: DMEM supplemented with 2 mM L-glutamine, 100 IU/ml penicillin and 100 µg/ml streptomycin.

Freezer mix: FBS supplemented with 10% sterile dimethyl sulfoxide (DMSO) (Sigma-Aldrich, Poole, U.K.).

FACS Buffer: Phosphate buffered saline (PBS) supplemented with 0.5% Bovine Serum Albumen (BSA) and 0.1% NaN3 sodium azide.

MACS Buffer: PBS supplemented with 0.5% BSA and 2 mM EDTA.

2.1.2 Separation of Peripheral Blood Mononuclear Cells (PBMCs)

50 ml of whole blood, obtained from the Welsh Blood Transfusion Service or directly *ex vivo* from healthy donors, was collected into a sterile 50 ml falcon tube (BD Biosciences) with 50 µl preservative-free heparin (Unihep, Leo®) at a final concentration of 1000 IU/ml. PBMC were generated by Axis-shield density gradient centrifugation. Peripheral blood was gently layered onto an equal volume of Axis-shield density gradient media (Lymphoprep^{TM}, STEMCELL Technologies, UK) and centrifuged for 10 minutes at 1800 rpm (561 g) with the brake off (Hireaus Megafuge 1.0). The buffy coat was removed from the interface using a sterile Pasteur pipette and placed into a sterile 50 ml falcon. Cells were washed twice in R0: 1800 rpm (561 g) for 10 minutes, followed by 1500 rpm (389 g) for 5 minutes. Cells were then suspended in R10 media and kept at 37 °C/5% CO_2. Cells intended for use as human γ-irradiated (30 Gy) allogeneic feeders were stored at 4 °C prior to use.

2.1.3 Counting cells with Trypan blue

Cells were counted and analysed for viability by combining 10 µl of cell suspension with an equal volume of 0.1% Trypan blue in phosphate-buffered saline (PBS) (Sigma-Aldrich) and loaded on to an improved Neubauer haemocytometer (Weber Scientific International Limited, Lancing, U.K.). Viable cells remain colourless, whilst non-viable cells appear blue at 100 times magnification on a light microscope (Nikon Eclipse TS100). The percentage of total cells counted that remained white equates to the viability of the cell culture.

2.1.4 Culture of Human $CD8^+$ T-cell clones

$CD8^+$ T-cells were grown from cryopreserved stocks in T25 tissue culture flasks, in CK media for 2 weeks following re-stimulation using 1 µg/ml Phytohaemagglutinin (PHA) with γ-irradiated allogeneic feeders (12 x 10^6 irradiated allogeneic PBMC from 2-3 different individuals in 12 ml of media per flask). The flask was upright and tilted at an angle for the first 5 days, before returning to vertical. Media was topped up on day 5 and changed on day 7, taking care not to disturb the pellet. Cells were counted and plated out into 24-well tissue culture plates on day 10. After 2 weeks, cells were maintained in CK media, or T-cell media.

2.1.5 Human $CD8^+$ T-cell clones used in this thesis

The following $CD8^+$ T-cell clones were used in this study (Table 2.1):

- ILA1, specific for the human telomerase reverse transcriptase (hTERT)-derived epitope ILAKFLHWL (residues 540-548) restricted by HLA A*201 (A2 hereafter) (Laugel et al., 2007b, Purbhoo et al., 2007).
- MEL2, MEL5 and MELc5, specific for the Melan-A-derived epitope ELAGIGILTV (residues 26-35) restricted by HLA A2 (Purbhoo et al., 2007, Laugel et al., 2007b).
- LC13, specific for the Epstein-Barr virus (EBV) EBNA3A-derived epitope FLRGRAYGL (residues 339–347) restricted by HLA B*0801 (B8 hereafter) (Macdonald et al., 2009, Burrows et al., 1994, Bridgeman et al., 2012).
- SB10, specific for the EBV BZLF1-derived epitope LPEPLPQGQLTAY (residues 52–64) restricted by HLA B*3508 (B35 hereafter) (Green et al., 2004, Tynan et al., 2005).

2.1.6 Separation of $CD8^+$ T-cells from fresh, directly *ex vivo* PBMC

Directly *ex vivo* PBMC were counted and resuspended in MACS buffer, before magnetically labelling with CD8 MicroBeads (human)(MACS® Technology, Miltenyi Biotec Ltd.), as per manufacturers instructions. The cells were then loaded onto a MACS MS column, which is placed in the magnetic field of a MiniMACS cell Separator. The MiniMACS cell Separator was then removed from the magnetic field, thus facilitating elution of the positively selected $CD8^+$ fraction, as per

Name	MHCI restriction	Epitope	Residue	Origin
ILA1	A*0201	ILAKFLHWL	540-548	hTERT
MEL2	A*0201	ELAGIGILTV	26-35	Melan-A
MEL5	A*0201	ELAGIGILTV	26-35	Melan-A
MELc5	A*0201	ELAGIGILTV	26-35	Melan-A
LC13	B*0801	FLRGRAYGL	339-347	EBV EBNA3A
SB10	B*3508	LPEPLPQGQLTAY	52-64	EBV BZLF1

Table 2.1: Human $CD8^+$ T-cell clones used in this thesis.

manufacturer's instructions. Cells were then washed, and resuspended in R10 media.

2.1.7 Generation of TCR-transduced $CD8^+$ T-cell lines

1 x 10^6 $CD8^+$ T-cells, separated directly *ex vivo*, were counted, and resuspended in 1ml R10 media. Cells were plated in a 24-well tissue culture coated plate. 25 µl resuspended Dynabeads® (Dynabeads® Human T-Activator CD3/CD28, ThermoFisher Scientific Inc., Invitrogen Life Technologies), were washed in an equal volume of MACS buffer. A MiniMACS cell Separator was used to facilitate buffer removal, before resuspending in 25 µl R10, which was subsequently added to the counted cells. IL-2 was supplemented at 30 IU/ml. Cells were incubated overnight at 37 °C/5% CO_2, and examined the next day for active proliferation. 500 µl Lentiviral particles (generated as described in section 2.1.13)(Table 2.2), resuspended in R10 supplemented with IL-2 at 30 IU/ml were added. Cells were incubated and examined every 24 hours. The media was changed/virus particles removed after 24-48 hours, dependant on cell health. Cells were cultured in CK media after 5 days, and sorted for transgene expression (rat CD2 (rCD2 hereafter) expression) using a modified FACSAriaII™ (BD Biosciences). Cells were sorted into R20 media, and rested overnight before expansion by re-stimulation using 1 µg/ml PHA with γ-irradiated allogeneic feeders. Cells were maintained in CK media and regularly stained to demonstrate maintained transgene expression.

Name of transTCR	MHCI restriction	Epitope	Residue	Origin
ILA1	A*0201	ILAKFLHWL	540-548	hTERT
C12C*	B*2705	KRWIILGLNK	263-272	HIV p24 Gag

* (Iglesias et al., 2011)

Table 2.2: Transduced $CD8^+$ T-cell lines generated in this thesis.

2.1.8 Cryopreservation storage of cells

5 x 10^6 cells were centrifuged at 1500 rpm (389 g) for 5 minutes then re-suspended in 1 ml freezer mix and transferred to a cryovial (Nunc). Cryovials were stored in 100% Isopropyl, Propan-2-ol (Mr.Frosty™, ThermoScientific) storage containers at -80 °C for 48 - 72 hours before being transferred to liquid nitrogen containers for long-term storage.

2.1.9 Thawing of frozen stocks

Cell stocks were rapidly thawed at 37 °C to minimize cell death, washed in R0 (1500 rpm (389 g), 5 minutes) to remove the DMSO before re-suspension in the appropriate culture media.

2.1.10 Generation of stable HLA A2-expressing C1R B-cell line

Endotoxin free pcDNA3.1 mammalian expression vectors (Life Technologies) with inserts encoding either the full length of the HLA A2, or one of its mutants: A2 DT227/8KA (Purbhoo et al., 2001), A2 A245V (Wooldridge et al., 2005), A2 Q115E (Wooldridge et al., 2007), A2/K^b A245V (Dockree et al., 2017), and A2/K^b (Wooldridge et al., 2010a), were generated and linearised, before inserting into the C1R B-cell line by electroporation. The C1R B-cell line is an Epstein-Barr Virus (EBV)–transformed, class I MHC negative immortal cell line (Storkus et al., 1987). C1R cells were split and fed with R10 media 24 hours before transfection because transfection efficiency is increased when B cells are actively dividing, and the population is >90% viable. For each transfection 10 x 10^6 C1R B cells were washed twice in R0 by centrifuging at 1500 rpm (389 g) for 5 minutes at room temperature, before resuspension in 500 µl of R0 and transfer to a sterile 0.4 cm electroporation

cuvette (Bio-Rad, Herts, UK) with 10 µg endotoxin-free linearised DNA (10 µl of 1 µg/µl). After gently mixing the cell suspension and DNA using a Pasteur pipette the cuvette was placed on ice for 5 minutes. Electroporation was performed using the following conditions for each DNA construct; Voltage = 250 V, Capacitance = 400 µF.

Electroporation was performed using a Gene Pulser Xcell™ electroporation system (Bio-Rad). The electroporated cells were then rested at room temperature for 10 minutes. After the addition of 500 µl warm R10, the suspension was gently transferred into a T25 flask with a further 12 ml R10 and subsequently cultured at 37 °C/5% CO_2. Stable transfectants were selected by adding 0.5 mg/ml G418 (Sigma-Aldrich) 72 hours after transfection. Cell health and viability was examined daily, as significant death was expected in the first 3 days following G418 addition, prior to recovery. The transfected C1R cell lines were sorted for A2 expression using a modified FACSAriaII™ (BD Biosciences) following staining with FITC-conjugated mouse anti-human HLA A2 antibody, specific clone BB7.2 (Biolegend®), before cloning by limited dilution. The clones were maintained in culture in R10 media, and regularly tested for HLA A2 and analysed by flow cytometry. All clones showed 100% HLA A2 expression, staining with similar MFIs.

2.1.11 Generation of C1R B-cell Clones by limited dilution

Cells were counted and resuspended at a concentration of 1 cell per 400 µl culture media. Cells were plated up in a round-bottomed 96-well tissue culture plate, 200 µl/well (i.e. 1 cell ever 2 wells). Control wells at 10 and 100 cells/well were also added. Plates were cultured at 37 °C/5% CO_2, replacing media as required and examined for growth after 10 - 14 days. Clones were stained with FITC-conjugated

mouse anti-human HLA A2 antibody, and examined by flow cytometry. Data acquired were compared in order to compare A2 expression levels. Clones expressing similar levels of A2 for each mutation were selected for expansion. Once expanded, C1R B-cells were maintained in culture in T200 tissue culture flasks. Clones were regularly stained for A2 expression whilst in culture.

2.1.12 The HEK 293T lentiviral packaging cell line

The HEK 293T cell line is a derivative of HEK 293 cells, a line originally derived from normal human embryonic kidney (HEK) cells by transformation with sheared Adenovirus-5 DNA (Graham et al., 1977). HEK 293T has been stably transfected to express the SV40 large T antigen (DuBridge et al., 1987), and, like its parent cell, is efficiently transducible with retroviruses. HEK 293T is an adherent cell line, maintained in culture in D10 media. Cultures reaching 100% confluence were washed in PBS to remove traces of serum (which contains a trypsin inhibitor), before incubation for 5-10 minutes with 0.5% trypsin in HBSS (Life Technologies). Flasks were gently agitated to encourage cells to detach from the plastic tissue culture surface. Cells were removed by gentle pipetting, washed to remove trypsin, and split.

2.1.13 $CaCl_2$ Transfection of HEK 293T cells and Production of Lentiviral particles

Lentivirus (LV) was generated by $CaCl_2$ transfection of HEK 293T packaging cells with four distinct plasmids of a 3rd generation LV packaging system. The pELN 3rd generation transfer vector was used in combination with pRSV.rev, pVSV-G, and

pMDLg/pRRE. HEK 293T cells were split, counted, and plated at 10^6 /ml, in 15 ml of D10 in a T175 flask. Following 24 hours, cell health and confluence were checked, and the media was removed and replaced with 12 ml of pH 7.9 media. Transfection mix (comprising 15 µg pELN, 18 µg pRSV.rev, 7 µg pVSV-G, and 18 µg pMDLg/pRRE), made up to 3 ml with pH 7.1 media (Table 2.3), was slowly added taking care to contact only the surrounding media rather than the adherent cells on the tissue culture surface. Following 12 - 18 hours, the media were removed, and replaced with 15 ml of D10. Virus was harvested, stored at 4 °C, and media replaced at 48 and 72 hours post transfection. The supernatant collections were pooled, and passed through a 0.45 µm filter. Pooled supernatant was added to 38.5 ml thin-walled ultracentrifuge tubes (Beckmann Coulter), topping up with media to ensure the tube is filled, and placed in a Beckmann Coulter SW28.1 rotor for ultra-centrifugation (Beckmann Coulter Optima L-100 XP) at 20,000 g for 2 hours at 4 °C. Following centrifugation, the supernatant was discarded, the pellet allowed to dry, and the virus resuspended in 2 ml of R10 media. Virus was aliquotted, snap frozen on dry ice, and stored at -80 °C.

2.1.14 Immortal T-cell Lines

Immortal cell lines used in this thesis are; the J.R.T3-T3.5 line (ATCC, 2014b, Schneider et al., 1977), the J.RT3-T3.5 NFAT GLuc line (provided by Dr. John Bridgeman), and the HUT78 H9 derivative (ATCC, 2014a, Chen, 1992, Beddoe et al., 2009). These lines are maintained in culture in R10 media. Cells were resuspended at a concentration of 10^6 /ml, and plated up in a 24 well tissue culture plate, 1 ml/well. 500 µl Lentiviral particles (generated as described above),

pH 7.1 media	D0 25 mM HEPES pH adjusted to pH 7.1 0.22 µm filtered
pH 7.9 media	D10 25 mM HEPES pH adjusted to pH 7.9 0.22 µm filtered
Transfection mix	15 µg pELN 18 µg pRSV.rev 7 µg pVSV-G 18 µg pMLDg/pRRE 50 mM $CaCl_2$ made up to 3 ml with pH 7.1 media

Table 2.3: $CaCl_2$ Transfection Media.

resuspended in R10, were added to each well. Either one or 2 viruses were added, and the well topped up to 2 ml with R10. Cells were incubated and examined every 24 hours. The media was changed/virus particles removed after 48 hours, dependant on cell health. Cells were expanded, and sorted for transgene expression using a modified FACSAriaII™ (BD Biosciences), into R20 media. Transgene expression was examined by staining for rCD2 expression, (FITC conjugated anti-ratCD2, specific clone OX-34, Biolegend®) which indicates transfection with TCR transgene, and CD8ß (anti-CD8ß, specific clone 2ST8.5H7, Beckman Coulter), which indicates CD8αß heterodimer expression. Cells were washed and expanded in R20 media, and then maintained in culture in R10 media, and regularly stained to ensure maintenance of phenotype. A list of immortal T-cell lines generated in this thesis is listed in Table 2.4.

2.2 Bacterial Culture

2.2.1 Bacterial Culture media

The following culture media were utilised in production of this thesis:

Luria-Bertani (LB) Broth: Tryptone 10 g/l, Yeast extracts 5 g/l and NaCl 10 g/l. pH adjusted to 7.0 with NaOH

LB Agar: Tryptone 10 g/l, Yeast extracts 5 g/l, NaCl 10 g/l and Agar 15 g/l. Media were poured into plates whilst still warm and fluid.

TYP Broth: Tryptone 16 g/l, Yeast extracts 16 g/l, NaCl 5 g/l and K_2HPO_4 1 g/l. pH adjusted to 7.0 with NaOH.

Parent Cell line	Trans-TCR	CD8 variant
J.RT3-T3.5	ILA1	$CD8^-$
J.RT3-T3.5	ILA1	CD8αß
J.RT3-T3.5	ILA1	CD8αS53Nß
J.RT3-T3.5 NFAT GLuc	ILA1	$CD8^-$
J.RT3-T3.5 NFAT GLuc	ILA1	CD8αß
J.RT3-T3.5 NFAT GLuc	ILA1	CD8αQ2K/S53Nß
J.RT3-T3.5 NFAT GLuc	ILA1	CD8αS53Nß
J.RT3-T3.5 NFAT GLuc	ILA1	CD8αßM2
J.RT3-T3.5 NFAT GLuc	ILA1	CD8αßM3
J.RT3-T3.5 NFAT GLuc	ILA1	CD8αßM4
J.RT3-T3.5 NFAT GLuc	MEL5	$CD8^-$
J.RT3-T3.5 NFAT GLuc	MEL5	CD8αß
J.RT3-T3.5 NFAT GLuc	MEL5	CD8αQ2K/S53Nß
J.RT3-T3.5 NFAT GLuc	MEL5	CD8αS53Nß
J.RT3-T3.5 NFAT GLuc	MEL5	CD8αßM2
J.RT3-T3.5 NFAT GLuc	MEL5	CD8αßM3
J.RT3-T3.5 NFAT GLuc	MEL5	CD8αßM4

J.RT3-T3.5 NFAT GLuc	LC13	$CD8^-$
J.RT3-T3.5 NFAT GLuc	LC13	CD8αß
J.RT3-T3.5 NFAT GLuc	LC13	CD8αS53Nß
H9	ILA1	$CD8^-$
H9	ILA1	CD8αß
H9	ILA1	CD8αQ2K/S53Nß
H9	ILA1	CD8αS53Nß
H9	ILA1	CD8αßM2
H9	ILA1	CD8αßM3
H9	ILA1	CD8αßM4
H9	MEL5	$CD8^-$
H9	MEL5	CD8αß
H9	MEL5	CD8αQ2K/S53Nß
H9	MEL5	CD8αS53Nß
H9	MEL5	CD8αßM2
H9	MEL5	CD8αßM3
H9	MEL5	CD8αßM4

Table 2.4: Immortal T-cell lines generated in this thesis.

Psi Broth: Tryptone 20 g/l, Yeast extracts 5 g/l and $MgSO_4$ 5 g/l. pH adjusted to 7.6 with KOH.

SOC Broth: Tryptone 20 g/L, Yeast extracts 5 g/l, NaCl 0.5 g/l, Potassium Chloride - 0.186 g/l, Magnesium Chloride Hexahydrate – 2.03 g/l, Magnesium Sulphate – 1.2 g/l and D-Glucose – 3.604 g/l.

All media were autoclaved (liquid cycle at 121 °C for 60 minutes) and cooled to <55 °C before addition of selection agent, carbenicillin or kanamycin, at 100 µg/ml.

2.2.2 Buffers

Tris-Acetate-EDTA (TAE) Buffer: 40 mM Tris, pH 7.6, 20 mM Acetic Acid and 1 mM EDTA.

Tris-EDTA (TE) Buffer: 10 mM Tris-HCl, pH 8.0 and 1 mM EDTA

Buffers were made with milliQ (double-distilled) H_2O and filtered to 0.45 µm.

2.2.3 Making chemically competent bacteria (Hanahan Method)

Buffers were made as follows: -

TbfI: Potassium acetate 30 mM, Rubidium chloride 100 mM, Calcium chloride 10 mM, Manganese chloride 50 mM, Glycerol 15%. Adjusted to pH 5.8 and filtered (0.2 µM).

TbfII: MOPS 10 mM, Calcium chloride 75 mM, Rubidium chloride 10 mM, Glycerol 15%. Adjusted to pH 6.5 and filtered (0.2 µM).

50 ml of Psi broth supplemented with tetracycline at 50 µg/ml, was inoculated with 50 µl bacteria (Table 2.5), and incubated at room temperature overnight. A further 100 ml of Psi broth was inoculated with 1 ml of the starter culture, and incubated at 37 °C, with gentle aeration (shaker set to 110 rpm) to A 550 = 0.45. Alternatively, in order to achieve greater competency, the starter culture was maintained on ice during the day, and 100 ml of Psi broth inoculated with 1 ml started culture was incubated at room temperature overnight, similarly to A 550 = 0.45.

The culture was chilled on ice for 15 minutes before pelleting the cells at 6000 rpm (7245 g) for 10 minutes in a pre-chilled Sorvall™ flask. Supernatant was discarded and replaced with 40% starting volume (40 ml) TbfI, and incubated on ice for 15 minutes. The cells were pelleted as previously, supernatant discarded, and resuspended in 5% starting volume (4 ml) TbfII. Cells were incubated on ice for 15 minutes before aliquotting (50 µl), snap freezing on dry ice, and storage at -80 °C (Hanahan, 1983).

2.2.4 Transformation of Chemically competent bacteria

Bacterial aliquots, stored at -80 °C, were thawed slowly on ice. ~50 ng of plasmid DNA was added to 50 µl of thawed competent bacteria, gently mixed with the pipette tip, and kept at 4 °C for 5 minutes. The bacteria were then heat-shocked for 90 s at 42 °C, then return to ice for a further 2 minutes. 100 µl of SOC media was then added to the bacteria, which were incubated at 37 °C, with shaker set to

E. coli strain	Application
TOP10	Plasmid amplification for transformation, sequencing or transfection.
XL10 gold	Plasmid amplification for transformation, sequencing or transfection. Suitable for large, lentiviral plasmids.
BL21 (DE3) pLysS	DE3 lysogen expresses T7 upon IPTG induction. The pLysS plasmid produces T7, thus reduces basal expression of the gene of interest.

Table 2.5: Chemically Competent Bacterial Strains.

220 rpm, for 30 minutes, before streaking onto agar plates impregnated with the appropriate antibiotic for the transformed plasmid. Plates were incubated overnight at 37 °C, alongside a negative control plate (containing bacteria only, no DNA) for every transformation.

2.2.5 Induced Target Gene Expression in Bacterial Culture

A single colony was picked from a plate of recently transformed BL21 (DE3) *E. coli,* and used to inoculate 30 ml of TYP media, supplemented with 100 µg/ml carbenicillin, and incubated overnight at 37 °C, agitated at 220 rpm. 1 l of carbenicillin-supplemented TYP media was inoculated with 5 ml of starter culture and agitated again at 37 °C, until OD_{600} reaches between 0.5 and 0.6, as measure by spectrophotometer (Biochrom, Cambridge, UK). A 1ml pre-induction sample was retained, and protein expression was induced by addition of 1 ml 0.5 mM dioxin free isopropyl-1-thio-β-D-galactopyranoside (IPTG; Melford Laboratories). Shaker speed was reduced to 110 rpm, and flasks were agitated for a further 3 hours post induction. A further (post-induction) sample was retained, before the culture was centrifuged at 4000 rpm (2772 g) for 20 minutes at 4 °C. The supernatant was discarded, and the bacterial pellet re-suspended in lysis buffer for immediate processing into inclusion bodies.

2.2.6 Glycerol Stocks

500 µl of bacterial starter culture was added to 500 µl 50% glycerol in a 1.5 ml lockable microcentrifuge tube (Eppendorf). Stocks were clearly labelled and stored at -80 °C, where they can be stored for several years, and used to reinitiate the bacterial culture without the need for re-transformation.

2.3 Molecular Biology

2.3.1 DNA Preparation – Starter Culture

The object DNA plasmid was transformed into either XL10 gold *E. coli* (large plasmids) or TOP10 *E.coli* (packaging plasmids) by heat shock treatment, expanded in SOC media and plated up on LB agar plates impregnated with an appropriate antibiotic for overnight incubation at 37 °C. A single bacterial colony was selected for inoculation into 5 ml LB broth, supplemented with selection antibiotics at 100 µg/ml and shaken for 8 hours at 37 °C and 220 rpm. Starter culture was used to make a glycerol stock, and for DNA miniprep, or to inoculate a culture broth for DNA maxiprep.

2.3.2 DNA plasmid Miniprep

5 ml of bacterial culture broth was centrifuged at 4000 rpm (2772 g) for 10 minutes, so pelleting the bacteria. The supernatant was discarded. Plasmid DNA was extracted using a commercially available DNA miniprep kit (Zyppy plasmid miniprep kit; Zymo Research, CA, USA), as per manufacturer's instructions. These kits are based upon the alkaline lysis method. DNA was eluted into nuclease free water (Ambion®, LifeTechnologies, ThermoFisher Scientific), or Elution Buffer, and stored at -20 °C.

2.3.3 DNA Plasmid Maxiprep

1 ml of bacterial starter culture was used to inoculate 400 ml of LB broth supplemented with the appropriate selection antibiotic at 100 µg/ml. The culture

was agitated overnight at 37 °C and 220 rpm. Bacterial cells were pelleted by centrifugation at 4000 rpm (2772 g) for 20 minutes. The supernatant was discarded, and the plasmid DNA extracted from the bacterial cells by use of a commercially available maxiprep kit (PureLink®, Invitrogen, ThermoFisher Scientific), based upon the alkaline lysis method. Extracted DNA was eluted into nuclease free water (Ambion®, LifeTechnologies, ThermoFisher Scientific), or Elution Buffer, and stored at -20 °C.

2.3.4 DNA Plasmid Maxiprep (Endotoxin-free)

400 ml of bacterial culture was pelleted as previously. This was transferred to an aseptically prepared tissue culture hood, where the supernatant was discarded, and plasmid DNA was extracted with a commercially available endotoxin-free maxiprep kit (Endofree® Plasmid Maxi Kit, Qiagen), based upon the alkaline lysis method. Extracted DNA was eluted into endotoxin-free elution buffer, into a sterile vessel, and stored at -20 °C.

2.3.5 DNA Quantification

1 µl of DNA was measured using a Nano-drop (Thermo Scientific) set to record at 260 nm wavelength. Nuclease free water (Ambion®, LifeTechnologies, ThermoFisher Scientific) was used as a blank reference. An absorbency of 1 at 260 nm was assumed to indicate a DNA concentration of 50 ng/µl (after the extinction coefficient for DNA was taken into account).

2.3.6 DNA Sequencing

Plasmid DNA was sent for sequencing by Eurofins Genomics. Samples were sent pre-mixed with primer, as per sample submission guide (https://www.eurofinsgenomics.eu/media/892645/samplesubmissionguide_valueredtubes_update_296x105_4c.pdf).

15 µl of DNA plasmid, at a concentration of 50 – 100 ng/µl, was placed in a clean 1.5 ml lock-safe tube (Eppendorf), together with 2 µl primer at 10 pmol/µl (total volume 17 µl). For each construct, both forward and reverse sequencing primers were sent, and sequencing was checked at each stage of the cloning process. Sequencing data were analysed using CLC Genomics workbench.

2.3.7 Restriction Digest

Restrictions enzymes (FastDigest®, ThermoFisher™) were used to target specific regions of DNA plasmids and to liberate DNA facilitating cloning. Restriction enzymes were selected using plasmid maps, and as indicated in the text. DNA was subjected to restriction digestion by these specific enzymes as per manufacturers instruction.

2.3.8 Agarose Gel Electrophoresis Separation and DNA Extraction

Agarose gels were composed of 1 % Ultrapure agarose (Invitrogen) dissolved with heat into TAE buffer. Once fully dissolved, the agarose was allowed to cool a little before the addition of x 10,000 SYBR® Safe DNA gel stain (5 µl in 50 ml) or Midori Green Advanced DNA Stain (2 µl in 50 ml), which was gently mixed before casting

the gel. Once the gel had set the running tank was topped up with TAE buffer. Samples were mixed with x 6 DNA loading dye (ThermoScientific™), and loaded onto the gel, and run alongside an appropriate volume of 1 kb DNA ladder (GeneRuler™, ThermoFisher™) 75 V, 200 mA for 30 minutes. Gels were examined using an ultraviolet (UV) transilluminator. DNA bands were excised and so liberated from the gel, and the DNA extracted from the gel using a commercial kit (Wizard® DNA Clean-Up kit, Promega, UK, or ZymoClean™ Gel DNA Recovery Kit, Zymo Research) according to the manufacturer's instructions.

2.3.9 Ligation of DNA Products

Vectors and inserts were ligated by mixing insert and vector at different ratios with 1U DNA ligase (T4 DNA ligase Promega) and 3 µl DNA ligase buffer (Promega) and made up to a final volume of 30 µl with nuclease-free water (Ambion®, LifeTechnologies, ThermoFisher Scientific). Ligation reactions were set up on ice, and incubated for 16 hours at 16 °C. The end product was stored at 4 °C throughout the day, before transformation into XL10 Gold *E. coli*.

2.3.10 Polymerase Chain Reaction (PCR)

PCR reactions were set up using high-fidelity DNA polymerase (Phusion®, NEB), in combination with high fidelity (HF) Phusion buffer (NEB), $MgCl_2$, and DMSO. dNTP aliquots, combining equal molar amounts of all four nucleotides, were stored at -20 °C, and discarded following a single use. Primers were diluted to 100 pmol/µl in TE buffer. Primers are listed in Appendix A. PCR conditions are indicated below (Table 2.6 & 2.7), with the annealing temperatures having been determined for each

primer pair used using the NEB website (http://tmcalculator.neb.com) A Mastercycler® Gradient (Eppendorf) was used.

2.3.11 Site Directed Mutagenesis (SDM)

Site Directed Mutagenesis (SDM) was used to introduce point mutations into the α-chain of CD8. The GeneArt® cloning vector CD8β.IRES.CD8α.pMK was used as the template for this, with sense and antisense primers being designed to amplify each point mutation (Q2>K, F48>Q, and S53>N).

Multiple reaction conditions were trialled for each mutation, with PCR cycling conditions as detailed below (Table 2.8). Subsequently, 1 µl of DpnI (FastDigest™, ThermoScientific™) and 5 µl 10 x FD Buffer (FastDigest™, ThermoScientific™), were added and incubated for 1 hour at 37 °C. The DNA was purified using a commercial kit (Wizard®, Promega), as per manufacturer's instructions. The cleaned product was transformed into TOP10 *E. coli*. Bacteria were cultured on Kanamycin impregnated agar plates overnight at 37 °C.

2.3.12 CD8 cloning strategy

The cloning cassette, CD8β.IRES.CD8α.pMK, the design and concept of which is discussed below (2.3.15), was obtained from GeneArt®. The CD8β.IRES.α construct was liberated from the pMK cloning plasmid by restriction digestion, and re-ligated into the pELN lentiviral plasmid. Multiple restriction sites throughout the cloning cassette facilitated manipulation of both the α- and β-chains, enabling substitution of mutated CD8 into the lentiviral vector. The pMK cloning plasmid contains the

Component	Volume / 50 µl	Final concentration
DNA, 10 - 50 ng	*Varies*	0.2 - 1 ng/ml
Primer 1 (forward)/ 10 pmol/µl	1.25 µl	0.25 µM
Primer 2 (reverse)/ 10 pmol/µl	1.25 µl	0.25 µM
50 mM $MgCl_2$	0.5 µl	0.5 mM
2.5 mM dNTP	5 µl	250 µM
DMSO	0.5 µl	0.5%
5 x HF Buffer	10 µl	1 x
Phusion polymerase	0.25 µl	0.01 U/µl
Nuclease-free H_2O	Up to 50 µl	-

Table 2.6: PCR Reaction Conditions

Stage	Name	Temperature	Time
1	Initial denaturing	94 °C	30 s
2 (Cycle x 30)	Denaturing Annealing Extension	94 °C 54 – 72 °C 74 °C	10 s 30 s 40 s
3	Final extension	74 °C	7 minutes
-	Hold	4 °C	∞

Table 2.7: PCR Cycling Conditions

Stage	Name	Temperature	Time
1	Initial denaturing	98 °C	30 s
2 (Cycle x 25)	Denaturing Annealing Extension	98 °C 72 °C 72 °C	10 s 30 s 5 minutes
3	Final extension	68 °C	10 minutes
-	Hold	4 °C	∞

Table 2.8: PCR Cycling Conditions for SDM

gene for resistance to kanamycin, and the smaller plasmid was suitable for transformation into TOP10 *E. coli,* thus bacteria transformed with this plasmid, were cultured in media supplemented with kanamycin at 100 µg/ml. The pELN lentiviral plasmid contains the gene for resistance to carbenicillin, and was suitable for transformation into XL10 gold *E. coli,* thus bacteria transformed with this plasmid were cultured in media supplemented with carbenicillin at 100 µg/ml. Products were screened at each stage of cloning, initially by restriction digestion of DNA product, or by colony PCR. Where these results were favourable, the product was sent for DNA sequencing (Eurofins).

2.3.13 Linearisation of DNA

Plasmid DNA for stable transfection of C1R B-cells must first be linearised in order for it to successfully integrate with host cell DNA. It is essential that this DNA be produced in an endotoxin-free manner. 50 µg of plasmid DNA was digested with 10 µl BglII (New England Biolabs), 20 µl of 10 x NEB buffer and 145 µl nuclease free water (Ambion®, LifeTechnologies, ThermoFisher Scientific). Plasmid DNA was subjected to restriction digestion by BglIII for 18 hours at 37 °C. Linearised DNA was run on a 1% agarose gel in order to measure digestion efficiency.

2.3.14 Ethanol Precipitation

400 µl of 100% ethanol (Sigma-Aldrich) was added to the linearised product, and incubated together at room temperature for 10 minutes. The reaction was then centrifuged for 10 minutes at 13,500 rpm (12,225 g), and the supernatant discarded. The DNA pellet was resuspended in 500 µl of 70% ethanol. Centrifugation was repeated,

supernatant once more discarded, and the final DNA pellet was resuspended in 50 µl of endotoxin-free water.

2.3.15 Designing of CD8ß.IRES.CD8α construct (Figure 2.1)

Previous work had utilised a CD8α.2A.CD8ß construct, however this has resulted in failure of heterodimer expression. For this thesis, a new construct was designed. The expression cassette was as follows: - CD8ß.IRES.CD8α (Figure 2.1B). It was hoped that this new design would overcome the preferential homodimer formation observed with the CD8α.2A.CD8ß construct, as it was anticipated that in this cassette, CD8ß would be synthesised in considerably larger (~10x greater) quantities than CD8α (Attal et al., 1999, Bouabe et al., 2008), estimated from the length of construct and the anticipated ribosomal drop-off rate. This rationale is further supported by the layout of the CD8α and CD8ß genes in man, with the CD8ß1 locus being located upstream to CD8α (DiSanto et al., 1993). The new CD8ß.IRES.CD8α expression cassette contained CD8ß and CD8α separated by an internal ribosome entry site (IRES), which directs ribosomes to initiate translation downstream of the stop codon in the first transgene, ensuring bicistronic expression of the two transgenes from the same transcript (Morgan et al., 1992, Szymczak et al., 2004). In addition, the 2A self-cleaving peptide was changed for an IRES promoter to avoid potential ribosomal skipping of peptides and associated mutations and other translation errors resulting from inefficient cleavage that have been reported with the 2A self-cleaving peptide (Szymczak et al., 2004). Another difference was the insertion of a STOP codon at the end of the CD8ß gene, thus the two proteins are produced separately. The new expression cassette was codon

A

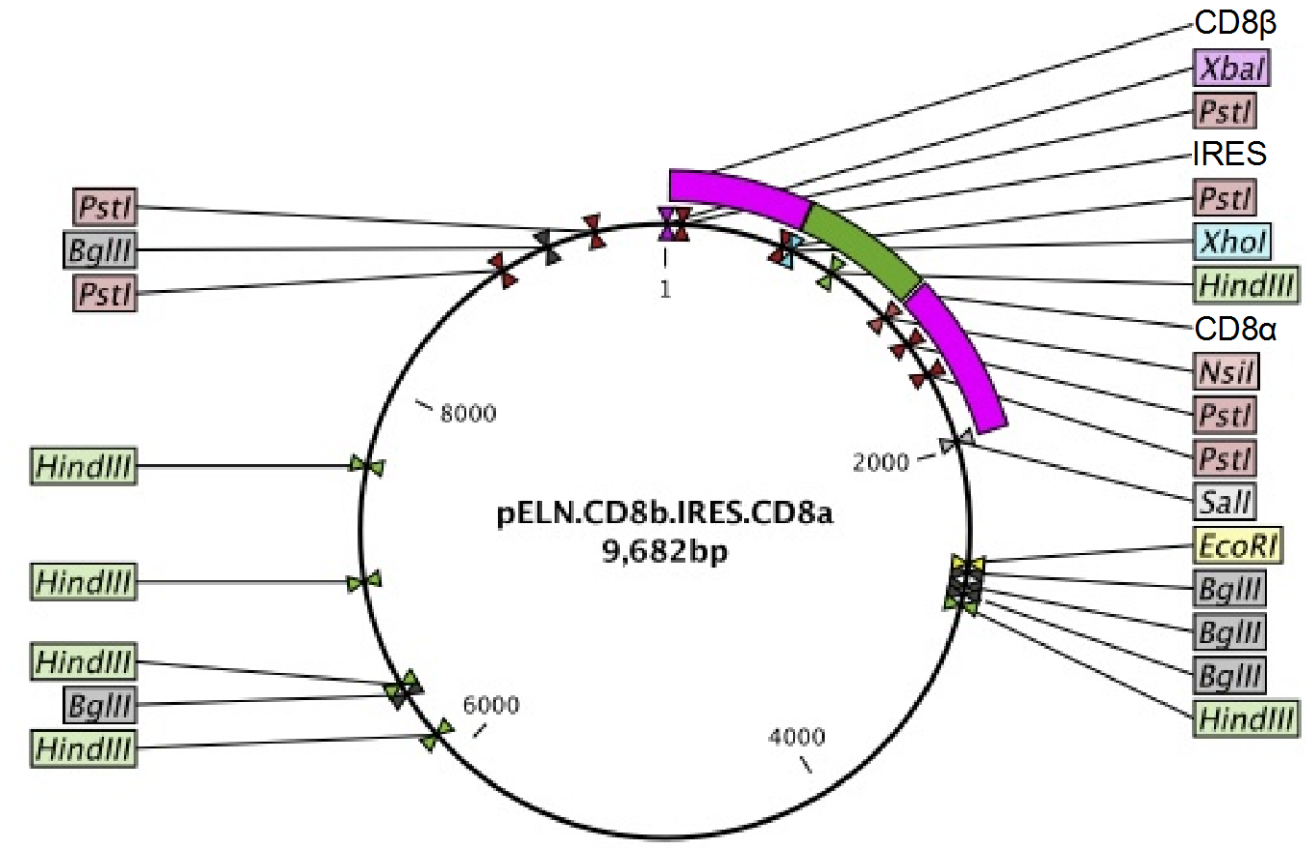

B

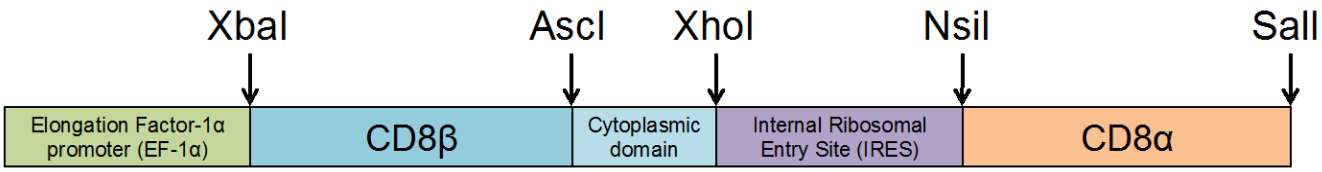

Figure 2.1: The pELN lentiviral plasmid, showing major restriction sites and inserted CD8ß.IRES.CD8α construct (**A**). Expanded schematic of the CD8 construct, CD8ß.IRES.α (**B**), shows the restriction enzymes used whilst working with this plasmid.

Once the whole plasmid had been cloned into the pELN lentiviral plasmid, mutations and variations were inserted into the construct, working with the packaging smaller pUC57 packaging plasmid. The mutated regions were then cut and cloned into the pELN. CD8 plasmid using the five main restriction enzymes utilised in this study; Xba1, AscI, Xho1, Nsi1, and Sal1.

optimised for mammalian expression by GeneArt, and cloned into the lentiviral packaging plasmid pELN, where its expression is controlled by the EF-1α promoter.

2.3.16 Cloning of the CD8αß expression cassette into the pELN lentiviral vector

The CD8ß.IRES.CD8α. construct was designed to contain a 5' XbaI and a 3' SalI restriction site flanking the expression cassette encoding CD8 (Figure 2.1). The CD8ß.IRES.CD8α. pMK cloning plasmid and the pELN lentiviral transfer plasmid were subjected to restriction digest with XbaI and SalI enzymes (Figure 2.2). The samples were separated on a 1% agarose gel. The liberated insert and backbone were excised, then purified and ligated using DNAligase. The resultant DNA plasmid was transformed into competent XL10 gold *E. coli* bacteria and cultured on carbenicillin plates. Colonies were picked and assessed for successful plasmid transduction by colony polymerase chain reaction (PCR), and by culture and miniprep, and DNA sequencing.

2.3.17 Site Directed Mutagenesis of CD8ß.IRES.CD8α.pMK to generate α-chain mutants and cloning into the pELN lentiviral plasmid

Site directed mutagenesis was used to introduce mutations into the existing DNA maxiprep of the CD8ß.IRES.CD8α.pMK cloning plasmid. The small size of this cloning plasmid facilitated mutation by this means. The resultant DNA was transformed into competent XL10 gold *E. coli* bacteria, which were cultured on kanamycin plates. Colonies were picked for culture in kanamycin selection media, and minipreps were performed on the resultant cell pellet to generate DNA for

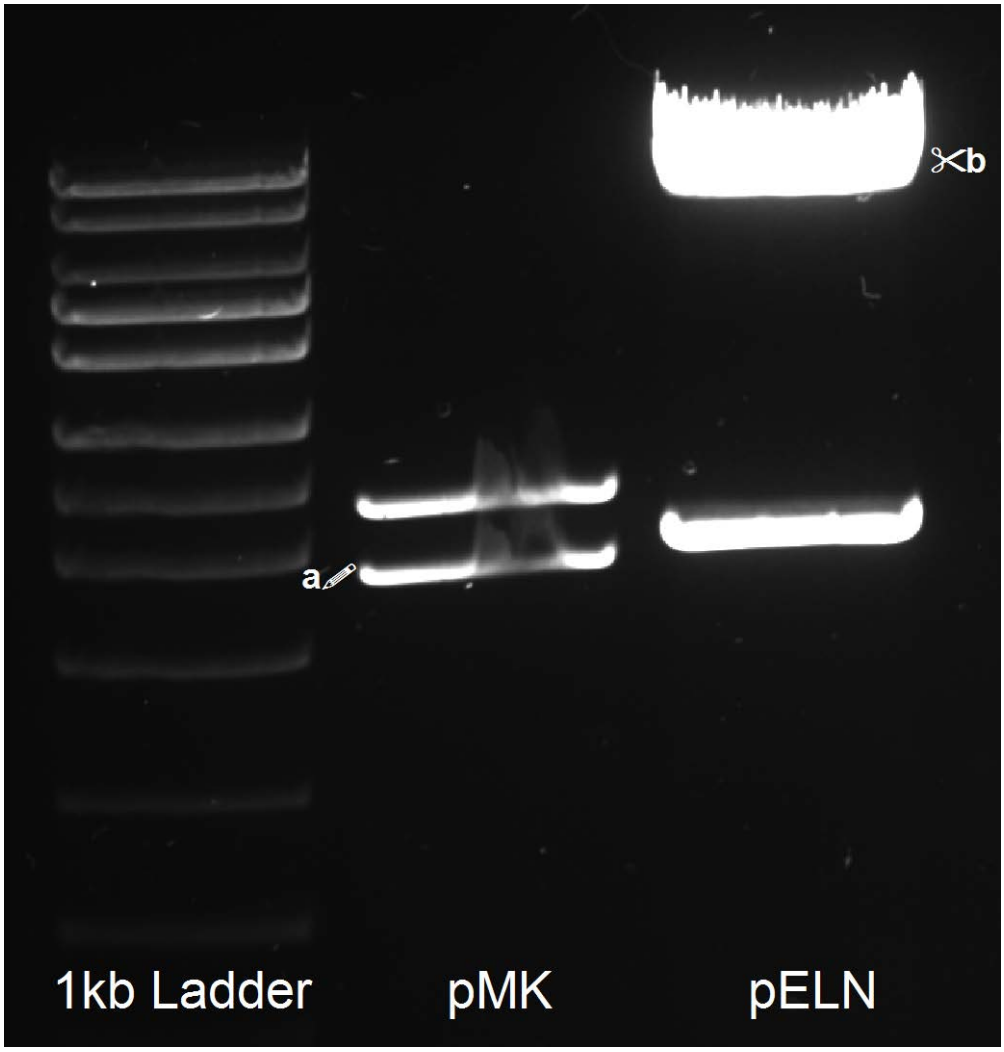

Figure 2.2: The cloning plasmid (pMK) and the lentiviral vector (pELN) were subjected to restriction digest by the enzymes XbaI and SalI.

The insert (a) and the lentiviral backbone (b) were liberated for ligation, before transformation of the resultant DNA product into chemically competent XL10 gold *E. coli*, for replication of the DNA plasmid. The successfully transformed bacteria can then be expanded in selection media (1% carbenicillin).

sequencing. Sequencing was performed at Eurofins MWG Operon, and confirmed the presence of each mutation, with DNA product being aligned to the wild type sequence (Figure 2.3 & Appendix C). DNA aliquots that contained the desired mutation were retained for cloning into the pELN lentiviral transfer plasmid.

2.3.18 Cloning of CD8α mutant variants into the pELN lentiviral plasmid

The CD8β.IRES.CD8α. insert was designed to contain a 5' NsiI and a 3' SalI restriction site flanking the CD8α transgene, meaning that the CD8α part of the construct could be substituted easily for each of the SDM mutants, liberating this piece only from the packaging plasmid and re-inserting it into the lentiviral backbone, ligating it into the region where the *wild type* CD8α had been removed using the same restriction sites. The CD8β.IRES.CD8α.pMK cloning plasmid for each α-chain mutant variant, and the CD8β.IRES.CD8α.pELN lentiviral transfer plasmid were subjected to restriction digest by the enzymes NsiI and SalI. The samples were separated on a 1% agarose gel. The liberated CD8α inserts and pELN backbone were excised and purified and subjected to ligation by DNAligase. The resultant DNA plasmid was transformed into competent XL10 gold *E. coli* bacteria and cultured on carbenicillin plates. Colonies were picked for expansion, and checked for successful transformation by colony polymerase chain reaction (PCR), and by miniprep and DNA sequencing.

2.3.19 Cloning of CD8β splice variants into the pELN lentiviral plasmid

The CD8β.IRES.CD8α. insert was designed to contain a 5' AscI restriction site in the trans-membrane region of the CD8β protein, and a flanking 3' XhoI restriction site

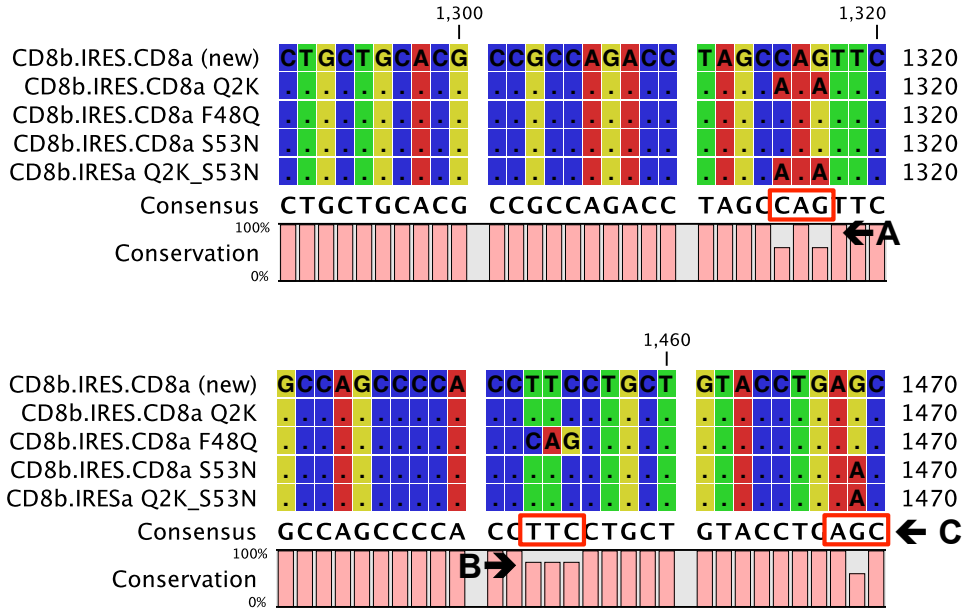

Figure 2.3: DNA Sequence of CD8β.IRES.α and each of its α-chain mutants; S53N, F48Q, and Q2K.

DNA preps obtained from lysed bacterial cultures were subjected to digestion as described in Figure 2.2. DNA preps, which could be digested in the correct manner, were selected for sequencing with the IRESfor primer (described in appendix C). The sequencing data was aligned with and compared to the sequences detailed for each mutant. Excerpts containing the mutations are depicted above, with the complete data set available in the appendices. The mutations Q2K (**a**), F48Q (**B**) and S53N (**C**) are highlighted at positions 1315, 1543, and 1468, respectively. (These positions are relative only to the start of the cassette sequence).

(Figure 2.1), thus the DNA encoding the CY-2 part of the cytoplasmic tail of the CD8β protein could be isolated. The pMK cloning plasmid, containing each of the splice variants, codon optimized for mammalian expression, was obtained from Genewiz (Figure 2.4). The restriction sites were located outside of the CY-2 variant sequence, and thus were present in all variants. The cloning plasmid containing all variants, and the pELN lentiviral plasmid, were subjected to restriction digest by AscI and XhoI. The samples were separated on a 1% agarose gel. The liberated CD8β CY-2 inserts and pELN backbone were excised and purified, then subjected to ligation by DNAligase. The resultant DNA plasmid was transformed into competent XL10 gold *E. coli* bacteria and cultured on carbenicillin plates. Colonies were picked preparation of miniprep DNA for sequencing. The M-2 and M-4 variants could not be separated on a gel, owing to their similar sizes (only 13 base pairs difference), thus could not be truly identified prior to the sequencing stage (Figure 2.4), thus the one band was used for cloning, and successful clones were identified by sequencing of the ligation products.

2.4 Protein Biochemistry

2.4.1 Buffers

The following buffers were used in this thesis:

Lysis Buffer: 10 mM Tris, 10 mM $MgCl_2$, 150 mM NaCl and 10% Glycerol**,**

Triton Wash Buffer: 0.5% Triton 100, 50 mM Tris, 100 mM NaCl and 10 mM EDTA.

Resuspension Buffer: 50 mM Tris, 100 mM NaCl and 10 mM EDTA.

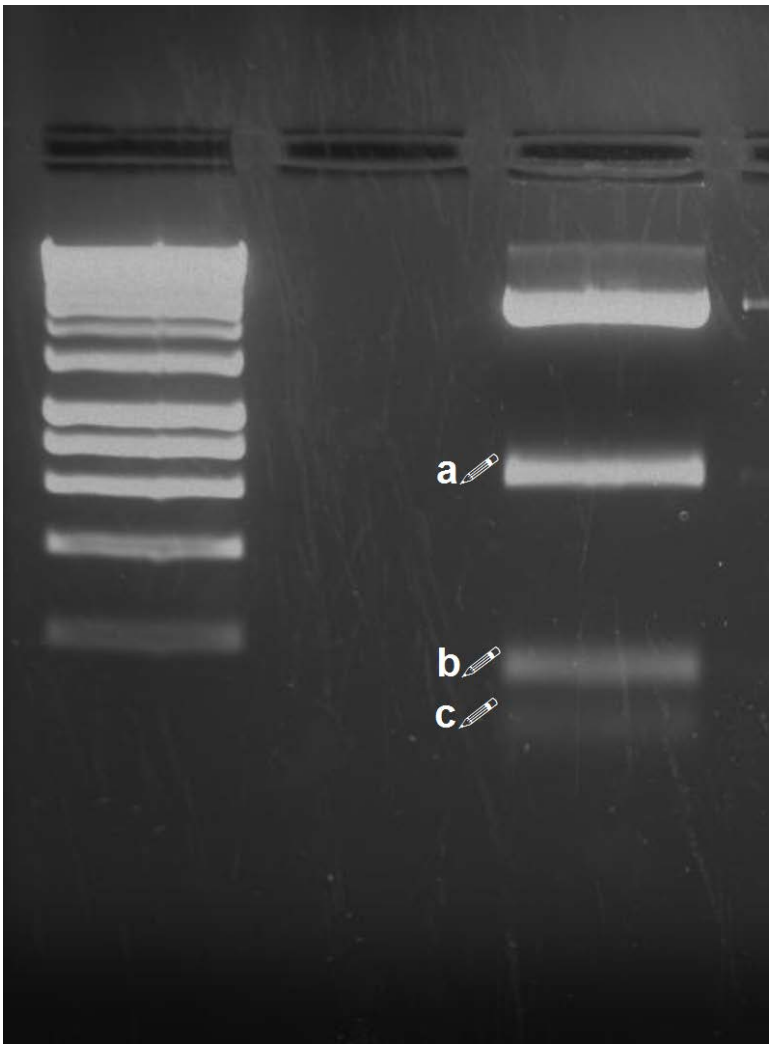

Figure 2.4: The CD8β cloning plasmid was subjected to digestion by AcsI and XhoI.
The packaging plasmid was designed to contain an AscI restriction site near the junction of the trans-membrane and cytoplasmic domains and flanked 3' by an XhoI site. The plasmid also contained the CY-2 domain of each of the β-chain splice variants; M2, M3 and M4, each also flanked by a 5' AscI and a 3' XhoI. The fractions were separated on a 2% agarose gel, allowing for liberation of the wild type M1 (**a**), the M2 and M4 CY-2 variants (**b**) and the M3 CY-2 variant (**c**). The M2 and M4 variants were treated as a single product prior to sequencing, owing to a size difference of only 13 base pairs.

(Data provided by Tomas Watkins)

Guanidine Buffer: 6 M Guanidine, 50 mM Tris, 2 mM EDTA and 100 mM NaCl.

Urea (Denaturing) Buffer: 8 M Urea, 50 mM Tris pH, 100 mM NaCl, 10 mM EDTA and10 mM Di-thio-3-etinol (DTT)(added immediately before use).

Refolding (REDOX) Buffer: 100 mM Tris, 400 mM L-Arginine, 2 mM EDTA,

6.5 mM cysteamine (added immediately before use) and 3.7 mM cystamine (added immediately before use).

Guanidine Denaturing Buffer: 6 M Guanidine, 50 mM Tris, 100 mM NaCl, 10 mM EDTA and 10 mM DTT (added immediately before use).

Refolding (REDOX) Buffer for CD8: 200 mM Tris, 500 mM L-Arginine, 10 mM EDTA, 6.5 mM cysteamine (added immediately before use) and 3.7 mM cystamine (added immediately before use).

SDS Non-reducing sample running buffer: 125 mM Tris pH 6.8, 4% Sodium dodecyl sulphate (SDS), 20% Glycerol and 20 µg/ml bromothenol blue.

SDS Reducing sample running buffer: 125 mM Tris pH 6.8, 4% Sodium dodecyl sulphate (SDS), 20% Glycerol, 20 µg/ml bromothenol blue and 10% DTT.

HBS-EP Biacore Buffer: 10 mM HEPES pH 7.4, 150 nM NaCl, 3.4 mM EDTA and 0.005% Surfactant P20.

2.4.2 Preparation of Protein Inclusion Bodies

Synthetic proteins used in this thesis (MHCI heavy (α-) chains (biotin tagged), ß2m, CD8α, TCRα and TCRß) were manufactured in D21 (DE3) pLys *E. coli*. The DNA sequence for the soluble (extracellular) part of these proteins is codon optimised

for prokaryotic expression, and cloned into the pGMT7 plasmid, where it is expressed under the control of the T7 promoter.

The bacterial pellet produced as described above was resuspended in 40 ml lysis buffer. The suspension was transferred to a 50 ml Falcon tube and lysed by sonication. 200 µl of 20 µg/ml DNase was added to the tube, which was then rocked for 30 minutes at room temperature. The inclusion bodies were then transferred to a clean Sorvall™ plastic flask, to which 100 ml of Triton wash buffer was added. The inclusion bodies centrifuged at 10,000 rpm (11952 g) for 20 minutes at 4 °C and the supernatant discarded. The pellet was the resuspended in 100 ml of resuspension buffer and centrifuged once again at 10,000 rpm (11952 g) for 20 minutes at 4 °C and a 500 µl sample taken for purity assessment before discarding the supernatant. The inclusion bodies were then dissolved in 15 ml of guanidine buffer, the concentration assessed by spectrophotometry, and stored at -80 °C.

2.4.3 Refolding of Soluble Biotinylated pMHCI monomers

30 mg of inclusion bodies for each MHCI heavy chain (*wild type* or each of its mutants) and ß2m were denatured by incubating separately in 10 ml of urea buffer at 37 °C for 30 minutes. 1 l of refolding buffer was pre-chilled to 4 °C, and stirred vigorously. To this was added first 1 ml of peptide (4 mg/ml in DMSO), followed by 30 mg of denatured ß2m, and then lastly 30 mg of denatured MHCI heavy chain. Gentle stirring was continued for 3 hours at 4 °C before transferring the refold to 12 kD cut-off dialysis tubing (Sigma-Aldrich) and dialysing against 12 l chilled dH_2O overnight, followed by dialysing against 12 l chilled 10 mM Tris pH 8.1 for 48 hours, changing the dialysis bucket for fresh 10 mM Tris once during this time.

The refold was filtered (0.45 µM) and loaded onto a 5 ml anion exchange column (Hi Trap Q HP; GE healthcare), which had previously been equilibrated with 10 mM Tris pH 8.1. The protein was then eluted over a salt gradient (0 - 500 mM NaCl in 10 minutes/10 mM Tris pH8.1). Protease inhibitors (1:100) (500 µM AEBSF, 1 µg/ml Aprotinin, 1 µM E-64, 500 µM EDTA and 1 µM Leupeptin; Calbiochem, UK) were added to eluted fractions, which were then stored at 4 °C whilst analysis by SDS-PAGE gel was performed. Correctly folded fractions, those showing a heavy chain band at ~35 kD and a ß2m band at ~12 kD, were retained, pooled, and concentrated to ~800 µl using a centrifugal filter device (Vivaspin® 20, Sartorius). The protein was then biotinylated overnight by addition of 100 µl BioMix A, 100 µl BioMix B and 1 µl (2.5 µg), Bir A enzyme (Avidity, Denver, USA), mixing well, and incubating at room temperature overnight. Excess Biotin was removed and the sample further purified by gel filtration into PBS using a Superdex HR 200 column (Amersham Pharmacia), which had previously been equilibrated into PBS. Fractions were again collected and pooled, and protease inhibitor added, before concentration was assessed by spectrophotometry. The monomer was then aliquotted and stored at -80 °C.

2.4.4 Refolding of Soluble αßTCR monomers

30 mg TCRα chain and 30 mg TCRß inclusion bodies were denatured by incubating separately with 10 ml of guanidine buffer at 37 °C for 30 minutes. 1 l of refolding buffer was pre-chilled to 4 °C, and stirred vigorously, and refolding initiated by the addition of the denatured TCRα and TCRß chains simultaneously. Stirring was continued for 3 hours at 4 °C before transferring the refold to 12 kD cut-off dialysis tubing (Sigma-Aldrich) and dialysing against 12 l chilled dH_2O overnight, followed

by dialysing against 12 l chilled 10 mM Tris pH 8.1 for 48 hours, changing the dialysis bucket for fresh 10 mM Tris once during this time.

The refold was filtered (0.45 µM) and loaded onto a 5 ml anion exchange column (Hi Trap Q HP; GE healthcare), which had previously been equilibrated with 10 mM Tris pH 8.1. The protein was then eluted over a salt gradient (0 - 500 mM NaCl in 10 minutes/10 mM Tris pH8.1).

Protease inhibitors (1:100) (500 µM AEBSF, 1 µg/ml Aprotinin, 1 µM E-64, 500 µM EDTA and 1 µM Leupeptin; Calbiochem, UK) were added to eluted fractions, which were then stored at 4 °C whilst analysis by SDS-PAGE gel was performed. Correctly folded fractions, those showing a α-chain band at ~28 kD and a ß-chain band at ~30 kD (reduced) and the whole monomer at ~58 kD (non-reduced), were retained, pooled and concentrated down to 1 ml using a centrifugal filter device (Vivaspin® 20, Sartorius). The sample further purified by gel filtration into PBS using a Superdex HR 200 column (Amersham Pharmacia), which had previously been equilibrated into PBS. Fractions were again collected and pooled, and protease inhibitor added, before concentration was assessed by spectrophotometry. The monomer was then aliquotted and stored at -80 °C.

2.4.5 Manufacture of Soluble CD8αα

3 x 60 mg aliquots of CD8α inclusion bodies were denatured separately at 10 minute intervals in 20 ml of guanidine buffer at 37 °C for 30 minutes each. The denatured CD8α inclusion bodies were added at 10 minutes intervals to 4 l of vigorously stirring, pre-chilled CD8 refold buffer. Stirring was continued for 1¾ hours at 4 °C. The refold was then concentrated to 150 ml using a MasterFlex L/S (Cole/Palmer) concentrator using a VivaFlow® 200 filter (Sartorius) using a 10 kD

cut off filter. Both the tubing and refold were maintained on ice throughout. The concentrated refold was then transferred to 12 kD cut-off dialysis tubing (Sigma-Aldrich) and dialysing against 8 l dH_2O overnight, followed by dialysing against 8 l chilled 10 mM 2-N-Morpholinoethanesulfonic acid (MES) pH 6.0 for 8 hours, then again overnight against fresh 10 mM MES.

The refold was diluted in 500 ml MES pH 6.0, filtered (0.45 µm), and loaded onto a 5 ml Hi Trap SP cation exchange column (GE healthcare) pre-equilibrated in 10 mM MES pH6 (Sigma-Aldrich). Protein was eluted from the column with a salt gradient (0 - 500 mM NaCl in 10 minutes/10 mM MES pH6.0). Fractions were analysed by SDS-PAGE gel (CD8α bands at ~13 kD (reduced) and CD8αα bands at ~26 kD (non-reduced)), and correct fractions were pooled and concentrated down to 1 ml using a low molecular weight cut off (MWCO) centrifugal filter device (Amicon® Ultra Ultracell-3, Merck Millipore). The sample further purified by gel filtration into PBS using a Superdex HR 200 column (Amersham Pharmacia), which had previously been equilibrated into PBS. Fractions were again collected and pooled, and protease inhibitor added, before concentration was assessed by spectrophotometry. The monomer was then aliquotted and stored at -80 °C.

2.4.6 Fast Protein Liquid Chromatography (FPLC) Trace

FPLC was utilised to elute and purify refolded protein fractions, and for buffer exchange. Examples of the traces obtained for ion exchange (IE) and gel filtration (GF) of refolded monomers: MHCI, αßTCR and CD8αα, are detailed in Appendix B.

2.4.7 SDS PolyAcrylamide Gel Electrophoresis (PAGE)

Proteins were separated and analysed using SDS-PAGE using the NOVEX NuPAGE® SDS-PAGE system (ThermoFisher™). Pre-cast gels, NuPAGE Novex 4–12% Bis-Tris Midi Gel w/ MOPS, were rinsed in dH2O prior to use. The gel was docked into the XCell SureLock™ Mini-cell Electrophoresis System, and the chamber filled with Nupage® MES running buffer. Samples were prepared by diluting 1:4 with running buffer, each sample being analysed with both reducing and non-reducing buffer. Samples were incubated at 95 °C for 5 minutes, prior to loading onto separate lanes of the gel, alongside the molecular weight ladder (PageRuler™ Plus pre-stained protein ladder, ThermoFisher™). Gels were run at 180 V for 40 minutes. The gel was removed from its casing, rinsed twice with dH2O before staining with Coomassie Blue Colloidal Stain Kit (ThermoFisher) by gentle agitation for 30 - 60 minutes, then de-staining for 1 – 2 hours with milliQ dH2O to allow visualisation.

2.4.8 Spectrophotometry

A Biomate spectrophotometer (ThermoScientific) was used to estimate protein concentration. Proteins were mixed well and samples for analysis were further diluted 1 in 100 in the buffer in which they were stored (guanidine buffer for inclusion bodies, PBS for monomers, or HBS-EP Biacore buffer for samples being prepared for SPR experiments). Furthermore the machine was made to blank reference with this same buffer prior to sample analysis. Readings were taken and recorded at 280 nm λ, and the protein concentration calculated using the dilution factor and the specific extinction coefficient the protein (calculated from the amino acid sequence).

2.4.9 Surface Plasmon Resonance (SPR)

Before SPR experiments, proteins must first be gel filtrated into HBS-EP Buffer to ensure purity / remove any aggregates, and to exchange into the Biacore buffer. This was done using a Superdex 200 HR column (Amersham Pharmacia) as previously described. CD8αα and αβTCR were concentrated to 100 μM and 150 μM, respectively, using a low MWCO centrifugal filter device (Amicon® Ultra Ultracell-3, Merck Millipore). SPR was performed using a BIAcore T100 machine (BIAcore AB). All reagents and proteins were kept at 4 °C, whilst experiments were carried out at 25 °C. A research grade CM5 sensor BIAcore chip was used.

The flow cell was activated using a mix of sulfo-*N*-hydroxysuccinimide (NHS) and 1-ethyl-3-(3-dimethylaminpropyl)-carbodimide hydrochloride (EDC) (O'Shannessy et al., 1992). The 1: 1 mix of 100 mM NHS and 400 mM EDC was flowed over the cell, followed by streptavidin solution (streptavidin 100μg/ml diluted in 10 mM Sodium Acetate, 0.1 mM EDTA, 1 mM NaCl, 1 mM DTT, pH 4.6), and finally 1 M ethanolamine-HCl pH 8.5. Each were injected for 600 s at a flow rate of 10 μl/min (O'Shannessy et al., 1992). Biotinylated pMHCI monomers diluted in HBS-EP BIAcore buffer were immobilized onto the chip surface at approximately 1000 response units (RU). Serial dilutions of analyte were prepared and flowed over the chip at a rate of 30 μl/min. The data generated were analysed using BIAevaluation 3.1, Microsoft Excel and Origin 6.1 software. The K_D values were calculated using a nonlinear curve fit (y = [P1x]/[P2 + x]).

2.4.10 Manufacture of pMHCI Tetramers

Streptavidin has four binding sites for biotin, thus needs to be combined with soluble pMHCI monomers in a 1:4 molar ratio for the construction of tetramers

(Wooldridge et al., 2005). Tetramers were conjugated to either R-phycoerythrin (PE) or Allophycocyanin (APC). The concentration of the pMHCI monomers was measured as described above. The volume of conjugated streptavidin required for each tetramer reaction in order to complete the saturation of streptavidin molecules, was calculated and added to the monomer in 5 equal aliquots at 20-minute intervals, mixing thoroughly each time. The reaction was carried out on ice and maintained in the dark. The tetramer was stored at 4 °C, protected against light degradation, for up to four weeks. During usage, it was monitored for signs of protein degradation.

2.5 Flow Cytometry

A list of antibodies used is detailed in Table 2.9.

2.5.1 Tetramer Staining of $CD8^+$ T-cell Clones

5×10^4 cells were resuspended in 40 µl of PBS and stained with fixable violet fluorescin amine dye (ViViD, Life Technologies) at a 1 in 800 dilution. Cells were washed and resuspended in 40 µl of FACS buffer and stained with either A2 DT227/8KA, A2 A245V, A2, A2 Q115E, A2/K^b A245V, or A2/K^b tetramers folded around the ELAGIGILTV peptide at 25 µg/ml for 20 min at 37 °C. Cells were washed twice and resuspended in 100 µl FACS buffer. Data were acquired using a FACSCanto flow cytometer, and analysed using FlowJo software.

Manufacturer	Species	Specific clone	Target	Fluorochrome	Dose per 40 µl test
Biolegend	Mouse	HCD14	CD14	Pacific Blue	0.5 µl
BD Bioscience	Mouse	rmC5-3	CD14	QD V500	2 µl
Biolegend	Mouse	HIB19	CD19	Pacific Blue	0.5 µl
BD Bioscience	Mouse	SJ25C1	CD19	QD V500	2 µl
Biolegend	Mouse	UCHT1	CD3	PerCP	0.5 µl
Biolegend	Rat	17A2	CD3	PE-Cy7	1 µl
Biolegend	Mouse	UCHT1	CD3	H7 APC	0.5 µl
Miltenyi Biotec	Mouse	M-T466	CD4	APC	2 µl
Miltenyi Biotec	Mouse	VIT4	CD4	PE-Cy7	2 µl
Miltenyi Biotec	Mouse	BW135/80	CD8	FITC	2 µl
Miltenyi Biotec	Mouse	RPA-T8	CD8	APC	2 µl
BD Bioscience	Mouse	RPA-T8	CD8	PE-Cy7	3 µl
BD Bioscience	Mouse	RPA-T8	CD8	QD V705	3 µl
Beckman Coulter	Mouse	IM2217U	CD8B	PE	2 µl
Biolegend	Mouse	BB7.2	HLA-A2	FITC	1 µl

Biolegend	Mouse	FN50	CD69	APC-Cy7	1 µl
Biolegend	Mouse	OX34	rat CD2	FITC	1 µl
Biolegend	Mouse	OX34	rat CD2	PE	0.5 µl
Biolegend	Mouse	IP26	αβTCR	FITC	1 µl
BD Bioscience	Mouse	D21-1351	MIP1ß	PE	1 µl
BD Bioscience	Mouse	B27	IFNγ	V450	3 µl
BD Bioscience	Rat	MQ1-17H12	IL-2	APC	4 µl
BD Bioscience	Mouse	MAb11	TNFα	PE-Cy7	3 µl
BD Bioscience	Mouse	H4A3	CD107a	BV785	(pre-titred)

Table 2.9: Antibodies used for flow cytometry in this thesis
(All targets are human unless otherwise stated)

2.5.2 A2 Staining of PBMC

Following isolation of fresh PBMC from healthy donors, 10^5 PBMC were counted and resuspended in 40 µl of PBS and stained with fixable violet fluorescin amine dye (ViViD, Life Technologies) at a 1 in 800 dilution. PBMC were washed and resuspended in 40 µl of FACS buffer then stained with 1 µl of αHLA-A2-FITC. Cells were incubated at 4 °C in the dark for 20 minutes, before washing in PBS and resuspending in FACS buffer. Cells were analysed using a FACSCanto flow cytometer. Data were analysed, and the HLA-A2 restriction of healthy PBMC donors recorded for later experiments.

2.5.3 Tetramer Staining of directly *ex vivo* PBMC

Following isolation of fresh PBMC from healthy donors, 10^5 PBMC were counted and resuspended in 40 µl of PBS and stained with fixable violet fluorescin amine dye (ViViD, Life Technologies) at a 1 in 800 dilution. PBMC were washed and resuspended in 40 µl of FACS buffer then stained with either A2 DT227/8KA, A2 A245V, A2, A2 Q115E, A2/K^b A245V, or A2/K^b tetramers folded around ELAGIGILTV at 0.5, 50, or 50 µg/ml for 20 min at 37 °C. PBMC were washed and resuspended in 40 µl of PBS, resuspended in FACS buffer, and stained with αCD14-PB, αCD19-PB, αCD3-PE-Cy7, αCD4-APC, and αCD8-FITC for 20 minutes at 4 °C. Cells were washed twice in PBS and fixed in 100 µl 1% paraformaldehyde (PFA). Data were acquired using a FACSCanto flow cytometer, and analysed using FlowJo software.

2.5.4 HLA-A2 Staining of C1R B-cells

C1R B-cells in culture were counted and 5 wells each containing 5 x 10^4 of each cell line were resuspended in 40 µl FACS buffer, and stained with fixable violet fluorescin amine dye (ViViD, Life Technologies) at a 1 in 800 dilution. A serial dilution of αHLA-A2-FITC in FACS buffer was prepared giving rise to a dilution of 1 in 1000, 1 in 2000, 1 in 4000, and 1 in 8000. Cells were washed and resuspended in 40 µl of either FACS buffer (unstained control) or each of the antibody dilutions. The cells were incubated for 15 minutes at 4 °C in the dark, before washing twice in PBS and resuspending in 100 µl of 1% PFA. Data were acquired using a FACSCanto flow cytometer, and analysed using FlowJo software.

2.5.5 Staining of Transduced Immortal Cell lines for Sorting

Lentivirally cells lines (J.RT3-T3.5 or H9) were counted and resuspended in FACS buffer at 10^6 /ml. 5 x 10^6 cells were re-suspended in 500 µl PBS and stained with fixable violet fluorescin amine dye (ViViD)(Life Technologies) at a 1 in 800 dilution for 5 minutes in the dark at room temperature, gently agitating throughout. Cells were then washed, re-suspended in 500 µl PBS, and stained with 2 µl αCD2-FITC, 5 µl αCD8ß-PE and 5 µl αCD8α-APC for 15 minutes at 4 °C in the dark, gently agitating throughout. Cells were then washed twice before re-suspending in FACS buffer. Cells were analysed and sorted using a modified FACSAriaIITM flow cytometer. Sorting was continued until 5 x 10^5 cells were obtained, or as many as possible.

2.5.6 Staining Immortal Cell Lines for Maintenance of Phenotype following expansion post-sorting

10^5 cells were counted and re-suspended in 40 µl PBS and stained with fixable violet fluorescin amine dye (ViViD)(Life Technologies) at a 1 in 800 dilution for 5 minutes in the dark at room temperature. Cells were then washed and re-suspended in 40 µl PBS and stained with appropriate antibodies (αCD8ß-PE, αCD8α-APC, and αrCD2-FITC, occasionally αTCRαß-FITC αCD3PerCP, αrCD2-PE, and αCD8α-PE-Cy7 were also used) for 20 minutes at 4 °C. Cells were washed twice in PBS and fixed in 100 µl 1% PFA. Data were acquired using a FACSCanto flow cytometer, and analysed using FlowJo software.

2.5.7 Tetramer Staining of J.RT3-T3.5 T-cell lines

5 x 10^4 cells of each of J.RT3-3.5 ILA1 TCR^+ $CD8\alpha\beta^-$, J.RT3-3.5 ILA1 TCR^+ $CD8\alpha\beta^+$, and J.RT3-3.5 ILA1 TCR^+ $CD8\alpha S53N\beta^+$ were counted and re-suspended in 40 µl PBS, before staining with fixable violet fluorescin amine dye (ViViD)(Life Technologies) at a 1 in 800 dilution for 5 minutes in the dark, at room temperature. Cells were washed in PBS, re-suspended in 40 µl PBS and stained with either A2 *wild type* (**A**) or A2 277/8 (**B**) tetramers folded around ILAKFLHWL at 25 µg/ml for 20 min at 37 °C in the dark. Cells were washed twice and fixed in 100 µl 1% PFA. Data were acquired using a FACSCanto flow cytometer, and analysed using FlowJo software. 2 x 10^4 events were captured, and dead and dying cells were excluded from analysis.

2.5.8 Activation of JR.T3-T3.5 lines

6 x 10^5 C1R A2 target cells were incubated in 50 µL of R2 media with peptide, added at the desired final concentration (10^{-4} – 10^{-10}, and 0 M). The target cells were pulsed with peptide for one hour before washing twice with R2 media. 3 x 10^5 of each J.RT3-3.5 T-cell line, suspended in 50 µL of R2 media, were applied to the peptide pulsed targets and incubated at 37 °C overnight. Cells were washed and re-suspended in 40 µl FACS buffer, before staining with fixable violet fluorescin amine dye (ViViD)(Life Technologies) at a 1 in 800 dilution for 5 minutes in the dark, at room temperature. Cells were washed in PBS, re-suspended in 40 µl FACS buffer and stained with αCD19-PB and αCD69-APC for 20 minutes at 4 °C, in the dark. Cells were washed twice with PBS and fixed in 100 µl 1% PFA. Data were acquired using a FACSCanto flow cytometer, and analysed using FlowJo software. 5 x 10^4 events were captured, and both $CD19^+$ and dead and dying cells (Pacific $Blue^+$) were excluded from analysis.

2.5.9 Intracellular Staining (ICS)

$CD8^+$ T-cell clones were rested overnight in R2 media. C1R B-cell targets were counted, plated at 5 x 10^5 / ml (2 x 10^4 / 50 µl / well) in R2 media, and pulsed with peptide at a final concentration of (10^{-2} – 10^{-8} M, and 0 M) for 1 hour. The serum-starved $CD8^+$ T-cells were counted, and resuspended at 10^6 / ml (5 x 10^4 / 50 µl) in R2, supplemented with 2 µl/ml brefeldin A (GolgiPlug; Sigma-Aldrich), 14 µl/ml monensin (GolgiStop; BD Biosciences), and 10 µl/ml αCD107a-FITC. $CD8^+$ T-cells were plated together with the peptide-pulsed targets (50 µl of T-cell suspension added per well of B-cell targets), thus giving a final concentration / well of 1 µl/ml brefeldin A, 7 µl/ml monensin, and 5 µl/ml αCD107a-FITC.

The cells were incubated together for 4 hours and 18 hours at 37 °C and in a 5% CO_2 atmosphere. Following incubation, cells were washed with PBS, and stained with LIVE/DEAD fixable Aqua dead cell stain (Invitrogen™, ThermoFisher) at a 1 in 1000 dilution for 10 minutes at room temperature, protected from light. Cells were washed and subsequently stained with αCD19-BV500, αCD3-H7 APC, and αCD8-QD V705 at 4 °C, in the dark, for 20 minutes. Cells were washed twice with PBS and subsequently resuspended in 200 µl BD Cytofix/Cytoperm then incubated at 4 °C for 20 minutes in the dark. Cells were washed thrice in 1 x Perm/Wash (BD Biosciences), before staining with αIFNγ-V450, αTNFα-PE-Cy7, αMIP1ß-PE and αIL-2-APC at 4 °C for 20 minutes. Cells were washed three times before resuspending in 200 µl Perm/Wash. Data was acquired using a modified FACSAria II flow cytometer (BD Biosciences) and analysed with FlowJo software (Tree Star).

2.6 T-Cell Activation Assays

2.6.1 Non-specific Activation by C1R B-cell targets

$CD8^+$ T-cell clones were rested overnight in R2 media. The serum-starved $CD8^+$ T-cells were counted and resuspended at 6 x 10^5 /ml (i.e. 3 x 10^4 / 50 µl). C1R B-cell targets were counted, and resuspended at 6 x 10^5 /ml, 1.2 x 10^6 /ml, 3 x 10^6 /ml, and 6 x 10^6 /ml (3 x 10^4, 6 x 10^4, 1.5 x 10^5, and 3 x 10^5 / 50 µl, respectively). Subsequently, 3 x 10^4 $CD8^+$ T-cells were plated, and incubated together with C1R B-cells stably transfected with similar levels of A2 or each of its mutants, at different E: T ratios for 4 or 18 hours at 37 °C. The supernatant was harvested and assayed by ELISA for IFNγ (R & D Systems), as per manufacturers instructions.

2.6.2 Chromium Release Killing Assay

10^6 C1R B-cell targets stably transfected with similar levels of HLA A2 or each of its mutants, were counted, and resuspended in 1 ml of R2 media. Each C1R cell line was labelled with 30 µCi of ^{51}Cr (PerkinElmer, Cambridge, UK), and incubated for 1 hour. Cells were washed twice, re-counted, and resuspended at a concentration of 5 x 10^3 per 100 µl R2 media. Each target was incubated together with rested and counted $CD8^+$ T-cell clones at different effector: target ratios. The cells were incubated together for 4 hours at 37 °C in a 5 % CO_2 atmosphere. Each species of target was also cultured alone (target spontaneous release) and with TritonX-100 (Sigma-Aldrich) at a final concentration of 5% (target total release). 15 µl supernatant was harvested from each and mixed with 150 µl OptiPhase Supermix Scintillation Cocktail (PerkinElmer). Plates were analysed using a liquid scintillator and luminescence counter (MicroBeta TriLux; PerkinElmer) with Microbeta Windows Workstation software (PerkinElmer). Specific lysis was calculated according to the following formula:

$$\left(\frac{\text{experimental release - target spontaneous release}}{\text{target total release - target spontaneous release}} \right) \times 100\%$$

2.6.2 Peptide Activation of $CD8^+$ T-cell clones

$CD8^+$ T-cell clones were rested overnight in R2 media. The serum-starved $CD8^+$ T-cells were counted and resuspended at 6 x 10^5 /ml (i.e. 3 x 10^4 / 50 µl). 6 x 10^4 C1R A2 target cells were incubated in 50 µL of R2 media with peptide at a final concentration of 10^{-5} – 10^{-11}, and 0 M at 37 °C for 1 hour, before washing twice in R2 media. The peptide pulsed targets were then incubated together with 3 x 10^4

$CD8^+$ T-cells at 37 °C for 4 or 18 hours. The supernatant was harvested, and assayed for IFNγ or MIP1ß by ELISA (R & D Systems), as per manufacturer's instructions.

2.6.3 Peptide Activation of H9 ILA1TCR$^+$ CD8α^{var}ß T-cell lines.

H9 ILA1 TCR$^+$ CD8α^{var}ß lines were rested in R2 for 48 hours. 6 x 10^4 C1R A2 target cells were incubated in 50 µL of R2 media with peptide, as described in later chapters for the ILA system, added at a final concentration of 10^{-2} – 10^{-8} and 0 M. The target cells were pulsed with peptide for two hours before washing twice and resuspending in 50 µl of R2 media. 3 x 10^4 of each H9 ILA1 TCR$^+$ CD8α^{var}ß line, suspended in 50 µL of R2 media, were applied to the peptide pulsed targets and incubated at 37 °C overnight. The supernatant was harvested and assayed for IL-2 or IL-10 by ELISA as per manufacturer's instructions.

2.6.4 Peptide Activation of J.RT3-T3.5 NFAT gluc lines.

The J.RT3-T3.5 NFAT gluc cell lines were rested in R2 media for 24 hours prior to activation experiments. 6 x 10^5 C1R A2 target cells were incubated in 50 µL of R2 media with peptide, added at a final concentration of 10^{-4} – 10^{-10}, and 0 M. The target cells were pulsed with peptide for two hours before washing twice with R2 media. 6 x 10^5 J.RT3-3.5 NFAT GLuc transTCR$^+$ CD8α^{var}ß T-cells were suspended in 50 µL of R2 media, and incubated together with the peptide-pulsed B-cell targets at 37 °C for 24 hours. Subsequently, the supernatant was harvested, and assayed for luciferase protein by bioluminescence as per manufacturer's instructions.

2.6.5 ELISA (R & D Systems)

ELISA kits for IFNγ and MIP1ß were supplied by R & D Systems, and were performed according to the manufacturer's instruction, using reagents as advised (DuoStop®)(Wash Buffer, Coating buffer, Diluent, Streptavidin HRP, Colour reagents A & B (Chromogen), Peroxide and STOP solution). Half-area 96 well plates were coated with 50 µl of capture antibody, diluted as per manufacturer's protocol. Plates were sealed and incubated overnight at room temperature, or for one hour at 37 °C. Plates were washed twice using an Atlantis 2 line microplate washer (Biochrom Asys Atlantis, Biochrom, UK). Plates were blocked for one hour with 150 µl blocking antibody, diluted as per manufacturer's instructions. Plates were washed, and 50 µl cell supernatant added, alongside 50 µl of a serially diluted standard solution. Plates were incubated at room temperature for 75 minutes, and subsequently washed, before adding 50 µl of detection antibody, diluted as per manufacturer's instructions added. Plates were incubated for a further 20 minutes, washed and 50 µl of streptavidin horseradish peroxidase (StrepHRP), diluted as per manufacturer's instructions, was added to wells. Plates were again washed, and 25 µl of each of colour reagent A and B (chromogen and peroxide) were added to wells, before incubating for up to 20 minutes, protected from light, until colour change was appropriately developed (using standards). 25 µl of STOP solution (sulphuric acid) was added to wells, and the plates were read immediately at 450 nm wavelength, using a reference of 570 nm (BioRad iMark microplate reader, BioRad).

2.6.6 *Gaussia* Luciferase Bioluminescence Assay

Gaussia luciferase (GLuc) is a reporter luciferase, expressed in mammalian cells that have been transduced with reporter plasmids (commercially available, NEB). The J.RT3-T3.5 NFAT GLuc line is transduced to express GLuc upon activation of through the NFAT (Nuclear factor of Activated T-cells) cascade. Upon activation, cells have high levels of reporter luciferase GLuc in their cytoplasm, and it is secreted into the surrounding media. Whilst these cells can be lysed for assay, the test was found to be sensitive enough for assay of supernatant alone.

Luciferase production, indicative of NFAT activation, was measured using a BioLux® *Gaussia* Luciferase assay kit (NEB), as per manufacturer's instructions. Briefly, the substrate was diluted in BioLux assay buffer 100:1. An opaque (white-walled) half-area 96-well plate (Corning) was used for the assay. 25 µl of the diluted substrate was added to each well, followed by 5 µl of the culture supernatant sample immediately prior to reading. A FLUOStar Optima spectrometer (BMG Labtech) was used to read the assay, set to read bioluminescence.

Chapter 3

$CD8^+$ T-cell specificity is compromised at a defined major histocompatibility complex class I/CD8 affinity threshold

3.1 Introduction

The CD8 co-receptor is capable of binding all MHCI complexes. It binds to the largely invariant region of the MHCI (Wooldridge et al., 2007, Gao et al., 1997b), thus its binding is unaffected by the presented peptide, and in doing so, enhances T-cell antigen sensitivity. The TCR has the potential to engage MHCI presenting both self and foreign peptides (Yachi et al., 2005, Colf et al., 2007). In addition, it has been suggested that the pMHCI/CD8 interaction may enable T-cell recognition at low copy numbers of specific pMHCI or low avidity ligands (Hampl et al., 1997). The pMHCI/CD8 interaction is characterized by very weak affinities (up to 100x weaker than the TCR/pMHCI interaction) and extremely rapid kinetics (K_{off} in the order of $18s^{-1}$) (Wyer et al., 1999, Huang et al., 2007, Hutchinson et al., 2003). These biophysical properties do, however, differ somewhat between species; for example murine CD8 binds the murine H-$2K^b$ MHCI with a K_D of ~ 30 μM, whereas human CD8 binds the comparable human HLA A*0201 (A2 hereafter) MHCI with a K_D of ~ 120 μM (Purbhoo et al., 2001). The significance of these species differences remains uncertain, however it has been suggested this may be due to differences in the size of the T-cell repertoire; the mouse having less TCRs in comparison to man (Arstila et al., 1999, Casrouge et al., 2000).

Previous studies have shown that as the pMHCI/CD8 interaction strength increases, so too does the sensitivity of the antigen specific T-cell response (Sun et al., 1995, Wooldridge et al., 2007, Sanders et al., 1991). The relationship is neither simple nor

direct: initially, the increase is disproportionate, with a x 1.5 fold increase in the strength of the pMHCI/CD8 interaction resulting in antigen sensitivity being increased by up to two orders of magnitude. Above a certain strength of pMHCI/CD8 interaction, this response becomes non-specific, leading to T-cell activation irrelevant of the specificity of the TCR or the nature of the presented ligand (Wooldridge et al., 2010a). Other studies have examined the effects of reducing the strength of the pMHCI/CD8 interaction (~ K_D = 500 μM) or abrogating its binding altogether (Xu et al., 2001, Gao et al., 2000) on $CD8^+$ T-cell activation. I intend to classify the effects of manipulating the strength of the pMHCI/CD8 interaction in more detail by examining the point at which $CD8^+$ T-cell activation becomes non-specific i.e. how far the strength of this interaction may be increased before the observed loss of specificity is seen. Defining this threshold has importance in the development of novel therapeutic approaches for patient benefit, where enhanced target killing may be desirable. In this instance, it is vital that the specificity of the TCR be maintained.

3.1.1 The Tripartite complex: CD8 as a co-receptor to the TCR/pMHCI interaction

Individual TCRs are capable of recognizing large numbers of pMHCI ligands (up to 10^6) (Wooldridge et al., 2012), and indeed this feature is quintessential to maintaining a T-cell repertoire that is poised to recognize all potential pMHCIs that could be encountered. Many of these 'possible' pMHCI ligands are not 'real' i.e. they do not occur in nature and will never be presented at the cell surface in the context of MHCI, nonetheless the promiscuity of the TCR remains an essential feature of an effective immune system. Whilst a plethora of pMHCI ligands may be recognized by a single TCR, the affinity of the TCR/pMHCI interaction can vary considerably, with the

recognition of pathogen derived pMHCI agonists being characterized by high affinity TCR/pMHCI interactions (mean K_D of ~ 8 μM) (Bridgeman et al., 2012) and TCR interactions with self-peptide MHCI (auto-antigens) being typified by much weaker TCR/pMHCI interactions (mean K_D of ~ 90 μM) (Bridgeman et al., 2012). Indeed, thymic selection of the T-cell repertoire relies on these very features; TCRs are selected which recognise self-antigen weakly. They do not encounter foreign antigens until presented with such a challenge, however the promiscuity of the TCR facilitates the likelihood that suitable T-cells may recognise and respond to the challenge. It is also believed that weak and on-going stimulation by self-antigens allows the naïve population and memory pool to persist in the periphery in the absence of a specific challenge (Goldrath and Bevan, 1999, Boyman et al., 2009, Anderton and Wraith, 2002). Antigens which can be found on neoplastic cells, whilst still self-antigens, are often subtly different from those expressed on healthy cells (Schumacher and Schreiber, 2015, Wang and Wang, 2017). TCRs which recognise cancer antigens very often do so at an affinity which falls between these two extremes, as one may expect with a peptide which is not completely foreign, and this may be one of the factors explaining how neoplasia may evade the immune system.

TCR engagement with specific pMHCI is necessary for $CD8^+$ T-cell activation, but is in most cases inadequate for a complete response (Holler and Kranz, 2003, Laugel et al., 2007a). Co-ligation of MHCI by CD8 is often necessary in order to elicit a complete response, particularly in the case of weaker affinity pMHCI ligands (Daniels and Jameson, 2000, Laugel et al., 2007b). CD8 interaction with the invariant region of the MHCI draws the two molecules together at the T-cell: target cell interface, co-localizing CD8-associated lck and intracellular CD3 (Rybakin et al., 2011).

3.1.2 CD8$^+$ T-cells and cancer

As has already been discussed, TCRs exist which recognise cancer-specific antigens. TCRs recognise self-MHC with an affinity typically weaker than foreign antigens, (mean K_D of ~ 90 μM) (Bridgeman et al., 2012), however significant overlap exists, and the highest TCR/pMHCI interactions documented to date (> 1 μM) are directed against foreign antigen ligands (Davis et al., 1998). Whilst we know these TCRs exist, this TCR/pMHCI interaction strength may in some instances be inadequate to clear the host's cancer, as is evidenced by the existence of this disease (Bridgeman et al., 2010b). Of the TCRs examined by Bridgeman *et al*, several cancer epitopes are recognised with an affinity not dissimilar to foreign. Indeed, the mean of the cancer interactions examined in this study is 41 μM, falling only a little lower than that of the foreign TCR/pMHCI interactions (32 μM). The persistence of these cancers in the host leads us to deduce that there must be further reasons for this apparent failure of the immune system to recognise and eliminate this challenge.

Cancer epitopes may be further sub-grouped on the basis of their encoding genes. Some arise *de novo* and are unique to certain cancers, one example being the A24-restricted peptide SYLDSGIHF, which is derived from a mutated ß-catenin gene found in melanomata (Robbins et al., 1996). Tumour antigens may also be non-mutated and cell-line specific, such as epitopes derived from the MART-1 melanoma-specific protein which include the A2-restricted 9-mer, AAGIGILTV, and the similar A2-restricted 10-mer, EAAGIGILTV (Kawakami et al., 1994, Ekeruche-Makinde et al., 2012, Kessler et al., 2011). Onco-foetal antigens are epitopes, which are normally, only found during foetal development, thus their existence in the mature host cell is indicative of pathology. An example of such is NY-ESO-1, which is normally, only found in the developing foetus and the human testis, but may also be expressed in melanoma (Chen et al., 2000, Jager et al., 1998). However, the existence of tumour-

reactive $CD8^+$ T-cells is often insufficient for tumour clearance, but is suggestive of a possible therapeutic approach, as enhancing this response may elicit improved patient survival.

Efforts to create vaccinations using these epitopes has failed to demonstrate effective responses in all but a very few cases, with T-cells being raised in inadequate numbers to result in a reduction in tumour burden (Brinkman et al., 2004, Parmiani et al., 2002). Benign lesions resulting from Human Papilloma Viridae (HPV) have shown some response to autologous vaccines, although such papillomatous 'warts' often auto-regress in time suggesting self clearance, as have equine sarcoids, in which bovine papilloma virus has also been implicated (Kinnunen et al., 1999, Otten et al., 1993). Cancers associated with this type of virus may be prevented or their instance reduced by this type of approach, an example being the HPV-associated cervical cancer vaccine, which prevents aggressive lesions (Schwarz et al., 2009). This vaccine is considered to significantly reduce HPV associated cancers, and is estimated to prevent approximately 70% of cervical cancers. It is now routinely used, at least in girls, in 71 countries (as of 2017) (World Health Organization. Electronic address, 2017).

In addition to this sub-optimal TCR/pMHCI interaction, tumours also utilise many other strategies to evade the host immune system, including down-regulation of pMHCI resulting in a low copy number being expressed at the cell surface, and the creation of an immunosuppressive tumour environment.

Whilst the existence of naturally occurring T-cells which recognise cancer epitopes, has been known for some time, it is only in the last decade that this clinical direction has been pursued in earnest. $CD8^+$ T-cells that recognise tumour antigens were

identified and cultured in the late 80s and early 90s (Jerome et al., 1991, Ioannides et al., 1991, Boon and van der Bruggen, 1996). The earliest work in this field went on to demonstrate that $CD8^+$ T-cells found within the tumour infiltrate were enriched for this type of TCR, and the term Tumour Infiltrating Lymphocyte (TIL) was first utilized. Early research went on to demonstrate that $CD8^+$ T-cells, when cultured and expanded *in vitro* are capable of reducing tumour burden and in some cases elicit tumour clearance (Rosenberg et al., 1986, Dudley and Rosenberg, 2003). This novel strategy in cancer immunotherapy, termed Adoptive Cell Transfer (ACT), utilized *ex vivo* expansion of TILs, and initial reports demonstrated improved patient survival. However, this therapy was still inadequate in some cases, and in recent years much work has been dedicated to improving tumour killing and thus patient survival.

3.1.3 The potential for CD8 manipulation as a method for enhancing ACT therapies

It has already been discussed that small increases in pMHCI/CD8 affinity can result in a disproportionately greater increase in $CD8^+$ T-cell activation (Wooldridge et al., 2007, Wooldridge et al., 2005). It has been demonstrated that super-enhancement of the CD8/pMHCI interaction results in a total loss of TCR antigen specificity resulting in blanket activation of all $CD8^+$ T-cells (Wooldridge et al., 2010a). It is reasonable to hypothesise that there exists a threshold above which the TCR loses specificity, and that increasing the CD8/pMHCI interaction, whilst staying beneath this threshold, should result in maximal enhancement in T-cell activation without the loss of specificity

3.1.4 Super-enhanced CD8 binding leads to total loss of T-cell antigen specificity

The pMHCI/CD8 interaction is characterized by very low solution binding affinities and extremely rapid kinetics. Although some variation exists between different MHCI alleles, due to polymorphisms that affect the CD8 binding site, the average pMHCI/CD8 interaction has a K_D ~ 145μM (K_D range of 100 - 220 μM). There are a small number of exceptions with even weaker pMHCI/CD8 solution binding affinities (K_D ~500 μM), such as HLA A*6801 and HLA A* 4801. The HLA-A*0201 (A2 hereafter) MHCI was chosen for use in this study. It's pMHCI/CD8 affinity falls in the middle of this range, close to the average (K_D ~130-145 μM). Introducing a glutamine (Q) > glutamic acid (E) mutation at position 115 of the MHCI alpha 2 domain has been shown to increase the pMHCI/CD8 solution binding affinity by ~ 1.5 fold (K_D ~ 87 μM) without any affect on TCR/pMHCI binding affinity (Wooldridge et al., 2007). This incremental increase in the strength of the pMHCI/CD8 interaction afforded a significant increase in the sensitivity of pMHCI antigen recognition (up to 100 fold) without any significant loss of T-cell specificity. In a subsequent study it was demonstrated that increasing the strength of the pMHCI/CD8 interaction by ~ 15 fold (K_D~ 10 μM) resulted in a complete loss of pMHCI recognition specificity (Wooldridge et al., 2010a). However the strength of the pMHCI/CD8 interaction at which $CD8^+$ T-cell activation specificity is lost has not been defined. This is the specific research question that I intend to answer in this thesis chapter.

3.1.5 Summary & Aims

$CD8^+$ T-cells are capable of recognizing and eliminating cancerous cells *in vivo*. This has sparked great interest in the use of cellular therapy against cancer. Owing to the

non-polymorphic nature of CD8, such a molecule used as a gene vaccine or transfectant would be globally applicable to enhance ACT systems, and thus a potentially invaluable tool for future potential immunotherapies. Barriers to the widespread use of this approach still exist. One of the most common problems is that 'natural' anti-cancer T-cells are not very antigen sensitive and as a result, not very effective at killing tumour cells. This is because cancer-specific TCRs are often characterized by affinities that are not sufficiently strong to elicit a robust response. One approach that can be used to circumvent this issue is to develop strategies that enhance the cancer-specific T-cell response by increasing the strength of the pMHCI/CD8 interaction. Due to the non-polymorphic nature of CD8, strategies to enhance the antigen specific T-cell response by increasing the strength of the pMHCI/CD8 interaction would be globally applicable to any system in which enhanced T-cell immunity is desirable such as the design of ACT.

Although there is significant scope to increase the strength of the pMHCI/CD8 interaction for therapeutic benefit, it has also been demonstrated that increasing the strength of the pMHCI/CD8 interaction by 10-fold results in complete loss of pMHCI antigen specificity. Before such therapies can be developed it is essential that this loss of TCR specificity is fully characterized. In this chapter, I aim to better characterise the strength of the pMHCI/CD8 interaction, and how it affects the T-cell response. To this end I will use a panel of MHCI variants with different pMHCI/CD8 affinities to determine the pMHCI/CD8 affinity threshold at which loss of pMHCI specificity occurs. Any effort to utilise CD8 manipulation to enhance ACT must ensure that the strength of the pMHCI/CD8 interaction falls short of this threshold to avoid catastrophic consequences for the patient.

3.2 Results

3.2 1 Generating a panel of MHCI mutants with a spectrum of CD8 binding affinities

To determine the pMHCI/CD8 affinity at which loss of pMHCI recognition specificity occurs, it was necessary to design a novel MHCI mutant with a pMHCI/CD8 interaction dissociation constant (K_D) of between 87 μM and 10 μM. In order to achieve this, I introduced an alanine (A) > valine (V) substitution at position 245 of A2/K^b (a fusion molecule comprising the α1/α2 peptide binding platform of HLA A2 and the α3 domain of H2-K^b) to give A2/K^b A245V. Surface plasmon resonance (SPR) confirmed that A2/K^b A245V interacts with CD8 with a K_D of 27.8 μM (Figure 3.1B) and importantly, does not affect the TCR/pMHCI interaction (Figure 3.1D). Construction of this novel MHCI mutant extends the panel of MHCI mutants that are available for performing comprehensive studies on the affect of varying the strength of the pMHCI/CD8 interaction. The complete panel consists of MHCI variants that exhibit abrogated (A2 DT227/8KA), weak (A2 A245V), *wild type* (A2), slightly enhanced (A2 Q115E), enhanced (A2/K^b A245V) and super-enhanced (A2/K^b) interaction with CD8 (Table 3.1). SPR measurements confirm that none of these MHCI mutations have any effect on the strength of the TCR/pMHCI interaction. This extended panel of MHCI mutations, which is represented as a schematic in Figure 3.2, were either introduced into soluble MHCI for the subsequent construction of pMHCI tetramers or expressed at the cell surface of C1R B-cells (Figure 3.3).

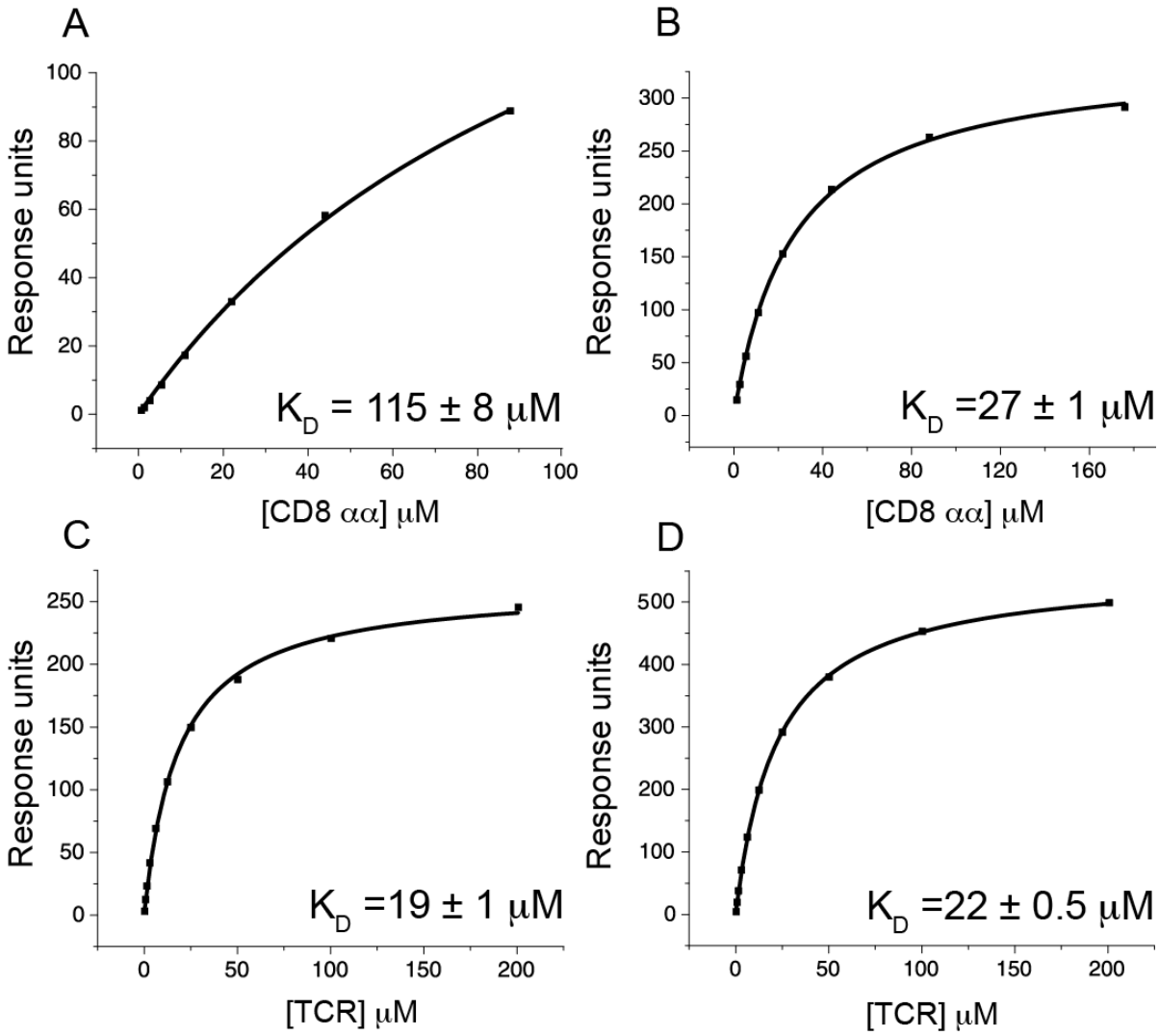

Figure 3.1: A2/K^{b}A245V exhibits enhanced affinity for CD8 without impacting the TCR/pMHCI interaction.

Biotinylated A2 (**A&C**) or A2/K^b A245V (**B&D**) pMHCI monomers folded around the heteroclitic ELAGIGILTV epitope were immobilized on a streptavidin-coated BIAcore chip. Serial dilutions of soluble human CD8αα (**A&B**) or MEL5 TCR (**C&D**) were flowed over the chip to measure equilibrium binding by surface plasmon resonance. Data were analysed using BIAevaluation 3.1, Microsoft Excel and Origin 6.1.

Location of Mutation	Description of Mutation	pMHCI/CD8 K_D (μM)
MHCI α3 domain	A2 DT227/8KA	> 10,000 (NTB) *
MHCI α3 domain	A2 A245V	498 *
wild type	no mutation	137 ± 9.7 *
MHCI α2 domain	A2 Q115E	98 ± 14.5 *
MHCI α3 domain	A2/K^b A245V	27.8 ± 0.7
MHCI α3 domain	A2/K^b	10.9 *

Measurements taken from Wooldridge *et al*, 2005, Wooldridge *et al,* 2007, and Wooldridge *et al*, 2010.
NTB: No detectable binding

Table 3.1: Summary of mutations examined in this chapter.
Table of HLA A2 mutations, and their respective affinity for CD8αα as measured by SPR. These point mutations in the MHCI molecule influence CD8 binding, without affecting TCR binding affinity (Wyer et al., 1999, Purbhoo et al., 2001, Xu et al., 2001, Wooldridge et al., 2007, Ekeruche-Makinde et al., 2012, Wooldridge et al., 2010, Clement et al., 2011, Huang et al., 2010).

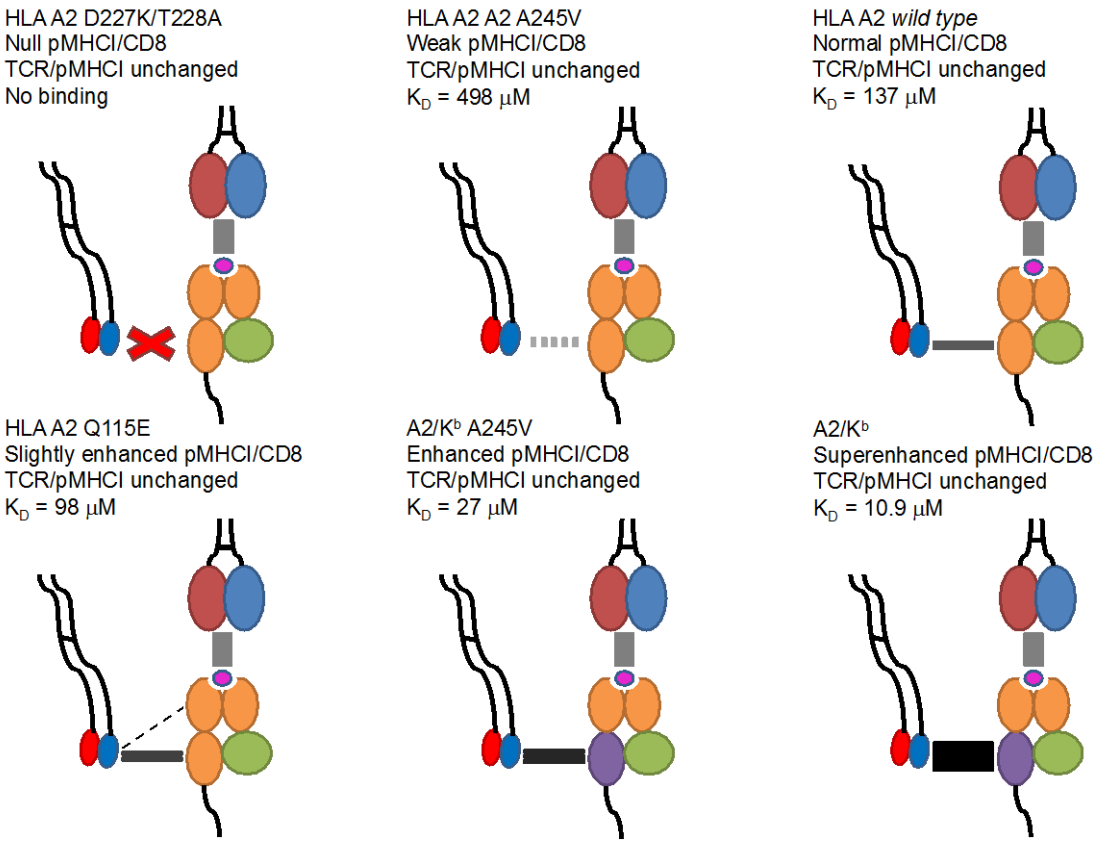

Figure 3.2: Schematic representation of the mutations used in this chapter
pMHCI/CD8 binding affinity of HLA A2 mutants demonstrating abrogated, decreased, normal, slightly enhanced (x1.5), enhanced (x5) and superenhanced (x10) affinity. The TCR binding platform and thus the interaction of the TCR with pMHCI remain unaffected by each of these mutations.

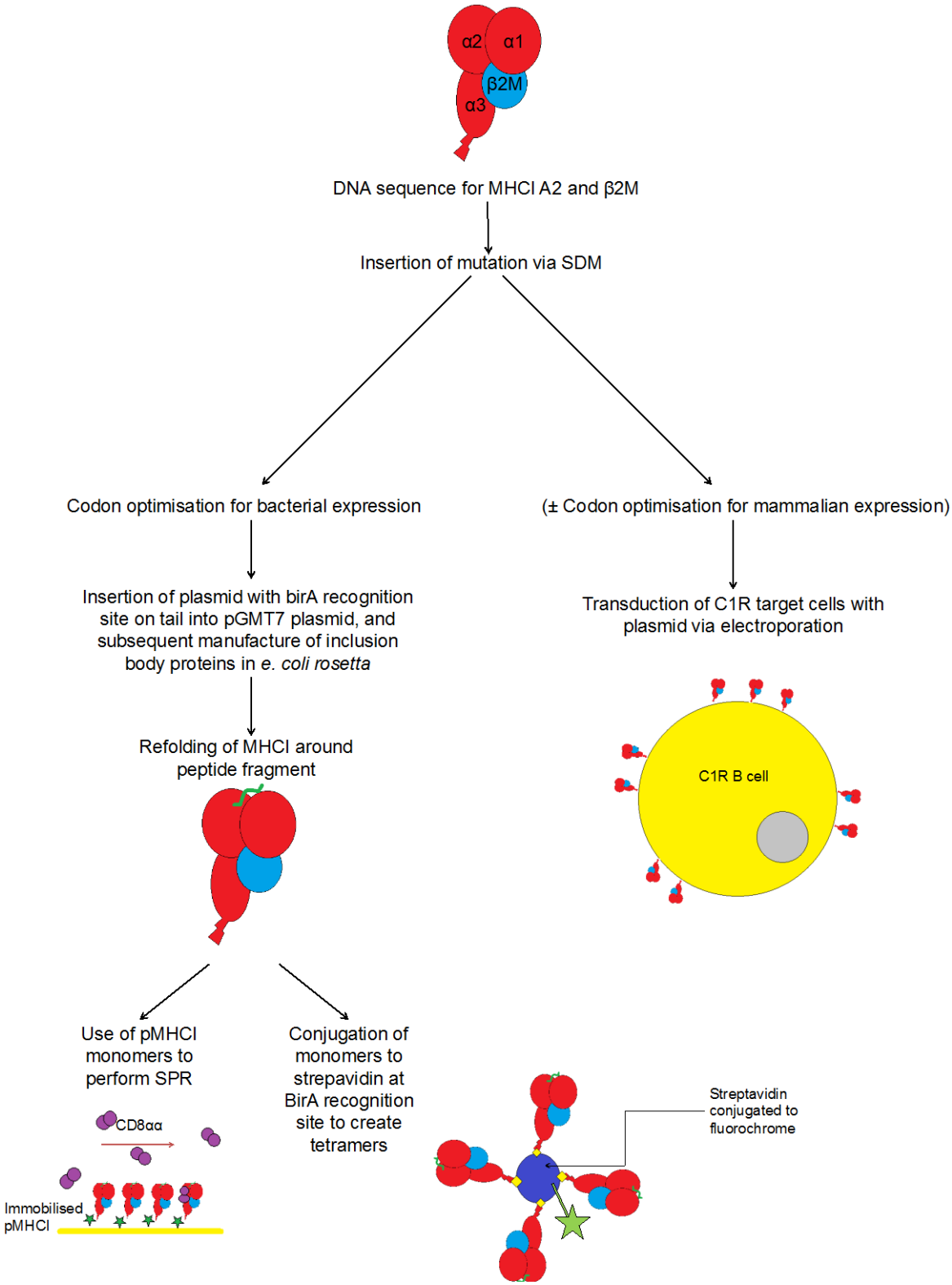

Figure 3.3: Mutations used in this study
Mutations were inserted into either synthetic monomers, which were used for SPR studies or to measure staining using multimer technology, or into stably transfected C1R targets for cell function assays.

3.2.2 Increasing the strength of the pMHCI/CD8 interaction results in enhanced recognition of pMHCI by the TCR

pMHCI monomers for each of the MHCI mutants described in Table 3.1, were created by refolding the heavy chain bearing each mutation around the peptide ELAGIGILTV, with human ß2m, and used to create pMHCI tetramers (Figure 3.3). ELAGIGILTV is a heteroclitic variant of the A2 restricted Melan-A/MART-1_{26-35} epitope, EAAGIGILTV. Monomeric pMHCI complexes bind cell surface TCRs with an extremely short half-life, and for this reason are unsuitable tools for examining cell-surface interactions. The use of multimers such as tetramers and dextramers is a well-documented means of overcoming this limitation, and examining cell surface interactions enabling us to characterize $CD8^+$ T-cells (Altman et al., 1996). Tetramers increase the valency to four by means of conjugation with streptavidin, which is in turn conjugated to a fluorochrome to facilitate examination of antigen specific T-cells by flow cytometry (Wooldridge et al., 2009). These tetramers were used to stain 3 different A2-restricted, ELAGIGILTV-specific $CD8^+$ T-cell clones: MEL2, MELc5 and MEL5 (Figure 3.4A-C).

In all cases, pMHCI tetramer staining where CD8 binding was abrogated (A2 DT227/8KA) was minimal, or indistinguishable from the unstained control. As the strength of the pMHCI/CD8 interaction increased, an increase in the level of pMHCI tetramer staining was observed, with maximal staining being seen with the $A2/K^b$ tetramer. The results clearly show enhanced recognition of specific pMHCI at the cell surface as the strength of the pMHCI/CD8 interaction is increased (Figure 3.4A-C). In addition, the data obtained appears to show a plateau effect such that increases in the strength of the pMHCI/CD8 interaction above a certain threshold (K_D < 30 µM) result in a minimal increase in pMHCI recognition as measured by tetramer staining (Figure 3.4C).

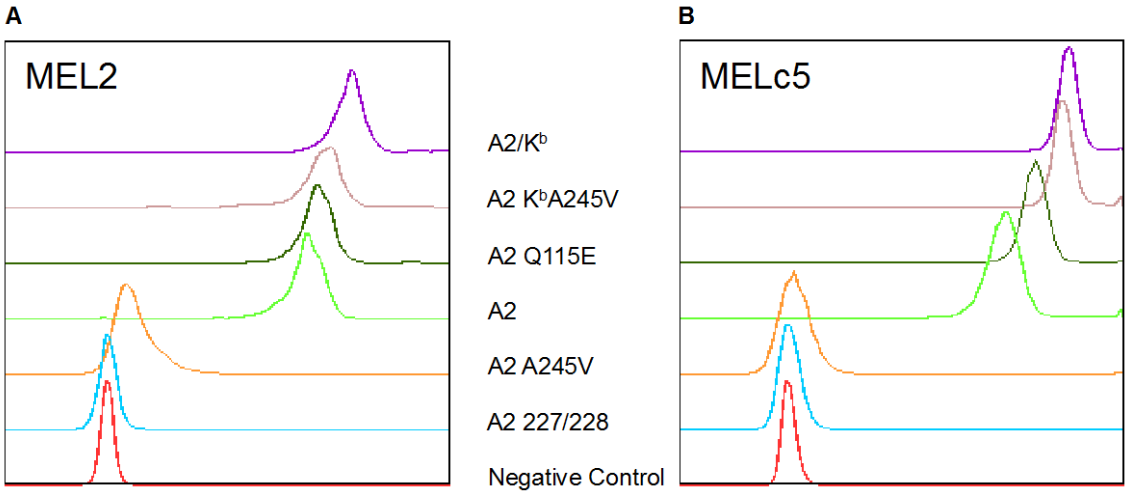
A
MEL2
B
MELc5
A2/Kb
A2 KbA245V
A2 Q115E
A2
A2 A245V
A2 227/228
Negative Control

C

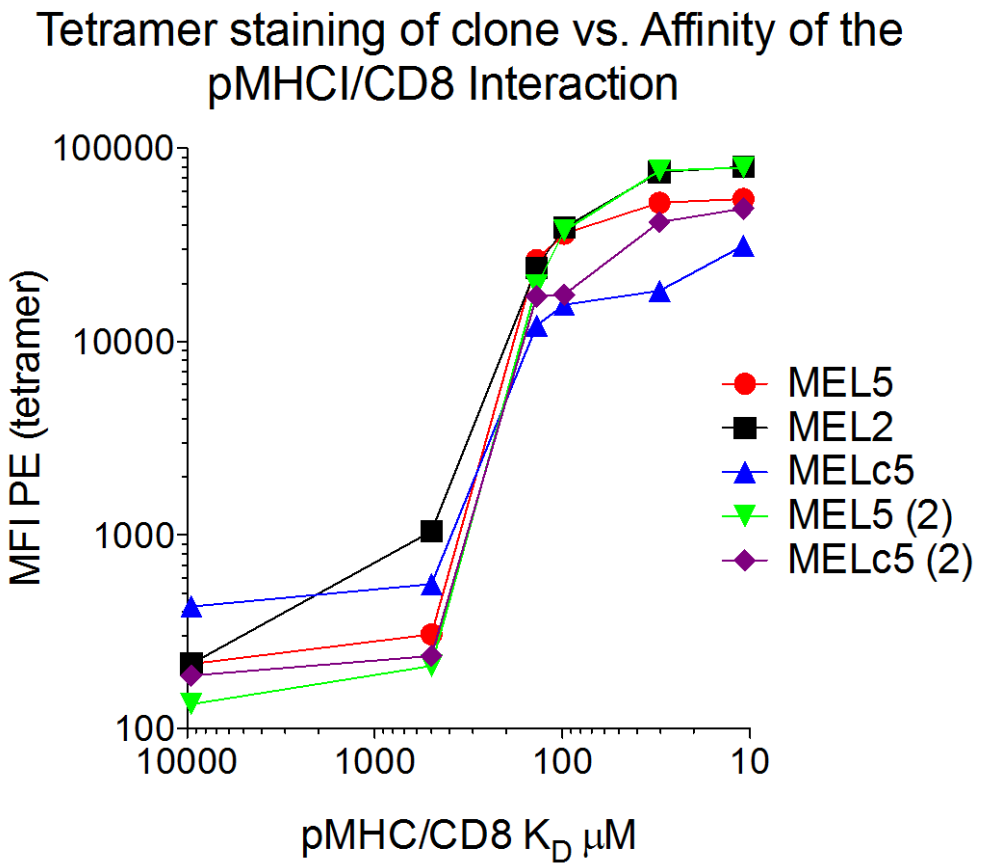
Tetramer staining of clone vs. Affinity of the pMHCI/CD8 Interaction
MFI PE (tetramer)
100000
10000
1000
100
10000
1000
100
10
pMHC/CD8 KD µM
MEL5
MEL2
MELc5
MEL5 (2)
MELc5 (2)

Figure 3.4: Tetramer staining vs. pMHCI/CD8 affinity of HLA A2-restricted ELAGIGILTV-specific clones

The effect of altering the strength of the pMHCI/CD8 interaction on tetramer staining of three HLA A*0201 ELAGIGILTV-specific $CD8^+$ T-cell clones was examined Cells were stained with either A2 DT227/8KA, A2 A245V, A2, A2 Q115E, $A2/K^b$ A245V or $A2/K^b$ tetramers folded around the ELAGIGILTV peptide. Data were acquired using a FACScanto flow cytometer, and analysed using FloJo software. Viable events are shown in histogram plots for the MEL2 clone (**A**) and the MELc5 clone **(B). C** depicts a summary of events recorded for all clones examined, as compared to the pMHCI/CD8 binding affinity of the mutants. These data are representative of multiple (>8) experiments.

3.2.3 Specificity of pMHCI recognition is compromised at a defined pMHCI/CD8 affinity threshold

An essential feature of the TCR is its unique and exquisite specificity, and it is well documented that tetramers replicate this in their staining (Burrows et al., 2000). Blood was obtained from healthy donors of known A2 restriction. Fresh PBMC were isolated from these donors and stained with the A2 mutant tetramer panel at 0.5, 5, and 50 µg/ml, then subsequently stained for CD14, CD19, CD3, CD4, and CD8. Live, $CD14^-$, $CD19^-$, $CD3^+$ cells were gated upon, as shown in Figure 3.5, to allow for examination of tetramer staining of $CD8^+$ T-cells (Figures 3.6 & 3.7).

No background staining was observed with wild type A2 tetramers in $A2^{pos}$ or $A2^{neg}$ (Figures 3.6 & 3.7). This is to be expected; in the absence of alloreactivity (which was not observed in any of the $A2^{neg}$ restricted donors examined), one would not expect $A2^{neg}$ restricted individuals to harbour TCRs specific for A2-restricted epitopes. A total loss of tetramer staining specificity was seen when donor PBMC were stained with the $A2/K^b$ tetramer, with over 85% of $CD8^+$ T-cells staining tetramer positive (Figures 3.6 & 3.7). This has previously been observed and published with $A2^{pos}$ donors (Wooldridge et al., 2010a), and here, the same pattern was observed with both $A2^{pos}$ and $A2^{neg}$ donors (Figures 3.6 & 3.7). These experiments were repeated multiple times (n>10) at a single tetramer concentration (25 µg/ml) and the same pattern was observed, although in earlier experiments the A2 specificity of the donor was not known. This supports my hypothesis that once pMHCI/CD8 affinity is enhanced above a certain level, this interaction becomes dominant over the TCR/pMHCI interaction. Here we see that irrelevant of the peptide ligand, or even the presenting MHCI, the interaction with CD8 becomes the driving force, with the kinetics being stabilised to such an extent as to facilitate tetramer staining even with little or no recognition of the pMHCI by the TCR itself.

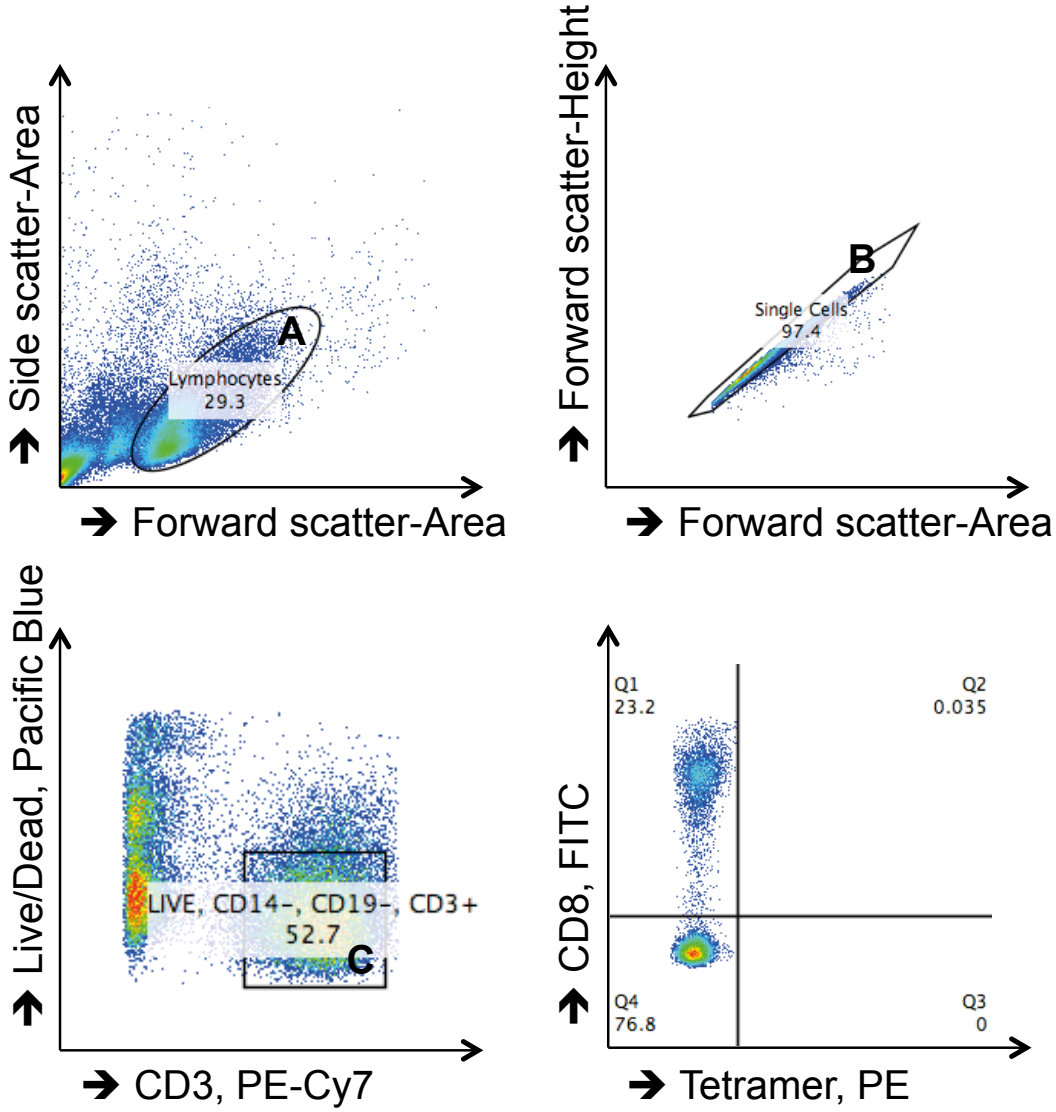

Figure 3.5: Gating Strategy employed for Figures 3.6 & 3.7:
Data were acquired using a FACScanto flow cytometer, and analysed using FloJo software. Data were plotted displaying forward scatter/side scatter area, and this plot was used to gate on a live lymphocyte population **(A)**. Data within this gate only were then plotted on a forward scatter area/height plot to enable doublets or dividing cells to be eliminated **(B)**. Live $CD3^+$ events were gated upon **(C)**. The resultant populations were taken forward for analysis. A quadrant gate was applied using the A2 tetramer applied at 50 µg/ml was used to set the gates for each figure. These gates were then applied to all samples analysed.

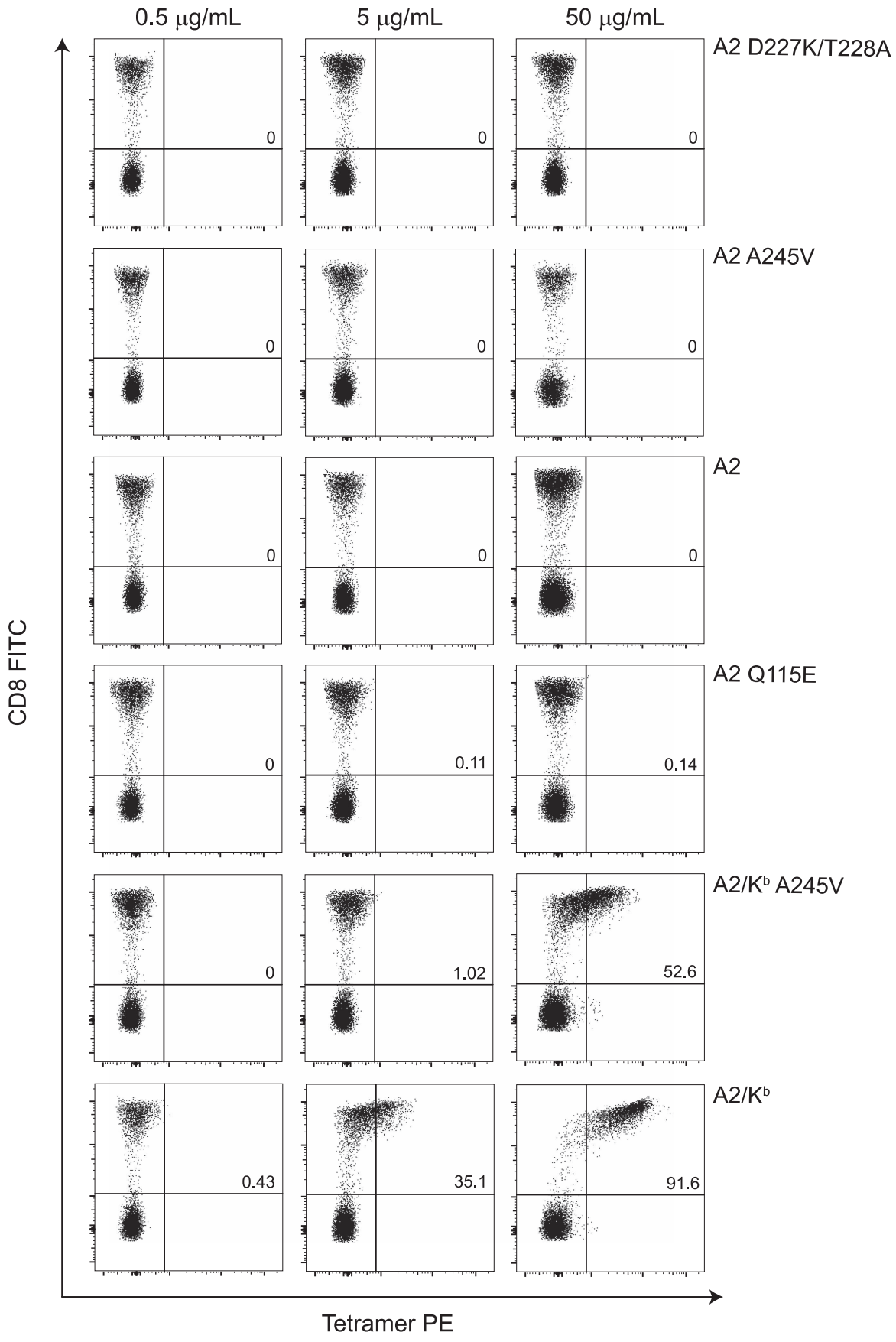
0.5 μg/mL
5 μg/mL
50 μg/mL
A2 D227K/T228A
A2 A245V
A2
A2 Q115E
A2/Kb A245V
A2/Kb
0
0
0
0
0
0
0
0
0
0
0.11
0.14
0
1.02
52.6
0.43
35.1
91.6
CD8 FITC
Tetramer PE

Figure 3.6: The effect of altering the strength of the pMHCI/CD8 interaction on tetramer staining of PBMC from an $A2^{pos}$ donor, directly *ex vivo*.

PBMC were obtained from a known $A2^{pos}$ donor. Following isolation, directly *ex vivo* PBMC were stained to exclude dead/dying cells, before staining with A2 DT227/8KA, A2 A245V, A2, A2 Q115E, $A2/K^b$ A245V or $A2/K^b$ tetramers folded around the ELAGIGILTV peptide at different concentrations. PBMC were then stained with antibodies (αCD14, αCD19, αCD3, αCD4, and αCD8before fixing in PFA for analysis by flow cytometry. Data were acquired using a FACScanto flow cytometer, and analysed using FloJo software. The data plotted represent the live, $CD3^+$ populations.

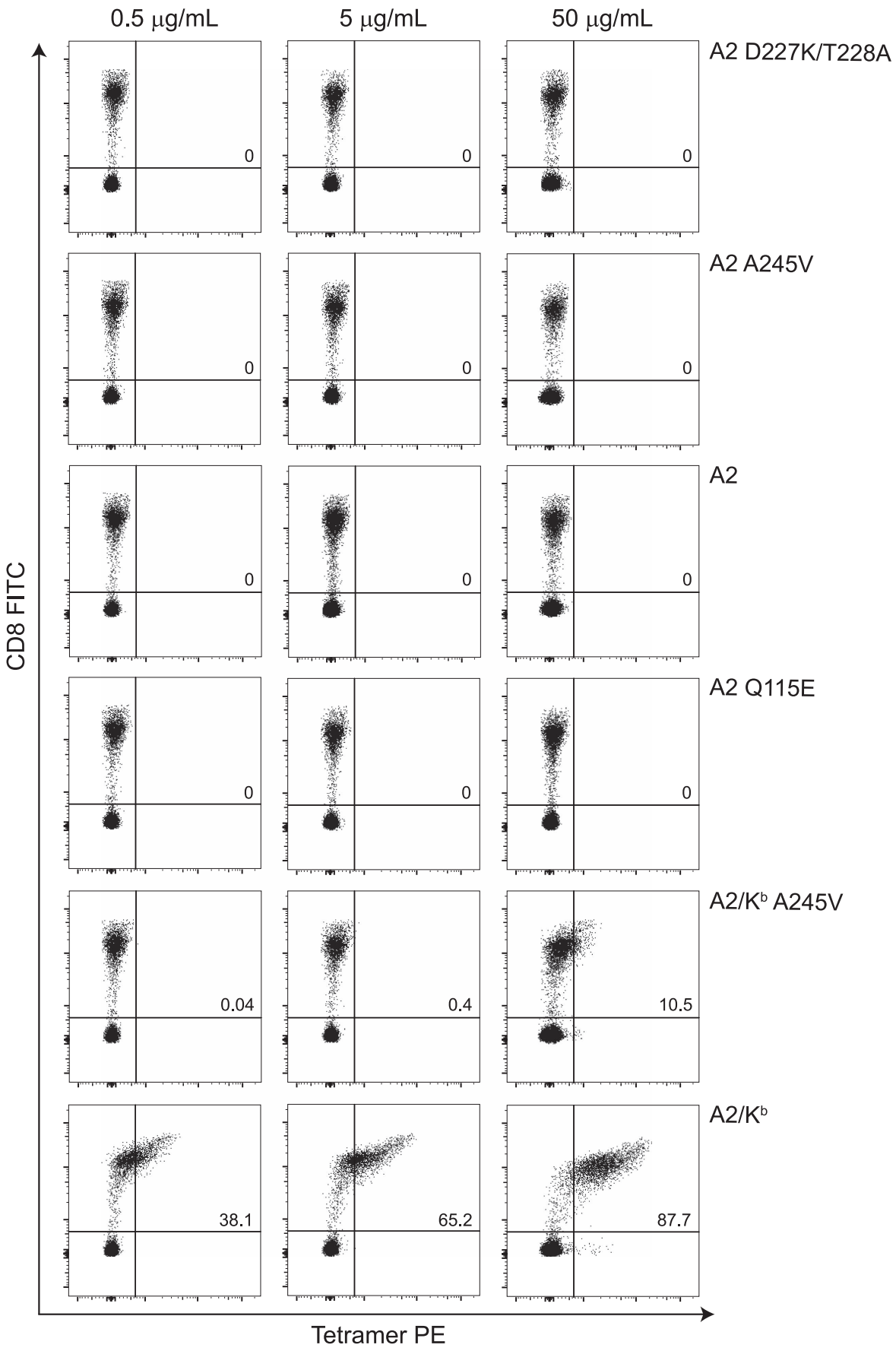
0.5 μg/mL
5 μg/mL
50 μg/mL
A2 D227K/T228A
A2 A245V
A2
A2 Q115E
A2/Kb A245V
A2/Kb
0
0
0
0
0
0
0
0
0
0
0
0
0.04
0.4
10.5
38.1
65.2
87.7
CD8 FITC
Tetramer PE

Figure 3.7: The effect of altering the strength of the pMHCI/CD8 interaction on tetramer staining of PBMC from an $A2^{neg}$ donor.

Following isolation, $A2^{neg}$ PBMCs were prepared and analysed in the same manner as those from $A2^{pos}$ donors (see Figure legend 3.6).

No loss of tetramer staining specificity was observed when staining with A2 Q115E tetramers, i.e. when pMHCI/CD8 was only slightly enhanced by ~ 1.5 fold. In both $A2^{pos}$ and $A2^{neg}$ donors, loss of specificity of the TCR was first observed in staining with A2/K^b A245V tetramers, and only at a staining concentration of 50 µg/ml (Figures 3.8). A more detailed study with tetramer staining at a broader range of concentrations in an $A2^{pos}$ donor was performed, the results of which are summarized in Figure 3.9. No loss of specificity was observed with the A2 DT227/8KA, A2 A245V, A2, or A2 Q115E tetramers. The A2/K^b A245V tetramer was also highly specific at ≤5 µg/ml, although some reactivity was observed with the same reagent at >5 µg/ml. Considerable background staining was apparent with the A2/K^b tetramer (Figure 3.9A). To clarify these data, we plotted non-specific staining as a function of tetramer concentration versus pMHCI/CD8 affinity (Figure 3.9B). In addition, two non-parametric tests (Friedman and Jonckheere-Terpstra) were conducted to examine the dependence of non-specific $CD8^+$ T-cell staining intensity on tetramer concentration and the K_D of the pMHC/CD8 interaction (Figure 3.10). These data clearly demonstrate that the loss of TCR specificity observed at the cell surface is not a gradual phenomenon, but that a rapid loss occurs once the apparent threshold of around K_D ~ 27-30 µM is exceeded.

3.2.4 T-cell activation specificity is compromised if the strength of the pMHCI/CD8 interaction is increased above a defined threshold

C1R B-cells (EBV transformed B-cells expressing little or no natural MHCI) were stably transfected with each of the A2 mutants, and the resulting lines were cloned to allow for selection of clones expressing similar levels of A2 (Figure 3.11). These clonal populations were then used to examine non-specific activation, in the absence

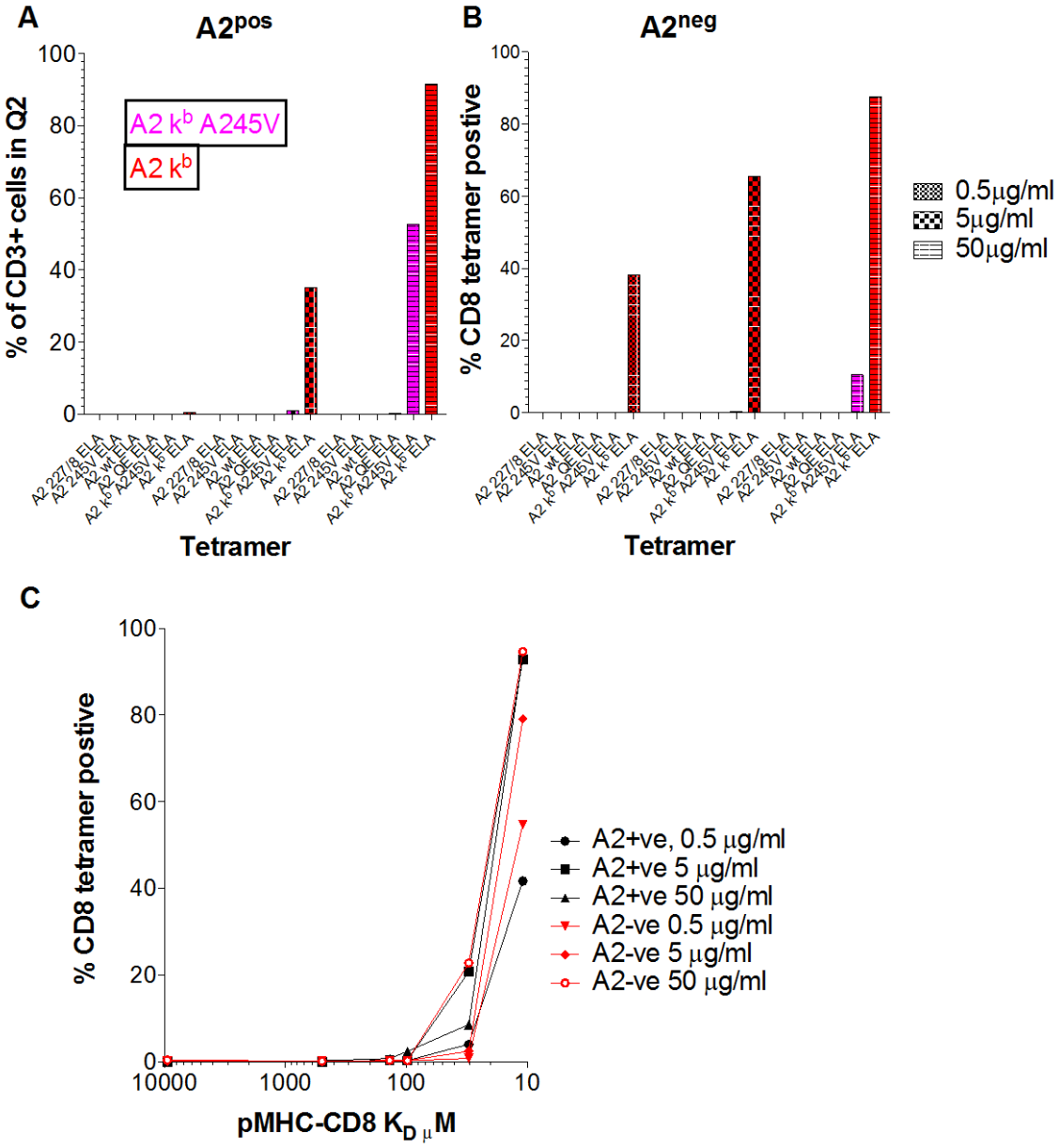

Figure 3.8: Similar staining patterns are seen in both $A2^+$ and $A2^-$ donors.
The data obtained for figures 3.6 & 3.7 may be summarized as above. The figure clearly shows that the first loss of TCR specificity, as measured by tetramer staining of fresh *ex vivo* PBMC is when the strength of the pMHCI/CD8 interaction is ≤ K_D of 30 µM. This is demonstrably true in both $A2^{pos}$ **(A)** and $A2^{neg}$ **(B)** donors, with all data being displayed on figure **C**.

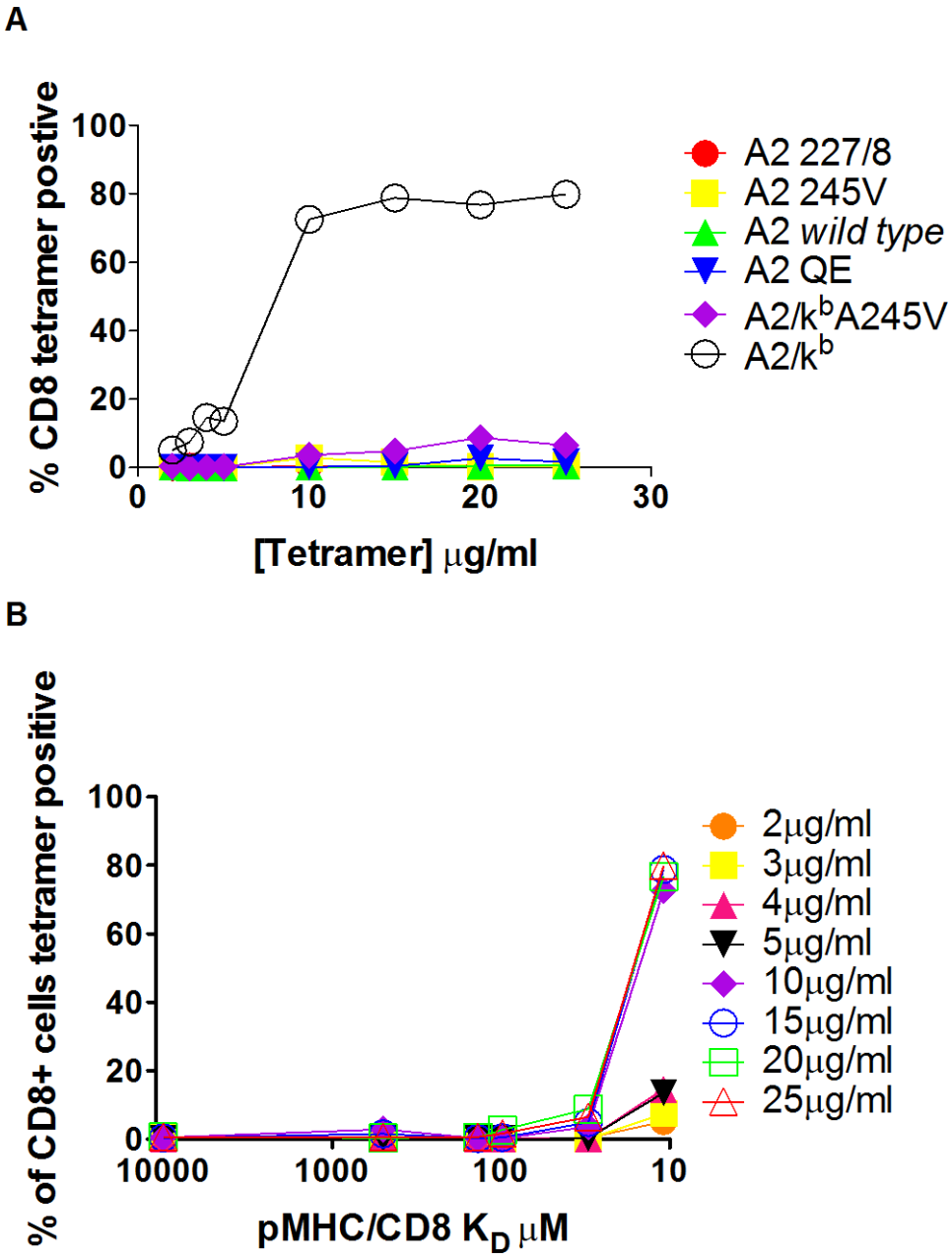

Figure 3.9: Detailed analysis of pMHCI tetramer binding specificity across a range of pMHCI/CD8 affinities in an $A2^{pos}$ donor: (A)

$A2^{pos}$ donor PBMCs were stained and analysed as described in the legend to Figure 5, with the exception that each tetramer was used at 2, 3, 4, 5, 10, 15, 20 or 25 µg/ml. **(B)** The same data is shown as % $tetramer^{+}$ $CD8^{+}$ T-cells versus pMHCI/CD8 affinity.

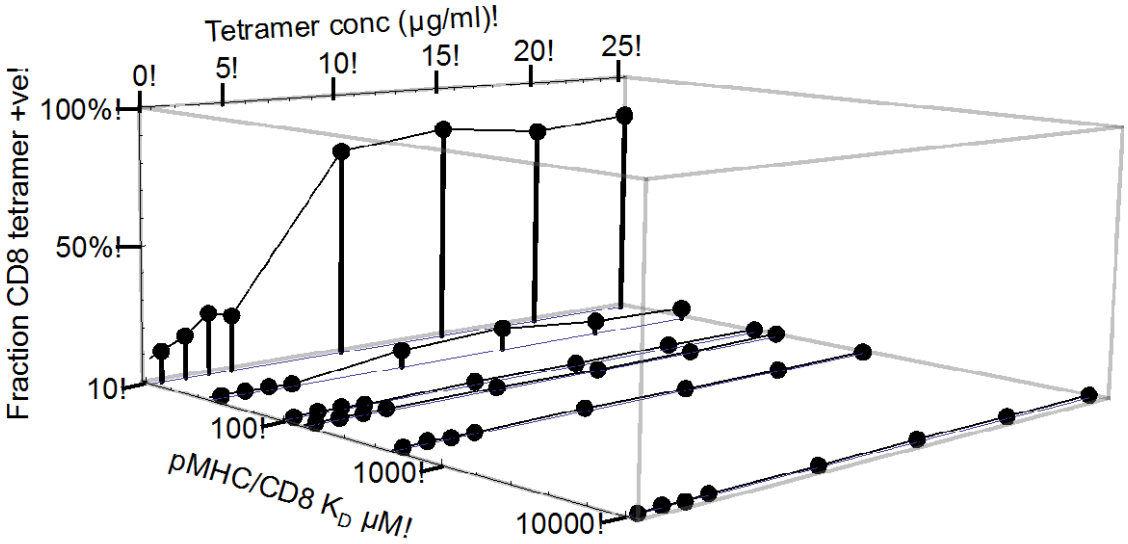

Figure 3.10: Statistical analysis of the data depicted in Figure 3.9 supported the significance of these finding:
The fraction of CD8 tetramer-positive cells varies with tetramer concentration ($P = 4.4\times10^{-3}$; Friedman test for tetramer effect); modest to strong evidence was found for the individual MHC variants (Jonckheere-Terpstra test for increasing dependence on tetramer concentration *P*-values: A2 227/8: 1.6×10^{-2}; A2 245V: 1.4×10^{-1}; A2: 1.4×10^{-1}; A2 QE: 1.0×10^{-2}; A2/K^bA245V: 5.4×10^{-2}; A2/K^b: 8.8×10^{-4}).The tetramer stain was strongly dependent on the dissociation constant of the pMHC/CD8 interaction ($P < 10^{-7}$; Jonckheere-Terpstra test for increasing dependence on K_D). The virtual absence of staining below K_D = 30 µM suggests that a value of this order of magnitude behaves a threshold value; whereas there was strong evidence for an effect of K_D on staining ($P = 3\times10^{-7}$; Friedman test), this effect was not detectable when data for the two lowest K_D-values were left out ($P = 1.7\times10^{-1}$; Friedman test, whereas $P = 6.2\times10^{-4}$ when only the lowest K_D-value was omitted).

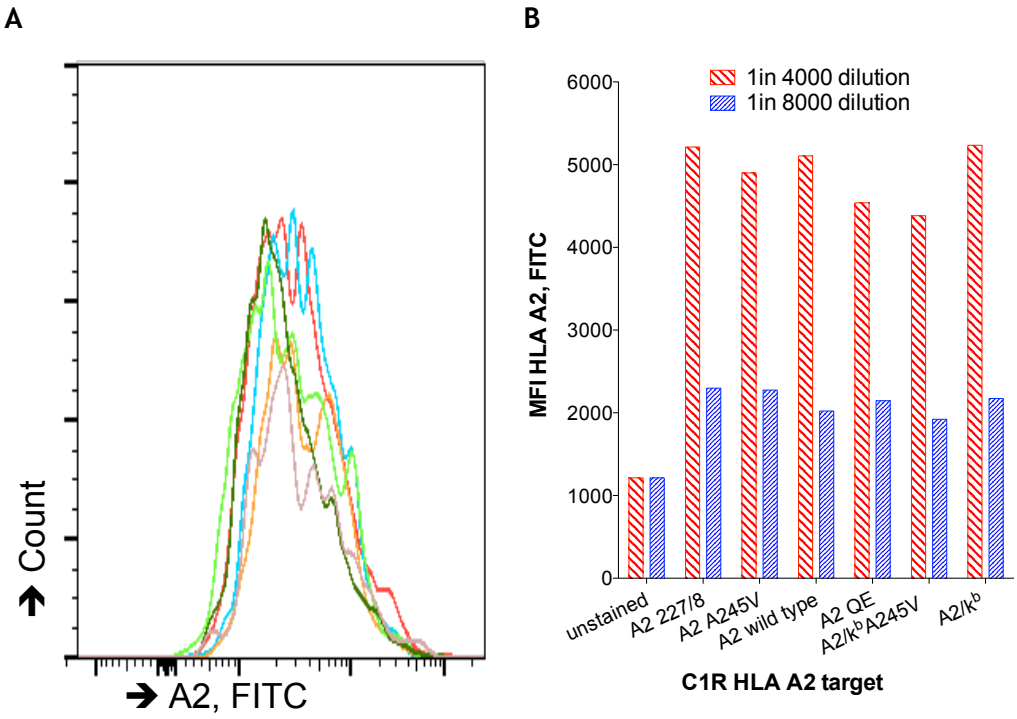

Figure 3.11: A2 staining of C1r targets
C1R B-cells of each species were stained with αA2 antibody. $2x10^4$ events were captured, and dead and dying cells were excluded from analysis. Viable events are shown in concatenated histogram plots for each of the C1R target lines (**A**), and these data are then summarized (**B**). The data shows that all cells lines express similar surface levels of HLA A2. The cell lines were regularly stained whilst maintained in culture to ensure phenotype was maintained, and these data are representative of multiple (>4) experiments.

of cognate peptide, of $CD8^+$ T-cell clones. $CD8^+$ T cells may achieve full activation in response to low pMHCI copy numbers; it has been shown that as few as 10 triple complexes may be required to elicit full calcium release, leading to synapse formation (Purbhoo et al., 2004). Therefore, it is possible that whilst the threshold for loss of TCR specificity as measured by tetramer staining appears to be in to region of K_D ~ 27-30 μM, owing to the low levels of cell surface pMHCI required to elicit a response, that this threshold may differ in the context of T-cell activation.

MEL5 was incubated overnight with C1R targets expressing each of the mutant MHCI shown in Figure 3.2, in the absence of cognate antigen. Following incubation, the resultant supernatant was harvested and assayed by ELISA for IFNg (Figure 3.12). After overnight incubation, non-specific IFNγ release was only observed in the presence of $A2/K^b$ C1R B cells. A similar pattern was observed when the supernatant was assayed for MIP1ß, however there was some non-specific activation in the presence of the C1R $A2/k^bA245V$ targets, however it was realised that the targets themselves release MIP1ß, making the data unreliable and flawed, thus this data is not shown.

Incubation of C1R A2 (or each of its mutants) targets together with $CD8^+$ T-cell clones resulted in increased non-specific target of targets as pMHCI/CD8 affinity and E:T ratio increased, however a marked increase was observed with the C1R $A2/k^b$ target compared to those bearing mutants with weaker affinity for CD8 (Figure 3.12).

These data indicate that $CD8^+$ T-cell activation specificity is maintained below a defined pMHCI/CD8 affinity threshold (KD~27 μM).

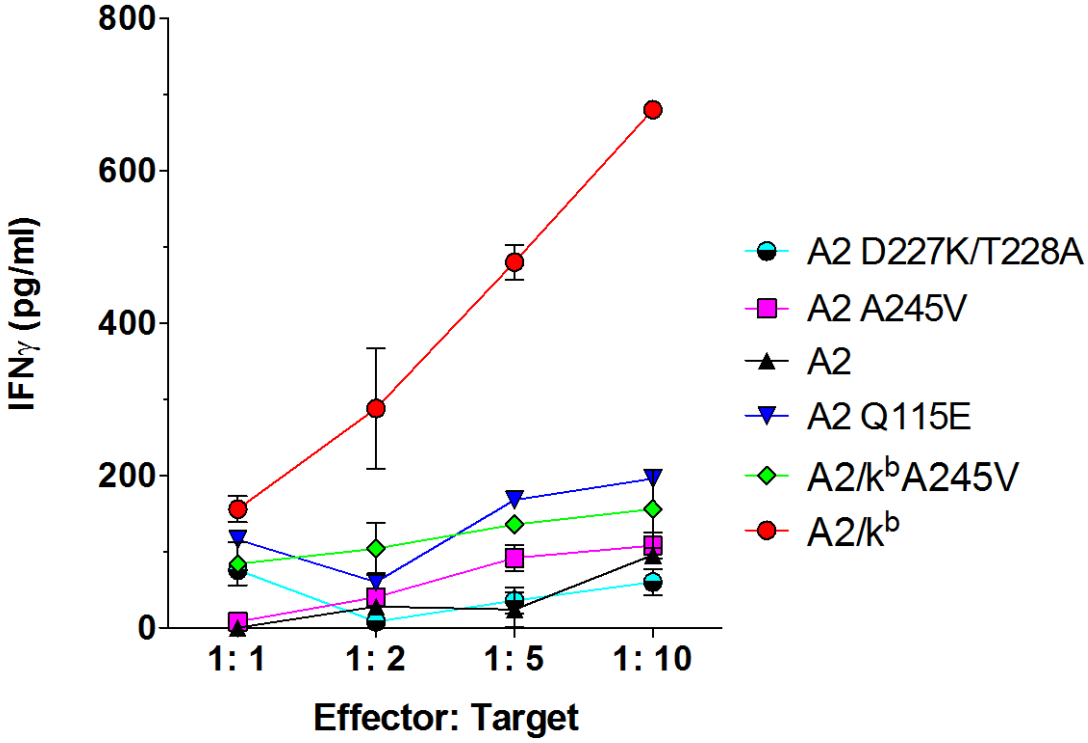

Figure 3.12: Surface expressed MHCI with superenhanced pMHCI/CD8 interaction affinity can activate CD8⁺ T-cells in the absence of cognate peptide.

Loss of TCR specificity is evident above a given threshold. MEL5 CD8⁺ clones were incubated with C1R A2 (*wild type* or each of its mutants) B-cells, at different E:T ratios for 18 hours at 37 °C. The supernatant was harvested and assayed by ELISA for IFNγ as per manufacturers instructions. The mean of two replicate assays, and their standard deviation, is plotted. The B-cell targets demonstrated no IFNγ release, and the background (IFNγ released by T-cells only) was subtracted in order to obtain the values plotted. This experimental protocol was repeated on four separate occasions, and these data are representative of the results obtained.

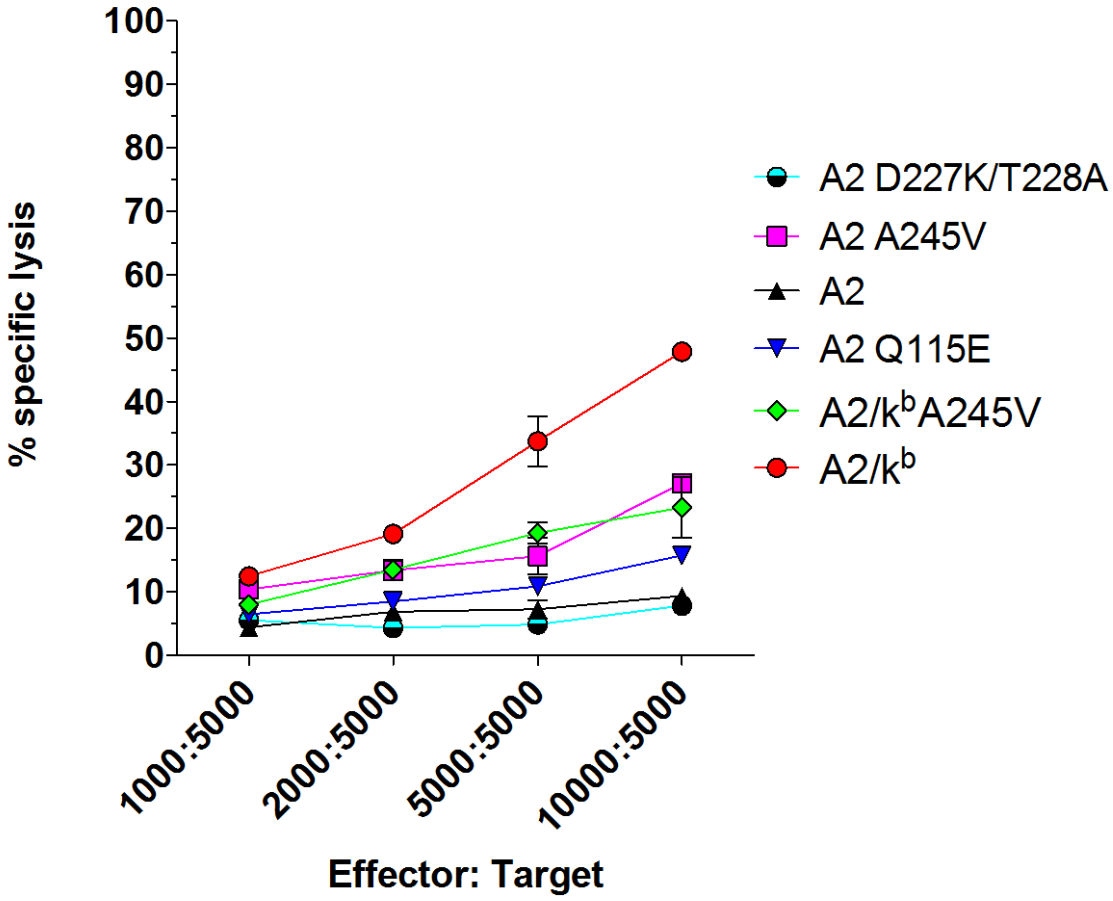

Figure 3.13: Surface expressed MHCI with superenhanced pMHCI/CD8 interaction affinity can cause non-specific lysis of target cells by $CD8^+$ T-cells in the absence of cognate antigen.

Targets, which had been previously labelled with ^{51}Cr, were counted and cultured together with counted Mel2 clones, alone (target spontaneous release), or with TritonX-100 (target total release). Cells were incubated at 37 °C for 4 hours, before harvesting supernatant for analysis using a liquid scintillator and luminescence counter in order to calculate specific lysis of targets. The mean of two replicate assays and their standard deviation is plotted. These assays were performed 3 times, and these data are representative.

3.3 Discussion

$CD8^+$ T-cells are capable of recognizing and killing cancerous cells *in vitro*. However, this interaction is very often sub-optimal, with the TCR/pMHCI interaction in the context of cancer epitopes being typified by a moderate to weak interaction affinity (K_D of ~ 90 μM) (Bridgeman et al., 2012). Non-self epitopes, for example those generated in response to viral challenge are characterized by a much stronger TCR/pMHCI interaction (K_D ~8 μM) (Bridgeman et al., 2012), and as a result of this, virally infected cells may be more readily recognized and eliminated by $CD8^+$ T-cells (Laugel et al., 2007b). Tumour Infiltrating Lymphocytes (TILs) have been effectively used to target cancer cells in a number of trials (June, 2007, Rosenberg and Dudley, 2009, Dudley et al., 2002). These T-cells are expanded *ex vivo* before being re-infused into the patient (June, 2007, Dudley et al., 2002). Whilst success rates vary between trials, it does appear that the effectiveness of this approach is compromised by the low affinity of naturally occurring anti-cancer TCRs which do not recognize these epitopes strongly enough to reliably eliminate established cancers (Morgan et al., 2006, Hinrichs and Rosenberg, 2014).

As has been discussed, in addition to sub-optimal ligand strength, tumours employ multiple strategies in order to evade the immune system.

Not only are cancer antigens very often of sub-optimal affinity, but they may also be of low avidity, with the tumour cells expressing low copy numbers of MHCI at the cell surface (La Rocca et al., 2014, Hicklin et al., 1999). Some tumours have been shown to down-regulate specific antigen, resulting in a reduction in cell surface MHCI in general and specific target pMHCI. Down-regulation of cell surface pMHCI has been shown to be linked to an unfavourable outcome in some cancer patients, suggesting that immune evasion by this means is an important mechanism in mortality and morbidity (Hanagiri et al., 2013).

Thus it becomes essential that if a TCR encounters its cognate ligand, adequate triggering should result. Not only can the tumour down-regulate these specific antigens, but it may also become resistant to immune-mediated destruction (Costello et al., 1999, Seliger, 2005, Bubenik, 2004, Topfer et al., 2011). Tumour cells may lose their ability to recognise signals for apoptosis and thus persist (Igney and Krammer, 2002, Topfer et al., 2011). They can also become more resistant to induced lysis by $CD8^+$ T-cells (Marincola et al., 2000, Igney and Krammer, 2002), thus if tumour clearance is to be achieved the T-cell response must be fully robust.

One strategy that has been employed in order to enhance tumour killing is the creation of 'high affinity TCRs'. Naturally occurring TCRs are isolated and clonotyped. These may be reintroduced into the host (Morgan et al., 2006), however success rates may be further enhanced by the introduction of mutations to enhance the TCR recognition of pMHCI (Hebeisen et al., 2013). It has been demonstrated that enhancement of the TCR beyond a certain point results in loss of specificity of the TCR, likely to be due to the TCR recognising the MHCI part of the pMHCI binding platform with such strength that the nature of the peptide becomes irrelevant (Holler et al., 2003).

In addition, one issue with this approach is that a new TCR must be designed for each epitope. The co-receptor CD8 is non-polymorphic in nature, and binds the invariant region of the MHCI molecule (Wooldridge et al., 2007). This makes this molecule an excellent candidate for the development of a more universal approach. Manipulation of the CD8 co-receptor itself in order to enhance the TCR response may generate a molecule that may be added to existing systems.

Potential target cells express a vast array of pMHCI on their cell surface, and the unique αßTCR of the $CD8^+$ T-cell must be able to distinguish between them. In this manner it may recognize self, dysregulated-self, or foreign peptide in order to

target cells for deletion. Whilst some TCR/pMHCI interactions are sufficiently strong to initiate TCR triggering in the absence of the co-receptor, for the most part its presence is absolutely required (Laugel et al., 2011, Knall et al., 1995). If this were not so, constant TCR recognition would occur. It has been postulated that this is the reason for the rapid kinetics and low affinities of the co-receptor; to prevent this from happening, thus allowing the TCR its unique specificity (Wyer et al., 1999). Complete loss of specificity of the TCR has been previously demonstrated when the pMHCI/CD8 is increased substantially above its natural limits to a similar affinity to that of foreign peptide TCR/pMHCI (Wooldridge et al., 2010a). It is evident therefore, that in order to maintain the unique specificity of the TCR, the pMHCI/CD8 interaction must be maintained within a defined window. I have created the mutated chimeric A/K^b A245V MHCI molecules in order to test this hypothesis. These molecules interact with CD8 with a K_D of a similar order to that of the murine pMHCI/CD8 interaction (Purbhoo et al., 2001).

In this chapter, I demonstrated a loss of TCR specificity, as measured by tetramer staining and cytokine production, where the pMHCI/CD8 interaction has a K_D that is less than 30 μM. Therefore, when the K_D of the pMHCI/CD8 interaction is < 30 μM, T-cell activation becomes CD8 driven and TCR-independent. In addition, the flow cytometry data collected would suggest that this effect is greatest where higher levels of cell surface CD8 are expressed; cells expressing highest levels of CD8 exhibit the greatest shift in tetramer staining (Figures 3.6 & 3.7).

I have also shown that above this threshold, increases in the strength of the pMHCI/ CD8 interaction result in minimal increases in the *specific* recognition of pMHCI. However below this threshold, small increases in pMHCI/CD8 result in relatively large increases in the recognition of cognate pMHCI as measured by

tetramer staining (Figure 3.4C). This phenomenon has large and direct implications for any future efforts to engineer CD8 for patient benefit.

Clement *et al* suggested that the A2/K^b chimeric molecules elicit activation in an 'antibody-like' manner (Wooldridge et al., 2010a). The cytoplasmic tail of CD8α brings with it to the TCR/pMHCI complex the early signalling kinase, lck, which acts to facilitate TCR signalling. I would hypothesise and argue that this effect, rather than inducing conformational changes in an antibody-like manner, is due to the dramatic changes in kinetics. My interpretation of the mathematical model put forward by Szomolay *et al* (Szomolay et al., 2013), is that either the TCR or the CD8 co-receptor may engage the pMHCI first. Under normal circumstances the very fast kinetics of CD8 would mean that it would engage and disengage far too rapidly for TCR engagement to occur concurrently, meaning that the TCR would need to engage first to allow the tripartite structure to form. However, if the kinetics are altered such that the off rate of CD8 is markedly decreased, this would allow this state to exist for longer, enabling fleeting TCR/pMHCI interactions, such as those potentially generated by an irrelevant peptide to allow TCR triggering to occur. It is reasonable to assume that the TCR samples the myriad of pMHCI presented at the target cell surface, thus very fleeting interactions must exist. If CD8 is already bound at this stage, and thus lck localized, this would facilitate non-specific triggering. If one considers this alongside the kinetic segregation model for T-cell activation as put forward by Davis and Van der Merwe (Davis and van der Merwe, 2006, van der Merwe and Davis, 2003), it becomes likely that if CD8 engages first, and remains *in situ,* lck will remain localised close to the CD3 ITAMs causing on going phosphorylation, however CD45 will be constantly acting to bring about de-phosphorylation, thus preventing triggering. As soon as a fleeting TCR engagement occurs, CD45 is excluded, facilitating rapid triggering as lck is already localised to the ITAMs. Moreover, it has been suggested that, rather than TCR triggering being

essential for T-cell activation, it is the formation of close-contacts which the TCR-pMHCI interaction creates which is important. Super-enhancement of the pMHCI/CD8 interaction will enable close contact formation in the absence of strong TCR recognition of the presented pMHCI (Chang et al., 2016). If this hypothesis is correct, it would also follow that those effector functions requiring greater TCR occupancy, such as IFNγ and target lysis, are likely to occur above a threshold, rather than in a stepwise manner, and that this threshold may appear to be higher than for example MIP1ß, which requires very low levels of TCR occupancy to stimulate release (Valitutti et al., 1996a, van den Berg et al., 2013).

In summary, I have demonstrated that a pMHCI/CD8 interaction K_D of ≤ 30 μM will lead to loss of the unique specificity of the TCR. In conclusion, CD8 must bind pMHCI with an affinity lower than this threshold in order to preserve the unique specificity of the TCR. Indeed, increases in pMHCI/CD8 above the wild type and below this threshold have been demonstrated to elicit the greatest increase in cognate pMHCI recognition. To properly utilize this knowledge for patient benefit, it would be useful to further characterize the effects of pMHCI/CD8 binding affinities which fall in between those examined (range K_D = 30 - 90 μM).

Chapter 4

CD8αß With Increased Affinity for pMHCI Enhances T-cell Activation

4.1 Introduction

CD8αß is constitutively expressed on cytotoxic $CD8^+$ T-cells, where it binds to the invariant region of MHCI, without interfering with the TCR binding platform (Wooldridge et al., 2007, Jiang et al., 2011, Gao et al., 1997a). The CD8 co-receptor acts extracellularly to stabilise the TCR/pMHCI interaction (Artyomov et al., 2010, Wooldridge et al., 2005). In addition, similarly to the CD4 co-receptor, it acts at an intracellular level to recruit lck (Gascoigne et al., 2011, Artyomov et al., 2010) to the CD3 complex (Beddoe et al., 2009), where it can bring about phosphorylation of ITAMs, the first step in downstream signalling from the TCR. As a result, CD8 can enhance T-cell antigen sensitivity by up to one million fold (Holler and Kranz, 2003). It has been demonstrated that CD8 co-receptor activity is not absolutely required for T-cell activation in the case of high affinity agonists (Laugel et al., 2011), and that dependence on CD8 is inversely proportional to TCR/pMHCI interaction affinity (Clement et al., 2016). However some studies have shown that $CD8^+$ T-cell function is incomplete in the absence of CD8 engagement, and only partial function such as target lysis is observed (Knall et al., 1995).

The pMHCI/CD8 interaction is characterised by weak affinities (100x weaker than most viral TCR/pMHCI interactions) and very rapid kinetics (18 s^{-1}) (Wyer et al., 1999, Wooldridge et al., 2003, Huang et al., 2007). It has previously been demonstrated that increasing the strength of the pMHCI/CD8 interaction above that which is physiologically normal, through manipulation of the MHCI molecule, results in an

enhanced $CD8^+$ T-cell response (Wooldridge et al., 2007), and that greatly enhancing the strength of the pMHCI/CD8 interaction results in loss of T-cell specificity, and activation irrespective of cognate ligand (Wooldridge et al., 2010a). In the previous chapter, I demonstrated that rather than being a gradual phenomenon, this loss of $CD8^+$ T-cell specificity occurs at a specific threshold ($K_D \leq 30$ μM). These studies have all involved manipulation of the pMHCI/CD8 interaction via mutation of the MHCI invariant region, at the binding site of CD8, however, it follows that manipulation of the pMHCI/CD8 interaction via mutation of the CD8 molecule itself could have similar affects.

4.1.1. CD8αα and CD8αβ

CD8 exists as a dimeric molecule, found in two forms at the cell surface; the heterodimeric CD8αβ which is constitutively expressed by cytotoxic $CD8^+$ T-cells, and the homodimeric CD8αα, which is found on more diverse populations including γδ T-cells, IELs and others, and seems to have a regulatory role (Norment and Littman, 1988, Das et al., 2003, Konno et al., 2002). The homodimeric isoform CD8ββ has been shown to theoretically exist under laboratory conditions in humans. However, it is unstable, rapidly degrades, has not been found to date in nature, and is of uncertain significance (Devine et al., 2000). Whilst *in vitro* studies have suggested that extracellular interactions between CD8αα or CD8αβ, and classical MHCI are comparable (Sun and Kavathas, 1997, Gangadharan and Cheroutre, 2004), the same is not true of the intracellular regions of these molecules. CD8α possesses in its cytoplasmic tail, two vicinal cysteine residues which, with a free Zn^{2+} ion, bind lck, thus as CD8 binds the pMHCI extracellularly, lck is localised in the TCR-CD3 complex, where it can act to phosphorylate the ITAMs (Artyomov et al., 2010).

One might suppose that CD8αα is capable of better co-receptor function than CD8αß as it is capable of recruiting two rather than one lck molecule, however the reverse appears to be true. It has been suggested that if two lck molecules are present in the tail of CD8αα, they sterically hinder the molecular interactions required for triggering (McNicol et al., 2007). This has been seen to dampen T-cell function, and the transient up-regulation of CD8αα in some cells where signalling suppression is required and has led to the hypothesis of a regulatory or inhibitory role for CD8αα (Cheroutre and Lambolez, 2008). CD8αα is capable of performing co-receptor function to the TCR/pMHCI interaction in the absence of CD8αß, albeit in a limited manner, although it inhibits T-cell function where CD8αß is present (Cawthon et al., 2001). CD8αα does not effectively support the activation of lower affinity pMHCI ligands, i.e. those that absolutely require CD8 (Renard et al., 1996). CD8αß performs far better as a co-receptor, both in terms of level of response and the ensuing degeneracy of the TCR. When one examines the breadth of the T-cell repertoire generated in its presence, it is evident that CD8αß is essential for full function and for thymic generation of a complete and robust T-cell repertoire (Zamoyska, 1994, Van Laethem et al., 2012).

4.1.2 Studies with Soluble CD8

The refolding of soluble human CD8αß is extremely challenging, largely due to the preference of CD8α to homodimerise, but also compounded by the difficulty of purification and separation, the instability of the small CD8 dimer (both CD8αα and CD8αß), and the high yields required for biophysical analysis owing to the weak affinity of the pMHCI/CD8 interaction. The small CD8αα molecule (26 kD) can be prone to precipitation at the concentration required for SPR (10 mg/ml), thus achieving these concentrations in the laboratory can prove tricky for the researcher.

Indeed, this was one of the reasons for Cole *et al*'s mutant design: to obtain a higher affinity CD8 that could be utilised at lower concentrations for crystallography studies. Studies into the biophysical properties of CD8αα and CD8αβ in the murine system, and its interactions with pMHCI suggest that the interaction is similar between the two molecules, and that they both interact with comparable affinities (Willcox et al., 1999, Wyer et al., 1999, Kern et al., 1998). Studies utilising human CD8αα suggest that the same is true in man (Gao et al., 1997a, Leahy et al., 1992).

4.1.3 High Affinity Soluble CD8αα

Cole *et al* generated a soluble CD8αα molecule, conceived through computational modelling and design, which was predicted and later demonstrated via SPR and crystallography, to exhibit enhanced binding for MHCI (Cole et al., 2005, Cole et al., 2007). Other mutants were briefly examined in this study, although none of these were demonstrated to have enhanced affinity for MHCI as measured by SPR (Cole et al., 2007). The α-chain mutation examined by Cole *et al* was a substitution of the serine residue at position 53, involved in contacts with the α2 domain of the MHCI heavy chain, for an asparginine (S53>N). Cole *et al* also substituted an alanine for the cysteine at position 33 (C33>A), however the purpose of this mutation was to eliminate the free cysteine from the α-chain, thus improving refolding efficiency and increasing the laboratory yield of synthetic CD8αα monomers.

4.1.4 Adoptive Cell Transfer for Cancer (ACT)

$CD8^+$ T-cells exist which are capable of recognising, and in many instances killing, cancer cells (Rosenberg et al., 1986). However, possibly owing to the similarity of

cancer ligands to self-antigens, this response is very often sub-optimal, falling somewhere between recognition of 'normal-self ligands' and recognition of 'pathogen-derived ligands'. Cancer cells may be recognised, but the response triggered is often inadequate to clear them, therefore neoplasia is able to persist in the host. Whilst naturally occurring $CD8^+$ T-cells can recognise cancer antigens in the context of MHCI, effective killing and clearance of the tumour by non-engineered T-cells is rare (June, 2007). In addition, tumours may adopt a number of mechanisms in order to evade the immune system, such as down-regulation of MHCI and the creation of an unfavourable environment for T-cell migration, proliferation, and activation (Seliger, 2005, Topfer et al., 2011).

ACT involves the *in vitro* expansion of the host's cells, and re-infusion of large numbers into the patient (Dudley and Rosenberg, 2003). The earliest studies of this technique as a potential cancer therapy involved the expansion of immune cells found within the tumour tissue (**T**umour **I**nfiltrating **L**ymphocytes: TILs) (Rosenberg et al., 1986, Topalian et al., 1987). Whilst these trials demonstrated some degree of efficacy, other researchers have gone on to explore ways of improving this response. In addition to the amount of work involved in generating TILs for expansion; invasive tissue biopsy (therefore solid tumours only) and digestion to isolate cells prior to expansion, the expansion of this mixed population means that the exact targets of the expanded cells is unknown, and very likely involves expansion of both inhibitory cells in addition to those involved in killing. This provides one possible explanation for the mixed responses to this type of therapy.

Therefore researchers have continued to explore other means of improving the T-cells used in ACT. The utilisation of $CD8^+$ T-cells obtained directly from separation of patient PBMC is considerably less invasive, involving only a blood sample. Engineering strategies to improve the response of these cells have thus far concentrated on the

TCR, either by manipulating the TCR itself (Hebeisen et al., 2013, Bridgeman et al., 2012, Morgan et al., 2006), or by the creation of chimeric antigen receptors (CARs), utilising the intracellular signalling component of the TCR-CD3 complex, but substituting the head of the TCR for an alternative recognition molecule (Bridgeman et al., 2010a, Bridgeman et al., 2010b, Haji-Fatahaliha et al., 2015). To date, manipulation of the co-receptor molecule has not been attempted, as a strategy to enhance the antigen sensitivity of cancer specific T-cells. If such an approach proved to be successful in enhancing the $CD8^+$ T-cell response then, owing to its non-polymorphic nature, this could potentially be a global strategy, ready to be added to any existing TCR-based ACT system.

4.1.5 Manipulating pMHCI/CD8 interaction affinity via cell surface CD8α

Whilst a previous study using soluble CD8αα has enabled us to identify a high affinity variant of CD8, for all of the reasons discussed above, it is essential that manipulations in a cell model be made to the heterodimer, CD8αß. To this end I first created a lentiviral construct enabling me to stably transduce cell lines with *wild type* CD8αß, described in chapter 2. Once efficacy of this model had been proven, further α-chain mutations were also introduced and used to generate lentiviral particles. Whilst Cole *et al* had successfully refolded soluble CD8αS53N in homodimeric form, it remained to be seen how this would refold alongside CD8ß, or traffic to the cell surface. The α-chain mutations trialled in this chapter are listed in Table 4.1.

Location of mutation	Description of mutation	pMHCI/CD8 K_D (μM)
Wild type	No mutation	137 ± 4.73
CD8α, extracellular domain	F48Q	NDB
CD8α, extracellular domain	Q2K	363 + 5.3
CD8α, extracellular domain	Q2K/S53N	Not measured
CD8α, extracellular domain	S53N/C33A*	30.8 + 1.5

Table 4.1: CD8α-chain mutations, and the affinity of the homodimer CD8αα for the pMHCI, as measured by SPR. Measurements are taken from a study by Cole et al, 2007 (Cole et al., 2007).

*The C33A mutation was introduced by Cole *et al* in order to remove the free cysteine residues, which can prove problematic to the structural biologist. Cole *et al* demonstrated no difference in binding when the *wild type* CD8αα was compared to the C33A mutant, thus they concluded that the C33A mutation had no impact on the pMHCI/CD8 interaction.

4.1.6 Immortal T-cell lines

In order to culture primary cells in the laboratory effectively, it is necessary to mimic *in vivo* growth conditions as closely as possible. In addition, these cells have a finite lifespan, and, owing to the re-stimulation process required in order to maintain them in culture, they can rapidly become exhausted. To circumvent these constraints, an immortal cell line model was selected in the first instance to allow optimisation of the transduction process. Immortal cell lines are cells that require no stimulation in order to keep growing and dividing. For this study, 3 immortal cell lines were utilised: the J.RT3-T3.5 line, the J.RT3-T3.5 NFAT GLuc line, and the HUT78 H9 derivative.

The J.RT3-T3.5 line, originally designated JM, was isolated from a 14-year-old boy with acute T-cell leukaemia in the 1970s (Schneider et al., 1977). The cells are commercially available (ATCC, 2014b), and widely utilised in research. They are a derivative of the E6-1 clone from the original jurkat line (ATCC TIB 152) first derived from this patient by Schneider *et al,* which has subsequently been mutated to lack the ß-chain of the TCR. Therefore, J.RT3-T3.5 cells do not naturally express either a TCR or CD3 at their cell surface, nor do they express any co-receptor. The endogenous α-chain remains functional if the ß-chain is replaced, and doing so restores CD3 expression (Ohashi et al., 1985). There are very few markers of activation for this cell line as the activation cascade is largely incomplete, however they retain the ability to up-regulate CD69 in response to activation through a transduced TCR, a feature that was exploited in this chapter.

The J.RT3-T3.5 NFAT GLuc line is derived from the J.RT3-T3.5 line, however, has been stably transduced to express luciferase in response to activation. Luciferase is a class of oxidative enzymes, which produce bioluminescence upon activation. This luminescence can be measured in intensity as a marker of cellular activation. The line was derived from a single clone following transduction, thus luciferase expression is the same for the same activation stimulus. Again, the endogenous ß-chain is lacking, thus there is no natural cell surface TCR or CD3 prior to transduction (Ohashi et al., 1985), although as previously, the theoretical potential for mis-pairing with the endogenous α-chain exists.

The $CD4^+$ HUT78 cell line was initially isolated from a 54-year-old lymphoma patient (Gootenberg et al., 1981, Chen, 1992, Mann et al., 1989). The HUT78 H9 derivative was further derived from this original line, and has since been shown to be near triploid in chromosome complement, with nearly 2/3 of its chromosomes being structurally altered (Chen, 1992). In addition, it has lost expression of the CD4 co-receptor. It retains an endogenous αßTCR, and, although this line is suitable for transduction, the theoretical possibility of mis-pairing and/or recognition through the endogenous TCR remains. The parental cell line was highly susceptible to HIV infection, and has been widely utilised in research of this virus (Chen, 1992). The HUT78 H9 cell line is widely available commercially for research (ATCC, 2014a). It is capable of producing the cytokines IL-2 and IL-10 in response to activation through a transduced TCR, a feature that was exploited in production of this thesis (Brigino et al., 1997, Chen, 1992).

Immortal cell lines have the benefits of continually dividing without the need for continued stimulus, thus they are easily transducible by lentiviral particles, and readily expand once stable transduction and enrichment has taken place. For these

reasons, they were an ideal starting point for initial exploration of my CD8 constructs and models, prior to any attempts to utilise this system in primary $CD8^+$ T-cells.

4.1.7 Aims

It has already been demonstrated that increasing the strength of the pMHCI/CD8 interaction acts to enhance T-cell activation (Wooldridge et al., 2010a, Wooldridge et al., 2007). However, in previous studies, increasing the strength of pMHCI/CD8 interaction was achieved by mutating MHCI. In this chapter, I aim to revisit this phenomenon, but instead by introducing point mutations into cell surface expressed CD8. The first aim was therefore to stably transduce cell lines to co-express a known TCR (Table 4.2) and the CD8αß co-receptor (or one of the α-chain mutants as summarised in Table 4.1), thus generating the tools required for this study. Secondly, I examined activation of these cell lines in response to the index peptide of the TCR, and then in response to known cross-reactive ligands (Table 4.3).

TCR name	Cognate ligand	Residue numbers	Origin	TCR/pMHCI K_D (μM)
ILA1	HLA A2 ILAKFLHWL	540-548	hTERT	36.6 ± 6.25
MEL5	HLA A2 ELAGIGILTV	26-35	Melan-A	18 ± 1
LC13	HLA B*0801 FLRGRAYGL	339-347	EBV EBNA3A	9 ± 0.4

Table 4.2: Summary of the TCRs used in this chapter, their cognate ligands, and the relative affinity of the TCR for these ligands.
(Laugel et al., 2007, Bridgeman et al., 2012, Burrows et al., 1994).

System	Peptide ligand	TCR/pMHCI K_D (μM)
ILA1	HLA A2 ILAKFLHWL	36.6 ± 6.25[1]
	HLA A2 ILAKFLHEL (8E)	>500[1]
	HLA A2 ILAKYLHWL (5Y)	242 ± 20[1]
	HLA A2 ILAKFLHTL (8T)	27.6 ± 4.71[1]
	HLA A2 ILGKFLHWL (3G)	3.7 ± 0.28[1]
LC13	HLA B*0801 FLRGRAYGL	9 ± 0.4[2]
	HLA B*4402 EEYLQAFTY	49 ± 0.2[2]

Table 4.3: Summary of the TCR systems used in this chapter, and the relative affinity of the TCR for cross-reactive ligands examined.

Measurements were taken from: -

1- Laugel *et al,* 2007
2- MacDonald *et al*, 2009
3- Bridgeman *et al,* 2012

(Laugel et al., 2007, Clement et al., 2011, Ekeruche-Makinde et al., 2012, Bridgeman et al., 2012, Macdonald et al., 2009).

4.2 Results

4.2.1 The generation of immortal J.RT3-T3.5 cell lines co-transduced with ILA1 TCR and CD8α^{var}ß

The J.RT3-3.5 parental cell line was co-transduced with wild type CD8αß and the ILA1 TCR, which is specific for the HLA A2 restricted hTERT telomerase derived epitope ILAKFLHWL (residues 540-548). Analysis of these cells demonstrated co-expression of both the ILA1 TCR and wild type CD8αß co-receptor (Figure 4.1A). Presence of the ILA1 TCR was confirmed by the detection of rat CD2 (rCD2, hereafter), the marker gene cloned into the lentiviral TCR construct which has been shown to correlate to TCR and CD3 expression (Figure 4.1A & B). Presence of the wild type CD8αß co-receptor was confirmed by positive staining with anti-CD8α antibody, and anti-CD8ß antibody. The two antibodies stained at similar levels, suggesting heterodimer expression
(Figure 4.1C).

In addition, the J.RT3-T3.5 parental cell line was transduced with the ILA1 TCR, and one of each of the CD8α-chain mutants; Q2>K, F48>Q, or S53>N (Table 4.1). Upon expansion, cells transduced with CD8αQ2Kß and CD8αS53Nß were demonstrated to express the heterodimeric co-receptor (Figure 4.1B & C). In contrast, J.RT3-T3.5 ILATCR rCD2^{+} lines transduced with CD8ß.IRESαF48Q failed to express any detectable CD8αß at the cell surface (Figure 4.1B)

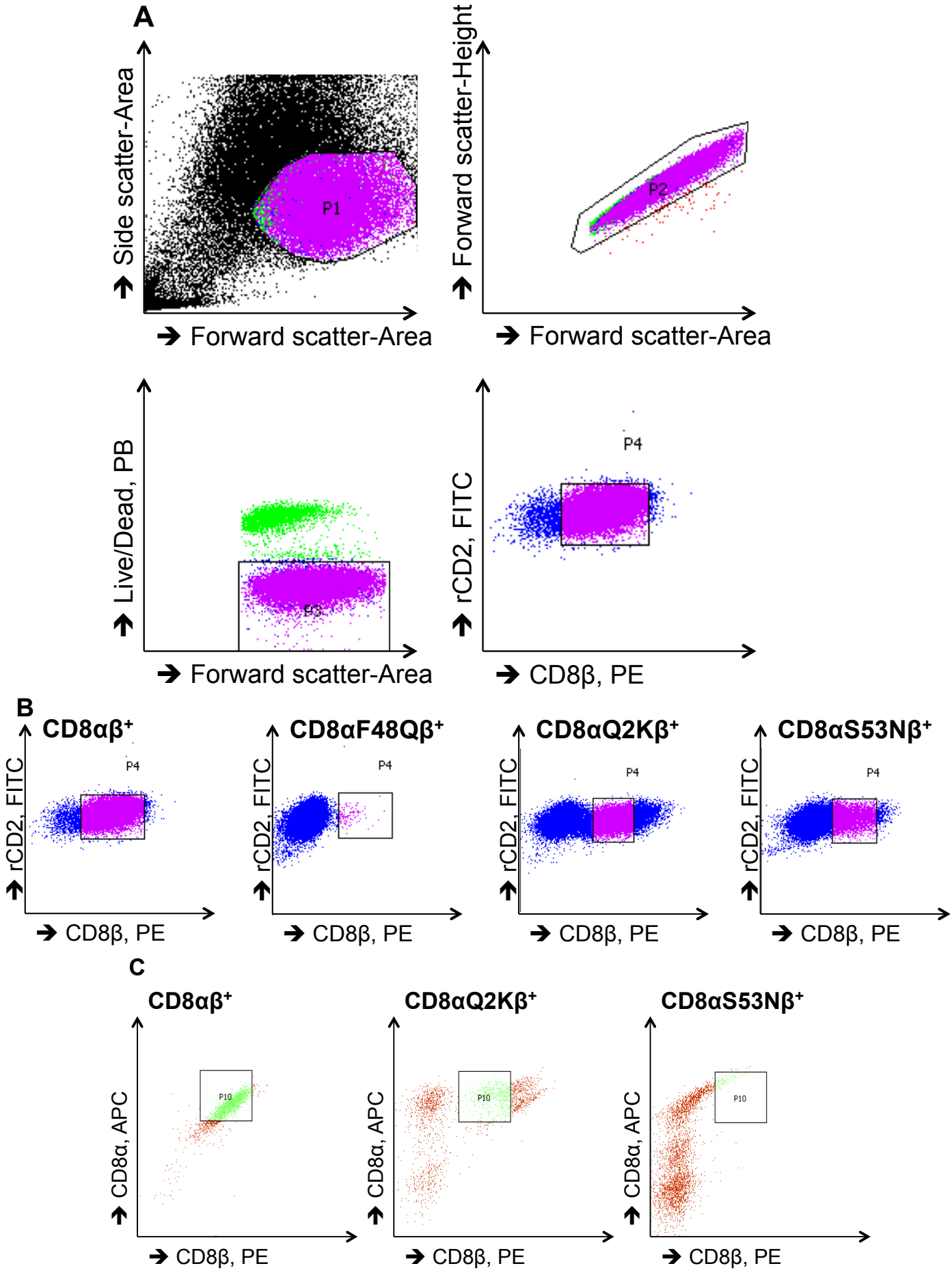
A
Side scatter-Area
Forward scatter-Area
P1
Forward scatter-Height
Forward scatter-Area
P2
Live/Dead, PB
Forward scatter-Area
P3
rCD2, FITC
CD8β, PE
P4
B
CD8αβ+
CD8αF48Qβ+
CD8αQ2Kβ+
CD8αS53Nβ+
rCD2, FITC
CD8β, PE
P4
C
CD8αβ+
CD8αQ2Kβ+
CD8αS53Nβ+
CD8α, APC
CD8β, PE
P10

Figure 4.1: J.RT3-3.5 ILA1 TCR$^+$ CD8α^{var}β$^+$ lines were stained for enrichment by TCR$^+$ CD8αβ$^+$ sorting:
Lentivirally transduced J.RT3-T3.5 lines, following expansion were stained with antibody (αrCD2, αCD8α, and αCD8β) to enable sorting by flow cytometry to enrich for TCR$^+$ CD8αβ$^+$ populations. Sorting was continued until 5 x 10^5 cells were obtained, or as many as possible, employing the gating strategy detailed (**A**). Cells were sorted into R20 media, and expanded, before re-staining to check for maintenance of phenotype. The first sort of cells lines (**B**) revealed failure to express CD8αF48Qβ at the cell surface, as measured by CD8β antibody staining. Following expansion, variant cell lines were found to express different levels of CD8αβ, thus were re-sorted (**C**). Despite repeated sorts, J.RT3-3.5 ILATCR$^+$ CD8αQ2Kβ$^+$ continued to stain highly for CD8β.

4.2.2 Establishing J.RT3-T3.5 ILA1 TCR$^+$ CD8αß$^+$ and J.RT3-T3.5 ILA1 TCR$^+$ CD8αS53Nß$^+$ cell lines with similar levels of TCR and CD8αß expression

J.RT3-T3.5 ILA1 TCR$^+$ CD8α^{var}ß$^+$ cell lines stained with anti-rCD2, anti-CD8α and anti-CD8ß antibodies were sorted using a modified FACSAria flow cytometer/cell sorter (Figure 4.1B & C). Following enrichment in this manner, the sorted cell populations were expanded and re-stained (Figure 4.2). J.RT3-T3.5 ILA1 TCR$^+$ CD8αß$^+$ and J.RT3-T3.5 ILA1 TCR$^+$ CD8αS53Nß$^+$ were found to express similar levels of cell surface TCR and CD8αß (Figure 4.2). Despite, repeated re-sorts, J.RT3-T3.5 ILATCR$^+$ CD8αQ2Kß$^+$ line expressed higher levels of CD8αß compared to wild type, and was therefore not used in subsequent experiments.

4.2.3 Increasing the strength of the pMHCI/CD8 interaction results in enhanced recognition of pMHCI by the TCR

J.RT3-T3.5 ILA1 TCR$^+$ CD8α^{var}ß$^+$ cell lines were stained with pMHCI tetramers loaded with cognate peptide for the ILA TCR, ILAKFLHWL (ILA, hereafter) (Purbhoo et al., 2007). Increased pMHCI tetramer staining of CD8$^+$ T-cells in the presence of the CD8 co-receptor, as compared to CD8$^-$ cells expressing the same TCR has previously been demonstrated (Campanelli et al., 2002), supporting the hypothesis that the CD8 co-receptor acts to enhance pMHCI recognition by the TCR. Here, I observed that pMHCI tetramer staining was increased as the strength of the pMHCI/CD8 interaction was increased, in a similar manner to that seen in Chapter 3 (Figure 3.4) (Dockree et al., 2017): The J.RT3-T3.5 ILA1 TCR$^+$ CD8αS53Nß$^+$ line stained with greater intensity than J.RT3-T3.5 ILA1 TCR$^+$ CD8αß$^+$, which in turn stained more than J.RT3-T3.5 ILA1 TCR$^+$ CD8αß$^-$ (Figure 4.3A). The same pattern, albeit with a lesser degree of staining, was

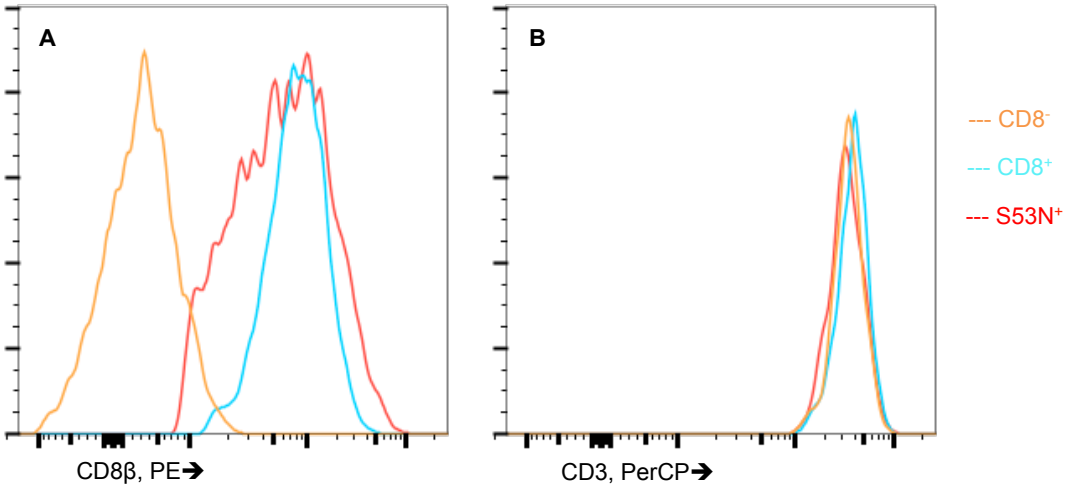

MFI	CD8β, PE (A)	CD3, PerCP (B)
CD8αβ⁻	342	36392
CD8αβ⁺	9927	39952
CD8αS53Nβ⁺	9823	35353

Figure 4.2: Staining of the J.RT3-3.5 ILA1 TCR⁺ CD8α^{var}β lines.
Sorted J.RT3-T3.5 ILA1 TCR⁺ CD8α^{var}β lines were stained with antibodies (αCD8β PE and αCD3 PerCP) post-expansion in order to check expression of the transgenes. Data were acquired using a FACSCanto flow cytometer, and analysed using FlowJo software. Data were concatenated into histogram plots, and an MFI obtained for CD8β (PE, **A**) and CD3 (PerCP, **B**). The data plotted represent the live, singlet populations. This experiment was repeated whilst the cell lines remained in culture to ensure that this phenotype was maintained.

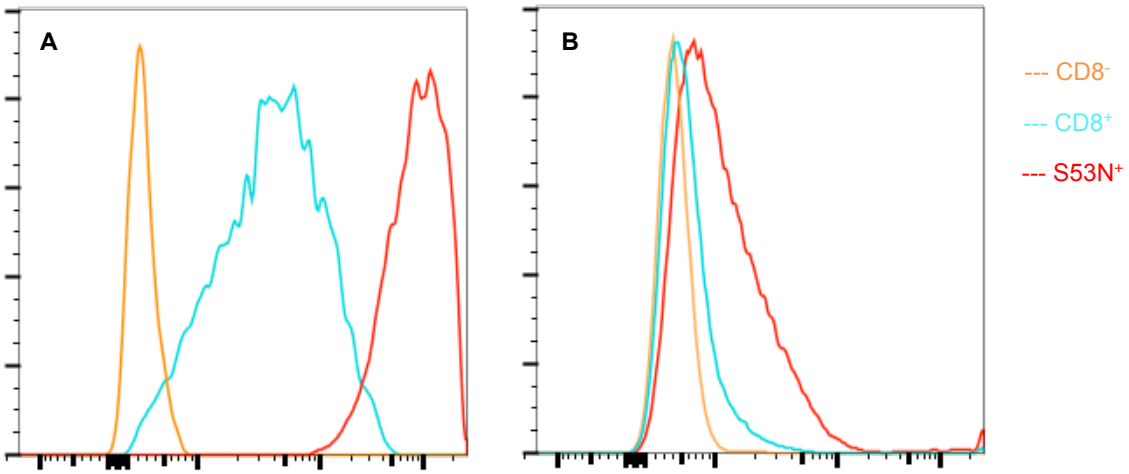

MFI tetramer, APC	A2 ILA ß2m (A)	A2 227/8 ILA ß2m (B)
CD8αß⁻	271	756
CD8αß⁺	6346	1738
CD8αS53Nß⁺	98624	3468

Figure 4.3: Tetramer staining of the J.RT3-3.5 ILA1 TCR⁺ CD8α^{var}ß lines:
The J.RT3-T3.5 ILA1 TCR⁺ CD8α^{var}ß T-cell lines were stained with either A2 *wild type* (**A**) or A2 277/8 (**B**) tetramers folded around ILA. Viable events are shown in concatenated histogram plots for each line. These figures show data representative of >6 repetitions (**A**), or 2 repetitions (**B**).

seen upon staining with a CD8 null pMHCI tetramer folded around ILA; A2 227/8 ILA, with minimal staining of J.RT3-T3.5 ILA1 TCR^+ $CD8\alpha\beta^-$, marginally more staining of J.RT3-T3.5 ILA1 TCR^+ $CD8\alpha\beta^+$, and increased staining of J.RT3-T3.5 ILA1 TCR^+ $CD8\alpha S53N\beta^+$ (Figure 4.3B).

4.2.4 CD8αß with increased affinity for pMHCI enhances T-cell antigen sensitivity

J.RT3-T3.5 ILA1 TCR^+ cell lines co-expressing either no CD8, *wild type* CD8αß, or high affinity CD8αß (S53N) were incubated for 24 hours with C1R A2 B-cells, which had been previously pulsed with the cognate ILA peptide. Assayed cells were stained with anti-CD19 antibody, in order to gate out the B-cell populations from analysis, and anti-CD69 antibody (Figure 4.4A). Increased antigen sensitivity is demonstrated in the presence of the *wild type* CD8αß co-receptor, indicating that the transduced co-receptor is capable of acting to increase the TCR recognition of the pMHCI, as it does when endogenously expressed in primary $CD8^+$ T-cells (Campanelli et al., 2002, Holler and Kranz, 2003). T-cell activation as measured by CD69 up-regulation is further enhanced in cells that express the mutant CD8αS53Nß co-receptor (Figure 4.4A). Data from four replicate experiments were subjected to statistical analysis and the differences shown to be significant (Figure 4.5).

$CD8^+$ T-cells are highly cross-reactive, with the degeneracy of the TCR being an essential feature for the maintenance of an effective T-cell response (Wooldridge et al., 2012, Laugel et al., 2011, Wooldridge et al., 2010b). The CD8 co-receptor has been shown to control cross-reactivity (Wooldridge et al., 2010b). The ILA1 TCR and its cross-reactive ligands have been well characterised in the literature (Purbhoo et al., 2007, Laugel et al., 2007b, Wooldridge et al., 2010b, Cole et al., 2008). Ligands

A

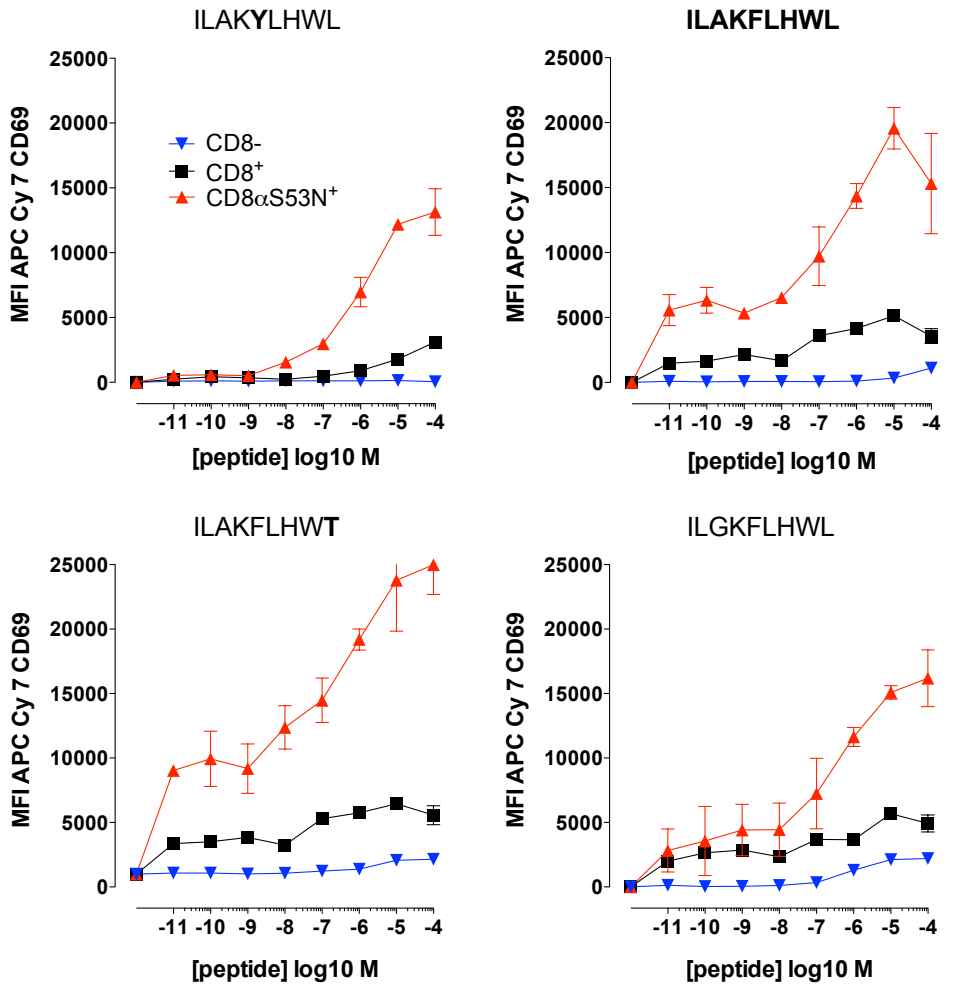
ILAKYLHWL
ILAKFLHWL
ILAKFLHWT
ILGKFLHWL
MFI APC Cy 7 CD69
[peptide] log10 M
CD8-
CD8+
CD8αS53N+
25000
20000
15000
10000
5000
0
-11 -10 -9 -8 -7 -6 -5 -4

B

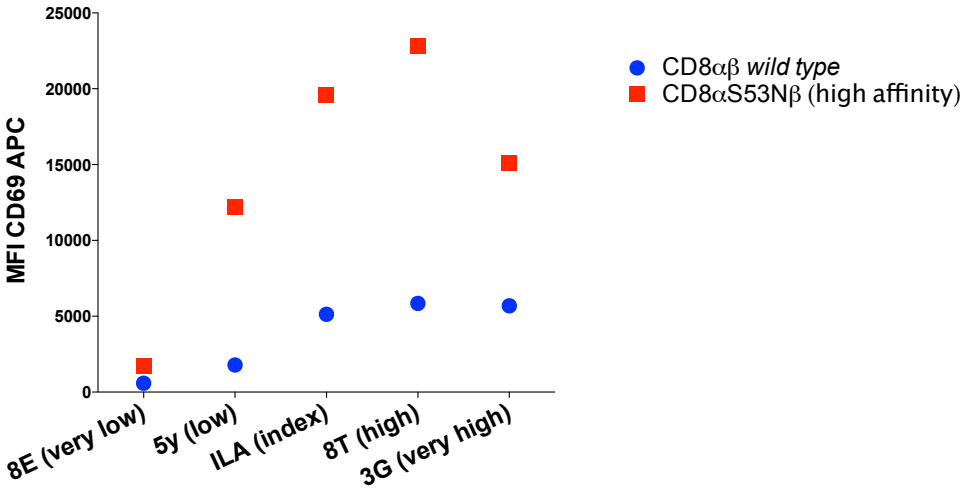
MFI CD69 APC
25000
20000
15000
10000
5000
0
8E (very low)
5y (low)
ILA (index)
8T (high)
3G (very high)
CD8αβ wild type
CD8αS53Nβ (high affinity)

Figure 4.4: Enhanced recognition of every ligand via the ILA TCR when co-receptor affinity for MHCI is increased: J.RT3-T3.5 ILA1 TCR^{+} CD8α^{var}β lines were incubated together with C1R B-cells, which had been pre-pulsed with peptide selected for the ILA system as described in Table 4.3. Following overnight incubation, cells were stained with Live/Dead stain, and with αCD19 PB and αCD69 APC-Cy7, so that dead/dying cells, and B-cells could be excluded from analysis, and activation of T-cells by CD69 up-regulation could be quantified. Viable effector T-cell (CD19^{-}) events were concatenated into histogram plots in order to obtain the MFI, and the data plotted is the mean of two replicate samples, and their standard deviation. Data were plotted comparing the activation of the different cell lines by the same ligand (**A**). Activation by ligands at 10^{-5} M peptide concentration was compared for J.RT3-3.5 ILATCR^{+} CD8αβ^{+} and J.RT3-3.5 ILATCR^{+} CD8αS53Nβ (*wild type* vs. high affinity CD8)(**B**). These data are representative of multiple identical experiments (n>4). Data plotted at the origin of the x-axis are obtained in the absence of exogenous peptide.

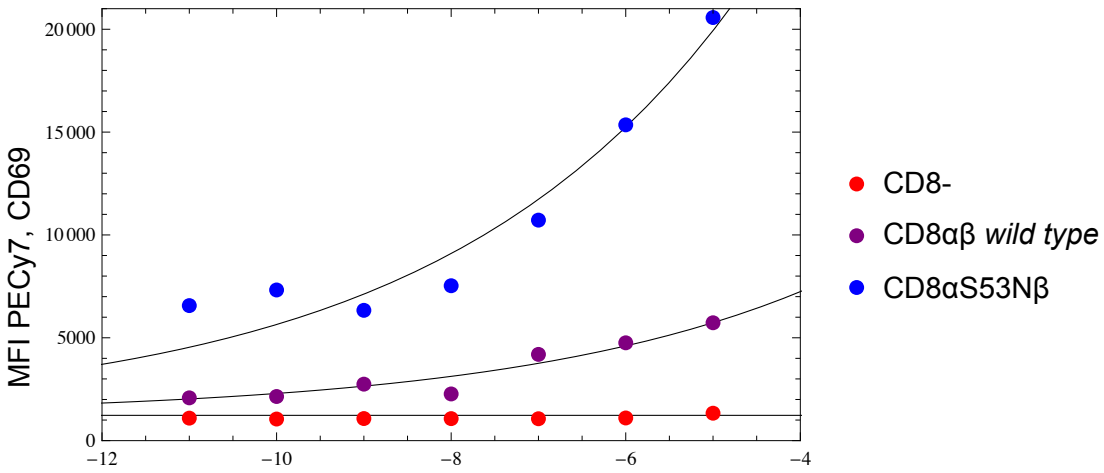

Figure 4.5: Cells transduced with enhanced affinity CD8 coreceptor are capable of significantly greater activation as measured by CD69 up-regulation when compared to the *wild type*.

Data obtained from the activation of J.RT3-3.5 ILATCR^{+} CD8αβ^{-}, J.RT3-3.5 ILATCR^{+} CD8αβ^{+} and J.RT3-3.5 ILATCR^{+} CD8αS53Nβ^{+} cells in response to C1R A2 targets pulsed with the cognate peptide ILA (as described in Figure 4.4) from four replicate experiments were used to calculate pEC50s (see appendix E). A representative example of curve fitting for the purpose of calculating pEC50s is shown in this figure (see appendix E for all other curve fits). The pEC50 data from each of these four replicate experiments were subjected to statistical analysis by Mann–Whitney U test in order to compare both the CD8^{-} and the high affinity CD8αS53Nβ^{+} cell lines to the *wild type*. Both lines were found to activate with pEC50s that were significantly different to the wild type, with a p value of 0.0210706 (S53N) and 0.00894157 (CD8^{-}), where n=4.

were selected from previous studies across a broad range of TCR/pMHCI interaction affinities; very low (ILAKFLHEL, 8E hereafter), low (ILAKYLHWL, 5Y hereafter), index (ILA), high (ILAKFLHTL, 8T hereafter), and very high, or CD8-independent (ILGKFLHWL, 3G hereafter) (Table 4.3) (Wooldridge et al., 2010b), and the same assay as described above was performed. There was increased CD69 staining with cell lines expressing CD8αS53Nβ as compared to *wild type* CD8 for every ligand examined (Figure 4.4A & B). These data demonstrate that enhancing the strength of the pMHCI/CD8 interaction by manipulating cell surface CD8 results in enhanced T-cell antigen sensitivity.

4.2.5 The HUT78 derivative H9 was successfully co-transduced with ILA1 TCR and one of the CD8αβ variants

The HUT78 derivative H9 cell line is capable of producing both IL-2 and IL-10 in response to activation (Brigino et al., 1997, Chen, 1992). Lentiviral particles were used to co-transduce this cell line with the ILA1 TCR, and one of the CD8αβvariants (either no CD8, *wild type* CD8αβ, or high affinity CD8αS53Nβ). The resultant cell lines were stained with anti-rCD2, anti-CD8α and anti-CD8β antibodies. Cells expressing similar levels of TCR (as indicated by $rCD2^+$) and CD8 (as indicated by $CD8\alpha^+$ $CD8\beta^+$) were gated upon and sorted in order to enrich for TCR^+ $CD8^+$ populations (Figure 4.6). The resultant sorted cells were expanded and re-stained. The data clearly demonstrate sustained expression of similar levels of TCR and CD8 on all cell lines (Figure 4.7).

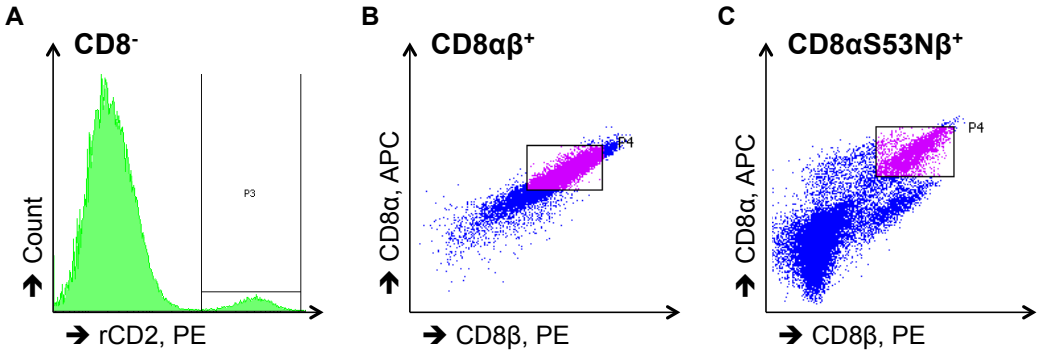

Figure 4.6: Generation of H9 ILA1 TCR$^+$ CD8α^{var}β cell lines:
HUT78 derivative H9 cells were transduced with lentiviral particles for the ILA1 TCR alone, or the ILA TCR and either *wild type* CD8αβ or the high affinity mutant CD8αS53Nβ. Following expansion, cell lines were counted and stained for sorting as follows: **A** H9 ILA1TCR$^+$ CD8$^-$, αrCD2 PE, or **B & C** H9 ILA1TCR$^+$ CD8αβ$^+$ (*wild type* or S53N), αrCD2 FITC, αCD8α APC, and αCD8β PE. Sorting was continued until 5 x 10^5 cells were obtained, or as many as possible. Viable, rCD2$^+$ events were gated upon, either for selection (**A**), or for gating further to enrich for a CD8α$^+$β$^+$ population (**B & C**). Cells were sorted into R20 media, and expanded, before re-staining to check for maintenance of phenotype.

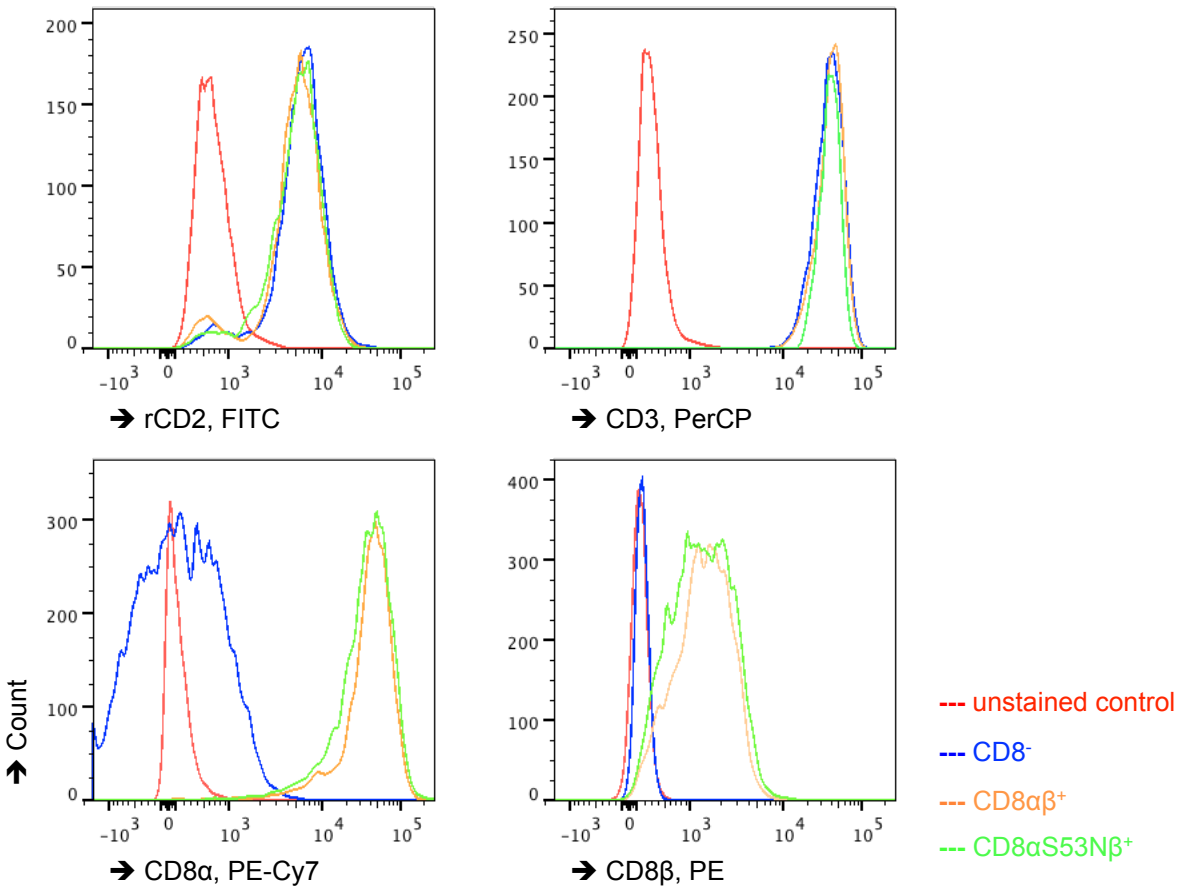

Figure 4.7: Expanded post-sort H9 ILATCR^{+} CD8α^{var}ß cell lines express similar levels of TCR at their cell surface, and, where expected, similar levels of CD8αß.

H9 ILA1TCR^{+} CD8α^{var}ß T-cell lines were expanded post sorting and stained with antibodies (αrCD2 FITC, αCD3 PerCP, αCD8α PE-Cy7 and αCD8ß PE) post-expansion in order to check expression of the transgenes. Data were acquired using a FACSCanto flow cytometer, and analysed using FlowJo software. The data plotted represent the live, singlet populations, concatenated into histogram plots. This experiment was repeated whilst the cell lines remained in culture to ensure that this phenotype was maintained.

4.2.6 CD8αß with increased affinity for pMHCI enhances the recognition of pMHCI by the ILA1 TCR, as measured by IL-2 release

Once expanded and expression levels of TCR and CD8αß had been confirmed, the resultant H9 cells lines were rested for 48 hours in order to reduce background. Cells were counted and incubated overnight with C1R A2 B-cells that had been previously pulsed with ILA, the index peptide for the transduced TCR. The supernatant was harvested after 18 hours, and subjected to analysis by ELISA for IL-2, as per manufacturers instructions. The data obtained demonstrates increased activation where the high affinity mutant co-receptor, CD8αS53Nß, is present, as evidenced by increased levels of IL-2 in the resultant supernatant (Figure 4.8). Data from three replicate experiments were subjected to statistical analysis and the differences shown to be significant (Figure 4.9)

4.2.7 CD8αß with increased affinity for pMHCI enhances the recognition of pMHCI by the ILA1 TCR, as measured by IL-10 release

A peptide activation of the H9 lines was performed, as for Figure 4.4, and the resultant supernatant subjected to analysis by ELISA for IL-10, as per manufacturers instructions. The five agonists used previously; 3G, 8T, ILA, 5Y and 8E, were used for peptide titrations. The data had at all but the highest peptide concentration a high background. Examination of the data generated at the maximum peptide concentration demonstrates that increasing the affinity of the CD8 co-receptor for the pMHCI results in enhanced T-cell activation to cognate and high affinity peptide variants, as measured by IL-10 cytokine production (Figure 4.10), however has little effect on lower affinity ligand.

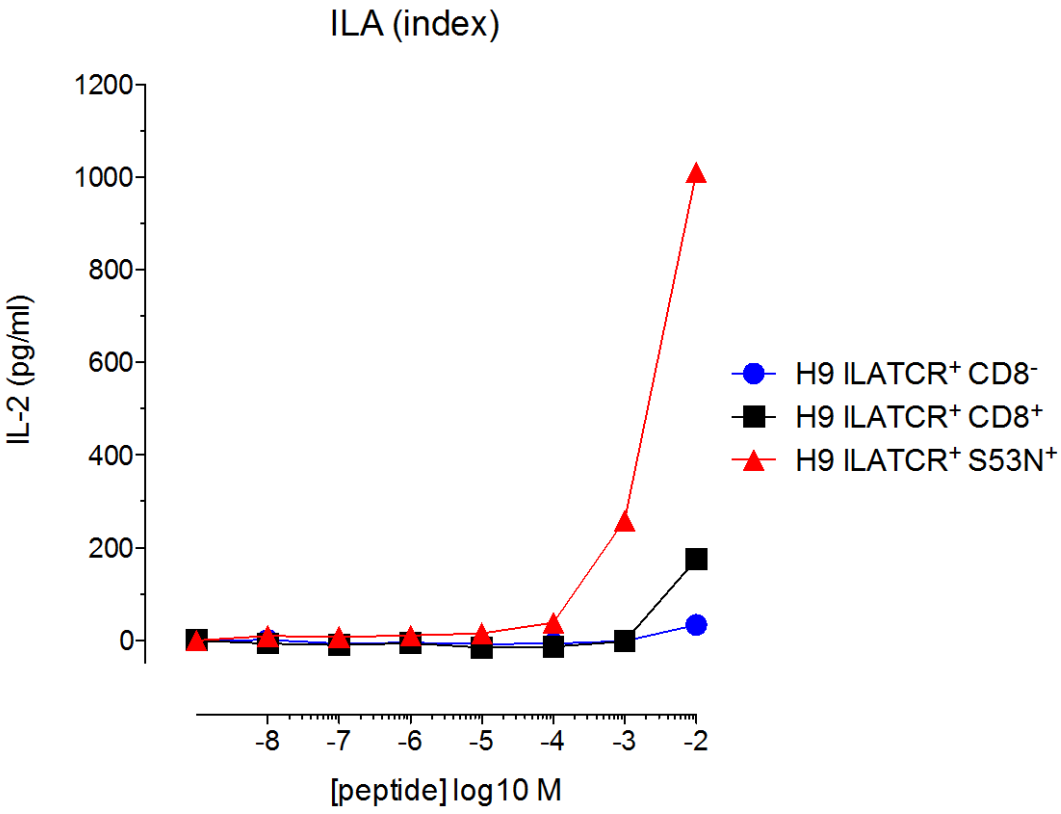

Figure 4.8: Enhanced recognition of index peptide (ILAKFLHWL) via the ILA TCR when co-receptor affinity is increased, as measured by IL-2 release.

Peptide-pulsed C1R A2 targets were incubated together with each of the H9 ILATCR^{+} CD8α^{var}ß lines at 37 °C overnight. The supernatant was harvested and assayed for IL-2 ELISA as per manufacturer's instructions. Data plotted represent the mean of two replicate assays and their standard deviation, however the standard deviation is so small as to not be visible on this chart. This assay was repeated four times, and these data are representative. Data plotted at the origin of the x-axis are obtained in the absence of exogenous peptide.

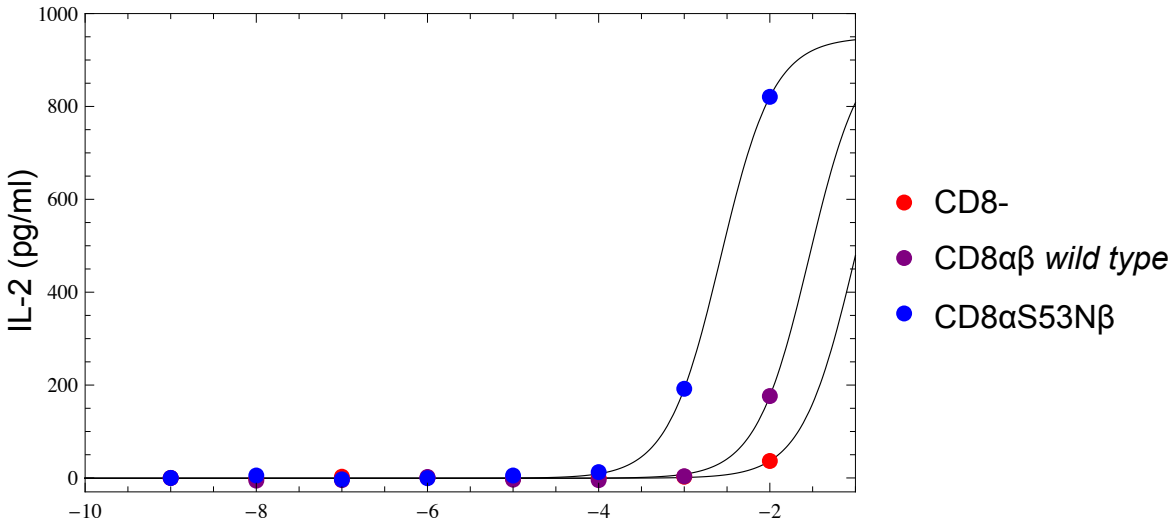

Figure 4.9: Cells transduced with enhanced affinity CD8 coreceptor are capable of significantly greater activation as measured by IL-2 release, when compared to the *wild type*.

Data obtained from the activation of H9 ILATCR^{+} CD8αß$^{-}$, H9 ILATCR^{+} CD8αSß$^{+}$ and H9 ILATCR^{+} CD8αS53Nß$^{+}$ in response to C1R A2 targets pulsed with the cognate peptide ILA (as described in Figure 4.4) from three replicate experiments were used to calculate pEC50s (see appendix E). A representative example of curve fitting for the purpose of calculating pEC50s is shown in this figure (see appendix E for all other curve fits). The pEC50 data from each of these four replicate experiments were subjected to statistical analysis by Mann-Whitney U test in order to compare both the CD8^{-} and the high affinity CD8αS53Nß$^{+}$ cell lines to the *wild type*. Both lines were found to activate with pEC50s that were significantly different to the wild type, with a p value of 0.011225 (S53N) and 0.0319112 (CD8^{-}), where n=3.

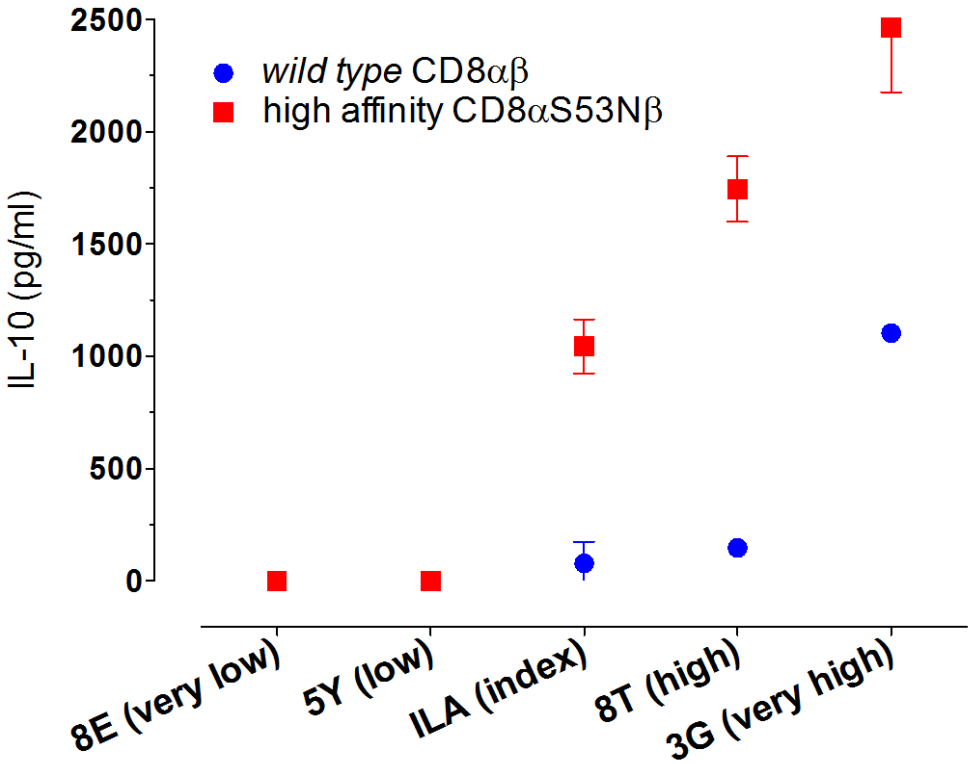

Figure 4.10: Enhanced recognition of every ligand via the ILA TCR when co-receptor affinity is increased, as measured by IL-10 release:
The activation experiment as described for Figure 4.7 was performed, including all the cross-reactive peptides for the ILA1 system described in table 4.3, and the resultant supernatant harvested and assayed for IL-10, as per manufacturer's instructions. The mean of two replicate readings and their standard deviation, as obtained at the highest peptide concentrations for high affinity and *wild type* are plotted.

4.2.8 The J.RT3-3.5 NFAT GLuc monoclonal line was successfully co-transduced with the ILA1, the MEL5, or the LC13 TCR, and one of the CD8αß variants

The MEL5 TCR was isolated and sequenced from the MEL5 clone, as described in Chapter 3. MEL5 was expanded in response to the peptide agonist, ELAGIGILTV, which is a heteroclitic variant of the A2 restricted Melan-A/MART-1_{26-35} epitope, EAAGIGILTV. Both the MEL5 T-cell clone and the TCR have been well characterised (Clement et al., 2011, Laugel et al., 2007b, Ekeruche-Makinde et al., 2012). LC13 is a public TCR, which has been well studied by many authors. Its cognate ligand is the B*0801 (B8 hereafter) restricted Epstein-Barr Virus (EBV) determinant FLRGRAYGL, derived from the latent Epstein-Barr Nuclear Antigen (EBNA) 3A (Burrows et al., 1990). Alloreactivity has also been documented against B*3501 (B35 hereafter) and allotopes restricted by B*4402 and B*4405 (Burrows et al., 1994, Burrows et al., 1995, Archbold et al., 2006). This TCR is interesting owing to its marked cross-reactivity extending into other MHCI-presented ligands (alloreactivity).

The J.RT3-3.5 NFAT GLuc line was co-transduced with the ILA1 TCR, MEL5 TCR or LC13 TCR, alongside either no CD8αß, *wild type* CD8αß or high affinity CD8αS53Nß. Following expansion, the transduced lines were stained as previously described, with anti-rCD2, anti-CD8α and anti-CD8ß, and sorted in order to enrich for $rCD2^{+}CD8\alpha\beta^{+}$ cells. The sorted populations were expanded, and re-stained to examine expression levels of rCD2, CD8α and CD8β. The data obtained demonstrated maintained expression of cell surface TCR and CD8α at similar levels (Figure 4.11A). Interestingly, and in contrast to previous cell lines, the CD8ß expression was more variable (Figure 4.11B), however the cells were double positive ($CD8\alpha^{+}$ $CD8\beta^{+}$) . As TCR and CD8α levels were similar on ILA1 TCR^{+}, MEL5 TCR^{+} and LC13 TCR^{+} J.RT3-3.5 NFAT GLuc lines, I decided to use them in subsequent activation assays.

A

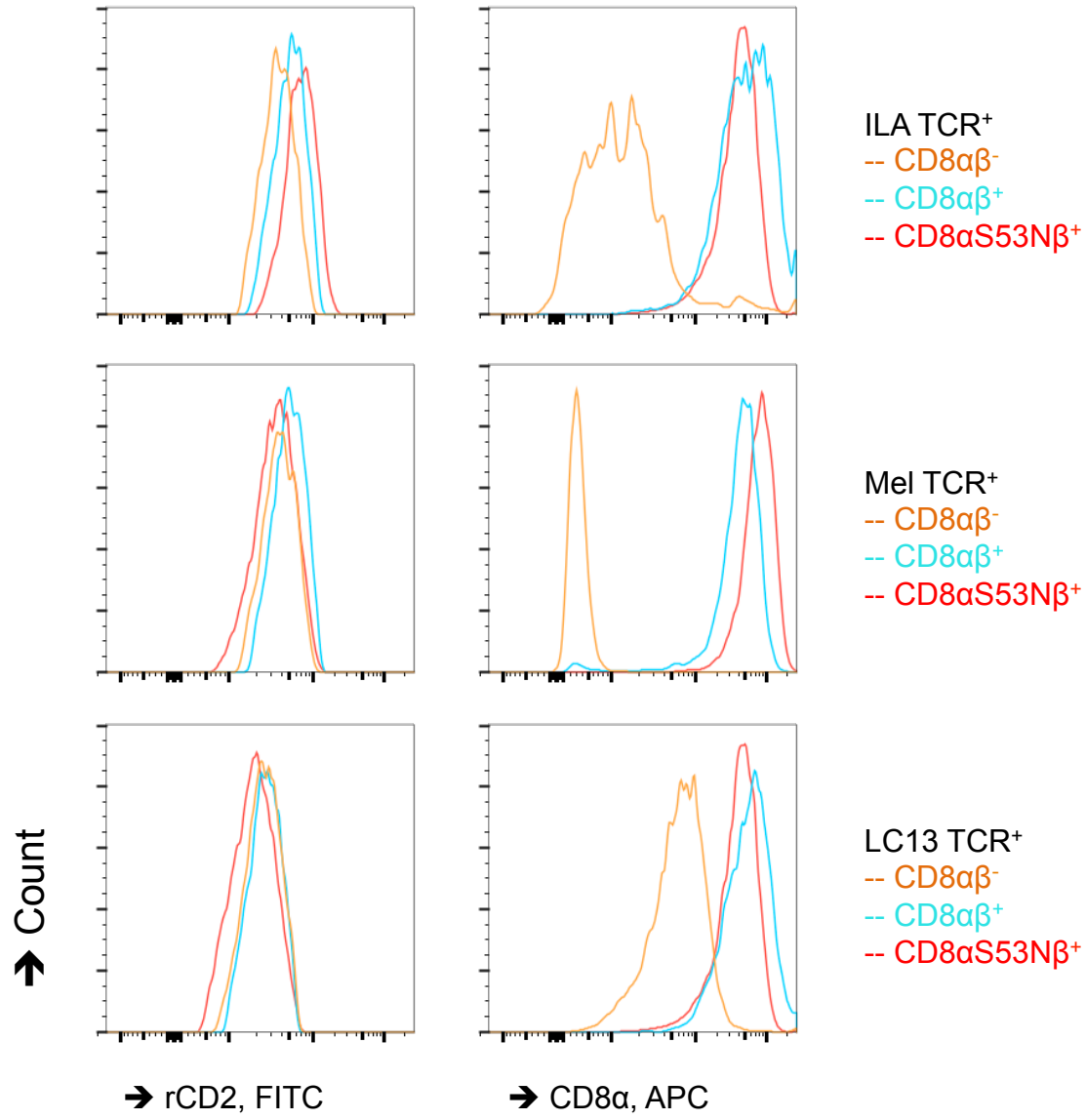
ILA TCR+
-- CD8αβ-
-- CD8αβ+
-- CD8αS53Nβ+
Mel TCR+
-- CD8αβ-
-- CD8αβ+
-- CD8αS53Nβ+
LC13 TCR+
-- CD8αβ-
-- CD8αβ+
-- CD8αS53Nβ+
➔ Count
➔ rCD2, FITC
➔ CD8α, APC

B

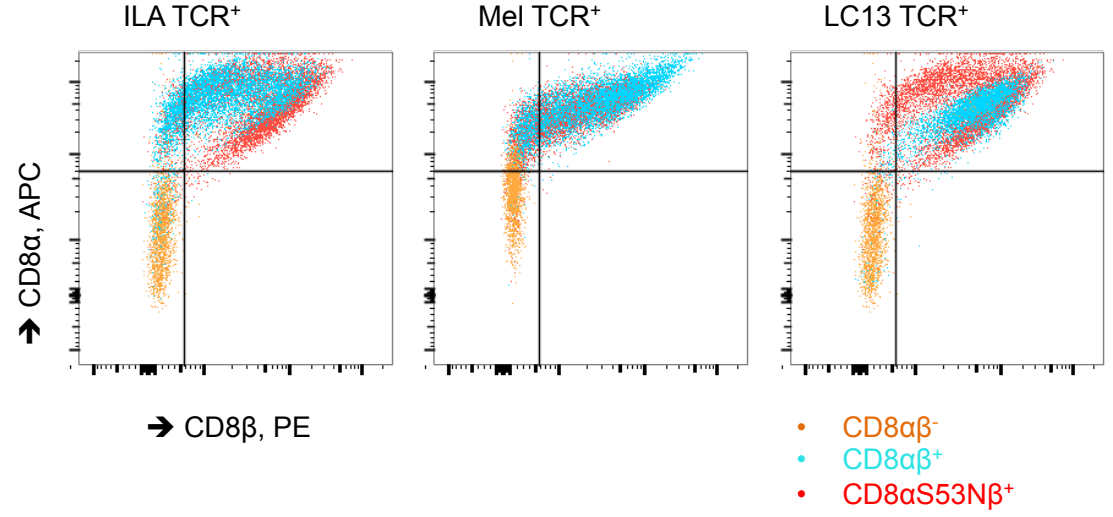
ILA TCR+
Mel TCR+
LC13 TCR+
➔ CD8α, APC
➔ CD8β, PE
• CD8αβ-
• CD8αβ+
• CD8αS53Nβ+

Figure 4.11: Expanded post-sort J.RT3-3.5 NFAT GLuc TCR *var*$^{+}$ CD8α^{var}ß cell lines express similar levels of TCR and, where expected, similar levels of CD8α.
Transduced cell lines had been sorted and enriched as previously, and following expansion, were stained with αrCD2 FITC, αCD8α APC, and αCD8ß PE. Data were acquired using a FACSCanto flow cytometer, and analysed using FlowJo software. The data plotted represent the live, singlet populations, concatenated into histogram plots (**A**), or dot plots (**B**).

CD8α staining of the Mel line was observed to be higher than that seen in other lines. This was in the $CD8^-$ line, which have never encountered a CD8 LV and so cannot be express CD8α as they have no endogenous CD8. No explanation could be offered for this, however, given that the CD8αß and CD8αS53Nß lines expressed higher levels when compared to this, I took this to be the normal negative staining for this line, and so proceeded with subsequent assays.

4.2.9 High affinity CD8 results in enhanced recognition of pMHCI by TCR, as measured by a bioluminescence assay

The J.RT3-3.5 NFAT GLuc line has been stably transduced as a reporter line of NFAT activation. This means that upon activation via the NFAT cascade, these cells will up-regulate and produce luciferase protein, which is released into the supernatant. Overnight peptide activation assays were performed as described, using serum-starved ILA1 TCR^+ or MEL5 TCR^+ J.RT3-3.5 NFAT GLuc cell lines and cognate peptide-pulsed C1R A2 B-cell targets. The harvested supernatant was then assayed for luciferase protein as per the manufacturers instructions (NEB BioLux® Gaussia Luciferase Assay Kit BioLux® Gaussia Luciferase Assay). The equipment available for reading of luminescence meant that only a single ligand could be analysed at any one time. The data shows increased luminescence, indicating increased luciferase protein into supernatant, following activation through NFAT by the cognate ligand with cell lines expressing the high affinity CD8αS53Nß co-receptor as compared to *wild type* (Figure 4.12).

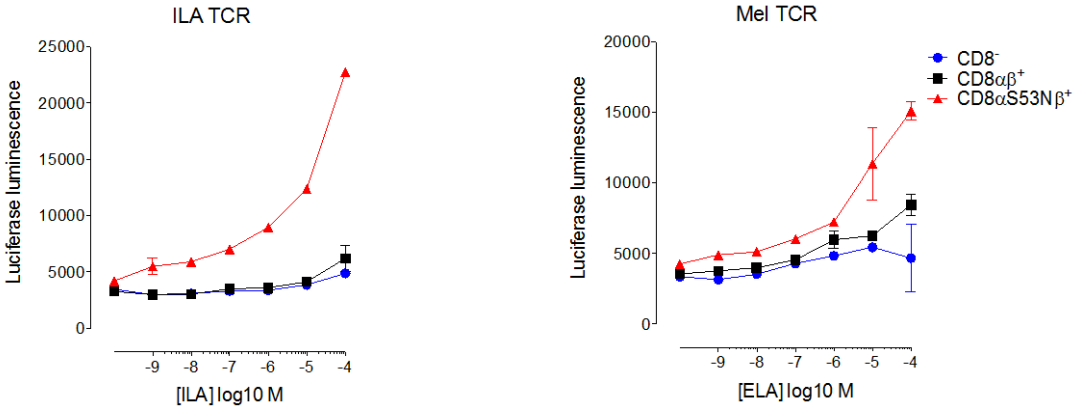

Figure 4.12: Cell lines transfected with high affinity CD8αS53Nß exhibit enhanced recognition of cognate ligand via the TCR compared to the *wild type* CD8αß co-receptor, as measured by NFAT-linked luciferase protein release.

C1R A2 target cells which had been pulsed with either the ELA or the ILA peptide, were incubated together with either the J.RT3-3.5 NFAT GLuc ILA1 TCR^{+} CD8α^{var}ß line or the J.RT3-3.5 NFAT GLuc MEL5 TCR^{+} CD8α^{var}ß line, at 37 °C for 24 hours. The supernatant was subsequently harvested, and assayed for luciferase protein by bioluminescence as per manufacturer's instructions. The data plotted represent the mean of two replicate assays and their standard deviation, and are representative of multiple experiments (n = 4). Data plotted at the origin of the x-axis are obtained in the absence of exogenous peptide.

These data demonstrate increased activation of NFAT through the TCR by cognate ligand as the pMHCI/CD8 affinity of the expressed co-receptor is increased, as measured by luciferase protein release into the supernatant.

4.2.10 High affinity cell surface CD8 affords increased activation via the LC13 TCR by both cognate and alloreactive ligands

The cognate ligand of the LC13 TCR is the B8-restricted epitope, FLRGRAYGL (FLR hereafter) (Burrows et al., 1990). LC13 has been shown to be alloreactive against B*4402 and B*4405 (Burrows et al., 1994, Burrows et al., 1995, Macdonald et al., 2009). Previously, the B*4405 restricted allotope has been identified as EEYLQAFTY (EEY hereafter), a proposed natural alloptope for the LC13 TCR (Macdonald et al., 2009, Bridgeman et al., 2012). Overnight peptide activation assays were performed using serum-starved J.RT3-3.5 NFAT GLuc LC13 TCR^{+} $CD8^{var}$ lines and T2 B-cell targets, which had been previously pulsed with either FLR or EEY peptides. The harvested supernatant was subjected to luciferase luminescence assay as per manufacturer's instructions. The data obtained from the assays shows increased activation where the CD8αß co-receptor is expressed at the cell surface, and that this activation is further enhanced when this is replaced with the CD8αS53Nß high affinity mutant co-receptor (Figure 4.13).

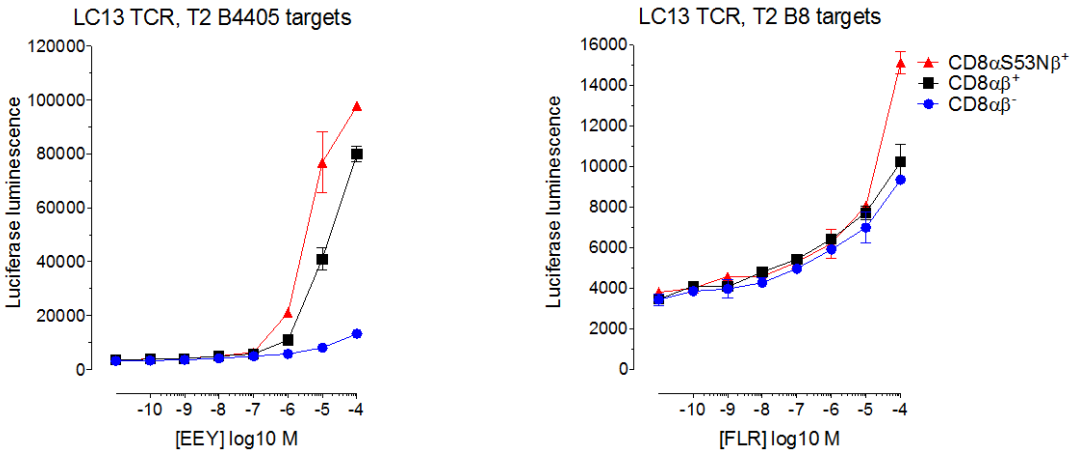

Figure 4.13: Cell lines transfected with high affinity CD8αS53Nß exhibit enhanced recognition of both the cognate ligand, and the allotope, via the LC13 alloreactive TCR compared to the *wild type* CD8αß co-receptor, as measured by NFAT-linked luciferase protein release.

T2 B*0801 target cells were pre-pulsed with the cognate ligand FLR, and T2 B*4405 alloreactive target cells were pre-pulsed with the mimotope EEY; each peptide being added at the desired final concentration (10^{-4} - 10^{-10}, and 0 M). Serum-starved J.RT3-3.5 NFAT GLuc LC13 TCR^{+} CD8α^{var}ß cells were applied to the peptide pulsed targets and incubated at 37 °C for 24 hours. The supernatant was harvested, and assayed for luciferase protein by bioluminescence as per manufacturer's instructions. The data plotted represent the mean of two replicate assays and their standard deviation, and are representative of two independent experiments. Data plotted at the origin of the x-axis are obtained in the absence of exogenous peptide.

Data demonstrate increased activation of NFAT through the TCR by both ligands as co-receptor affinity for the pMHCI is increased.

4.3 Discussion

$CD8^+$ T-cells are capable of recognising MHCI-presented cancer epitopes. Indeed, cancer has been described by some as a failure of the immune system (Swann and Smyth, 2007, Finn, 2012). If we consider that an important role of the immune system is constant and on-going surveillance for dysregulated cells, then neoplastic cells should be recognised and eliminated before they are grossly evident in the host. Tumours that present as recognisable pathology have already evaded those $CD8^+$ T-cells capable of recognising their unique onco-antigens. Therefore, $CD8^+$ T-cells are capable of recognising cancer epitopes, but their inadequate response can allow the tumour to persist, and grow, in the host. This chapter represents attempts to examine the enhancement of the antigen-specific T-cell response to onco-antigens by manipulation of the CD8αchain, specifically to enhance the affinity for MHCI.

The data sets generated from activation of all transduced immortal cell lines examined in this chapter (TCR^+ $CD8\alpha^{var}$ß) by cognate ligand, presented in the context of MHCI expressed by B-cell targets all demonstrated the same trend, that increasing the affinity of CD8αß for MHCI by manipulation of the α-chain results in increased antigen sensitivity. This was the case for all ligands examined, including low affinity ligands, where activation was detectable in these assays. Whilst this obviously has implications for enhanced recognition of cancer cells by $CD8^+$ T-cells, it also needs to be considered that enhanced recognition of all other ligands recognised by the TCR was observed.

It remains to be seen what effect the use of high affinity CD8 will have on cross-reactivity with self, and the importance of a robust investigation into the effect of increasing the strength of the pMHCI/CD8 interaction on the promiscuity of the TCR, is recognised. TCR promiscuity is an essential feature of $CD8^+$ T-cells,

rendering them capable of recognising the vast number of potentially harmful challenges that might exist (Mason, 1998, Sewell, 2012). The range of ligands, which may be recognised by a single TCR, is variable. Some may be highly promiscuous; a TCR recognising over 10^6 different peptide ligands was characterised by Wooldridge *et al* (Wooldridge et al., 2012). It is recognised that autoimmune TCRs, such as the one characterised in this publication, tend to be more cross-reactive, and that TCRs recognising foreign ligands recognise the fewest epitopes, in some cases as few as 10^2, however the average is of the order of 10^5 (Wooldridge et al., 2012, Sewell, 2012). As has been mentioned already, there is a great need to fully characterise the effect that the use of high affinity CD8 has on TCR promiscuity. The data obtained for this chapter demonstrated that, in the case of CD69 up-regulation, an early and low-occupancy indicator of T-cell activation, the S53N mutation enhanced T-cell activation for all ligands examined, even with very low affinity for the TCR. Extrapolation of these data may suggest that such a mutation would greatly increase TCR promiscuity. It should also be noted, that in the case of CD69 expression, the basal level of CD69 expression is higher in CD8αS53NΒ lines as compared to the *wild type*. Interestingly, when one examines readouts such as IL-2 and IL-10, the weaker affinity ligands examined did not exhibit enhanced activation, giving hope to the possibility that increasing the affinity of the CD8 co-receptor may not dramatically increase the promiscuity of the TCR in a manner which could prove detrimental to the patient.

It has already been noted in Chapter 3 that increasing the strength of the pMHCI/CD8 interaction above a defined threshold resulted in non-specific activation. For this reason, it is essential that the effect of enhancing pMHCI/CD8 interaction on cross-reactivity be fully classified. To this end, I attempted to transduce primary T-cells with the lentiviral particles in order to examine this system in primary cells, however, at the time of writing, this had proved

problematic. Limits of the jurkat system utilised in this chapter include the inability to respond to combinatorial peptide library screens, owing to poor sensitivity of effector function read-outs. Thus, examination of the high affinity CD8αS53NB in primary cells remains an essential goal for the continuation of this work.

The affinity of the pMHCI/CD8 interaction of the S53>N α-chain mutant homodimer for HLA A2-Tax and the HLA A24-EBV, was measured by Cole *et al* to be around 30 μM (Cole et al., 2007). This is very close to the affinity at which we recognise loss of specificity of the TCR (Dockree et al., 2017), as discussed in Chapter 3. If we are to utilise such an enhancement in pMHCI/CD8 interaction for patient benefit, it is anticipated that a mutation with a lesser degree of enhancement above the wild type would be more likely to be useful. As was demonstrated in chapter 3, enhancement of the pMHCI/CD8 affinity above this threshold results in loss of TCR specificity, with potentially catastrophic consequences for the host. It is anticipated that an enhancement of pMHCI/CD8 affinity similar to that of the Q115>E mutation examined in chapter 3 would be of more use for future strategies (Wooldridge et al., 2007, Dockree et al., 2017).

In conclusion, the jurkat model utilised in this chapter has provided valuable early insights into the ability of high affinity CD8 molecules to enhance $CD8^+$ T-cell activation, and their potential for enabling $CD8^+$ T-cells to elicit a more robust response to cancer ligands. The system requires further testing, and very likely the examination of further CD8 mutations. We have already approached a molecular modeller in order to identify further mutants for study. It has been suggested that CD8 has a key role in the control of T-cell cross-reactivity (Wooldridge et al., 2010b, van den Berg et al., 2007, Szomolay et al., 2013), narrowing the focus of

the TCR within its potential cross-reactive ligands. This will be examined in more depth in the next chapter.

Chapter 5

Manipulation of the pMHCI/CD8 interaction has the effect of 're-focussing' the TCR by re-arranging the relative potencies of its cross-reactive ligands

5.1 Introduction

CD8 has been shown to enhance and modulate the antigen-specific T-cell response (Garcia et al., 1996, Laugel et al., 2011, Miceli and Parnes, 1991), by reducing the TCR/pMHCI dissociation rate by over 50% and facilitating downstream triggering by recruitment of the TCR/CD3 complex to lipid rafts (Wooldridge et al., 2005, Gakamsky et al., 2005). Mathematical modelling has enabled us to consider the effect of altering the strength of the pMHCI/CD8 interaction on the relative potencies of TCR ligands and thus upon TCR degeneracy (Szomolay et al., 2013). van den Berg *et al* predicted that changes in the cell surface density of CD8 could alter T-cell functional avidity for agonists, and rearrange the relative potencies of each potential agonist (van den Berg et al., 2007). The ability to re-arrange the relative potency hierarchy of TCR agonists could act to facilitate a robust response to antigenic challenge, whilst damping down the response to self-ligands and thus avoiding autoimmunity, and has been described as a 'focussing effect'.

Mathematical modelling has enabled us to predict that a similar 'focussing effect' will be seen if one examines activation data obtained over a range of different pMHCI/CD8 interaction affinities. This suggests that for any given pMHCI ligand, there would be an optimal pMHCI/CD8 affinity which would afford maximal functional sensitivity. A deeper understanding of this mechanism would allow us to exploit this phenomena for patient benefit; it could be possible to design a CD8 molecule with a

defined affinity for the target MHCI which would result in greatest antigen sensitivity to a given cancer pMHCI ligand. This would enable us to optimise existing ACT systems.

5.1.1 TCR Degeneracy

Whilst early authors considered that a TCR possessed only a single pMHCI ligand, with each individual T-cell targeting a specific challenge, it very quickly became evident that this could not possibly be the case. It has been suggested that there exists ~10^{15} different pMHCI possibilities; how then could a T-cell repertoire of 2.5 x 10^7 (Nikolich-Zugich et al., 2004) recognise all of these antigens if each TCR had only a single designated target ligand? Therefore TCRs must be highly degenerate, and this promiscuity is an essential feature of an effective immune response. The promiscuous nature of the TCR has been documented in the literature since the early 1990s (Lopez et al., 1993, Wraith et al., 1992, Dedeoglu et al., 1992, Colombani, 1990, Burrows et al., 1994), however attempts to further classify this have been limited, examining only a small number of peptide ligands as compared to the entire peptide universe of all possible pMHCI ligands. Wooldridge *et al* utilised a combinatorial peptide library (CPL) screen to classify TCR promiscuity, identifying a single autoimmune TCR, which is capable of recognising over 10^6 different pMHCI ligands (Wooldridge et al., 2012). Whilst this example is considered to be highly cross-reactive, even as compared to other TCRs, 10^5 ligands is considered to be the average scope of recognition, and this degeneracy of the TCR is taken to be an essential feature of T-cell biology (Mason, 1998, Wooldridge et al., 2010b, Sewell, 2012).

5.1.2 CD8 can control T-cell cross-reactivity

Wooldridge *et al* examined the cross-reactivity of the TCR over a range of different pMHCI/CD8 affinities (Wooldridge et al., 2010b). Their data demonstrated that only a small number of pMHCI ligands are recognized in the absence of pMHCI/CD8 binding (CD8-independent ligands). As the strength of the pMHCI/CD8 interaction is increased, the number of pMHCI ligands recognised was also increased. This led the authors to conclude that CD8 controls T-cell cross-reactivity, ensuring that the immune system is able to mount a robust response to infected or dysregulated cells, whilst remaining quiescent in the face of self-antigens, mounting only the minimal response required in order to maintain the naïve and memory pool.

The study described above also observed that altering the strength of the pMHCI/CD8 interaction changed the pattern of pMHCI recognition (Wooldridge et al., 2010b). Further mathematical modelling predicted that increasing the strength of the pMHCI/CD8 interaction could enhance the recognition of one pMHCI ligand, whilst reducing the response to others, thus adjusting the relative potency. It was predicted that adjusting the CD8 co-receptor density at the cell surface could be a means by which this might be achieved *in vivo* (van den Berg et al., 2007, Szomolay et al., 2013). Whilst the effect of altered CD8 levels at the cell surface are hypothesised in this model, the exact means by which the T-cell might achieve this are unclear, however I propose a possible explanation in section 7.1.2.

5.1.3 Aims

It has been suggested that manipulation of CD8 co-receptor density is the means by which the T-cell is able to re-arrange the relative potencies of its potential ligands. It has been further hypothesised that a similar "focussing effect" may be observed via

manipulation of the pMHCI/CD8 interaction affinity. In this chapter, I have probed this role of CD8 further by examining how altering the strength of the pMHCI/CD8 interaction by manipulating cell surface CD8 affects recognition of a range of cross-reactive ligands with different TCR/pMHCI affinities. In order to do this, I have utilised the following jurkat lines: J.RT3-3.5 ILA1 TCR^+ $CD8\alpha\beta^-$, J.RT3-3.5 ILA1 TCR^+ $CD8\alpha\beta^+$ and J.RT3-3.5 ILA1 TCR^+ $CD8\alpha S53N\beta^+$, and H9 ILA1 TCR^+ $CD8\alpha\beta^-$, H9 ILA1 TCR^+ $CD8\alpha\beta^+$ and H9 ILA1 TCR^+ $CD8\alpha S53N\beta^+$. In addition, I examined activation of the MEL5 $CD8^+$ T-cell clone in response to a range of cross-reactive ligands with different TCR/pMHCI affinities presented in the context of the mutant A2 panel described in chapter 3 (Table 3.1).

System	Peptide ligand	TCR/pMHCI
ILA1	A2 ILAKFLHWL	36.6 ± 6.25[1]
	A2 ILAKFLH**E**L (8E)	>500[1]
	A2 ILAK**Y**LHWL (5Y)	242 ± 20[1]
	A2 ILAKFLH**T**L (8T)	27.6 ± 4.71[1]
	A2 IL**G**KFLHWL (3G)	3.7 ± 0.28[1]
MEL5	A2 ELAGIGILTV	18 ± 1[1]
	A2 EL**T**GIGILTV (3T)	82 ± 4[2]
	A2 **FAT**GIGIITV (FAT, 8I)	3 ± 0.4[3]

Table 5.1: Summary of the TCR systems used in this chapter, and the relative affinity of the TCR for cross-reactive ligands examined.

Measurements were taken from: -

1- Laugel *et al,* 2007
2- Clement *et al*, 2011
3- Ekeruche-Makinde *et al*, 2012

The majority of these ligands were found using combinatorial peptide library (CPL) screen technology.

(Ekeruche-Makinde et al., 2012, Clement et al., 2011, Laugel et al., 2007).

5.2 Results

5.2.1 Increasing the strength of the pMHCI/CD8 interaction re-arranges the relative potencies of ILA1 TCR agonists

The affinity of the ILA1 TCR for its cognate and cross-reactive pMHCI ligands has been well characterised in the literature (Purbhoo et al., 2007, Laugel et al., 2007b, Wooldridge et al., 2010b, Cole et al., 2008). pMHCI ligands spanning a broad range of TCR/pMHCI interaction affinities were selected: very low (ILAKFLH**E**L, 8E hereafter), low (ILAK**Y**LHWL, 5Y hereafter), index (ILA), high (ILAKFLH**T**L, 8T hereafter), and very high, or CD8-independent (IL**G**KFLHWL, 3G hereafter) (Table 5.1) (Wooldridge et al., 2010b).

To examine activation induced by different TCR agonists in the context of different pMHCI/CD8 affinities, J.RT3-3.5 ILA1 TCR$^+$ cell lines co-expressing either no CD8, *wild type* CD8αß, or high affinity CD8αS53Nß were incubated for 24 hours with C1R A2 B-cells, which had been previously pulsed with the range of pMHCI ligands listed above (Figure 5.1). pEC50 values were obtained for all J.RT3-3.5 ILA1 TCR$^+$ cell lines activated against all pMHCI ligands using simultaneous curve fitting (Table 5.2, Figure 5.2 & Appendix D). In the absence of CD8, the CD8-independent agonist, 3G, was the best activator, and the following activation hierarchy was observed: 3G>8T>ILA>5Y (Figure 5.1 & 5.2, and Table 5.2). 8E is not shown because neither this nor 5Y elicited any CD69 up-regulation in the absence of CD8. This activation hierarchy is directly correlated with the strength of the TCR/pMHCI interaction (Cole et al., 2008, Laugel et al., 2007b) (Figure 5.1 & 5.2, and Table 5.2). When the ILA1 TCR was co-expressed with *wild type* CD8αß, the observed hierarchy of activation was: 8T>3G>ILA>5Y>8E (Figure 5.1 & 5.2, and Table 5.2). Whereas, transduction with the high affinity CD8αß co-receptor, CD8αS53Nß, resulted in the following activation

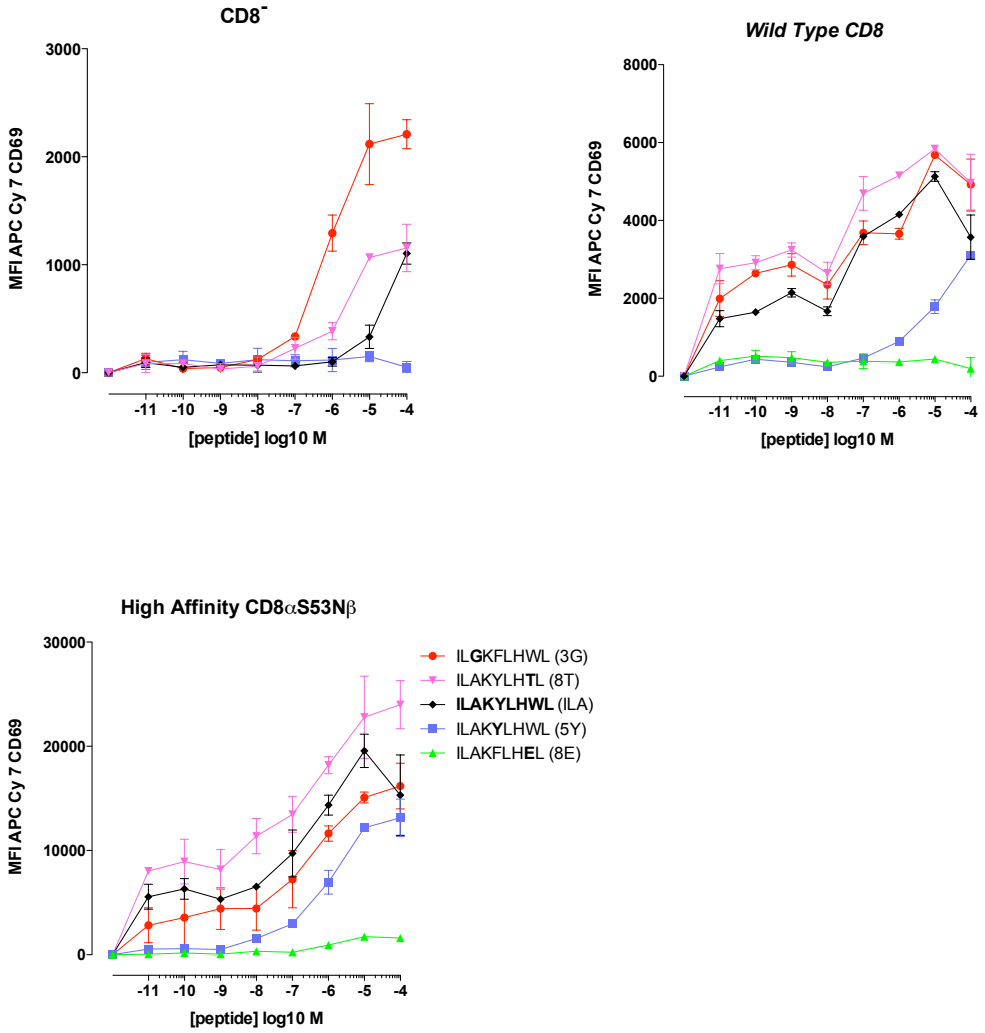

Figure 5.1: Altering the pMHCI/CD8 interaction affinity has the effect of altering the relative potencies of different pMHCI ligands as seen by the TCR.

Data obtained from the assays plotted in Figure 4.4 were re-plotted in order to compare activation of each cell line in response to different pMHCI ligands. For the sake of simplicity, the 8E peptide was omitted from the $CD8^-$ plot as no activation as measured by CD69 up-regulation was observed, and the data overlaid that of the 5Y peptide. The data represent the mean and standard deviation of two replicate assays, and the data at the origin of the x-axis is obtained in the absence of exogenous peptide.

Ligand / CD8 variant	5Y	ILA	8T	3G
CD8$^-$	-1952.15	-10.3357	-8.22473	-5.35621
CD8αß$^+$	-4.86265	-1.73276	-0.69812	-1.21762
CD8αS53Nß$^+$	1.16908	3.71495	5.39886	2.82922

Table 5.2: Scaled pEC50s for the J.RT3-T3.5 ILA1TCR system

The data portrayed in Figure 5.1 were used to generate scaled dose response curves. These data were then used to generate pEC50s, scaled to the weakest ligand presented in the context of the weakest pMHCI/CD8 interaction. In order to do so, the data were treated as a single batch for analysis, the assumption being that all cell lines share the same maximum output level. Given that all cells were treated in an identical manner, that the target cells were the same, and that each J.RT3-T3.5 ILA1TCR$^+$ CD8^{var} line originated from the same parent cell line, this assumption is warranted.

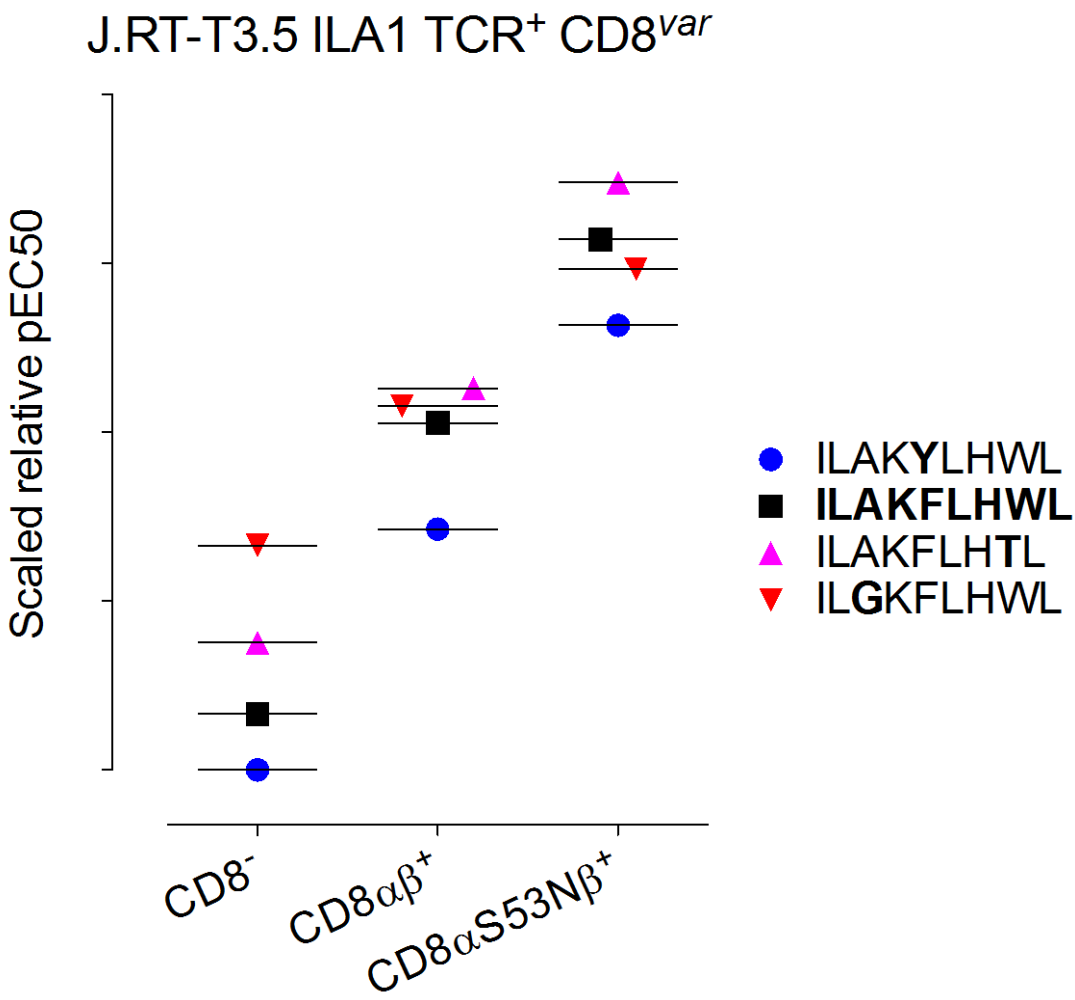

Figure 5.2: Re-arrangement of the scaled relative potencies of ligands as pMHCI/CD8 interaction affinity is increased.
The data tabulated in Table 5.2 is presented in the Figure above. The pEC50s have been scaled relative to each other. The pEC50 value for activation of the J.RT3-T3.5 ILA1 TCR^{+} $CD8^{-}$ line by 5Y is null and as such is plotted as 0.

hierarchy: 8T>ILA>3G>5Y>8E (Figure 5.1 & 5.2, and Table 5.2). These data suggest that enhancing the affinity of cell surface CD8 for pMHCI has the effect of re-arranging the relative potencies of agonists for the ILA1 TCR.

5.2.2 High affinity CD8 results in a reduced response to high affinity ligands

Once expanded and expression levels of ILA1 TCR and CD8 had been confirmed, the resultant H9 cells lines were rested for 48 hours in order to reduce background. Cells were counted and incubated overnight with C1R A2 B-cells that had been previously pulsed with the range of pMHCI ligands listed above. The supernatant was harvested after 18 hours, and subjected to analysis by IL-2 ELISA. The weaker affinity ligands, 5Y and 8E elicited no detectable response. For the index peptide ILA, activation was enhanced by the expression of wild type CD8αß and further enhanced by the expression of high affinity CD8αß (S53>N) (Figure 5.3A), consistent with results in chapter 5. For the higher affinity ligands (8T and 3G), activation was also enhanced by the expression of wild type CD8αß but interestingly, this was not further enhanced by the expression of high affinity CD8αß (S53>N). In fact, for both 8T and 3G, activation with high affinity CD8αß (S53>N) was lower in magnitude than that observed with wild type CD8αß (Figure 5.3A).

Interestingly, when I examined the effect of increasing the strength of the pMHCI/CD8 interaction on the relative potencies of ILA, 8T and 3G, a shift in the hierarchy of specific responses via the TCR was observed (Figure 5.3B & 5. 4, and Table 5.3). For H9 ILA1 TCR^+ lines with no CD8αß or expressing the *wild type* CD8αß co-receptor, the order of ligand potency observed was: 3G=8T>ILA>5Y (Figure 5.3B & 5.4, and Table 5.3). However, for H9 ILA1 TCR^+ lines expressing the high affinity co-

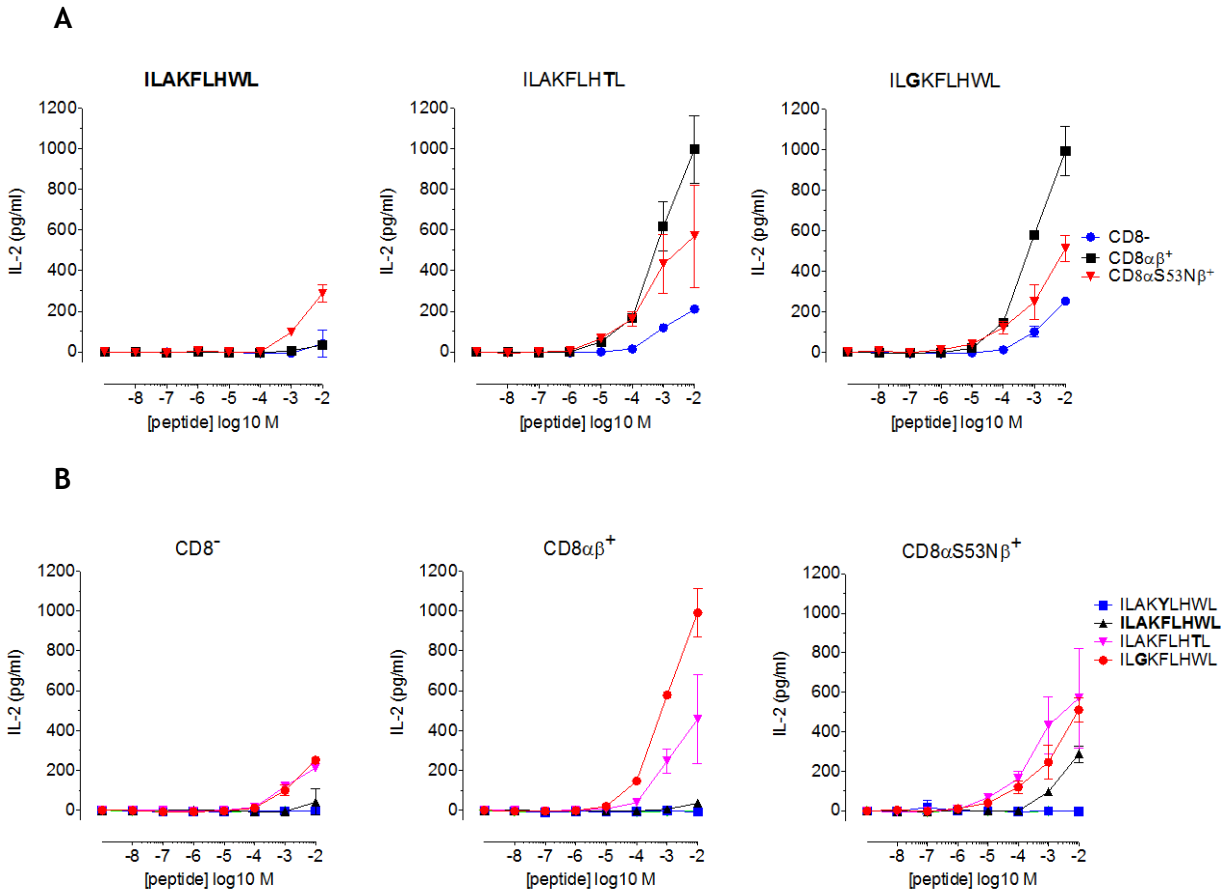

Figure 5.3: Increasing the pMHCI/CD8 affinity reduces activation through the TCR as measured by IL-2 release for higher affinity agonists.

Peptide-pulsed targets (peptides as described in Table 5.3 for the ILA system) added at the indicated concentrations, were incubated together with each of the H9 ILA1 TCR$^+$ CD8α^{var}β lines, at 37 °C overnight. The supernatant was subsequently harvested and assayed for IL-2 by ELISA. Data plotted represent the mean and standard deviation of two replicate assays, and are representative of 3 replicate experiments. The data sets closes to the origin of the x-axis represent data obtained in the absence of any exogenous peptide. Data sets are plotted to compare activation of different cell lines by the same ligand (**A**), and activation of the same cell line by different ligands (**B**).

Ligand / CD8 variant	5Y	ILA	8T	3G
CD8$^-$	-4.74167	-1.71556	0.115127	0.235721
CD8αβ$^+$	-53.2726	-1.7405	1.00874	2.18829
CD8αS53Nβ$^+$	-3.88575	0.3525	1.49607	1.16599

Table 5.3: Scaled pEC50s for the H9 ILA1TCR system.
The data portrayed in Figure 5.2 were used to generate scaled dose response curves. These data were then used to generate pEC50s, scaled to the weakest ligand presented in the context of the weakest pMHCI/CD8 interaction. In order to do so, the data were treated as a single batch for analysis, the assumption being that all cell lines share the same maximum output level. Given that all cells were treated in an identical manner, that the target cells were the same, and that each H9 ILA1TCR$^+$ CD8^{var} line originated from the same parent cell line, this assumption is warranted.

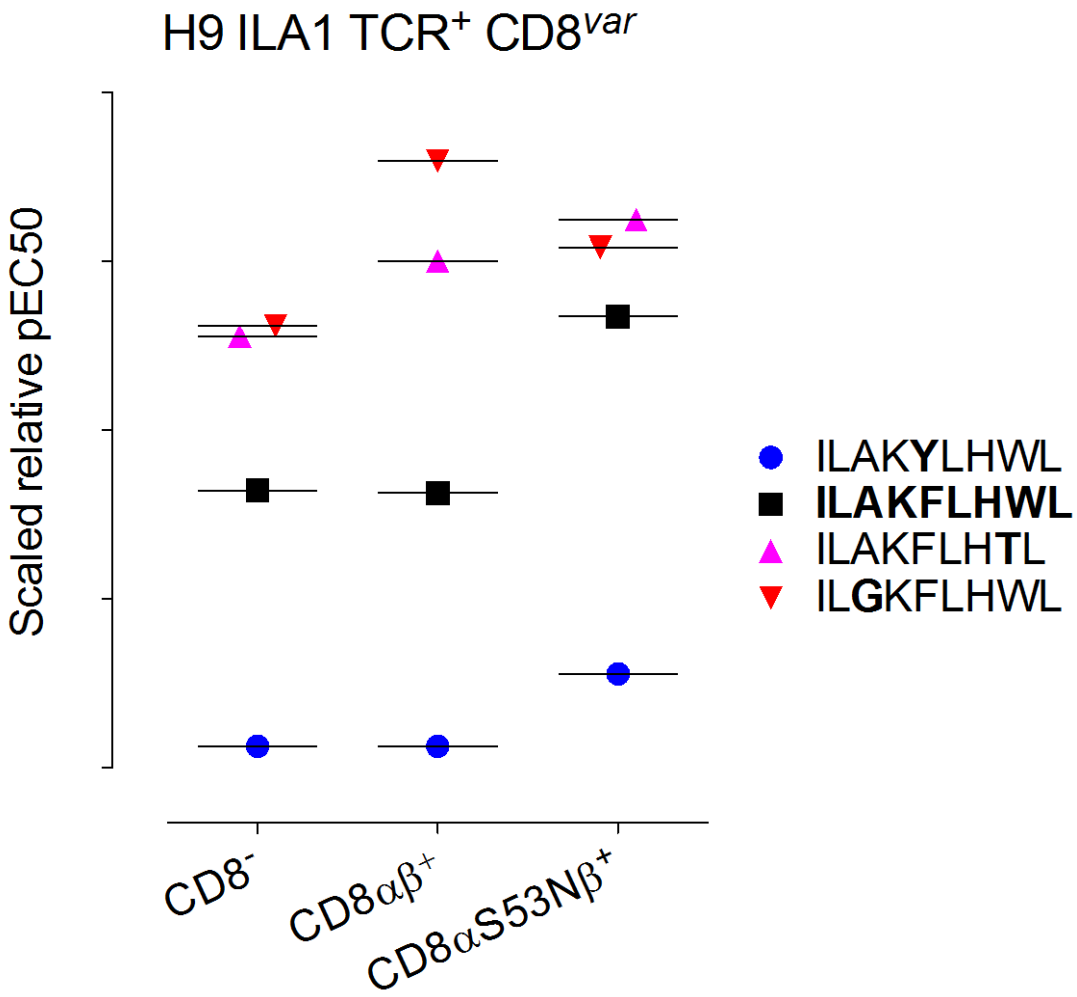

Figure 5.4: Re-arrangement of the scaled relative potencies of ligands as pMHCI/CD8 interaction affinity is increased.
The data tabulated in Table 5.2 is presented in the Figure above. The pEC50s have been scaled relative to each other. The pEC50 value for activation of the H9 ILA1 TCR^+ $CD8^-$ line by ILA is null and as such is plotted as 0.

receptor, CD8αS53NΒ, the following hierarchy of ligand potency is seen: 8T>3G>ILA>5Y (Figure 5.3B & 5.4, and Table 5.3). Therefore a shift in activation hierarchy as the strength of the pMHCI/CD8 interaction is increased was also observed in the H9 system (when effector function was measured by IL-2 release), albeit more subtle than the shift observed in the J.RT3-T3.5 system, as measured by CD69 up-regulation (Figure 5.1 & 5.2). The shift in hierarchy was not measurable by IL-10 release resulting from identical assays in the same H9 system (n=3).

5.2.3 Altering the strength of the pMHCI/CD8 interaction by manipulation of MHCI facilitates 'focussing'

C1R A2 targets utilised in Chapter 3 of this thesis in order to examine non-specific activation of $CD8^+$ T-cells were used to further examine the 'focussing effect' observed above. A panel of cross-reactive ligands recognised by the MEL5 TCR with different TCR/pMHCI affinities were selected from previously published studies (Table 5.1). These ligands had been identified using CPL technology. The ligands selected were ELAGIGILTV (index peptide, ELA), the weak affinity agonist EL**T**GIGILTV (3T hereafter), and the high affinity agonist **FAT**GIGI**I**TV (FAT hereafter) MEL5 $CD8^+$ T-cells clones were counted and rested overnight in R2 media in order to reduce the background readout. C1R A2 B-cells expressing either wild type or mutant MHCI were counted and pulsed for two hours with either index or a cross-reactive ligand as indicated (Figure 5.5). Targets were then washed and the MEL5 $CD8^+$ T-cell clone added, then incubated overnight. The resultant supernatant was harvested and assayed for IFNγ by ELISA.

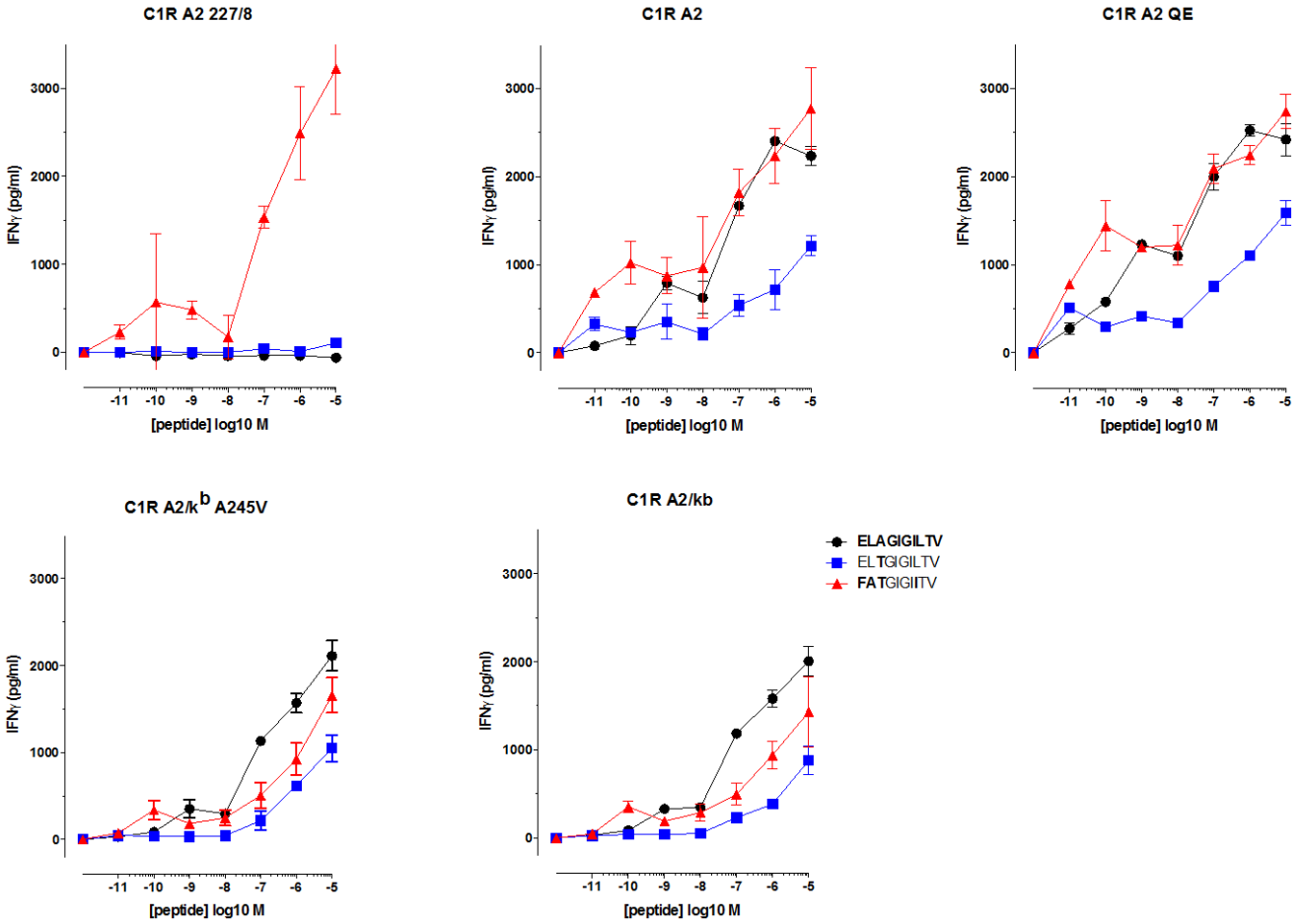

Figure 5.5: Altering the strength of the pMHCI/CD8 interaction by manipulation of MHCI facilitates 'focussing'

C1R A2 target cells were pulsed with peptide, as described in Table 3.1 for the MEL5 system, added at the concentration indicated, and subsequently incubated together with serum-starved MEL5 $CD8^{+}$ T-cells at 37 °C overnight. The supernatant was harvested and assayed by ELISA for IFNγ. The mean and standard deviation of two replicate assays is plotted. Experimental assays were repeated on six occasions, and these data are representative. The data sets at the origin of the x-axis are obtained in the absence of exogenous peptide. Data is displayed to depict activation using different target cells, and thus differing pMHCI/CD8 interaction strength, by the same peptide.

I observed that when the pMHCI/CD8 interaction is abrogated (A2 227/8 MHCI), the only robust response made by the MEL5 $CD8^+$ T-cell clone is to the high affinity ligand, FAT (Figure 5.5), and no activation was seen in response to either the cognate (ELA) or reduced affinity (3T) agonists. Therefore, the activation hierarchy observed in the absence of pMHCI/CD8 engagement was: FAT>ELA=3T (Figure 5.5 & 5.6, and Table 5.4). The activation hierarchy observed when cross-reactive ligands were presented in the context of *wild type* pMHCI was: FAT=ELA>3T (Figure 5.5 & 5.6, and Table 5.4). As pMHCI/CD8 interaction affinity is increased, I observed a shift in this hierarchy, through FAT>ELA>3T (A2 QE) to ELA>FAT>3T (A2/KbA245V) to ELA>FAT>3T ($A2/K^b$) (Figure 5.5 & 5.6, and Table 5.4). Plotting the same data to show how activation of the same ligand in different B-cell targets, i.e. pMHCI/CD8 is varied, we can observe which pMHCI interaction elicits the greatest T-cell response to the same TCR agonist (Figure 5.7).

Ligand / A2 variant	ELTGIGILTV	ELAGIGILTV	FATGIGIITV
A2 227/8	-2.63907	-1243	5.8255
A2	2.8892	5.5501	6.1982
A2 Q115E	3.788	6.2565	6.6447
A2 K^b A245V	2.1098	4.5299	3.4376
A2 K^b	1.5917	4.5109	3.2516

Table 5.4: pEC50s obtained by single batch analysis for the Mel System.

The data portrayed in Figure 5.3 were used to generate scaled dose response curves. These data were then used to generate pEC50s, scaled to the weakest ligand presented in the context of the weakest pMHCI/CD8 interaction. In order to do so, the data were treated as a single batch for analysis, the assumption being that all cell lines share the same maximum output level. Given that all cells were treated in an identical manner, and that all target cell lines originated from the same C1R parent line, with the same clone being applied to each, this assumption is warranted.

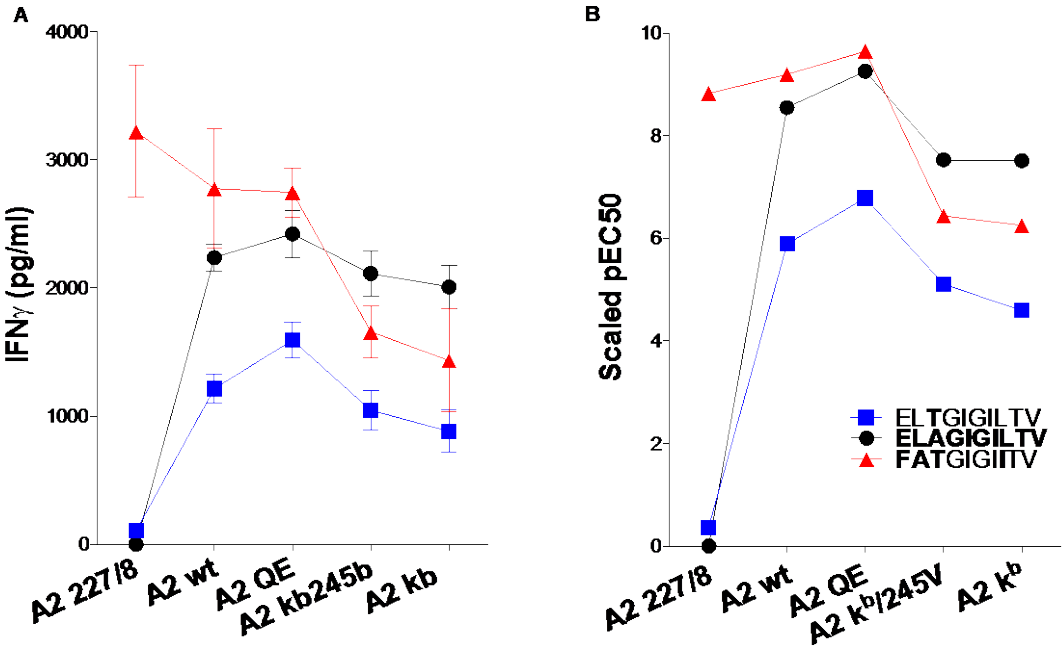

Figure 5.6: Altering the strength of the pMHCI/CD8 interaction by manipulation of MHCI facilitates 'focussing'

A The relative potencies of the ligands examined for Figures 5.3 and 5.5 are compared at a peptide concentration of 10^{-5} M. **B** The data generated above was displayed as scaled dose response curves, which could then be used to calculate pEC50s, thus allowing comparison of the relative potencies of the TCR agonists when considered over the whole curve. pEC50s are scaled relative to the weakest agonist and the lowest CD8/pMHCI affinity. In order to generate pEC50s, these data were treated as a single batch analysis, the assumption being that all cell lines share the same maximum output level. Given that all cells were treated in an identical manner, and that all target cell lines originated from the same C1R parent line, with the same clone being applied to each, this assumption is warranted. Activation by ELAGIGILTV-A2 227/8 represented a null result, and as such is drawn as 0. pEC50s are summarised in Table 5.2.

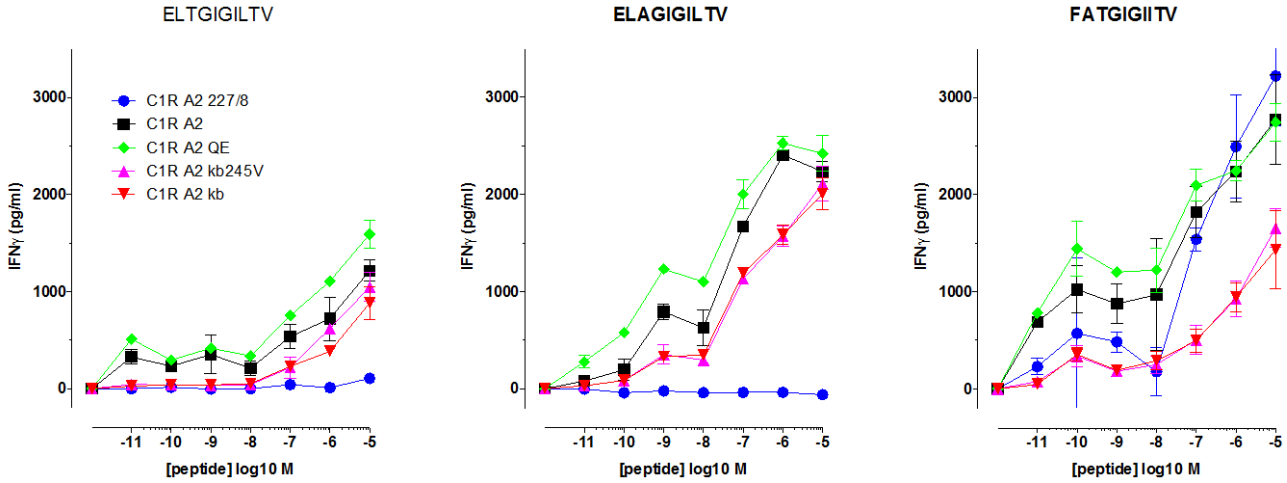

Figure 5.7: Rearrangement of the relative potencies of different TCR agonists as pMHCI/CD8 is altered.

The data generated for Figure 5.3 was re-plotted to compare activation of the MEL5 clone by different peptide ligands presented by different target cell lines.

5.3 Discussion

The binding of both TCR and CD8 is usually necessary to trigger downstream signalling with the exception of very potent TCR agonists or a greatly enhanced pMHCI/CD8 interaction (the A2/K^b mutant) (Wooldridge et al., 2010a, Laugel et al., 2007b, Cole et al., 2012). It has been recognised that dependence on CD8 is inversely related to TCR/pMHCI affinity; high affinity ligands may act as agonists in the absence of CD8, whilst poor agonists have an absolute requirement for co-receptor function, and moderate agonists which have a partial requirement for CD8 (Cole et al., 2012). Mathematical modelling has suggested that CD8 may exert a differential affect on the functional sensitivity of different ligands (van den Berg et al., 2007, Szomolay et al., 2013). It is predicted that *in vivo* this effect is likely to be achieved by alteration of the CD8 co-receptor density at the cell surface (van den Berg et al., 2007, Szomolay et al., 2013). It seems probable that manipulating the affinity of the pMHCI/CD8 interaction is likely to have a similar effect and thus may be a useful tool to manipulate the functional sensitivity of the TCR to differing affinity ligands (Szomolay et al., 2013, van den Berg et al., 2007). It would appear from experimental data that enhancing the strength of the pMHCI/CD8 interaction may increase the sensitivity of the TCR to a sub-optimal ligand, whilst the same enhancement may make an already favourable interaction less so, thus resulting in a 'focussing' effect.

It is uncertain why this effect was not observed when examining IL-10 release by the H9 system, although the different TCR occupancies required may offer an explanation. In short, this discrepancy reiterates the need for more robust testing of multiple systems in order to more fully classify this effect.

I have examined both the ILA1 and MEL5 system experimentally, altering the strength of the pMHCI/CD8 interaction both by manipulating the CD8 molecule

itself, and by manipulating the CD8 binding region of the MHCI molecule. Similar effects were observed in both systems and with different functional read-outs (Figures 5.1 – 5.7). For a given pMHCI ligand, enhancing the strength of the pMHCI/CD8 interaction initially results in enhancement of the T-cell response, however, further enhancement of this interaction resulted in the pMHCI ligand becoming sub-optimal, and if this is increased further the pMHCI ligand may become an increasingly poor agonist. The exception is very high affinity pMHCI ligands, which serve best as agonists to the TCR in the absence of CD8 or presence of wild type CD8. These observations are made most evident to see, if one rearranges the data in order to display the shift in ligand activation hierarchy as the pMHCI/CD8 interaction affinity is altered (Figure 5.1, 5.3 & 5.5).

On the basis of the data generated in this chapter, I propose the model detailed in Figure 5.8. In order for a ligand to function as an optimal agonist, a complex balance exists between the TCR/pMHCI affinity and the pMHCI/CD8 affinity. The relationship appears to be an inverse one; i.e. where TCR/pMHCI is relatively high (a strong agonist) then optimal activation through the TCR is achieved with a relatively low (or even absent) pMHCI/CD8 affinity. The converse is also true; a weak agonist may function as an effective TCR agonist if pMHCI/CD8 affinity is artificially increased beyond what is physiological normal. The model predicts that increasing the pMHCI/CD8 affinity would act to alter the relative potencies of different ligands for the TCR, so that response to weaker agonists may be enhanced whilst the response to stronger agonists may be reduced. Indeed the experimental data generated in this chapter is consistent with this prediction, and mathematical modelling has yielded a similar prediction (Figure 5.9), although in

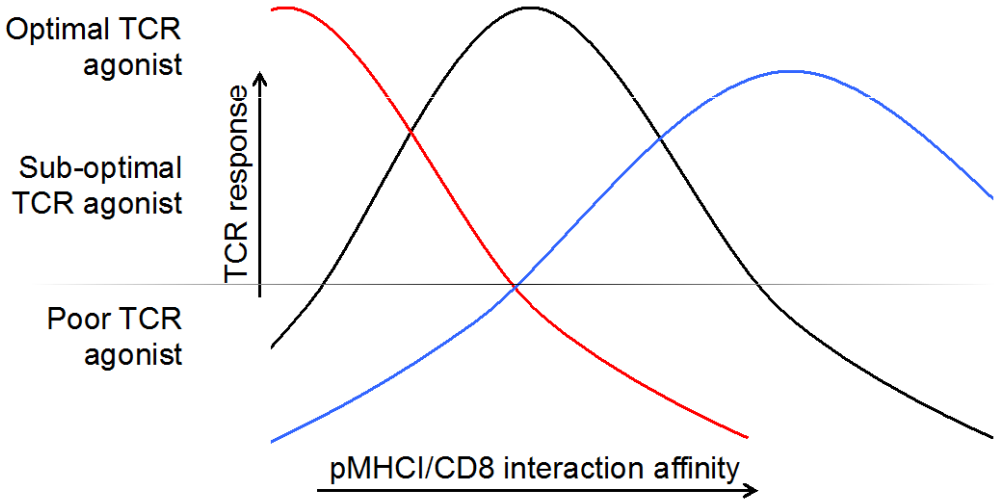

Figure 5.8: A hypothetical model of how altering the strength of the pMHCI/CD8 interaction influences the recognition of ligands with different affinities for the TCR.
The absence of CD8 renders a normally optimal agonist (**-black**) sub-optimal, and possibly too weak to elicit a T-cell response. A CD8 independent agonist (**-red**) can be weakened by the presence of CD8, and if the pMHCI/CD8 interaction is enhanced, it may cease to act as an agonist. Conversely a weak TCR agonist (**-blue**) can be stabilised by an enhanced affinity pMHCI/CD8 interaction, thus it may act as an effective agonist to the TCR.

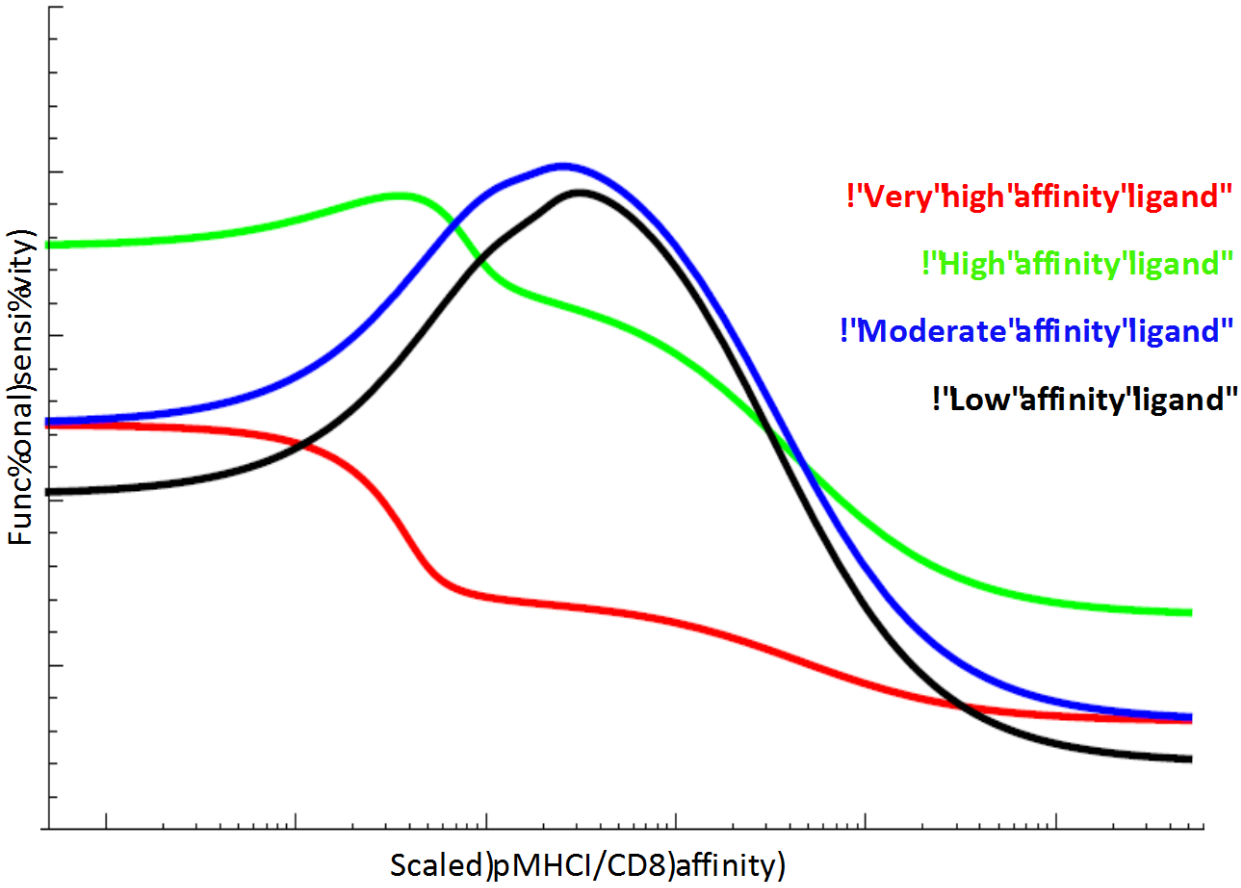

Figure 5.9: Predicting the effect that increasing the pMHCI/CD8 interaction affinity has on the functional sensitivity of the TCR.

Depicted is a mathematical model predicting the TCR response to different agonists as pMHCI/CD8 interaction affinity is varied, provided by Barbara Szomolay and Hugo van den Berg, University of Warwick (Szomolay and van den Berg, 2014, Szomolay et al., 2013, van den Berg et al., 2007).

this model it is predicted that both moderate and low affinity ligands will be co-enhanced at similar pMHCI/CD8 interaction affinities. Whilst this is a model, and as such subject to multiple variables, if enhancement of pMHCI/CD8 results in enhanced response to all of these ligands at similar affinities, then the implications at this level of enhancement is huge, with enhancement of the pMHCI/CD8 interaction potentially resulting in a marked increase in TCR promiscuity. Further examination of this area of CD8 biology is indicated in order to characterise this *in vivo*. This may be an important feature if one is to consider utilising CD8 manipulations for therapeutic gain.

I have previously discussed that as a non-polymorphic molecule necessary to perform a co-receptor function in $CD8^+$ T-cells, CD8 could be ideal to enhance the activity of adoptively transferred $CD8^+$ T-cells, as it could be globally applicable. The inherent cross-reactivity of the TCR has previously been discussed (Sewell, 2012, Mason, 1998). If increasing the pMHCI/CD8 affinity were to increase the TCR response to every single one of its multiple agonists, then the ramifications for cross-reactivity are vast, however, the data as discussed in this chapter would suggest that this is not the case, rather that altering the strength of the pMHCI/CD8 interaction serves to redefine the TCR/pMHCI interaction affinity at which agonists are 'optimal'. However, the effect of increasing the pMHCI/CD8 interaction affinity on cross-reactivity requires robust testing.

The reasons for this 'focussing' effect are likely to be linked to the kinetics of both the TCR/pMHCI and pMHCI/CD8 interactions. The pMHCI/CD8 interaction is characterised by very rapid kinetics ($K_{off} > 18\ s^{-1}$) (Wyer et al., 1999, Gao et al., 2000), and a relatively weak affinity (average K_D 145 μM), with notable outliers being far weaker (Bridgeman et al., 2012, Cole et al., 2012, Hutchinson et al., 2003). TCR/pMHCI interactions have been recorded over a far broader range; < 10

μM (viral epitopes) - > 250 μM (autoimmune). The off-rates are also highly variable between epitopes, with the strongest interactions tending to have the longest off-rates. If we consider the kinetics of the tri-partite structure as this pertains to TCR triggering, we can see why both TCR and CD8 co-receptor kinetics are important to, and dependent upon, each other.

In order for the TCR triggering to occur, both TCR and CD8 need to co-engage simultaneously. The triple structure must remain intact for long enough to allow phosphorylation of all ITAMs, facilitating downstream signalling. The structure then dissociates freeing the TCR; multiple single TCR events being required for full triggering. When a ligand is optimal, both molecules rapidly co-engage, remain engaged and triggering rapidly ensues. A weak agonist has a faster off rate and a shorter dwell time, thus is more likely to dissociate before phosphorylation of all ITAMs has occurred, making triggering less likely. Enhancement of the pMHCI/CD8 interaction has the effect of stabilising the TCR/pMHCI interaction, thus increasing the dwell time of the TCR. This enables weaker affinity ligands to initiate TCR triggering before the structure can dissociate. A strong TCR agonist, with a slow K_{off} will rapidly engage the TCR, and owing to its greater dwell time, will remain bound. CD8 independent agonists may form sufficiently stable interactions with the TCR to initiate TCR triggering without CD8 co-receptor help. In this instance, a high affinity co-receptor may still engage, facilitating ITAM phosphorylation and downstream signalling; however both interactions now have slower kinetics. The dwell time is directly related to both the TCR/pMHCI interaction affinity, and the pMHCI/CD8 interaction affinity, thus when both interactions are strong, the dwell time is greatly increased. The structure cannot dissociate, so further signalling cannot occur. The internalnalisation of the TCR, the recycling of pMHCI, and serial activation is thought to be essential for full and robust activation of the T-cell (Valitutti et al., 1995).

At one end of the spectrum are those interactions capable of initiating T-cell activation without co-engagement of the second receptor. CD8-independent ligands do not require CD8 in order to facilitate T-cell activation, and, as has been discussed, in some instances the agonist is so strong that the presence of the co-receptor can actually damp down the T-cell response. These agonists are however still limited by the specificity of the TCR itself. CD8 is non-polymorphic and binds the invariant region of the MHCI, thus may bind any MHCI. When this interaction affinity is increased above a certain point, specific activation through the TCR is not required, as was discussed in Chapter 3, and the co-receptor is capable of bringing about T-cell activation in an antibody like manner (Wooldridge et al., 2010a, Dockree et al., 2017).

The data presented in this chapter suggest a possible means by which CD8 can modulate the $CD8^+$ T-cell response. I have demonstrated that by manipulating the pMHCI/CD8 interaction affinity the relative potency of different pMHCI ligands presented in the context of the same MHCI is re-arranged. CD8 is uniform and mostly non-polymorphic in nature, thus it is evident that this is not the means by which CD8 modulates the specificity of the TCR *in vivo*, however it does provide some insights that it is possible to 're-focus' the TCR, and give some clues as to possible means by which this can be achieved. It has been considered that the same effect might be achieved by manipulating the levels of CD8 expressed at the cell surface. Increased co-receptor density has been postulated as a possible functional analogue for increased interaction affinity (Park et al., 2007).

In summary, this chapter has highlighted a further way in which the CD8 co-receptor may be essential in $CD8^+$ T-cell biology. The focussing effect described here may be essential to the host in terms of damping down cytotoxic responses to potent ligands thereby avoiding both catastrophic damage to host tissues and T-cell

exhaustion in the event of chronic infection. The exact mechanism by which this is achieved *in vivo* remains uncertain, but modulation of cell surface CD8 co-receptor levels has been postulated and will be probed in more depth in the next chapter.

Chapter 6

The level of CD8αß expressed at the cell surface can affect $CD8^+$ T-cell activation

6.1 Introduction

The heterodimer CD8αß is constitutively expressed at the surface of cytotoxic $CD8^+$ T-cells (Janeway, 1992). During TCR engagement, CD8αß co-engages the target pMHCI simultaneously with the TCR, where it acts to stabilise, enhance and fine-tune the antigen-specific T-cell response, and is thus termed the 'co-receptor' (Wooldridge et al., 2005, Janeway, 1992, Miceli and Parnes, 1991, Garcia et al., 1996). In man, CD8αß is largely non-polymorphic and binds the invariant region of the pMHCI, thus binds different MHCI alleles with similar affinities (although outliers do exist), meaning that it may perform co-receptor function to multiple pMHCI to which the highly promiscuous TCR is capable of recognising (Bridgeman et al., 2012, Wooldridge et al., 2012, Wooldridge et al., 2010b). In addition to stabilising the tri-partite structure extracellularly, CD8αß acts to deliver lck to the CD3 ITAMs thus facilitating downstream signalling (Arcaro et al., 2001, Artyomov et al., 2010, Gascoigne et al., 2011, Veillette et al., 1988, Bosselut et al., 1999).

6.1.1 The level of CD8αß expressed at the cell surface

The levels of CD8αß expressed at the cell surface of $CD8^+$ T-cells can vary both between populations, and in the same T-cell over time.

Different effector phenotypes have been described following activation, with different functions being attributed to $CD8^{high}$ versus $CD8^{low}$ populations (Kienzle et

al., 2004, Martinez, 2010). Some authors have described cell divisions giving rise to daughter cells expressing different levels of CD8, $CD8^{high}$ and $CD8^{low}$, resulting in two distinct populations with different roles and phenotype (Chang et al., 2007, Gerlach et al., 2013, Feinerman et al., 2008).

These differences in CD8 expression have been described by some as existing due to the asymmetrical division of transcription factors such as c-Myc (Do and Li, 2016, Feinerman et al., 2008). Indeed, manipulation of c-Myc has been suggested as a potential vehicle for the manipulation of CD8, and in doing so affecting the T-cell response. Do and Li suggest that this may be utilised for patient benefit in the development of novel cancer therapies (Do and Li, 2016). Feinerman *et al* describe an inverse relationship between levels of cell surface CD8 and the absolute number of ligands required for T-cell activation, whilst the percentage of the overall population that is capable of responding remains mostly unchanged (Feinerman et al., 2008). In addition, T-cell function is intrinsically linked to CD8 expression. In most instances, loss of cell surface CD8 leads to reduced tetramer staining (Demotte et al., 2002, Drake et al., 2005).

6.1.2 The $CD8^{high}$ and $CD8^{low}$ Phenotypes

T-cells ($CD3^+$ cells) may be split into six subsets based upon their CD4 and CD8 expression at the cell surface: $CD4^-CD8^-$, $CD4^+CD8^-$ (CD4 T-cells), $CD4^+CD8^{low}$, $CD4^+CD8^{high}$, $CD4^-CD8^{low}$, and $CD4^-CD8^{high}$ (Orru et al., 2013). Thus there are two distinct subsets for each of the CD8-expressors (DP and $CD8^+$ T-cells); $CD8^{low}$ and $CD8^{high}$ (also occasionally termed $CD8^{dim}$ and $CD8^{bright}$, respectively). Both $CD8^{high}$ and $CD8^{low}$ $CD8^+$ T-cells may be $CD28^+$ or $CD28^-$ (effector or memory), suggesting that $CD8^{high}$ and $CD8^{low}$ subsets represent a separate phenotype. An IL-2 rich environment

favours the differentiation of naïve $CD8^+$ T-cells into only $CD8^{high}$ effector cells, whereas in the presence of IL-4 both $CD8^{high}$ and $CD8^{low}$ phenotypes result, with plasticity between these two latter subtypes being demonstrated in response to IL-4 (Olver et al., 2013, Kienzle et al., 2004, Apte et al., 2008). T-cell clones produced in the absence of IL-4 are unable to produce IL-4, maintain a neutral environment, and remain $CD8^{high}$ effector T-cells. They produce perforin, granzymes and IFNγ and are cytolytic of targets (Kienzle et al., 2004, Kienzle et al., 2002). $CD8^{high}$ T-cells produced in the presence of IL-4 maintain the ability to produce IL-4, but otherwise have a cytotoxic phenotype. In contrast, $CD8^{low}$ T-cells, are able to produce IL-4 but otherwise have limited cytolytic function.

It is debated whether these two last subsets cycle between the two states under the influence of IL-4, where IL-4 and IFNγ reciprocally control CD8 expression, and thus effector phenotype (Apte et al., 2008, Kienzle et al., 2004, Olver et al., 2013, Kienzle et al., 2002). $CD8^{low}$ T-cells may exhibit long-term survival, and whilst they are only weakly cytotoxic, have been shown to demonstrate anti-tumour activity (Olver et al., 2013). Given the similarity of tumour antigens to self, it is possible that this down-regulation of CD8 and plasticity between the IL-4-derived subsets is an essential feature to avoid cross-reactivity with self. It should be noted that these $CD8^{low}$ subsets represent distinct and sustained populations, and are entirely different from the transient down-regulation of CD8 at the cell surface seen in $CD8^+$ effector cells which is normal following stimulation and activation via the TCR (Kao et al., 2005, Xiao et al., 2007).

6.1.3 Evidence for tuning of T-cell function

Following T-cell activation, there is a transient down-regulation of cell surface CD8 and TCR, and a reduction in T-cell antigen sensitivity (Garcia et al., 1996, Xiao et al., 2007). Others have suggested that CD8 levels at the cell surface remain unchanged however binding of CD8 and TCR to the pMHCI is reduced thus affecting function (Kao et al., 2005, Drake et al., 2005). It has been suggested that up-regulation of cell surface CD8 allows more efficient recognition of low affinity and low avidity ligands (Takada and Jameson, 2009b). Naïve T-cells expressing low levels of CD8 on their cell surface are therefore weakly stimulated by self-antigen encountered in the periphery (Sprent and Surh, 2011, Surh and Sprent, 2008, Takada and Jameson, 2009a). It is likely that this low level of weak stimulation allows them to continue to exist, since long-term survival of the T-cell is impaired in the absence TCR stimulation (Takada and Jameson, 2009b, Park et al., 2007).

Whilst this low level recognition, and partial activation of T-cells by self pMHCI is necessary for the persistence of these cells, it is evident that complete activation and targeting of self-ligands can occur resulting in autoimmune disease. The very fact that activation may occur to the same ligands and result in these two different consequent activities would suggest that the T-cell is capable of modulating its response. Indeed, it is essential that if the T-cell requires autologous stimulation in order to maintain the naïve pool in the long term, that a regulatory mechanism exists in order to prevent complete activation and thus widespread autoimmunity. CD8 levels at the cell surface are adjusted according to the specificity of the TCR (Park et al., 2007). This chapter will attempt to explore the possibility that altering the levels of cell surface CD8 is a mechanism by which the antigen sensitivity of the TCR can be modulated, and levels of T-cell cross-reactivity can be controlled.

6.1.4 Factors that control of CD8αß expression

Cell surface CD8αß levels are altered in response to various cytokines. CD8 is up regulated in the presence of IFN-γ and down regulated in response to IL-4 (Apte et al., 2008). These cytokines reciprocally result in increased or decreased levels of CD8α mRNA, suggesting that they are responsible for, or involved in, the switching on (IFN-γ) or off (IL-4) of the CD8α gene (Apte et al., 2008). CD8ß does not exist on its own in nature, nor in the form of the CD8ßß homodimer, thus control of the CD8α gene ultimately results in control of cell surface CD8αß expression (Devine et al., 2000, DiSanto et al., 1988, Gorman et al., 1988).

6.1.5 TCRs are inherently cross-reactive

An essential feature of the TCR is its promiscuity, enabling the T-cell to recognise and respond to a multitude of different peptide ligands (Wooldridge et al., 2012, Mason, 1998). Whilst it is recognised that a single TCR may be highly cross-reactive, potentially recognising an average of 10^5 different peptide ligands, not all of these are 'real', or encountered in nature. The TCR recognises a range of ligands with varying affinity, thus the T-cell response is similarly variable. The exact mechanism by which it differentiates between different ligands is uncertain. A role for CD8 in controlling T-cell cross-reactivity has been postulated (Wooldridge et al., 2010b, van den Berg et al., 2007).

6.1.6 Altering the pMHCI/CD8 interaction affinity alters the 'focus' of the TCR

It has been demonstrated in previous chapters, that altering the strength of the pMHCI/CD8 interaction affects the resultant T-cell response. Different TCR/pMHCI interactions are differently affected by these manipulations, leading to preferential activation of different affinity ligands, or, more simply, an alteration of the activation hierarchy when different peptide ligands are considered and compared. As has been discussed, this is true whether the manipulation of pMHCI/CD8 is achieved by altering the MHCI/CD8 binding region, or by manipulation of the CD8 molecule itself. Whilst it is evident that the non-polymorphic CD8 molecule itself remains unchanged *in vivo*, there are differences in the pMHCI/CD8 binding affinity between different MHCI alleles owing to differences in the invariant MHCI binding region, and, although the exact role of these natural variants remains unclear, it is possible that they are of biological significance.

A better understanding of this possible focussing mechanism is important if CD8 is to be utilised in adoptive transfer systems; if the copy number of the transgene controls expression levels, the transduced cell will be unable to alter expression levels at the cell surface. The potential implications if CD8 expression levels are indeed involved in focussing between ligands are that the cell will be unable to alter which ligands are best recognised. If we are able to identify the levels required for best activation against a given agonist, then cells expressing the desired level of CD8 may be selected for expansion, enabling optimal ACT.

6.1.7 Aims

Here, I hypothesise that the level of CD8αß expression at the cell surface can have a dramatic affect on T-cell antigen sensitivity. In order to examine the effect that different levels of cell surface CD8αß exert on T-cell activation, I have used the jurkat model described in previous chapters transduced with a well-characterized TCR and different levels of cell surface CD8αß. The drive of previous manipulations has been to identify a means by which a designer co-receptor may be used to augment existing ACT systems. It therefore becomes important to identify the optimal level of CD8αß expression required for effective target killing by $CD8^+$ T-cells. It is possible that this 'ideal level' varies between different affinities of TCR agonist, and classifying these factors will enable researchers to build a designer T-cell, fine-tuned to target cancer, and optimise ACT cancer therapies to achieve high success rates.

6.2 Results

6.2.1 Cell Lines co-transfected with *wild type* CD8αß and the ILA1 TCR co-express similar levels of TCR and broad range of the CD8αß co-receptor.

The JRT3-T3.5 cell line was co-transfected with ILA1 TCR and the co-receptor CD8αß. Flow cytometric analysis of these cells demonstrated co-expression of both the ILA1 TCR and CD8αß. Presence of the TCR was confirmed by positive staining with anti-rCD2 antibody, with anti-CD3 antibody, and with anti-αßTCR antibody. Presence of the CD8αß co-receptor was confirmed by positive staining with anti-CD8α antibody, and anti-CD8ß antibody (Figure 6.1). Staining confirmed expression of similar levels of TCR in transduced cell lines (Figure 6.2A). A wide range of CD8αß expression was observed, ranging from CD8αß$^-$ to a high level of CD8αß expression (Figure 6.2B). Staining confirmed similar levels of CD8α and CD8ß were expressed across this range, suggesting expression of the heterodimer (Figure 6.1).

6.2.2 ILA1 TCR$^+$ CD8αß$^+$ lines sorted for expression of different levels of cell surface CD8αß maintained their phenotype following sorting/enrichment.

J.RT3-T3.5 ILA1 TCR$^+$ CD8αß$^+$ cell lines stained with anti-rCD2, anti-CD8α and anti-CD8ß were sorted using a modified FACSAria flow cytometer/cell sorter, selecting for populations expressing either no CD8, or low, moderate and high levels of CD8αß at the cell surface (Figure 6.2B). Following enrichment in this manner, the sorted cell populations were expanded and re-stained. J.RT3-T3.5 ILA1 TCR$^+$ CD8αß$^-$, J.RT3-T3.5 ILA1 TCR$^+$ CD8αß^{low}, J.RT3-T3.5 ILA1 TCR$^+$ CD8αß^{med}, J.RT3-T3.5 ILA1 TCR$^+$ CD8αß^{high}

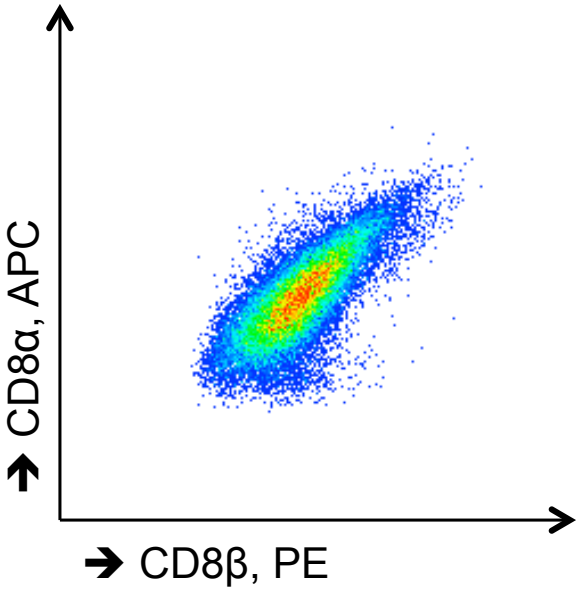

Figure 6.1: JRT3-3.5 ILA1 TCR$^+$ CD8αβ$^+$ cell line expresses CD8α and CD8β in equal proportions, suggesting expression of the CD8αβ heterodimer.

The J.RT3-3.5 ILA1 TCR$^+$ cell line was stably transfected with CD8αβ. The resultant cell line was expanded, and enriched for CD8αβ$^+$ cells. These cells were stained for FACs Canto analysis with ViViD Live/Dead stain, APC-conjugated anti-CD8α antibody and PE-conjugated anti-CD8β antibody. Live events were recorded.

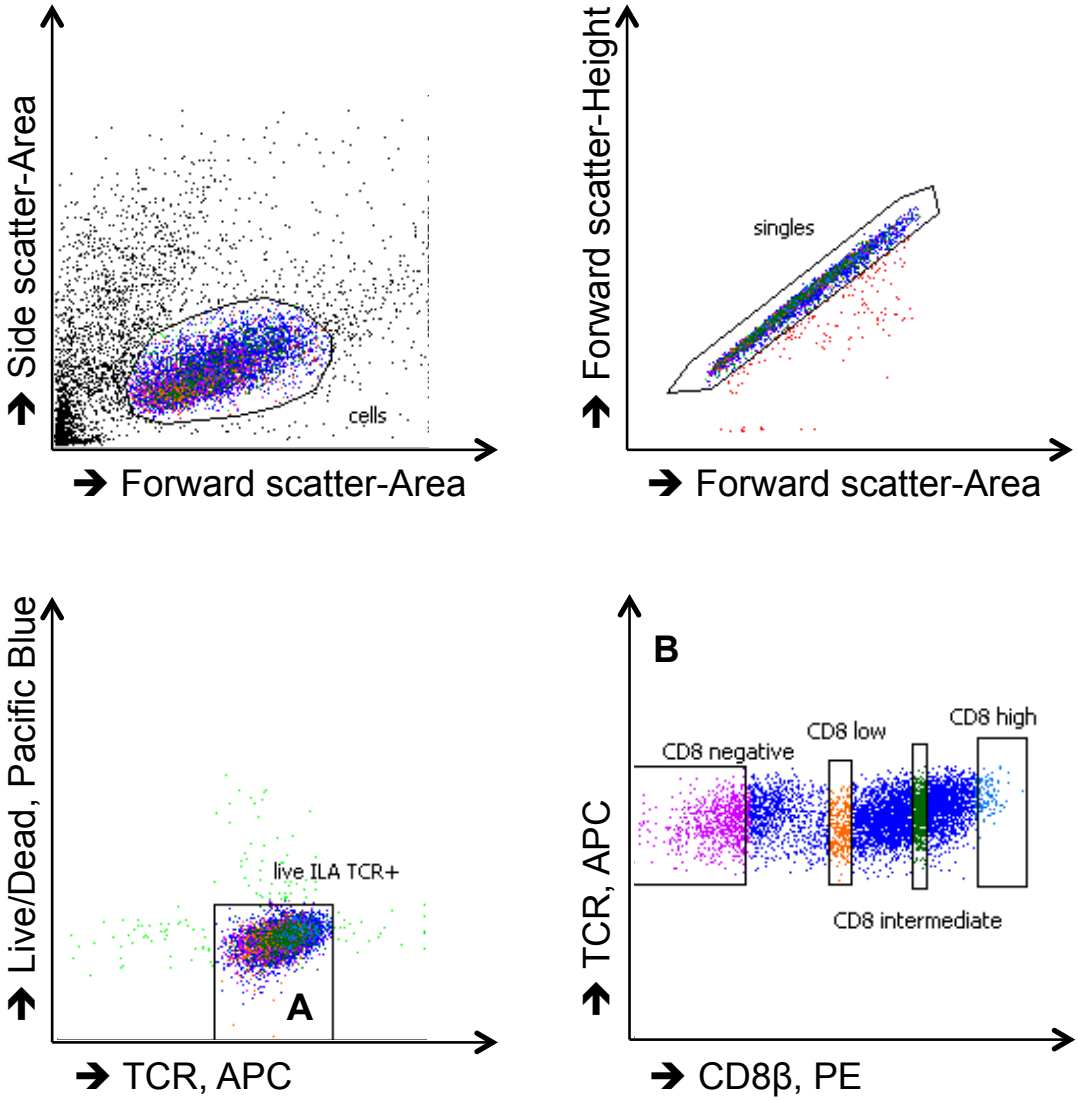

Figure 6.2: JRT3-3.5 ILA1 TCR$^+$ CD8αβ$^+$ cell line was sorted into CD8$^-$, CD8^{low}, CD8^{medium}, and CD8^{high} populations.
The J.RT3-3.5 ILA1 TCR$^+$ CD8αβ$^+$ cell line was stained with ViViD Live/Dead stain, anti-CD8β PE-conjugated antibody and anti-rat CD2 FITC-conjugated antibody. Cells were sorted using a modified FACSAriaII flow cytometer. Non-viable, rat CD2$^-$ events only were excluded (**A**) and the cell line was sorted into CD8β$^-$, and CD8β^{low}, CD8β^{medium}, and CD8β^{high} populations (**B**) for expansion.

were found to maintain relative expression levels of both the TCR and CD8αß at the cell surface (Figure 6.3A-C).

6.2.3 Increased level of cell surface CD8αß results in enhanced pMHCI tetramer staining.

When clonal primary $CD8^+$ T-cells (MEL5 clone) stained with tetramers loaded with their cognate ligand (ELA) and anti-CD8 antibody are gated upon in order to examine the $CD8^{low}$ and $CD8^{high}$ populations separately, the following trend can be observed; clones with higher levels of cell surface CD8 exhibit greater tetramer staining as compared to clones expressing lower levels of cell surface CD8. This trend is the same irrelevant of the pMHCI/CD8 interaction affinity (Figure 6.4A & B).

6.2.4 Increasing the level of CD8αß at the cell surface has a negative impact on the recognition of cognate pMHCI ligand.

J.RT3-T3.5 ILA1 TCR^+ cell lines co-expressing different levels of CD8αß were incubated for 24 hours with C1R A2 B-cells, which had been previously pulsed with the ILA peptide. Assayed cells were stained with anti-CD19 antibody in order to gate out the B-cell populations from analysis, and anti-CD69 antibody, and fixed before data capture by flow cytometry. Live, $CD19^-$ events were recorded in order to obtain CD69 MFI. The mean of two replicates was plotted (Figure 6.5A). The results show that the J.RT3-T3.5 ILA1 TCR^+ line is capable of being activated via the transduced TCR by cognate ligand, as evidenced by increased CD69 expression as peptide concentration is increased. Increased activation is demonstrated in the presence of the CD8αß co-receptor, indicating that the transduced co-receptor is capable of

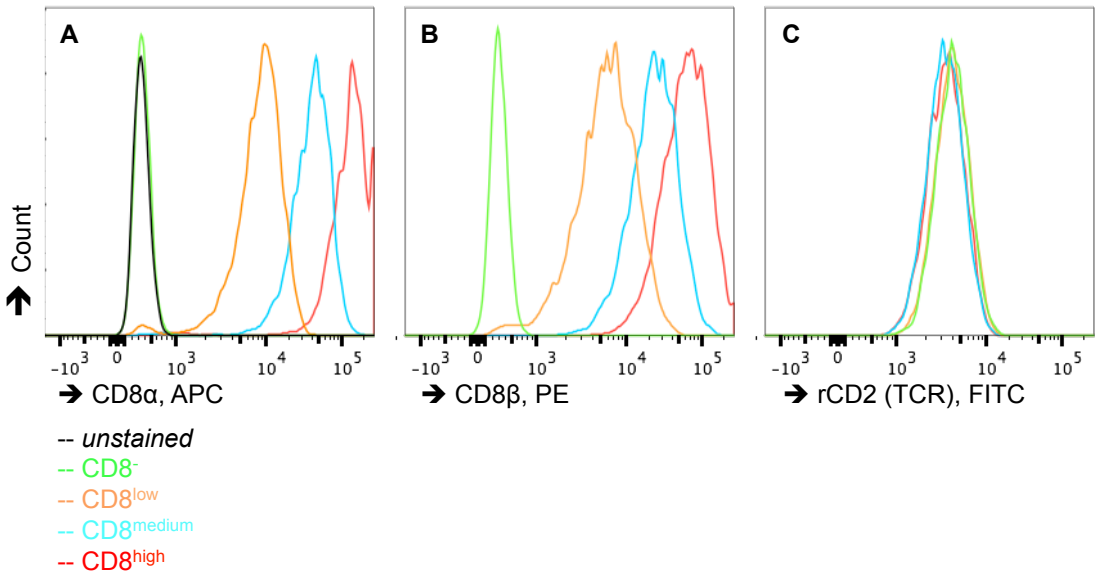

Figure 6.3: Sorted JRT3-3.5 ILA1 TCR$^+$ CD8αβ$^-$, JRT3-3.5 ILA1 TCR$^+$ CD8αβ^{low}, JRT3-3.5 ILA1 TCR$^+$ CD8αβ^{medium}, and JRT3-3.5 ILA1 TCR$^+$ CD8αβ^{high} maintain their phenotype following expansion.

Following sorting (Figure 6.2) and expansion, the JRT3-3.5 ILA1 TCR$^+$ CD8αβ$^-$, JRT3-3.5 ILA1 TCR$^+$ CD8αβ^{low}, JRT3-3.5 ILA1 TCR$^+$ CD8αβ^{medium}, and JRT3-3.5 ILA1 TCR$^+$ CD8αβ^{high} cell lines were stained with ViViD Live/Dead stain, and with anti-CD8α APC-conjugated antibody, anti-CD8ß PE-conjugated antibody and anti-rat CD2 FITC-conjugated antibody. Viable events were recorded, and the data were concatenated into histogram plots. Expression of CD8α (**A**), CD8ß (**B**) and TCR as indicated by rat CD2 marker gene expression (**C**), were compared between cell lines.

A

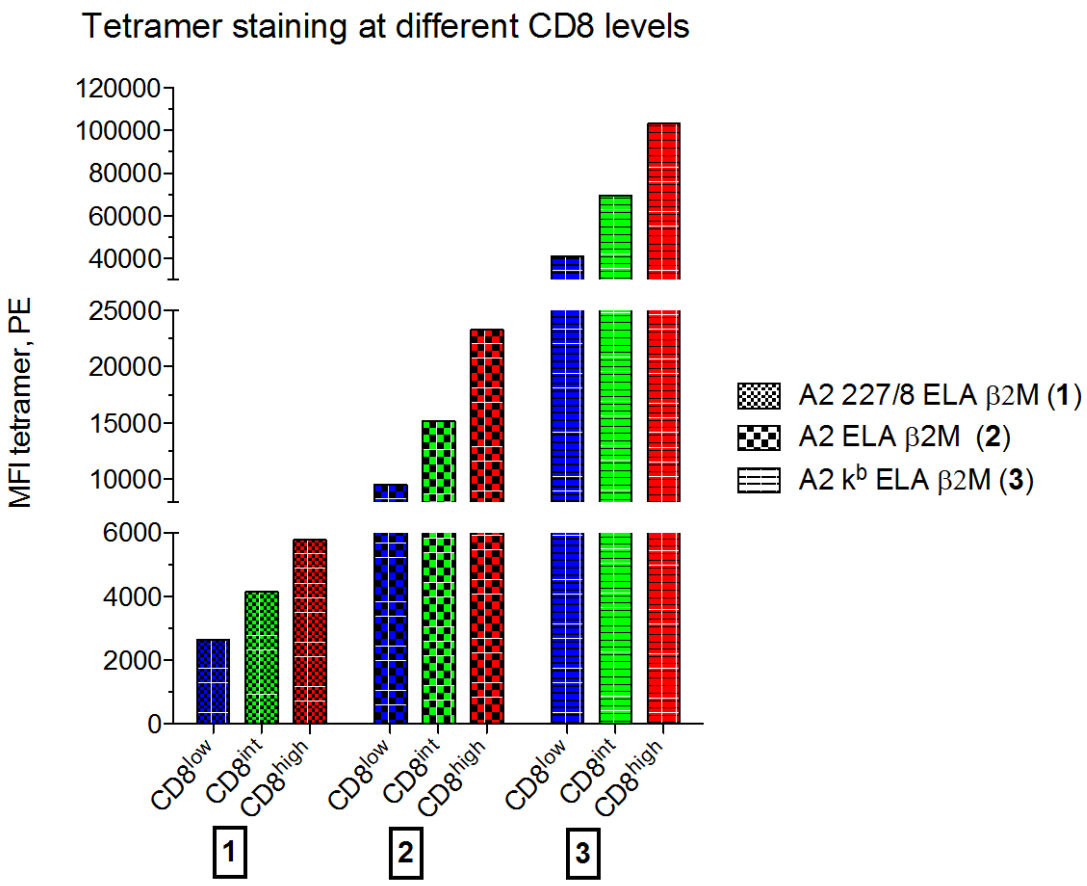

B

		low CD8	medium CD8	high CD8
A	A2 227/8	2657	4137	5777
B	A2 wild type	9537	15184	23279
C	A2 k^b	41017	69426	103115

Figure 6.4: $CD8^+$ T-cell clones stained with cognate tetramer demonstrate greater staining where higher levels of CD8 are found at the cell surface.

The MelanA-specific $CD8^+$ T-cell clone, MEL5, was stained with ViViD Live/Dead stain, anti-CD8 APC-conjugated antibody, and PE-conjugated tetramer loaded with cognate peptide bound to either wild type HLA A2 or HLA A2 bearing either the 227/8 or $A2/K^b$ mutations as described previously. Data were recorded using a FACSCanto flow cytometer. Live events were recorded, and gated to show $CD8^{low}$, $CD8^{medium}$, and $CD8^{high}$ expressing populations. Tetramers staining within these gates were concatenated into histogram plots and compared for each pMHCI/CD8 affinity The MFIs were calculated using FlowJo software, which are tabulated (**B**) and depicted (**A**).

A

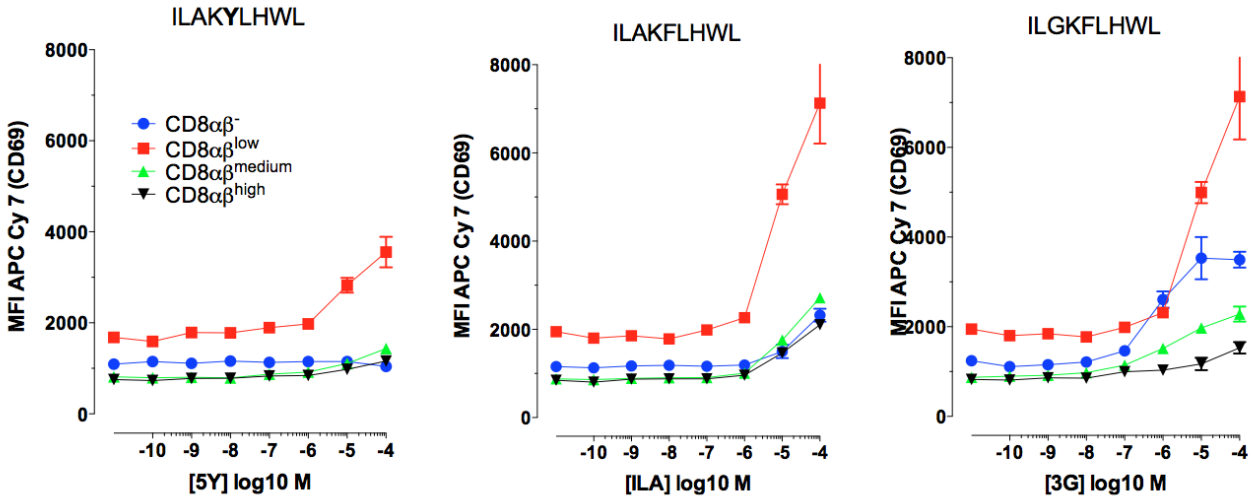
ILAKYLHWL
ILAKFLHWL
ILGKFLHWL
MFI APC Cy 7 (CD69)
8000
6000
4000
2000
0
CD8αβ-
CD8αβlow
CD8αβmedium
CD8αβhigh
-10 -9 -8 -7 -6 -5 -4
[5Y] log10 M
[ILA] log10 M
[3G] log10 M

B

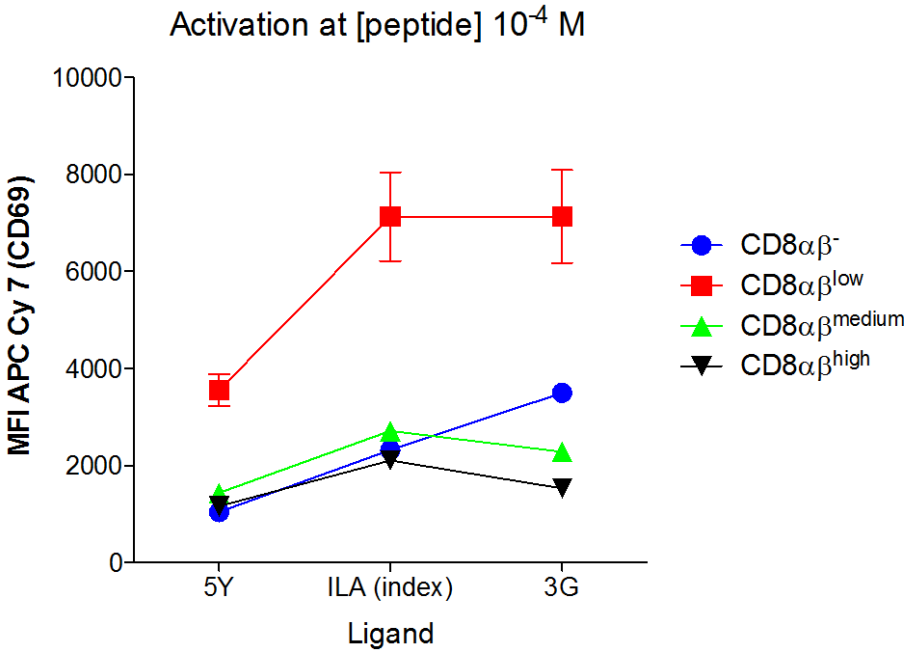
Activation at [peptide] 10-4 M
MFI APC Cy 7 (CD69)
10000
8000
6000
4000
2000
0
5Y
ILA (index)
3G
Ligand
CD8αβ-
CD8αβlow
CD8αβmedium
CD8αβhigh

Figure 6.5: J.RT3-T3.5 ILA1 TCR$^+$ CD8αß^{low} demonstrated greatest response to peptide activation as measured by CD69 up-regulation for all agonists.

Peptide pulsed C1R A2 targets (either one of 5Y, ILA and 3G peptides), as previously described for the ILA system, added at the desired final concentration (10^{-4} – 10^{-10}, and 0 M), were incubated together with each of the J.RT3-T3.5 ILA1 TCR$^+$ CD8αß^{levels} cell lines, overnight. Cells were then stained and fixed for data capture by flow cytometry. Viable effector T-cell (CD19$^-$) events were concatenated into histogram plots in order to obtain the MFI of CD69, and the data represent the mean and standard deviation of two replicate samples. Data points at the origin of the x-axis are generated in the absence of exogenous peptide. Data were plotted comparing the activation of the different cell lines by the same ligand (**A**). Activation by ligands at 10^{-4} M peptide concentration were compared (**B**). These data are representative of multiple experiments (n>4).

acting to increase the TCR recognition of pMHCI, as it does when endogenously expressed in primary $CD8^+$ T-cells. However cell lines expressing higher levels of CD8αß ($CD8αß^{medium}$ and $CD8αß^{high}$) exhibited poorer activation as measured by CD69 up regulation compared to cell lines expressing the lowest level of CD8αß ($CD8αß^{low}$), indicating that optimal activation by cognate ligand is achieved at lower levels of CD8 expression ($CD8αß^{low}$) (Figure 6.5A).

6.2.5 Increasing the level of CD8αß at the cell surface has a negative impact on the recognition of low and high affinity pMHCI ligands.

J.RT3-T3.5 ILA1 TCR^+ cell lines co-expressing different levels of CD8αß were incubated for 24 hours with C1R A2 B-cells, which had been previously pulsed with either the low affinity 5Y- or the high affinity 3G-peptide ligand. Assayed cells were stained with anti-CD19 antibody in order to gate out the B-cell populations from analysis, and anti-CD69 antibody. Data were collected by flow cytometry. The results show that the J.RT3-T3.5 ILA1 TCR^+ line is capable of being activated through the transduced TCR by cross-reactive ligands identified for the ILA system (Laugel et al., 2007b), as evidenced by increased CD69 expression as peptide concentration is increased. Greater activation was observed by the high affinity 3G- ligand (Figure 6.5B).

For each ligand, increased activation is demonstrated in the presence of the CD8αß co-receptor, as compared to $CD8^-$ cells, as with the cognate ligand. When we examine activation by the high affinity 3G peptide agonist, the greatest response is still observed in the J.RT3-T3.5 ILA1 TCR^+ $CD8αß^{low}$ line, however we can see increased response by $CD8^-$ cells as compared to the higher CD8 expressing lines (J.RT3-T3.5 ILA1 TCR^+ $CD8αß^{medium}$ and J.RT3-T3.5 ILA1 TCR^+ $CD8αß^{high}$). For all

ligands examined, cell lines expressing higher levels of CD8αß ($CD8\alpha\beta^{medium}$ and $CD8\alpha\beta^{high}$) exhibited poorer activation as measured by CD69 up regulation compared to cell lines expressing the lowest level of CD8αß ($CD8\alpha\beta^{low}$), indicating that optimal activation for all ligands examined is achieved at lower levels of CD8 expression ($CD8\alpha\beta^{low}$) (Figure 6.5A & B).

6.2.6 Activation via the ILA1 TCR when CD8 binding is abrogated is greatest at the lowest level of CD8αß expression.

J.RT3-T3.5 ILA1 TCR^+ cell lines co-expressing different levels of CD8αß were incubated for 24 hours with C1R A2 227/8 B-cells, which had been previously pulsed with the 5Y, ILA, or 3G- peptide ligand. Assayed cells were stained with anti-CD19 antibody in order to gate out the B-cell populations from analysis, and anti-CD69 antibody. Data was collected by flow cytometry. For each ligand, activation was less when CD8 binding was abrogated compared to the wild type C1R A2 targets, and for lower affinity ligands (5Y and ILA) activation was minimal at all concentrations of peptide, thus only data for the 3G-ligand depicted any discernable difference in activation, and as such, is the only data shown in Figure 6.6. As with the wild type A2 targets, greatest activation was observed in the J.RT3-T3.5 ILA1 TCR^+ $CD8^{low}$ cell line. The J.RT3-T3.5 ILA1 TCR^+ $CD8^{medium}$ and J.RT3-T3.5 ILA1 TCR^+ $CD8^{high}$ cell lines responded less well to 3G than the J.RT3-T3.5 ILA1 TCR^+ $rCD2^+$ $CD8^-$ cell line (Figure 6.6)

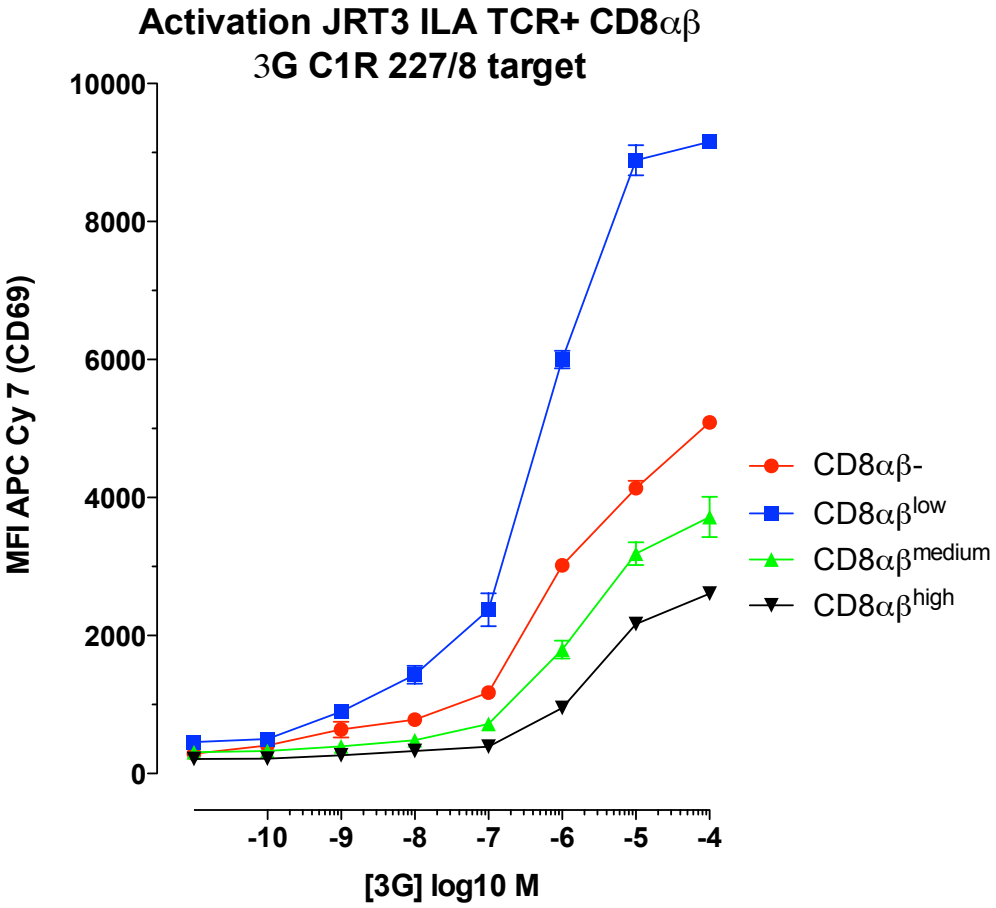

Figure 6.6: Where CD8 binding is abrogated J.RT3-T3.5 ILA1 TCR$^+$ CD8^{medium} and J.RT3-T3.5 ILA1 TCR$^+$ CD8^{high} lines respond less well to the CD8-independent 3G-agonist than J.RT3-T3.5 ILA1 TCR$^+$ CD8$^-$.

Peptide (3G) pulsed C1R A2 227/8 targets were incubated together with each J.RT3-3.5 ILA1 TCR$^+$ CD8αß^{levels} line overnight. Cells were stained and fixed for data acquisition using a FACScanto flow cytometer, and analysed using FlowJo software. Viable effector T-cell (CD19-) events were concatenated into histogram plots in order to obtain the MFI of CD69, and the data represents the mean and standard deviation of two replicate samples. The data sets at the origin of the x-axis are generated in the absence of exogenous peptide. These data are representative of two assays.

6.2.7 The J.RT3-T3.5 ILA1 TCR$^+$ CD8^{med} and J.RT3-T3.5 ILA1 TCR$^+$ CD8^{high} cell lines express CD8αß at greater levels than those observed naturally.

The J.RT3-T3.5 ILA1 TCR$^+$ CD8αß^{var} cell lines, primary CD8$^+$ T-cell clones (ILA1 and MEL5), and PBMC directly *ex vivo* were counted and stained with anti-CD8ß antibody. Cells were twice washed and then fixed in 1% PFA. Live, CD8$^+$ events were recorded in order to obtain MFIs. The mean of two replicates was plotted. These data demonstrate that the J.RT3-T3.5 ILA1 TCR$^+$ CD8αß^{low} express CD8 at levels similar to, or slightly higher than a primary CD8$^+$ T-cell clones, and higher than *ex vivo* CD8$^+$ cells isolated from PBMC. The J.RT3-T3.5 ILA1 TCR$^+$ CD8αß^{med} line expresses CD8 at a level approximately 5 x greater than the primary CD8$^+$ T-cell clones examined, and the J.RT3-T3.5 ILA1 TCR$^+$ CD8αß^{high} line expresses CD8αß at a level approximated 10 x greater than the primary CD8$^+$ T-cell clones examined (Figure 6.7).

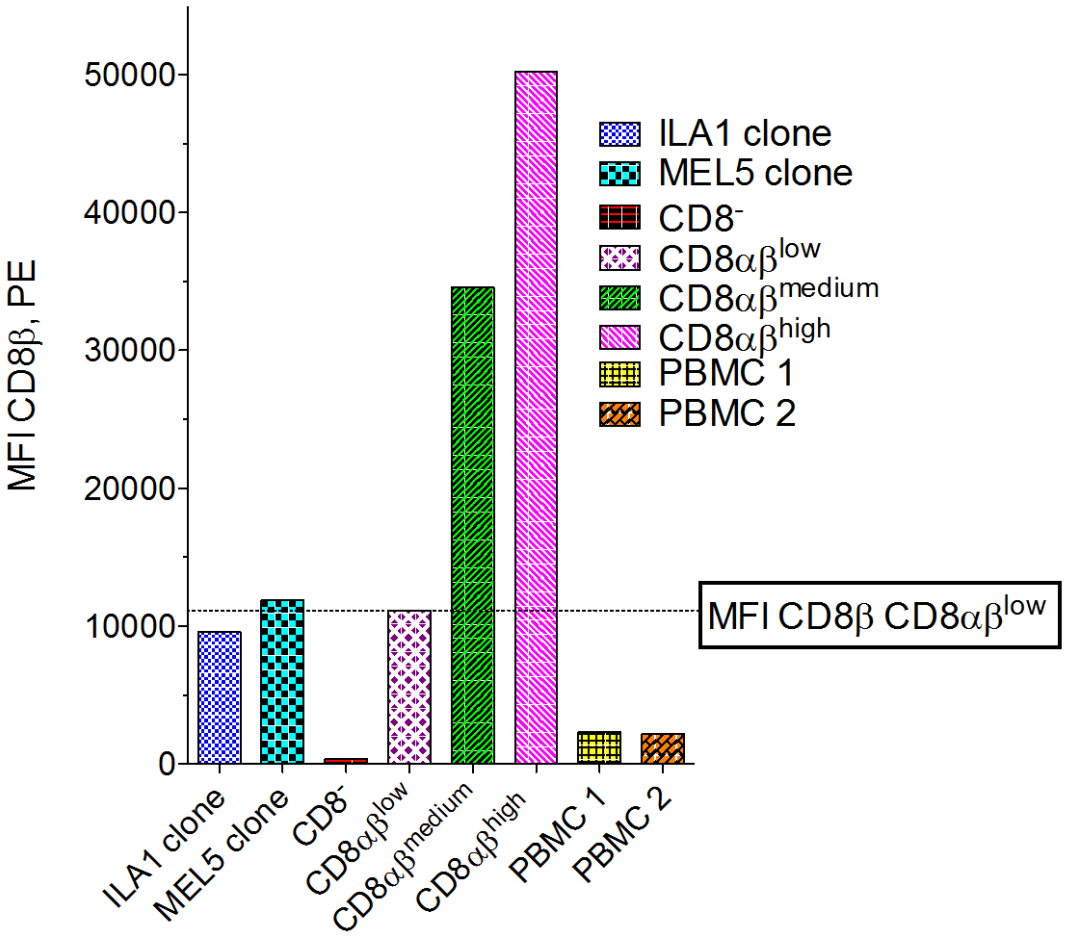

Figure 6.7: The J.RT3-3.5 ILA1 TCR$^+$ CD8αß^{low} cell line expresses similar levels of CD8αß at its cell surface as compared to CD8$^+$ T-cell clones in culture.

5 x 10^4 cells of each population were counted and stained with ViViD Live/Dead stain and anti-CD8ß PE-conjugated antibody, before fixing for data acquisition by flow cytometry. LIVE, CD8$^+$ events were recorded in order to obtain and MFI. These data are representative of n=3 replicate experiments.

6.3 Discussion

Previous chapters have concentrated on the strength of the pMHCI/CD8 interaction, and the effect of manipulating this on the ensuing T-cell response, however *in vivo* this interaction affinity is fixed. It has also been proposed that alteration of absolute levels of CD8 expressed at the cell surface may be a means by which the cell may regulate its response to pMHCI antigen (Takada and Jameson, 2009b, Park et al., 2007, van den Berg et al., 2007). Moreover, it has been suggested by some authors that alteration of the density of CD8αß co-receptors available may elicit a similar effect to manipulating to pMHCI/CD8 affinity on modulating the specific ligand focus of the TCR (van den Berg et al., 2013). In this chapter, I have utilised a jurkat model in order to examine the effect of altering the level of cell surface expressed CD8 on $CD8^+$ T-cell activation. In so doing, by the nature of the jurkat model, the CD8 levels present on the cell surface are fixed; the cell is no longer able to up- or down-regulate its co-receptor. Indeed demonstration of maintenance of phenotype was a key feature of experimental design (Figure 6.3).

The data demonstrates enhanced tetramer staining with increased cell surface CD8 expression, both within and outside of the normal physiological ranges for CD8 expression. Tetramer staining is a measurement of TCR/pMHCI binding at the cell surface, rather than of downstream signalling, as evidenced by enhanced tetramer staining with enhanced pMHCI/CD8 affinity tetramers, irrelevant of the ligand (Wooldridge et al., 2010a), The data obtained upon peptide activation of the jurkat lines expressing different levels of CD8 demonstrated the greatest activation by the $CD8^{low}$ cell line for all ligands examined; low, index and high affinity. This is in contrast to what is seen with tetramer staining of these lines (data not shown). Upon comparing the CD8 levels found in these cell lines to those seen upon the

surface of $CD8^+$ T-cell clones in culture, and $CD8^+$ T-cells directly *ex vivo*, we see that only the JRT3-T3.5 ILA1 TCR $CD8^{low}$ line expresses CD8 at levels close to the apparent physiological median. The JRT3-T3.5 ILA1 TCR $CD8^{med}$ and JRT3-T3.5 ILA1 TCR $CD8^{high}$ lines express CD8 at levels that are at least 5x and 10x respectively, those found in primary cells. Whilst it is possible that levels are so high as to hinder cell surface kinetics and movement within the cell membrane, this is unlikely, as evidenced by the enhanced tetramer staining seen in the JRT3-T3.5 ILA1 TCR $CD8^{med}$ and JRT3-T3.5 ILA1 TCR $CD8^{high}$ cell lines.

When CD8 binds the pMHCI concurrently with the TCR, it acts to deliver kinases such as lck to the CD3 complex, necessary for downstream triggering (Artyomov et al., 2010). It seems likely that when CD8 is found at the cell surface in levels so much greater than those found in nature (Figure 6.7), that many of these molecules would not have an associated lck, indeed the CD8 levels may be far in excess of the lck available. CD8 binding will therefore result in enhanced tetramer staining owing to the greater number of CD8 molecules to stabilise and bind the tetrameric pMHCI molecules, however, in the absence of the cytoplasmic counterpart to this interaction; the delivery of lck to the CD3 ITAMs, downstream triggering does not take place. It could be considered that CD8 acts as a competitive inhibitor to itself, where CD8 binds, thus blocking the biologically active CD8 with lck associated (CD8-lck hereafter) from binding. Additional studies using lck, both free in the cytosol and fused to the CD8ß tail of our trans-CD8αß, would be beneficial in testing this hypothesis, and work is underway to create the necessary constructs.

Another approach to examine this hypothesis could be to determine the ratio or absolute numbers of CD8 and lck within the cell membrane. Levels of these molecules could be examined with the use of antibodies by Western Blotting assays

or via immunohistochemistry, both of which detect these molecules with the use of mAbs. Förster Resonance Energy Transfer (FRET) could also be considered, and this non-invasive technique for examining molecular interactions would provide detailed information on the interaction of cell surface molecule. This technique may also be considered for fine-tuning a means of examining the differences between different levels of CD8 expression at the cell surface (Shrestha et al., 2015).

It has been previously alluded to that the $CD8^+$ T-cells transiently down-regulate CD8 upon antigenic stimulation via its TCR (and co-receptor binding of the pMHCI), thus activated $CD8^+$ T-cells express lower levels of CD8 at the cell surface (Xiao et al., 2007, Paillard et al., 1990). van den Berg *et al* examined the polyfunctionality of the ILA1 $CD8^+$ T-cell clone in response to its cross-reactive ligands (van den Berg et al., 2013). These data, provided by Dr. Kristin Ladell, were re-visited. The level of CD8 expressed by this clone following antigenic stimulation via its TCR by different ligands, presented in the context of C1R A2 and C1R A2 227/8 targets (CD8 binding abrogated) is detailed in Figure 6.8. The data evinces that CD8 expression by the ILA1 $CD8^+$ T-cell clone post activation is greater when the peptide ligand is presented in the context of HLA A2 227/8 as compared to the wild type, i.e. abrogation of CD8 binding of the MHCI gives rise to a lesser degree of CD8 down-regulation at the cell surface. This is true for every peptide ligand examined, as is as expected: CD8 enhances the antigen specific T-cell response, thus abrogation of its binding engenders less activation via the TCR. With the exception of the 3G8T super-agonist, the general trend of the data is such that as TCR/pMHCI is increased, so too is CD8 down-regulation in response to activation, and this is true for both A2 and A2 227/8. This is as expected: increasing the strength of the TCR/pMHCI interaction promotes a heightened T-cell response; and, greater

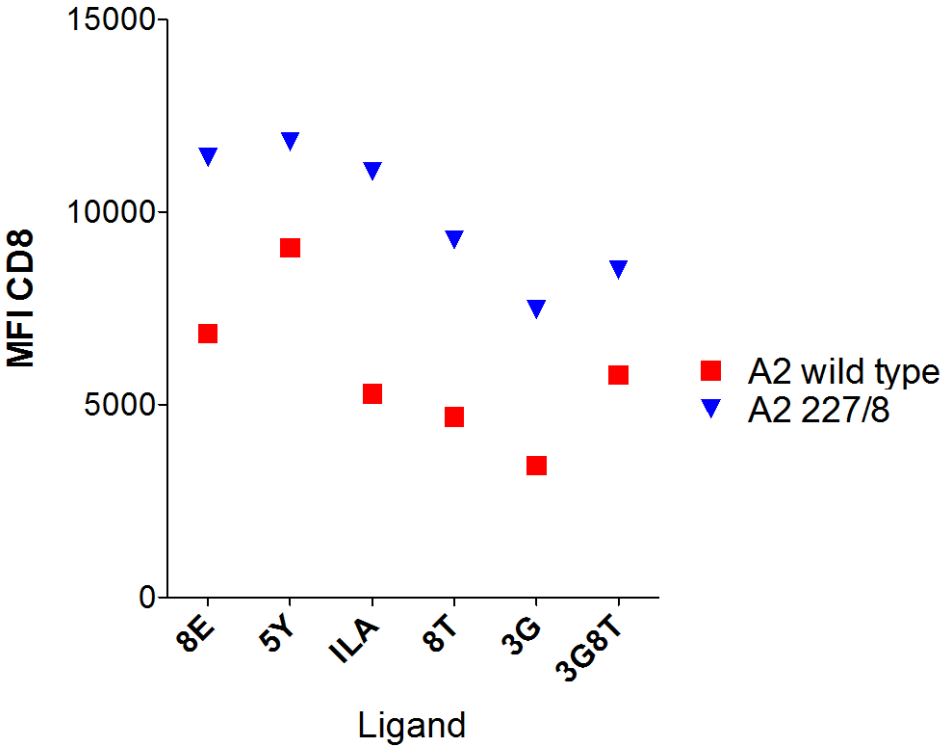

Figure 6.8: CD8⁺ T-cell clones stimulated by peptide presented in the context of pMHCI that does not bind CD8 express higher levels of CD8 at their cell surface.
The ILA1 clone was incubated together with C1R A2 and C1R A2 227/8, which had been previously pulsed with peptide as described (van den Berg et al., 2013). Cells were stained with anti-CD19, anti-CD3 and anti-CD8, and viability stain, before lysing to facilitate further staining for intracellular markers of activation (ICS). Data were acquired using a modified FACSAriaII flow cytometer, and FCS files re-analysed in order to create the above figure. This figure represents CD8 expression by the ILA1 clone, when stimulated by different TCR agonists presented in the context of C1R A2 and C1R A2 227/8 (abrogated CD8 binding). The data displayed in this figure are provided by Dr. John Bridgeman and Dr. Kristin Ladell. Multiple replicates of these experiments were repeated. (van den Berg et al., 2013). In addition, this assay has been repeated multiple times against single peptide agonists (n>8), using this ILA CD8⁺ T-cell clone, and other CD8⁺ T-cell clones, and these data are representative.

activation foments greater CD8 down-regulation, so lesser expression. Interestingly, the $CD8^{high}$ line still activates least well, even where CD8 binding is abrogated. This could suggest that CD8 exerts an effect beyond its extracellular interaction with the pMHCI. Another possibility is that the high levels of CD8 remove free lck from the cytosol, making activation more difficult.

If we further revisit the data provided by van den Berg *et al* (Figure 6.9) (van den Berg et al., 2013), an apparent change in ligand activation hierarchy when CD8 low versus high populations are compared is observed, similar to the 'focussing effect' observed where the strength of the pMHCI/CD8 interaction is manipulated (Chapter 5). It is recognised that these changes are minimal for most effector functions, and may be explained by the $CD8^{low}$ gate likely comprising the most-activated $CD8^{+}$ T-cells, however, this is also true of those activated by a weaker agonist, where the trend appears to be such that the $CD8^{high}$ gated cells demonstrate greater activation. This observation clearly merits further exploration. These data would suggest that the differences seen in the $CD8^{+}$ T-cell clone are small. In previous chapters of this thesis, the jurkat model has proved very useful for creating larger differences in the system, thus garnering more compelling evidence, however, the jurkat model developed thus-far for this chapter is clearly inadequate, and further work to create a better system, such as the CD8-lck chimera discussed above is plainly indicated.

It becomes apparent that aside from the strength of the pMHCI/CD8 interaction, the absolute numbers of CD8 molecules expressed at the cell surface represents a further means by which T-cell antigen sensitivity could be manipulated in order to facilitate a more robust response to low affinity ligands, such as cancer ligands. This is another aspect of $CD8^{+}$ T-cell function that must be better understood in order to build potential novel therapies for cancer, and augment and hone existing

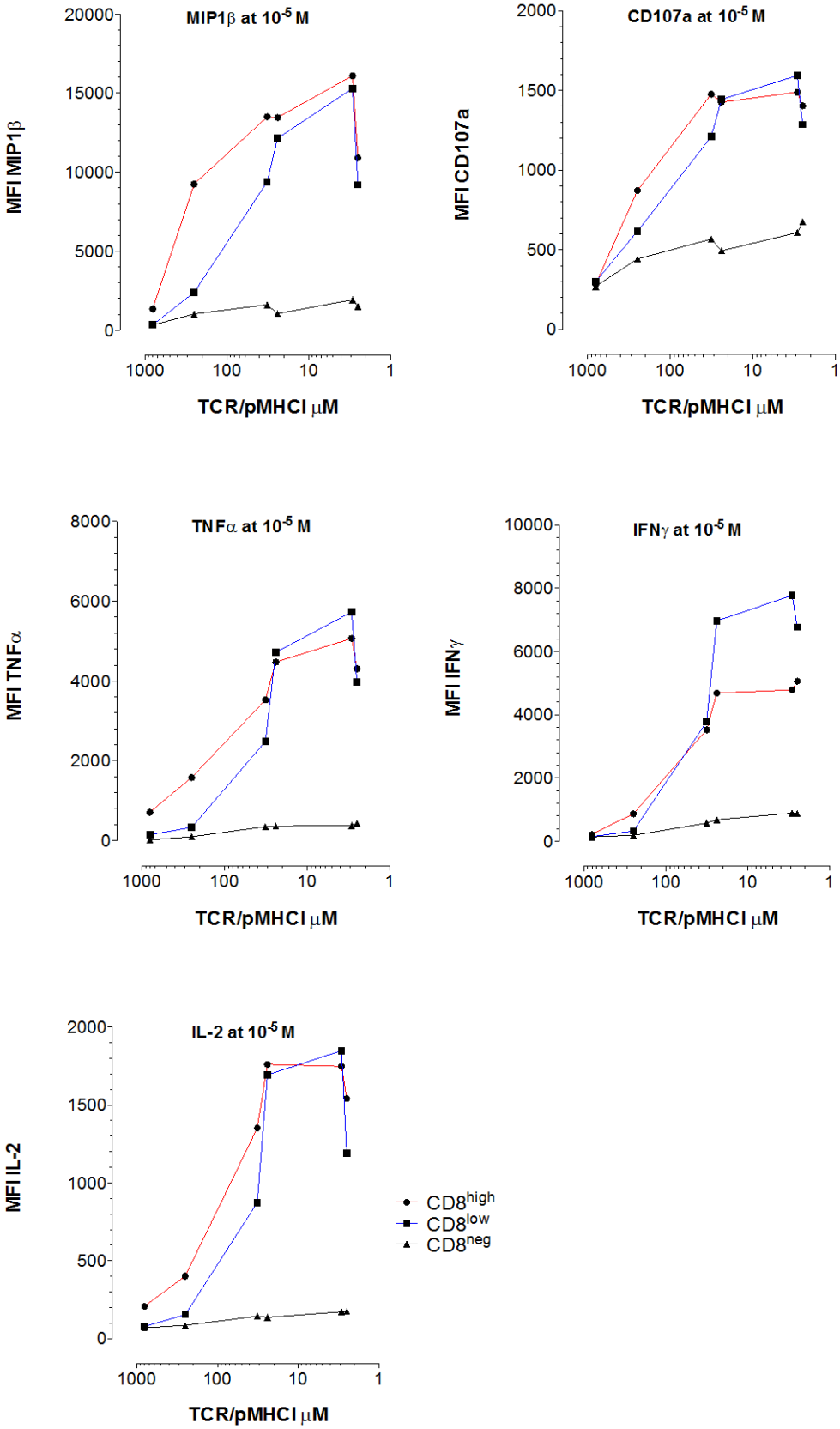
MIP1β at 10-5 M
MFI MIP1β
20000
15000
10000
5000
0
1000
100
10
1
TCR/pMHCI μM
CD107a at 10-5 M
MFI CD107a
2000
1500
1000
500
0
TNFα at 10-5 M
MFI TNFα
8000
6000
4000
2000
IFNγ at 10-5 M
MFI IFNγ
10000
IL-2 at 10-5 M
MFI IL-2
CD8high
CD8low
CD8neg

Figure 6.9: The relative potencies of TCR ligands is re-arranged by expression of different levels of CD8 at the cell surface of $CD8^+$ T-cell clones.

ILA1 clones were incubated together with C1R A2, which had been previously pulsed with peptide as described (van den Berg et al., 2013). Cells were stained with anti-CD19, anti-CD3 and anti-CD8, and viability stain, before lysing to facilitate further staining for intracellular markers of activation (ICS). Data were acquired using a modified FACSAriaII flow cytometer, and FCS files re-analysed in order to create the above figure. Experiments were repeated multiple times for publication (van den Berg et al., 2013). Data were provided by Dr. Kristin Ladell and were re-analysed as follows. Non-viable, $CD19^+$ ($V500^+$) events were excluded from analysis. $CD3^+$ events were examined and, cells were gated into $CD8^-$, $CD8^{low}$, and $CD8^{high}$ populations. Cytokine expression was examined for each of these populations to obtain an MFI. $CD8^+$ T-cell activation at [peptide] 10^{-5} M, as measured by cytokine expression by each CD8 population, in response to different TCR agonists, is depicted. TCR agonists are displayed on the x-axis as a product of their TCR affinity (TCR/pMHCI interaction affinity).

adoptive transfer systems. The data generated in this chapter demonstrate the importance of ascertaining the level of CD8 expression that engenders the optimal CD8 T-cell response before CD8 can be utilised in an adoptive transfer system.

Chapter 7

Final Discussion

7.1 Findings and Implications

7.1.1 Overview

In the production of this thesis I have furthered our understanding of the role that the CD8 co-receptor plays in T-cell activation. Moreover I have characterised the effects of manipulating the affinity of the pMHCI/CD8 interaction outside of its normal physiological range. I have established a means of enhancing the antigen specific T-cell response by enhancing the strength of the pMHCI/CD8 interaction, and quantified the point at which this manner of manipulation results in widespread non-specific activation, which would be deleterious to the host. I have probed the dynamic kinetics of the TCR/pMHCI and pMHCI/CD8 interactions, and discussed the co-relationships of these, further probing the means by which the TCR focus may be altered. And finally, I have conducted experimental work, which demonstrates that it is possible to alter T-cell antigen sensitivity by altering the level of cell surface CD8.

In contemplating the implications of these new aspects of T-cell biology, I have considered the potential therapeutic advantage of manipulation of CD8. Some researchers are exploring means by which increased affinity TCRs may be utilised in cancer immunology. This thesis examines in detail the role and function of the CD8 and its potential to enhance affinity and that this may help advise future therapeutics.

7.1.2 The strength of the pMHCI/CD8 interaction and its effect on T-cell antigen specificity

Whilst the CD8 co-receptor functions at extremely low pMHCI/CD8 interaction binding affinities, the average being K_D = 130 μM (Bridgeman et al., 2012), the strength of the pMHCII/CD4 interaction is lower still (K_D >2.5 mM) (Jonsson et al., 2016), leading us to conclude that the T-cell co-receptors have evolved to perform their function of augmenting the TCR/pMHC interaction at uniquely low affinities. It has been demonstrated that super-enhancement of the strength of the pMHCI/CD8 interaction results in a total loss of T-cell antigen specificity (Wooldridge et al., 2010a). Wooldridge *et al* described this as activating the T-cell in an 'antibody-like manner', when the strength of the pMHCI/CD8 interaction was increased 15-fold. However, Wooldridge *et al* had previously demonstrated that a small increase in the pMHCI/CD8 interaction affinity (1.5 fold) resulted in an enhanced T-cell response to its cognate antigen (Wooldridge et al., 2007), and it seemed logical that the impact of pMHCI/CD8 interaction affinities falling between this slight enhancement in the strength of the pMHCI/CD8 interaction (1.5 fold) and the super-enhanced interaction (15 fold) merited further study.

In Chapter 3, I demonstrated that rather than a gradual loss of T-cell antigen specificity as the strength of the pMHCI/CD8 interaction is increased, a sudden loss of T-cell antigen specificity is observed at a defined threshold. I subsequently characterised the defined affinity threshold beyond which the pMHCI/CD8 affinity may not be increased without loss of the exquisite specificity of the TCR (Dockree et al., 2017). Enhancement of the pMHCI/CD8 interaction strength beyond this threshold would result in catastrophic effects in the host; in all likelihood, widespread autoimmunity, and the potential inducement of cytokine storms. These findings suggest that there is an affinity window between this threshold and the

typical pMHCI/CD8 interaction affinity that could be exploited in order to potentially enhance the antigen specific T-cell response to weaker affinity ligands, such as cancer antigens.

7.1.3 The development of new tools to study cell surface CD8

The CD8 molecule exists at the cell surface as a dimeric molecule, as the homodimer, CD8αα, or the heterodimer, CD8αß. Additionally, it has been shown that it may (rarely) exist as a CD8ßß homodimer (Devine et al., 2000), although *in vitro* it has been shown that CD8α is absolutely required for trafficking of CD8 to the cell surface, thus the CD8ßß homodimer cannot be found at the surface of cells (Zamoyska, 1994). The heterodimer, CD8αß, is constitutively expressed on the cell surface of cytotoxic T-lymphocytes, thus these are more correctly termed $CD8^+$ T-cells, where it acts as co-receptor to the TCR/pMHCI interaction. Structural biologists have long recognised the preference of CD8 to homodimerise; human CD8αß has thus far proved difficult to refold, and as a consequence the crystal structure remains unsolved. In chapter 4, I designed and made a construct which when transduced into cells, enables expression of CD8αß at the cell surface. The creation of a means to alter cell surface expressed CD8αß provided me with a valuable research tool with which to further probe CD8 biology, allowing me to manipulate CD8 via both the α and ß chains, and in addition to alter the levels of CD8 expressed at the cell surface.

7.1.4 High Affinity CD8αß

A high-affinity CD8 α-chain mutation designed by a molecular modelling approach was previously characterised in the form of a soluble CD8αα molecule (Cole et al., 2007, Cole et al., 2005). The enhanced affinity of the S53>N CD8α mutant for MHCI was confirmed by SPR, and crystallography studies identified enhanced and additional contacts as compared to CD8αα *wild type* (Cole et al., 2007). Data obtained in experiments detailed in Chapter 5 clearly demonstrate that the same S53>N CD8α mutation inserted into the heterodimeric cell surface expressed CD8αß co-receptor also exhibits enhanced affinity for the pMHCI and results in enhanced T-cell antigen sensitivity, even to low affinity pMHCI ligands. High affinity CD8 mediated a statistically significant enhancement of T-cell antigen sensitivity in multiple systems, a feature which may be of great benefit when considering means of enhancing the T-cell's response to weaker affinity agonists.

In chapter 3, increased tetramer staining as the strength of the pMHCI/CD8 interaction was increased, was clearly demonstrated, thus it is logical to conclude that the enhanced staining observed with pMHCI tetramer corresponds to increased pMHCI/CD8 affinity. In addition, pMHCI tetramer staining with the HLA A2 mutants examined in chapter 3 exhibited little or no staining with the abrogated A2 227/8 tetramer as compared to the unstained control. When the J.RT3-3.5 ILA1 TCR^{+} $CD8^{var}$ lines were stained with the CD8 null (A2 227/8) ILA tetramer, only very slight staining was observed in the $CD8^{-}$ and $CD8^{+}$ lines as compared to the unstained control. However, a shift in staining was observed when the CD8αS53Nß co-receptor was expressed at the cell surface, suggesting that in the presence of this high affinity co-receptor, CD8 binding is no longer entirely abrogated by this DT227/8>KA mutation. This would imply that this particular mutation is too great an enhancement to be of use in ACT systems, however points us towards a new

goal in identifying one which is suitable, potentially closer to the strength of the Q115>E mutation examined in Chapter 3.

7.1.5 Altering the Focus of the TCR ('CD8-Focussing')

The CD8αß co-receptor serves to enhance, stabilise and tune the antigen-specific T-cell response to specific peptide ligands, presented in the context of MHCI molecules expressed on the surface of target cells. Each $CD8^+$ T-cell espresses an unique αßTCR, which facilitates the recognition of different peptide ligands, whilst the CD8αß co-receptor is largely non-polymorphic, binding as it does the invariant region of the pMHCI. Moreover the unique αßTCR is highly promiscuous, and is capable of recognising an average of 10^6 different peptide ligands (Wooldridge et al., 2012, Sewell, 2012). In Chapter 5, the potential role of CD8 in modulating pMHCI recognition by the TCR, or 'focussing' of the TCR, was probed.

Manipulation of the strength of the pMHCI/CD8 interaction alters the focus of the TCR such that as the strength of the pMHCI/CD8 interaction is increased, the focus of the TCR is moved away from higher affinity ligands. Moreover, lower affinity ligands are elevated in their potency. Indeed the augmentation of the T-cell response is not uniform across the board, thus CD8 appears to exert a differential effect on the TCR, resulting in rearrangement of the relative potency hierarchy of its cross-reactive ligands. This was predicted by mathematical modelling (van den Berg et al., 2007), however this is the first time that the strength of the pMHCI/CD8 interaction has been manipulated by altering cell surface CD8, thus is the first time that this phenomenon has been explored using this approach.

That TCRs must be cross-reactive is taken as dogma, however the mechanism by which the T-cell is able to control its own degeneracy, thus avoiding autoimmunity

and ensuring adequate response to challenge is unclear. Every single TCR must be autoreactive; otherwise the T-cell would have suffered death by neglect in the thymus. Additionally, it has been suggested that on-going weak self-stimulation is very likely the means by which the resting T-cell population is maintained. When the T-cell encounters and recognised foreign challenge, the response is rapid and robust, resulting in target deletion. We must ask what is different?

As has been mentioned, TCR ligands tend to fall within defined ranges. Autoimmune pMHCI are recognised with relatively weak affinities, conversely foreign peptide antigens are recognised far more strongly, some of these being CD8-independent, i.e. they do not require co-receptor help in order to facilitate downstream triggering and thus T-cell activation. Ligand affinity is intrinsically linked to on rate and thus to dwell time (Holler and Kranz, 2003, Laugel et al., 2007b). The CD8 co-receptor has been shown to stabilise the TCR/pMHCI interaction and thus increase dwell time of the ligand by over 2-fold (Holler and Kranz, 2003, Luescher et al., 1995), and in doing so increase the probability of full ITAM phosphorylation, thus initiating downstream signalling (Szomolay et al., 2013).

Complete-cell activation requires serial TCR triggering (Valitutti et al., 1995), so in order for T-cell activation to occur the triple structure must dissociate before the TCR can be re-cycled to allow the process to occur again. High affinity TCR ligands have a longer dwell time, and as a consequence do not absolutely require CD8 co-receptor help in order for downstream signalling to occur. Indeed, for very high affinity super-agonists, their ability to bring about serial triggering may be hampered by the CD8 co-receptor because the triple structure is now too stable and fails to dissociate. Conversely, the short dwell time of a weak affinity agonist

means that triggering cannot occur without CD8 co-receptor assistance because the TCR/pMHCI interaction is too fleeting for full ITAM phosphorylation to occur.

The data that I have presented in Chapter 5 supports this. Furthermore, if the pMHCI/CD8 affinity is enhanced by manipulation of either the CD8 molecule itself, or the CD8 binding region of the MHCI, then the triple structure is further stabilised and takes longer to dissociate. The probability of downstream signalling before dissociation is increased, however the focus of the TCR is moved away from high affinity agonists because they are now unable to bring about the serial triggering required. This novel aspect of CD8 biology may open up new means of enhancing the $CD8^+$ T-cell response to cancer ligands, which tend to be of weaker affinity than those pertaining to foreign challenge.

7.1.6 The effect of the level of CD8αß expression on T-cell activation

I have convincingly demonstrated the manner in which the focus of the TCR may be altered by manipulation of the strength of the pMHCI/CD8 interaction. Whilst it has been considered likely for sometime that the CD8 co-receptor may control cross-reactivity (Wooldridge et al., 2010b), it should be evident, given the non-polymorphic nature of the CD8 molecule, that this is not the means by which the T-cell is able to focus between its degenerate ligands. When van den Berg *et al* predicted the phenomenon of CD8 mediated TCR 'focussing', manipulation of the absolute levels of CD8 expressed by the cell at the cell surface was postulated as the means by which focussing may be brought about *in vivo*. Whilst I have been unable to generate a jurkat model robust enough to allow me to probe this aspect of CD8 biology in more detail, I have re-analysed an existing activation dataset, and the findings may go some way to support this theory.

It has been recognised for sometime that upon activation, $CD8^+$ T-cells down regulate cell surface CD8. I put forward the hypothesis that this is *because* they are focussing the TCR. High affinity ligands with a longer dwell time form stable TCR/pMHCI complexes, and as such require minimal CD8 co-receptor help. Indeed, in order for serial triggering to occur, they require the structure to dissociate. To this end CD8 is down-regulated resulting in a reduced probability of CD8 co-receptor co-engagement owing to its reduced density at the cell surface. Weaker ligands absolutely require this co-receptor help in order to stabilise the TCR/pMHCI interaction for long enough to initiate triggering, consequently CD8 expression must remain high. If one considers that weaker affinity ligands are potentially self-reactive, thus a low level of signal propagation in order to maintain the T-cell population is all that is required, since robust activation would result in autoimmune disease, then it makes sense that this should be so. It also goes some way to explain why those cancer agonists that fall between these two extremes may be missed by the immune system.

The mechanism by which the cell may achieve this is unclear, however it seems likely that this should be in response to activation, as it is evident that the cell could have no way of pre-determining the nature of the peptide ligand which the TCR engages. The T-cell's response to TCR triggering is to down-regulate CD8 at the cell surface. I suggest that the cell surface CD8 levels will continue to fall until the TCR becomes focussed, thus in the case of strong TCR ligands low levels of CD8 are observed. These lower levels provide less CD8 co-receptor help to the TCR/pMHCI interaction and so stabilisation of the TCR/pMHCI is afforded, however in the instance of stronger ligands, this is sufficient for triggering, thus serial engagement may rapidly and efficiently occur. Weaker agonist require more co-receptor help; the TCR must remain engaged with the pMHCI for sufficiently long for full iTAM phosphorylation (Szomolay et al., 2013), which owing to the less

stable TCR/pMHCI interaction, requires increased co-receptor help to stabilise the triple complex. If cell surface CD8 levels fall too far then triggering cannot occur. At this point, CD8 levels stop falling. An increase in CD8 levels at this point will result in the correct level of CD8 to provide optimal co-receptor help, i.e. the TCR is 'focussed' upon this ligand.

7.1.7 The level of cell surface CD8 must be maintained within a defined range for normal T-cell function

It is apparent that the levels of CD8αß present of the surface of a T-cell do indeed affect T-cell function, as evidenced by the existence of sub-types expressing different levels of CD8; the $CD8^{high}$ and $CD8^{low}$ phenotypes. These two $CD8^{+}$ T-cells subsets have been shown to have differing function with the $CD8^{low}$ expressers being of low cytotoxicity as compared to the $CD8^{high}$ phenotype (Kienzle et al., 2004). Whilst the jurkat model which I created in order to explore the effect of manipulating the level of CD8 at the cell surface did not allow me to do so comprehensively, I believe that I have used this data to demonstrate the need for maintaining cell surface CD8 levels within a defined range, similar to that which has evolved in nature. Increasing the level of cell surface CD8 outside of this "normal" range, resulted in reduced T-cell antigen sensitivity. I believe that the most probable explanation for this observation is that the CD8 co-receptor acts to deliver lck to the TCR-CD3 complex, thus if the level of cell surface CD8 greatly outstrips that of lck within the cell, then co-receptor function is hampered. In future, building a chimeric CD8-lck molecule would allow me to explore the effects of increasing cell surface CD8 levels outside of the physiologically range. I have designed a construct whereby the lck is fused to the tail of CD8α by means of a serine linker, although this remains to be tested *in vitro*.

7.1.8 The ß-chain Splice variants

The ß-chain of CD8 has been touched upon as another potential means of manipulating the T-cell response, but has not been probed in great depth. Human CD8ß has been shown to exist in four possible alternatively splice variants (M-1 – M-4), which differ in their cytoplasmic tails (Thakral et al., 2013, Thakral et al., 2008, Giblin et al., 1989, DiSanto et al., 1993). These have been shown to originate from two additional exons acquired during recent evolution through a common human and chimpanzee ancestor (Nakayama et al., 1992). The M1 isoform is homologous to murine CD8ß, and is therefore considered to be the wild type. It predominates in naïve T-cells, where expression of the corresponding mRNA for these isoforms is shown to be M-1 > M-4 > M-2 > M-3. The M-4 isoform has been demonstrated to be up-regulated in effector memory populations, where it appears to enhance response to APC at least 2-fold when compared to the wild type (Thakral et al., 2013). The exact mechanism by which the CD8ß gene is controlled, creating the various transcripts, and the relative expression and role of each of these splice variants, is poorly understood.

Differential expression of the ß-chain splice variants across different T-cell subsets would suggest that they may act differently and thus play different roles in $CD8^+$ T-cell activation, as evidenced by enhanced cytokine production observed by $CD8^+$ T-cells with increased expression of the M-4 isoform (Thakral et al., 2013). Thus the ß-chain splice variants may represent another means by which the antigen-specific T-cell response may be manipulated in order to create the most robust response to a given antigen. The information could be utilised for patient benefit in order to tailor an optimal ACT by combining the TCR with a fully optimised co-receptor for the cancer target. The ß-chain may also be considered as a potential target for

manipulation. Although, SPR studies to classify and examine mutations *in vitro* via SPR studies would be more difficult owing to the fact that as discussed above, refolding of human CD8αß is extremely challenging.

Other authors have noted enhanced T-cell response with ß-chain mutations in the extracellular domain which are presumed to enhance the affinity of the pMHCI/CD8 binding interaction (Devine et al., 2006). The stalk-region of the ß-chain is also considered to confer better co-receptor function to the CD8αß molecule. Whilst it is possible that this could be further explored in our quest for a 'designer co-receptor', it seems more likely to the author that this is further evidence for the need for a heterodimeric co-receptor, rather than as potential area for manipulation or improvement.

The alternatively spliced transcripts, which result in the ß-chain splice variants, are differentially expressed in different populations, thus it seems likely that they have different effects on cell function. Whilst their expression and prevalence in primary cells has been explored, a fully robust understanding of the effect which they exert upon $CD8^+$ T-cell function, and how they may act differently as co-receptors needs to be fully understood. Whilst these splice variants differ in their cytoplasmic tails, and cannot therefore be classified and examined by *in vitro* SPR studies, I have demonstrated that they can be transduced into cells, where they are capable of acting as co-receptor to a transduced TCR. However, time limitations and limitations with the equipment to measure effector responses from the J.RT3-3.5 NFAT GLuc cell lines precluded an analysis of how these splice variants affect antigen specific T-cell activation, but did serve to demonstrate that this is an avenue which merits further exploration in future. Preliminary data is detailed in Appendix E.

7.1.9 Optimisation of the CD8 co-receptor

When we talk about wishing to optimise a response, to a molecule, we need to first consider why this is not optimal in the first place? Why has CD8 evolved the way that it has if the response is not 'optimal'? The answer is simple. CD8 has multiple roles in T-cell biology. It has a role in the thymic selection of TCRs. It must also provide co-receptor help when required, augmenting the $CD8^+$ T-cell response, where necessary, enabling the immune system to mount a robust response to both foreign pathogens and dysregulated cells. Additionally, it must maintain a low-grade recognition of self-ligands, whilst avoiding autoimmune disease. I would argue that if we consider all of these roles, and the areas where they may contradict one another, then the CD8αß molecule is already fully optimal. However, I would argue that the main thrust of discussions in this thesis has been the potential to optimise the T-cell response by means of manipulating CD8, in order to augment the T-cell response to cancer ligands; ligands that require a full and robust response however are of lower affinity than those associated with foreign challenge. To this end, it seems important from the results generated that any attempts to utilise such a manipulated CD8 molecule for therapeutic gain should be robustly tested, and the effect on cross-reactivity in the host fully probed.

7.1.10 Engineering CD8 as a potential means of augmenting ACT strategies

$CD8^+$ T-cells are capable of recognizing cancer antigens presented in the context of MHCI on neoplastic cells. In addition to the various strategies that tumours employ in order to evade the immune system, the TCR/pMHCI interaction itself is

sometimes sub-optimal in the case of cancer antigens, which is probably due to their similarity to self-antigens. Some cancer antigens are recognised by the TCR with a much weaker affinity than those of pathogen-derived antigens, typically with a K_D of 10-100 μM, as compared to 8 μM, respectively (Bridgeman et al., 2012), although there is overlap meaning that for some ligands this is not always the case. This discrepancy in TCR recognition of foreign vs. neoplastic-self pMHCI goes some way to explain why the immune system is capable of effectively clearing many pathogens, but appears to be far less efficient at eliminating cancer. The 'ideal' TCR/pMHCI interaction affinity has been suggested to be around 10 μM (Zhong et al., 2013), and whilst there do exist cancer epitopes which when presented by the MHCI have an affinity for the TCR of this order, they are far less common than weaker cancer ligands. The potential for enhancement of the T-cells response to cancer ligands as a means of improving ACT has been demonstrated by the creation of 'designer TCRs', which recognise the cancer pMHCI with enhanced affinity.

The failure of peptide vaccines to induce an adequate immune response to clear tumours would suggest that endogenous TCRs are inadequate for this challenge. Various ACT strategies to overcome this failing have already been discussed; *ex vivo* priming and expansion of TILs, genetic engineering with 'designer TCRs' or the creation of CARs, along with the potential problems and inadequacies in each system. It has been previously mentioned that for many of these systems, the approach must be tailored to the individual tumour in order to avoid toxicity due to the attack of other tissues. The CD8 co-receptor is a largely non-polymorphic molecule in man, and binds the invariant region of every pMHCI, acting to stabilise and enhance the $CD8^+$ T-cell response (Wooldridge et al., 2005). It has been discussed how this feature of CD8 could make this molecule an ideal target for manipulating the $CD8^+$ T-cell response, and as such a system would be globally

applicable. Although data generated with the S53>N CD8α mutant in Chapter 5 provides proof of principle data that increasing the strength of the pMHCI/CD8 interaction by manipulating cell surface CD8 can result in enhanced T-call antigen sensitivity, the fact that the affinity of this mutant is near to the affinity threshold beyond which non-specific T-cell activation is observed means that this mutant is not suitable for incorporation into ACT strategies. However, if a mutation could be generated which has a pMHCI/CD8 affinity similar to that of the MHCI Q115>E mutation, then data suggests that this would be of value in augmenting the T-cell response, whilst still maintaining T-cell antigen specificity.

The data presented suggests that manipulation of the CD8 molecule may afford a means by which the T-cell response may be manipulated, however thus far this has only been examined in a jurkat model, and robust testing in primary cells is required before the value of this approach could be considered further.

7.2 Future Work with enhanced affinity CD8

7.2.1 SPR Studies

The mutation examined in this thesis, S53>N, was identified by Cole *et al* by computational design, and was examined in the context of solubilised extracellular α-chain homodimers (Cole et al., 2007, Cole et al., 2005). The S53>N mutation provides a larger side chain, enhancing contacts between the MHCI α3 domain and the mutation, which is located in the CDR-like loops of CD8α. Enhanced affinity of CD8αα for HLA A2 of 30 μM was demonstrated using SPR, compared to a K_D of 127μM for the *wild type* CD8αα. Assumptions are made that CD8αα and CD8αß interact with pMHCI with comparable affinities, based upon this being the case in the murine system, however it is uncertain whether this true, or if the mutation

may affect this. In the absence of structural studies of *wild type* CD8αß, SPR studies of the heterodimer possessing this mutation are unlikely in the near future. It is recognised that SPR studies with the CD8αß heterodimer would be a far more accurate means of assessing the affinity of this molecule of its pMHCI ligand *in vitro*, and that the refolding of soluble CD8αß remains a goal for structural biologists studying T-cell cell surface interactions.

The data presented in this thesis suggest that this mutation greatly enhances the pMHCI/CD8 interaction. Enhanced tetramer staining in the presence of CD8αS53Nß compared to *wild type* CD8αα suggests that K_{on} is enhanced by this mutation. Tetramer decay studies will provide information with regards to the off rate (Laugel et al., 2007b, Holmberg et al., 2003). Preliminary experiments (data not shown) demonstrated greater stability of tetramer binding in the presence of the CD8αS53Nß co-receptor, although this experiment requires repetition, and thus was not included in this thesis.

7.2.2 Primary Cells

A goal for this thesis was the examination of this mutation in primary cells. This would enable the quantification of this mutation and its effect on cross-reactivity with self. A combinatorial peptide library (CPL) screen can be used to examine the cross-reactivity of the TCR (Wooldridge et al., 2012), thus comparison of screens obtained where the wild type co-receptor is present will enable quantification of the effect of this mutation on TCR promiscuity. The jurkat model has not proved sufficiently robust to enable this kind of screening.

Unfortunately, efforts to transduce primary cells with both TCR and CD8, resulted in a cell population which failed to undergo more than a single expansion before

crashing, meaning cell numbers were too small to facilitate the use of a CPL screen.

Many strategies had been employed in efforts to infect primary cells with both lentiviral particles, and results are improving, and it is hoped that revisiting this in future will enable the generation of these primary cells.

A further goal for these cells is to use them in experiments with tumour banks. For example, can primary cells transduced with the Mel TCR and with CD8αS53Nß recognise Melanoma tumour cells? Can they target and kill these cells, and, most importantly, can they do so better than the wild type? The jurkat model could have been used with these tumour banks to prove enhanced recognition of 'real' tumour antigens *in vitro*, thus further demonstrating the potential value of this study.

7.2.3 An 'Ideal' Affinity for CD8 to enhance T-cell function.

A 1.5 fold enhancement in pMHCI/CD8 affinity has been shown to enhance the T-cell response without the loss of specificity of the TCR probed in Chapter 3 (Wooldridge et al., 2007, Dockree et al., 2017), thus it follows that a mutation in CD8 of a similar order is more likely to be of value for the enhancement of the T-cell response to weaker affinity agonists in a clinical setting. Indeed, the Q115>E mutation of the MHCI heavy chain has been utilised by researchers for the identification of low avidity T-cell populations (Wooldridge et al., 2009, Melenhorst et al., 2008). Such a mutation could be useful in a clinical setting in any setting where enhancement of T-cell response is desirable, however, as has been discussed, many cancer agonists are recognised by TCRs with affinities lower than that which would give rise to the most robust response. Whilst it is recognised that there are numerous other reasons why cancers escape the immune system, and

that some cancer agonists are demonstrably of suitably high affinity to induce a cytotoxic response from the CD8 T-cell, the success of some enhanced affinity TCR ACT systems to treat some cancers demonstrates that, at least in some settings, this approach may be beneficial to the patient.

7.2.4 Murine Models

Following the identification of a potentially useful CD8 mutation resulting in only mild enhancement in T-cell function, and robust of this *in* vitro, a translational model to further test this novel approach is required. Murine models are frequently used prior to therapeutic trials. Owing to the vast species differences in CD8 biology between these two species, this would need to be carefully considered.

Murine CD8 recognises murine MHCI with an affinity approximately 5x greater than its human counterpart (Hutchinson et al., 2003, Kern et al., 1998, Willcox et al., 1999, Gao et al., 1997a). The reason for this is uncertain, however it is assumed that murine $CD8^+$ T-cells must be more cross-reactive than in man in order to provide a sufficient T-cell repertoire, owing to the fact that the number of TCRs available must be reduced due to differences in their size. For this reason, a fully humanised mouse model would need to be considered.

7.2.5 Patient Safety

It has been discussed in some detail the need for further examination of this system, particularly in primary cells, largely due to the concerns of the affect of such an approach on the cross-reactivity of the TCR, meaning that the generation of autoimmune disease in the host is a potential cause for concern.

Whilst I have stated that one benefit of the use of CD8 to enhance the T-cell response is that such a molecule could be globally applicable, individual testing of the effect in each specific host would be an essential part of any pre-clinical suitability screening. T-cells destined for ACT would need to be screened, however the simplest means of doing so against the hosts unique tissue type, would be by the use of directly *ex vivo* PBMC as targets.

One of the greatest concerns with the enhancement of the T-cell response to tumour antigens is the potential for 'on-target, off-tumour' toxicity; whereby the engrafted T-cell successfully target the tumour cells, however activity against normal self tissues bearing similar (or autoreactive antigens) is also enhanced, leading to toxicity in the host. Some toxicities in patients are tolerated where the side effects are considered to be preferable to the disease, however it is recognised that sometimes in these systems, despite rigorous testing, unexpected toxicities occur; deaths have been reported following the use of high-affinity designed TCRs (Linette et al., 2013), and the enhancement of pMHCI/CD8 affinity as a means of enhancing the T-cell response would pose similar concerns for patient safety.

Further safety features may be built into transduced cells. Cells can be made incapable of division, thus any deleterious effects would cease with the life of the cells, however this is a poor solution in the case of anti-cancer therapy, where one is hoping that the T-cells will persist and continue immune surveillance to control the tumour or prevent its return, thus perpetuating remission.

Another approach is to introduce into the cell a gene switch as a means by which the T-cell's activity may be controlled. Engrafted cells may be designed such that their activity may be initiated or terminated by administration of, for example, antibiotics such as tetracycline (Stieger et al., 2009, Jin et al., 2014). Transgene

expression in engrafted cells may be controlled in this manner, enabling the clinician to control the function and behaviour of the engrafted cells *in vivo,* meaning that the harmful activity of these cells may be ceased if deleterious bystander activity or autoimmunity occurs.

Suicide genes have also been used as a means of enhancing the safety of ACT systems (Straathof et al., 2003, Griffioen et al., 2009). Inducible caspase, inducible Fas and CD20 have been considered as a means of controlling overgrowth transplanted cells, leading to induced apoptosis of the engrafted cell populations in the event of over-proliferation and over-activity.

Potential enhancement of the activity of the endogenous TCR by enhanced affinity trans-CD8 is another potential cause for concern as effects could be hugely unpredictable and vary from patient to patient, as well as from one engrafted cell to another. Mis-pairing of trans-TCR with the endogenous can also add a further dynamic to the unpredictability of activity of transduced cells for adoptive transfer, and the addition of an enhanced affinity CD8 to the system may very well cause further problems. To this end, the removal of the endogenous TCR may be necessary to improve safety. TALENs have been used in some CAR systems to remove the endogenous α-chain, thus (along with CD52 removal) rendering the engrafted T-cells less sensitive to the lymphodepleting agent Alemtuzumab which may be administered concurrently in lymphoma therapy (2017, Qasim et al., 2017), however a similar strategy could be considered to remove the endogenous TCR is enhancement of the endogenous TCR is proved to be a cause of concern for patient safety.

7.3 Summary and future directions

The data presented in this thesis has implications for the development of a novel way of augmenting ACT systems. A better understanding of the means by which modulation of the $CD8^+$ T-cell response can be achieved and how we can fine tune its response to alternate ligands will enable the development of future systems whereby the TCR may be tuned or 'focussed' to target ligands, enabling us to ensure ACT systems remain focussed to the cancer target of choice, as opposed to other cross-reactive ligands within the spectrum of TCR agonists which the $CD8^+$ T-cell is potentially able to recognise. Whilst the examples examined within this thesis are far from ready to be taken forward, further exploration in this area has great potential for identification and design of a model which may become ready to be taken forward to aid in design of novel ACT systems for patient benefit.

Future studies need to focus on a detailed examination of a range of CD8 mutations falling between the *wild type*, and defined loss of specificity threshold ($K_D \leq$ 30μM). A robust examination of this system over such a range would enable a better quantification of the effects that increasing the strength of the pMHCI/CD8 interaction has on T-cell antigen sensitivity, and the effects that this is likely to have on TCR focus. Furthermore, this system still requires testing in primary cells, and doing so would enable probing of the effects that these mutations have on cross-reactivity with self.

The effect exerted by altering levels of cell surface CD8 upon the antigen specific T-cell response requires probing in more detail. Whilst it is predicted that altering the levels of CD8 at the cell surface and in so doing the receptor density, is likely the means by which the cell alters the focus of its TCR *in vivo*, this hypothesis has not been examined. The effect of drastically increasing cell surface CD8 expression has been shown to be inhibitory to T-cell activation, thus it remains to either probe

this effect within a much narrower window, something which proved impossible in the jurkat model used in this thesis, or to pursue alternative strategies, such as the CD8-lck chimera. It is anticipated that more detailed examination of this area of CD8 biology will equip us with the tools necessary to build a designer co-receptor to augment sub-optimal ACT systems.

Appendices

Appendix A

Primers Used in this thesis

Name	Sequence
IRES for	5' GGC CAA AAG CCA CGT GTA TAA GAT AC 3'
pELN seq rev	5' CAT AAA GAG ACA GCA ACC AG 3'
Xba kozac for	5' GCT AGC TCT AGA GCC GCC ACC ATG 3'
IRES rev	5' CTG GGG TTG TGC CGC CTT TGC AGG TG 3'
CD8α int for	5' GAG TTG CTC AGG GCG 3'
CD8α int rev	5' CAG CGC CCT GAG CAA 3'
pMK seq for	5' CAG TCA CGA CGT TGT AAA AC 3'
T2A for	5' GGC GAC GTC GAG GAA AAC CCC GGG 3'
T2A rev	5' GCT TCC GCG TCC CTC GCC AGA TCC GG 3'
pcDNA3.1 F	5' CTG GCT AGC GTT TAA ACG GGC CC 3'
pcDNA3.1 R	5' AAT TCT GCA GAT ATC CAG CAC AGT G 3'
T7 for	5' TAA TAC GAC TCA CTA TAG GG 3'
CD8α F48Q sense	5' GCT GCC AGC CCC ACC CAG CGT CTG TAC CTG AGC 3'
CD8α F48Q antisense	5' GCT CAG GTA CAG CAG CTG GGT GGG GCT GGG AGC 3'
CD8α Q2K sense	5' GCC GCC AGA CCT AGC AAA TTC AGA GTC TCC CCC 3'
CD8α Q2K antisense	5' GGG GGA CAC TCT GAA TTT GCT AGG TCT GGC GGC 3'
CD8α S53N sense	5' CAC CTT CCT GCT GTA CCT GAA CCA GAA CAA GCC 3'
CD8α S53N antisense	5' GGC TTG TTC TGG TTC AGG TAC AGC AGG AAG GTG 3'
m Q2K mt for	5' GCT GCT GCA CGC CGC CAG ACC TAG CAA A 3'
m Q2K mt rev	5' GTC CGG TCC AGG GGG GAC ACT CTG AA 3'
m S53N mt for	5' AAC CAG AAC AAG CCC AAG GCC GCC 3'
m S53N mt rev	5' CAG GTA CAG CAG GAA GGT GGG G 5'

Table A.1: Primer sequences

Name	-mer	Application(s)	Vector	Plasmid(s)
IRES for	26	Sequencing Colony PCR	CD8β.IRES.α	pMK, pELN
pELN seq rev	20	Sequencing Colony PCR	CD8β.IRES.α	pMK, pELN
Xba kozac for	24	Sequencing Colony PCR	CD8β.IRES.α	pMK, pELN
IRES rev	26	Sequencing Colony PCR	CD8β.IRES.α	pMK, pELN
CD8α int for	15	Sequencing	CD8β.IRES.α	pMK, pELN
CD8α int rev	15	Sequencing	CD8β.IRES.α	pMK, pELN
pMK seq for	20	Sequencing	CD8β.IRES.α	pMK, pELN
T2A for	24	Sequencing	TCRα.2A.β	pMK, pELN
T2A rev	26	Sequencing	TCRα.2A.β	pMK, pELN
pcDNA3.1 F	23	Sequencing		pcDNA3.1
pcDNA3.1 R	25	Sequencing		pcDNA3.2
T7 for	20	Sequencing		pGMT7
CD8α F48Q sense	33	SDM	CD8β.IRES.α	pMK
CD8α F48Q antisense	33	SDM	CD8β.IRES.α	pMK
CD8α Q2K sense	33	SDM	CD8β.IRES.α	pMK
CD8α Q2K antisense	33	SDM	CD8β.IRES.α	pMK
CD8α S53N sense	33	SDM	CD8β.IRES.α	pMK
CD8α S53N antisense	33	SDM	CD8β.IRES.α	pMK
m Q2K mt for	28	SDM	CD8β.IRES.α	pELN
m Q2K mt rev	26	SDM	CD8β.IRES.α	pELN
m S53N mt for	24	SDM	CD8β.IRES.α	pELN
m S53N mt rev	22	SDM	CD8β.IRES.α	pELN

Table A.2: Primer names and applications

Appendix B

Protein Biology Supplementary Data

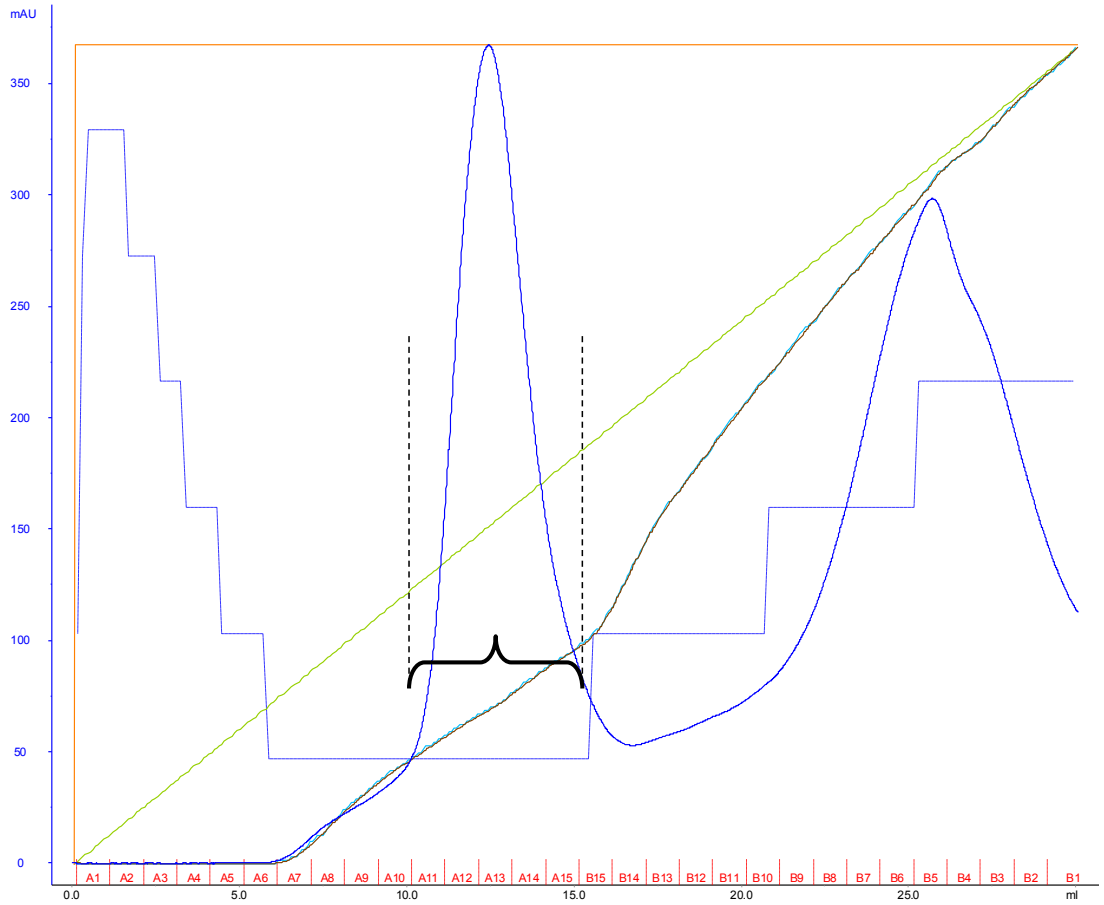

Figure B.1: Ion exchange MHCI.
The FPLC trace obtained for ion exchange (IE) of a typical HLA A2 monomer. Retained fractions (A11 – A15 inclusive) to be taken forward for concentration, biotinylation, and gel filtration (GF) are indicated.

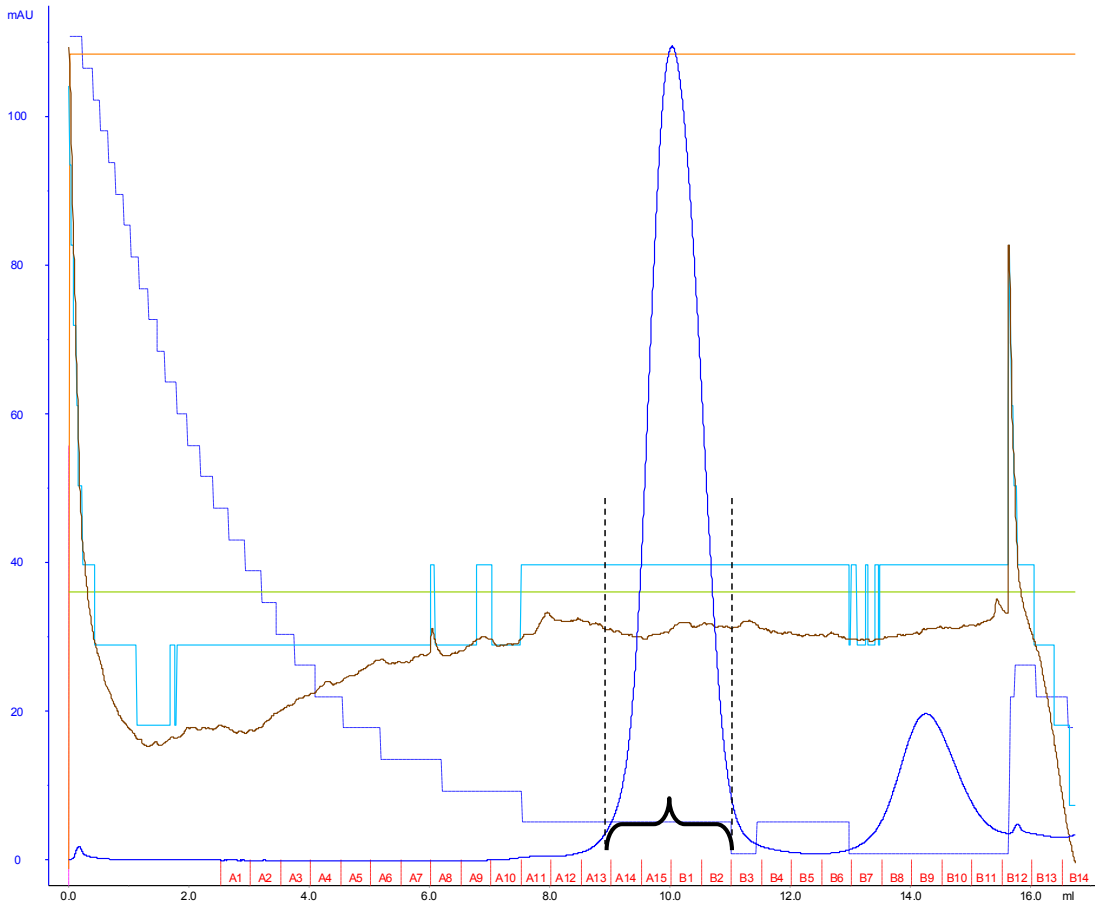

Figure B.2: Gel Filtration of MHCI.
The FPLC trace obtained for GF of a typical HLA A2 monomer. Retained fractions (A14 – B2 inclusive) to be taken forward for use in experiments are indicated.

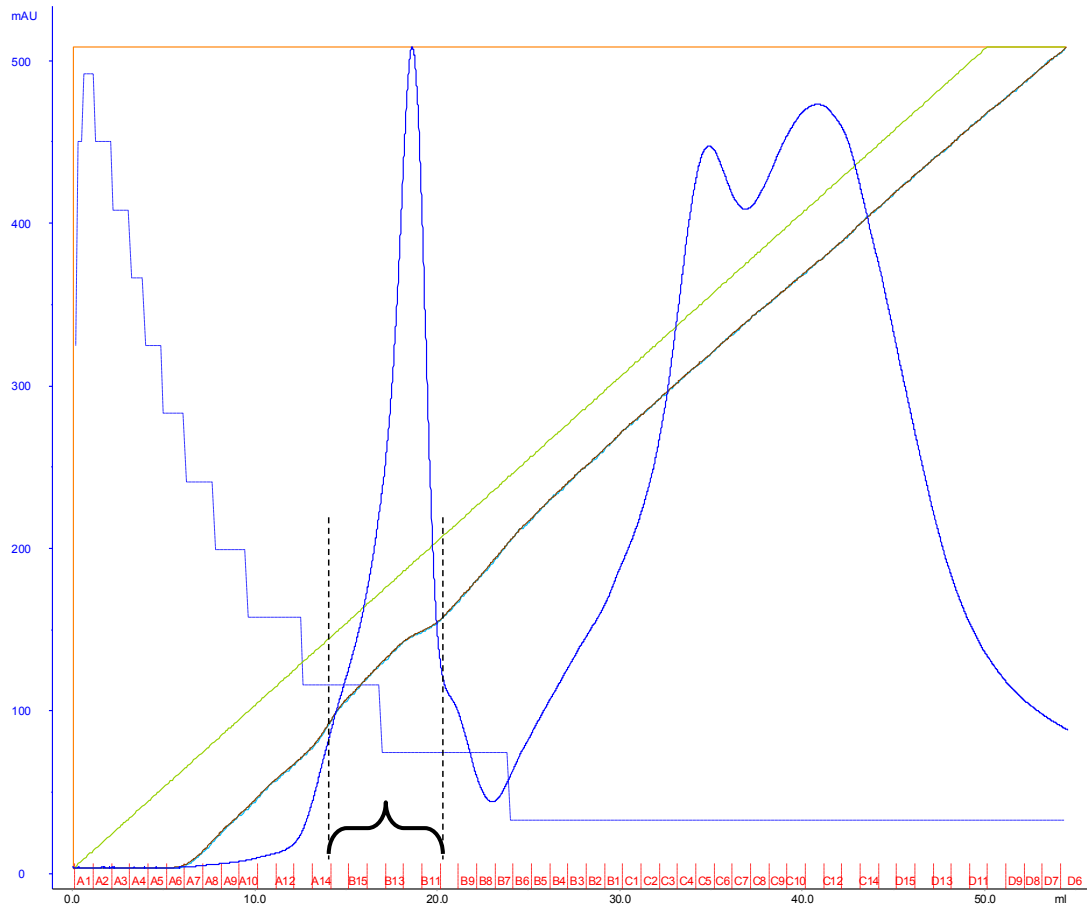

Figure B.3: Ion exchange TCR.
The FPLC trace obtained for IE of the MEL5 αβTCR monomer. Retained fractions (A15 – B11 inclusive) to be taken forward for concentration and GF are indicated.

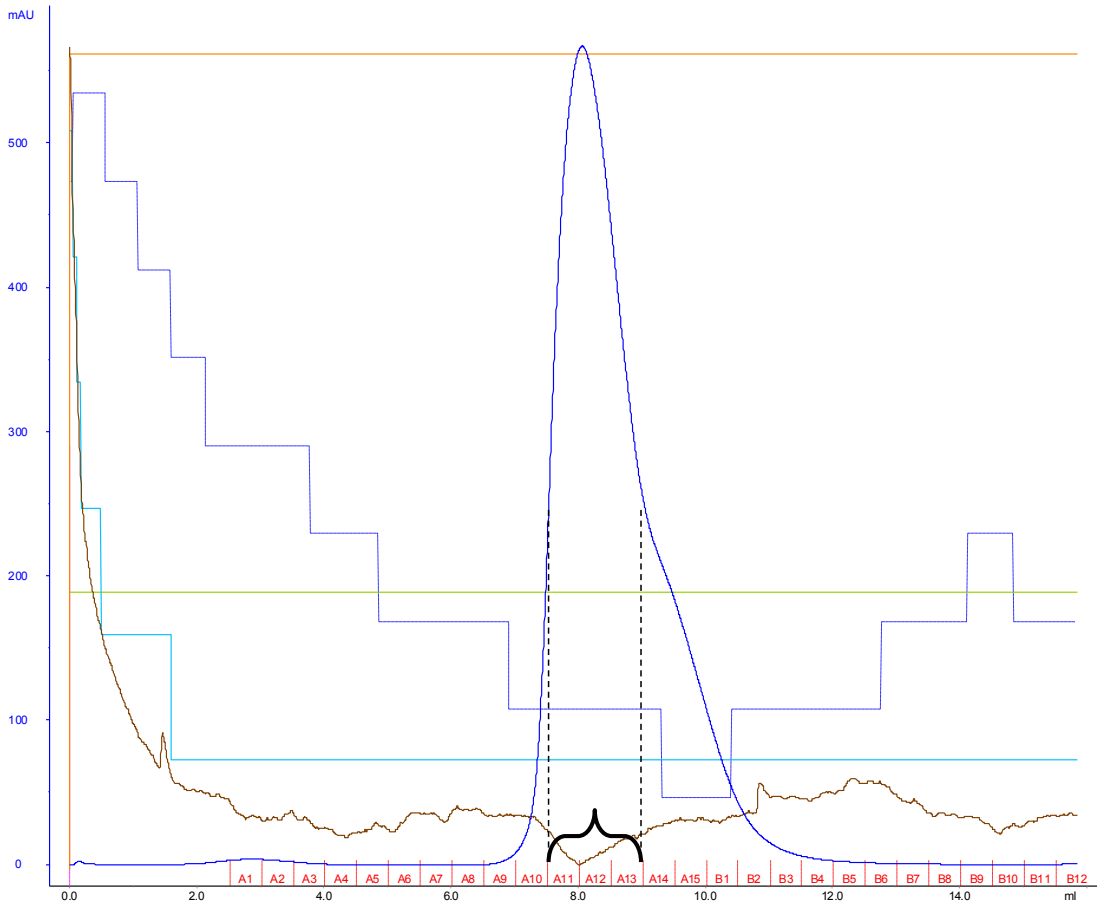

Figure B.4: Gel Filtration of TCR.
The FPLC trace obtained for GF of an αβTCR (MEL5) monomer. Retained fractions (A11 – A1 inclusive) to be pooled and taken forward for use in experiments are indicated.

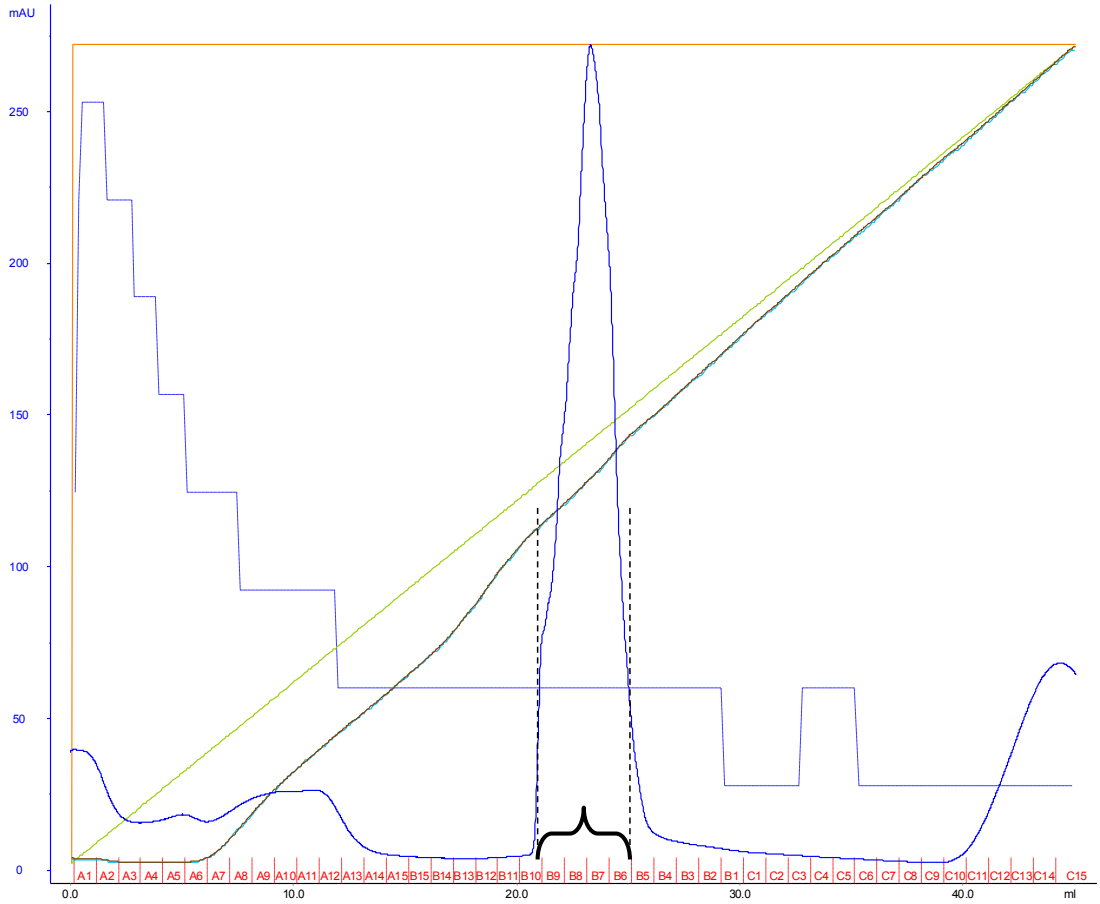

Figure B.5: Ion exchange CD8.

The FPLC trace obtained for IE of the CD8αα monomer. Retained fractions (B9 – B6 inclusive) to be taken forward for concentration and GF are indicated.

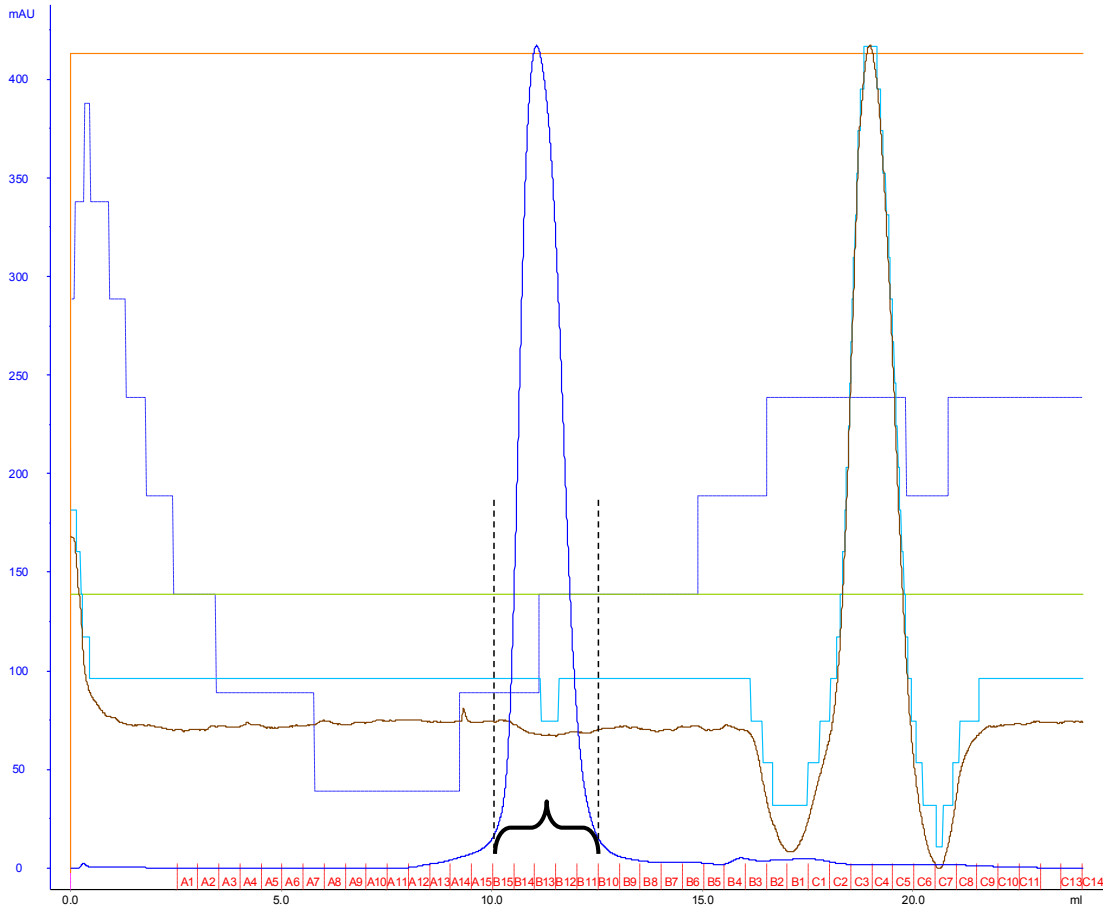

Figure B.6: Gel Filtration of CD8.

The FPLC trace obtained for GF of CD8αα monomer. Retained fractions (B15 – B11 inclusive) to be pooled and taken forward for use in experiments are indicated.

Appendix C

Sequence CD8α and α-chain Mutations

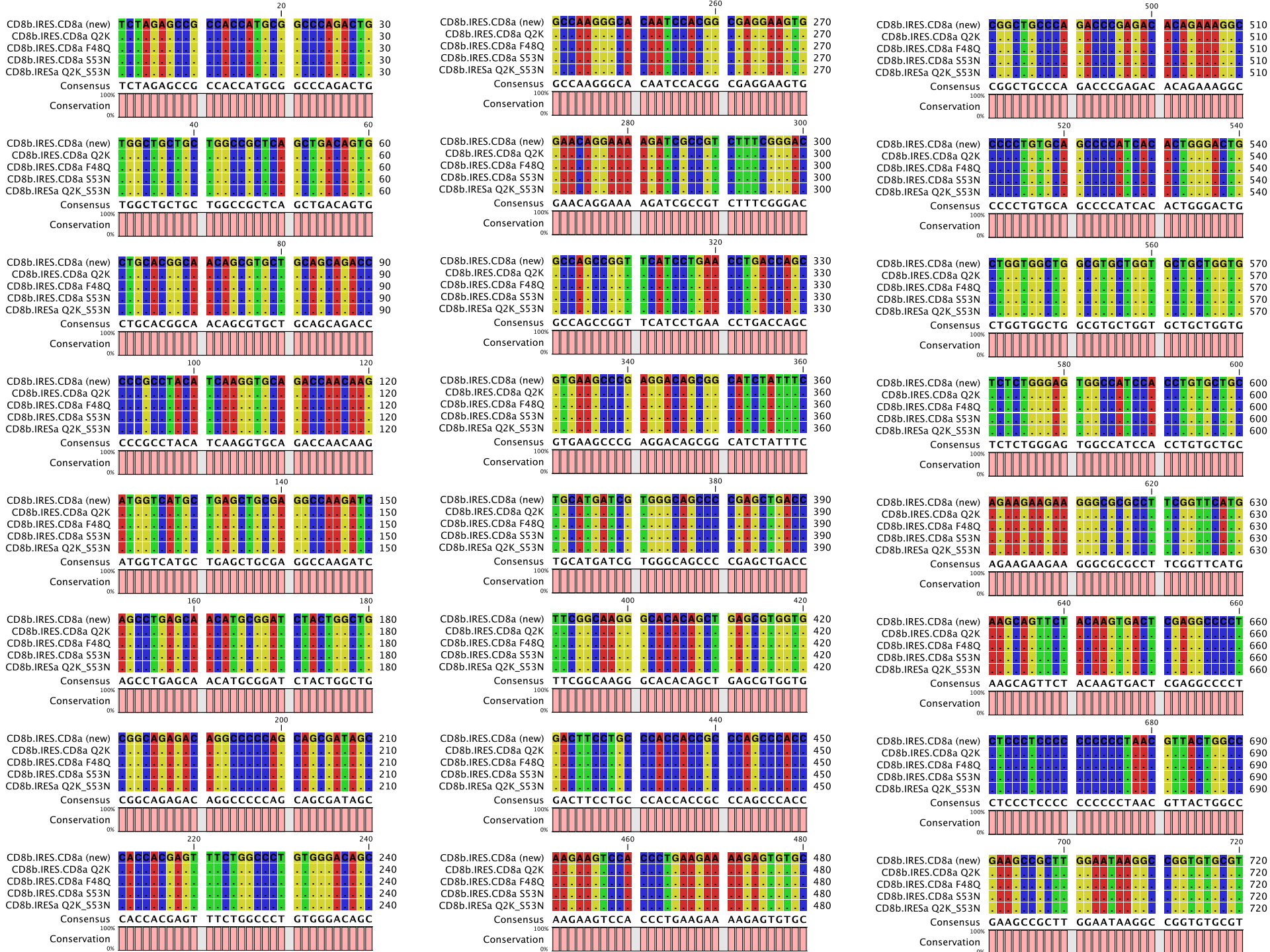
CD8b.IRES.CD8a (new)
CD8b.IRES.CD8a Q2K
CD8b.IRES.CD8a F48Q
CD8b.IRES.CD8a S53N
CD8b.IRESa Q2K_S53N
Consensus
Conservation
100%
0%
TCTAGAGCCG CCACCATGCG GCCCAGACTG
TGGCTGCTGC TGGCCGCTCA GCTGACAGTG
CTGCACGGCA ACAGCGTGCT GCAGCAGACC
CCCGCCTACA TCAAGGTGCA GACCAACAAG
ATGGTCATGC TGAGCTGCGA GGCCAAGATC
AGCCTGAGCA ACATGCGGAT CTACTGGCTG
CGGCAGAGAC AGGCCCCCAG CAGCGATAGC
CACCACGAGT TTCTGGCCCT GTGGGACAGC
GCCAAGGGCA CAATCCACGG CGAGGAAGTG
GAACAGGAAA AGATCGCCGT CTTTCGGGAC
GCCAGCCGGT TCATCCTGAA CCTGACCAGC
GTGAAGCCCG AGGACAGCGG CATCTATTTC
TGCATGATCG TGGGCAGCCC CGAGCTGACC
TTCGGCAAGG GCACACAGCT GAGCGTGGTG
GACTTCCTGC CCACCACCGC CCAGCCCACC
AAGAAGTCCA CCCTGAAGAA AAGAGTGTGC
CGGCTGCCCA GACCCGAGAC ACAGAAAGGC
CCCCTGTGCA GCCCCATCAC ACTGGGACTG
CTGGTGGCTG GCGTGCTGGT GCTGCTGGTG
TCTCTGGGAG TGGCCATCCA CCTGTGCTGC
AGAAGAAGAA GGGCGCGCCT TCGGTTCATG
AAGCAGTTCT ACAAGTGACT CGAGGCCCCT
CTCCCTCCCC CCCCCCTAAC GTTACTGGCC
GAAGCCGCTT GGAATAAGGC CGGTGTGCGT


CD8b.IRES.CD8a (new)
CD8b.IRES.CD8a Q2K
CD8b.IRES.CD8a F48Q
CD8b.IRES.CD8a S53N
CD8b.IRESa Q2K_S53N
Consensus
Conservation
100%
0%
740
750
760
780
800
810
820
840
860
870
880
900
920
930
940
960
980
990
1,000
1,020
1,040
1,050
1,060
1,080
1,100
1,110
1,120
1,140
1,160
1,170
1,180
1,200
1,220
1230
1,240
1,260
1260
1,280
1290
1,300
1,320
1320
1340
1350
1360
1380
1400
1410
1420
1,440
1440
TTGTCTATAT GTTATTTTCC ACCATATTGC
CGTCTTTTGG CAATGTGAGG GCCCGGAAAC
CTGGCCCTGT CTTCTTGACG AGCATTCCTA
GGGGTCTTTC CCCTCTCGCC AAAGGAATGC
AAGGTCTGTT GAATGTCGTG AAGGAAGCAG
TTCCTCTGGA AGCTTCTTGA AGACAAACAA
CGTCTGTAGC GACCCTTTGC AGGCAGCGGA
ACCCCCCACC TGGCGACAGG TGCCTCTGCG
GCCAAAAGCC ACGTGTATAA GATACACCTG
CAAAGGCGGC ACAACCCCAG TGCCACGTTG
TGAGTTGGAT AGTTGTGGAA AGAGTCAAAT
GGCTCTCCTC AAGCGTATTC AACAAGGGGC
TGAAGGATGC CCAGAAGGTA CCCCATTGTA
TGGGATCTGA TCTGGGGCCT CGGTGCACAT
GCTTTACATG TGTTTAGTCG AGGTTAAAAA
AACGTCTAGG CCCCCCGAAC CACGGGGACG
TGGTTTTCCT TTGAAAAACA CGATGATAAT
ATGCATGCCG CCACCATGAT GGCCCTGCCC
GTGACAGCCC TGCTGCTGCC TCTGGCTCTG
CTGCTGCACG CCGCCAGACC TAGCCAGTTC
AGAGTGTCCC CCCTGGACCG GACCTGGAAC
CTGGGCGAGA CAGTGGAACT GAAGTGCCAG
GTGCTGCTGA GCAACCCCAC CAGCGGCTGC
AGCTGGCTGT TCCAGCCTAG AGGCGCCGCT
A

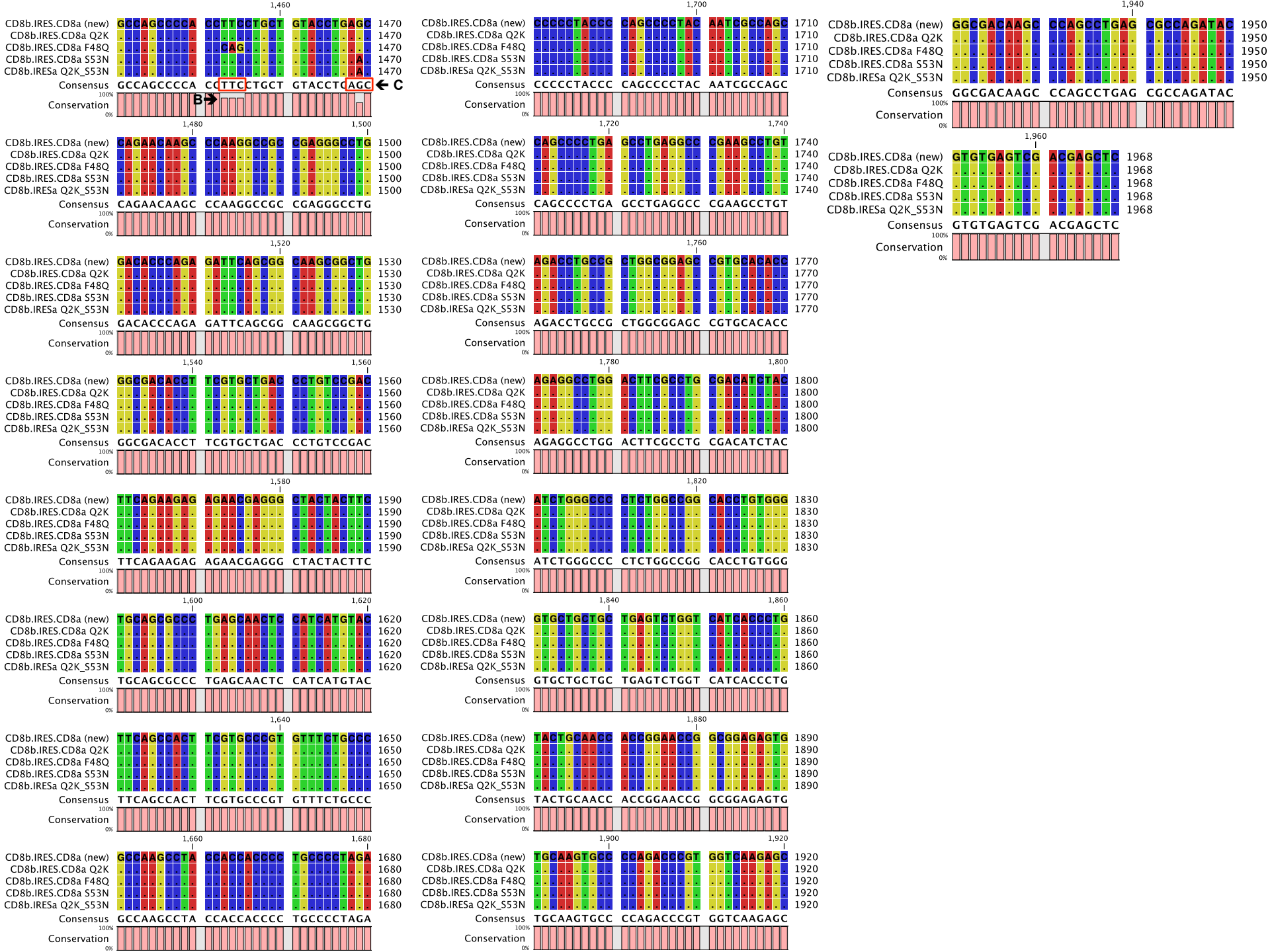
CD8b.IRES.CD8a (new)
CD8b.IRES.CD8a Q2K
CD8b.IRES.CD8a F48Q
CD8b.IRES.CD8a S53N
CD8b.IRESa Q2K_S53N
Consensus
Conservation
100%
0%
B
C
1,460
1,480
1,500
1,520
1,540
1,560
1,580
1,600
1,620
1,640
1,660
1,680
1,700
1,720
1,740
1,760
1,780
1,800
1,820
1,840
1,860
1,880
1,900
1,920
1,940
1,960
GCCAGCCCCA CCTTCCTGCT GTACCTGAGC 1470
CAGAACAAGC CCAAGGCCGC CGAGGGCCTG 1500
GACACCCAGA GATTCAGCGG CAAGCGGCTG 1530
GGCGACACCT TCGTGCTGAC CCTGTCCGAC 1560
TTCAGAAGAG AGAACGAGGG CTACTACTTC 1590
TGCAGCGCCC TGAGCAACTC CATCATGTAC 1620
TTCAGCCACT TCGTGCCCGT GTTTCTGCCC 1650
GCCAAGCCTA CCACCACCCC TGCCCCTAGA 1680
CCCCCTACCC CAGCCCCTAC AATCGCCAGC 1710
GAGCCCCTGA GCCTGAGGCC CGAAGCCTGT 1740
AGACCTGCCG CTGGCGGAGC CGTGCACACC 1770
AGAGGCCTGG ACTTCGCCTG CGACATCTAC 1800
ATCTGGGCCC CTCTGGCCGG CACCTGTGGG 1830
GTGCTGCTGC TGAGTCTGGT CATCACCCTG 1860
TACTGCAACC ACCGGAACCG GCGGAGAGTG 1890
TGCAAGTGCC CCAGACCCGT GGTCAAGAGC 1920
GGCGACAAGC CCAGCCTGAG CGCCAGATAC 1950
GTGTGAGTCG ACGAGCTC 1968

Appendix D

Best Fit Curves Used to generate pEC50s

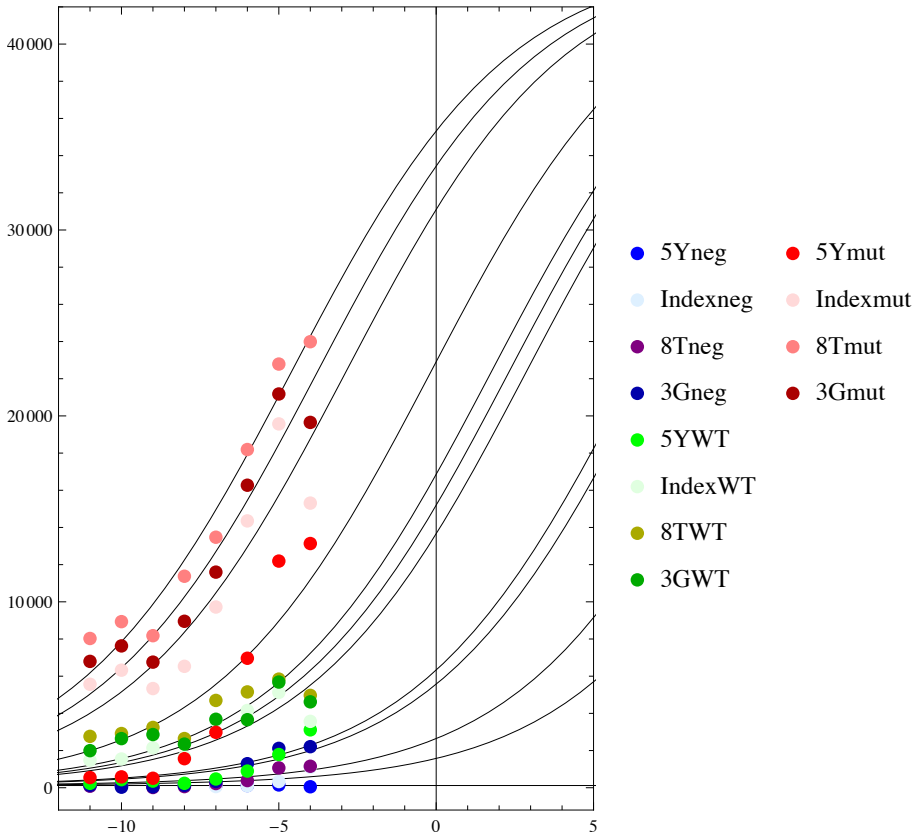

Figure D.1: J.RT3-T3.5 ILA1 TCR^{+} CD8^{var}
neg = CD8^{-}
WT = CD8αß$^{+}$
Mut = CD8αS53Nß$^{+}$
Best fit curves were applied to the data presented in Figure 5.1. The group were treated as a single batch (assumptions discussed in the main body of this thesis), and the curves used to generate pEC50s (Table 5.2), which were then scaled relative to each other in order to generate Figure 5.2.

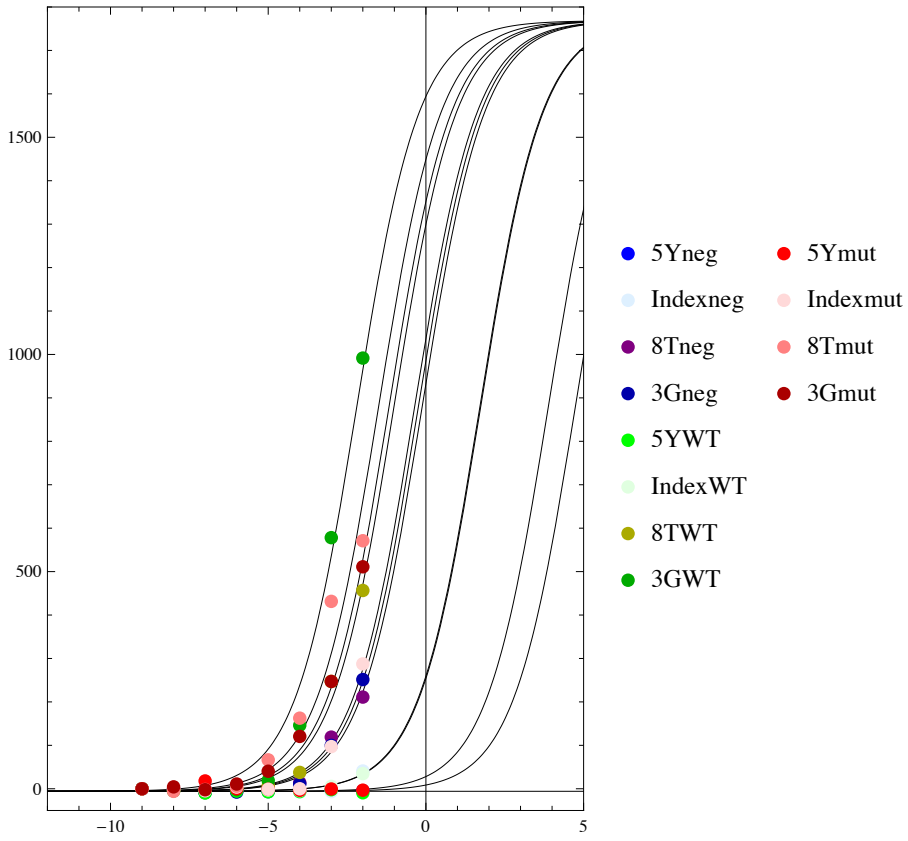

Figure D.2: H9 ILA1 TCR^{+} CD8^{var}
neg = CD8^{-}
WT = CD8αß$^{+}$
Mut = CD8αS53Nß$^{+}$
Best fit curves were applied to the data presented in Figure 5.3. The group were treated as a single batch (assumptions discussed in the main body of this thesis), and the curves used to generate pEC50s (Table 5.3), which were then scaled relative to each other in order to generate Figure 5.4.

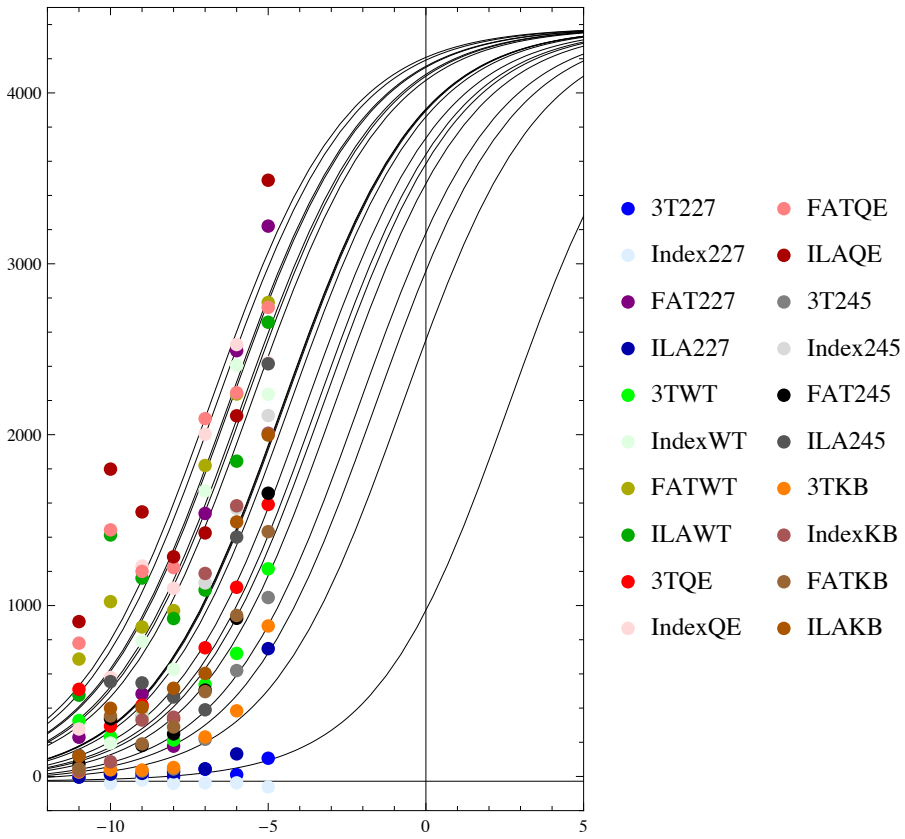

Figure D.3: MEL5 CD8⁺ T-cell clone, C1R A2 (or mutant) targets.
Best fit curves were applied to the data presented in Figure 5.5 & 5.7. The group were treated as a single batch (assumptions discussed in the main body of this thesis), and the curves used to generate pEC50s (Table 5.4 and Figure 5.6), which were then scaled relative to each other in order to generate Figure 5.6.

Appendix E

Supplementary Figures; The ß-chain Splice Variants

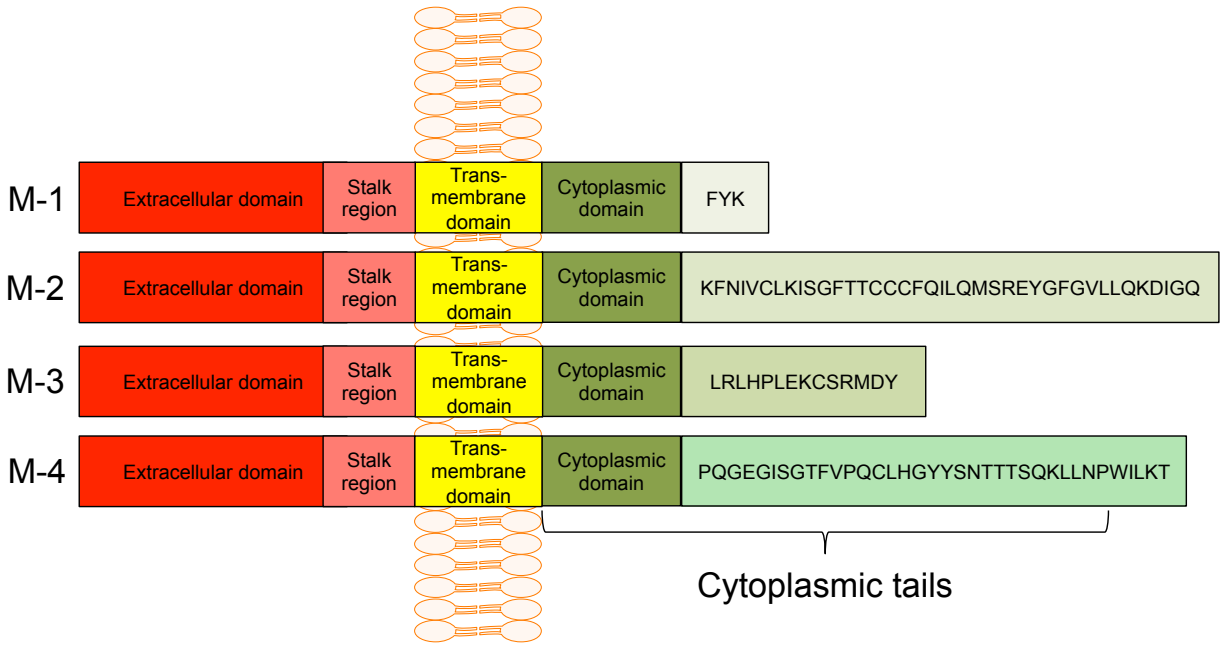

Figure E:1: CD8 ß-chain splice variants:
Four alternatively spliced variants have been described in man, resulting from alternative transcription of two exons, acquired in a common human/chimpanzee ancestor (DiSanto, Smith et al. 1993, Thakral, Dobbins et al. 2008, Thakral, Coman et al. 2013). The alternative transcriptions result in four distinctly different mRNA transcripts, giving rise to four different ß-chain alleles, which differ in their cytoplasmic domain as detailed above.

		ß-chain			
		M-1	M-2	M-3	M-4
α-chain	*wild type*	αß	αß	αß	αß
	S53>N	αß	αß	αß	αß

Table E.1
CD8αß co-receptor variants utilised in this thesis.

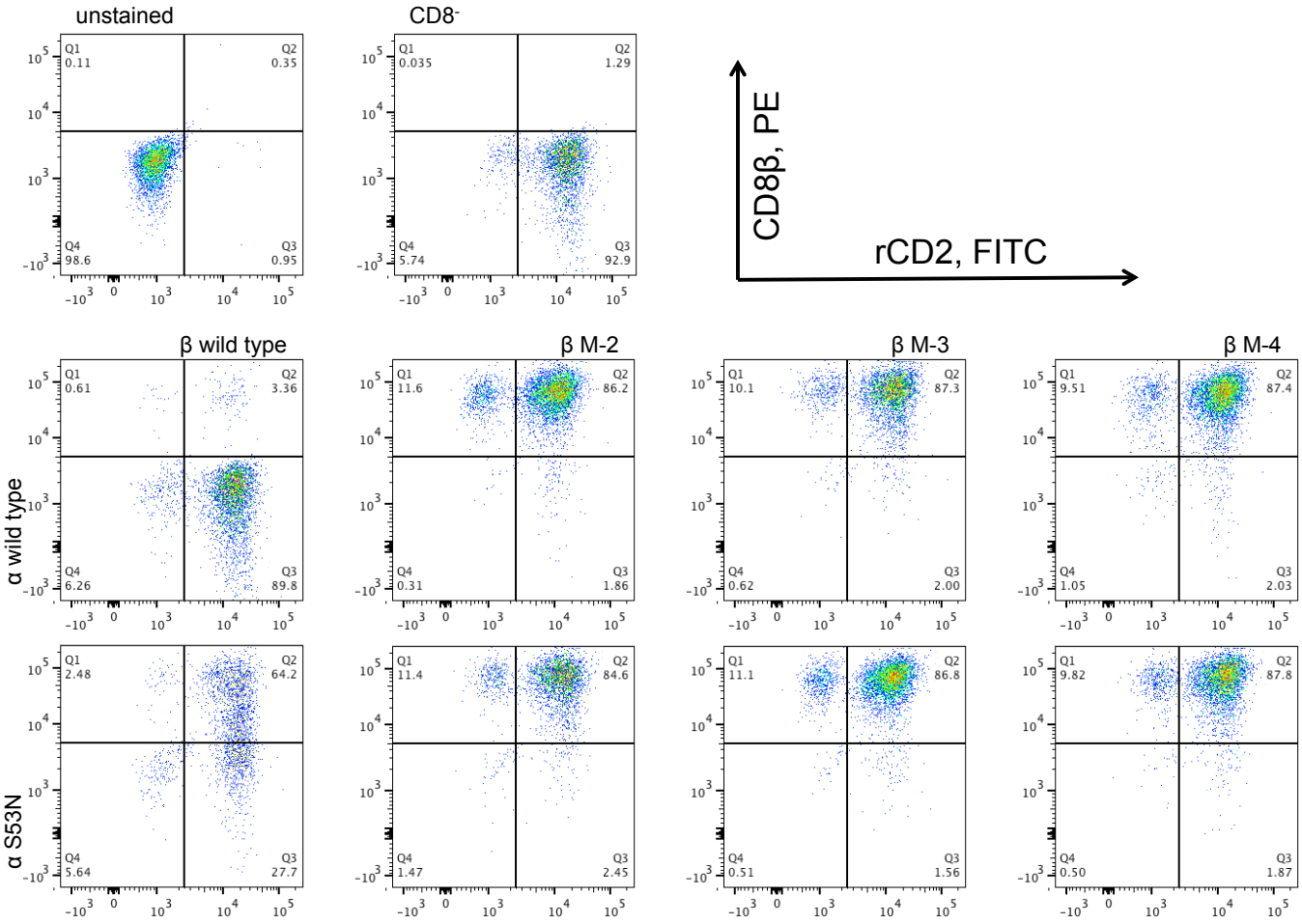

Figure E.2: The J.RT3-3.5 NFAT gluc. cell line was transduced with the both MEL5 TCR, and a CD8αß co-receptor as detailed in table F.1. Following expansion, the resultant cell lines were stained to demonstrate expression of the TCR and the co-receptor.

5 x 10^4 cells of each line were counted and re-suspended in 40 µl PBS and stained with fixable violet fluorescin amine dye (ViViD)(Life Technologies) at 1 in 800 dilution for 5 minutes in the dark, and at room temperature. Cells were then washed and re-suspended in 40 µl PBS and stained with 0.5 µl anti-rat CD2 antibody (FITC-conjugated), 2 µl anti-CD8α antibody (APC-conjugated), and 2 µl anti-CD8ß antibody (PE-conjugated) for 20 minutes at 4°. Cells were washed twice and fixed in 100 µl 1% paraformaldehyde. Data were acquired using a FACSCanto flow cytometer, and analysed using FlowJo software. The data plotted represent the live, singlet populations, concatenated into dot plots showing presence of TCR (as demonstrated by rCD2 staining) and CD8αß (as demonstrated by CD8ß staining). The double positive (Q2) populations for each line were selected for enrichment before further expansion and re-staining to confirm phenotype was maintained.

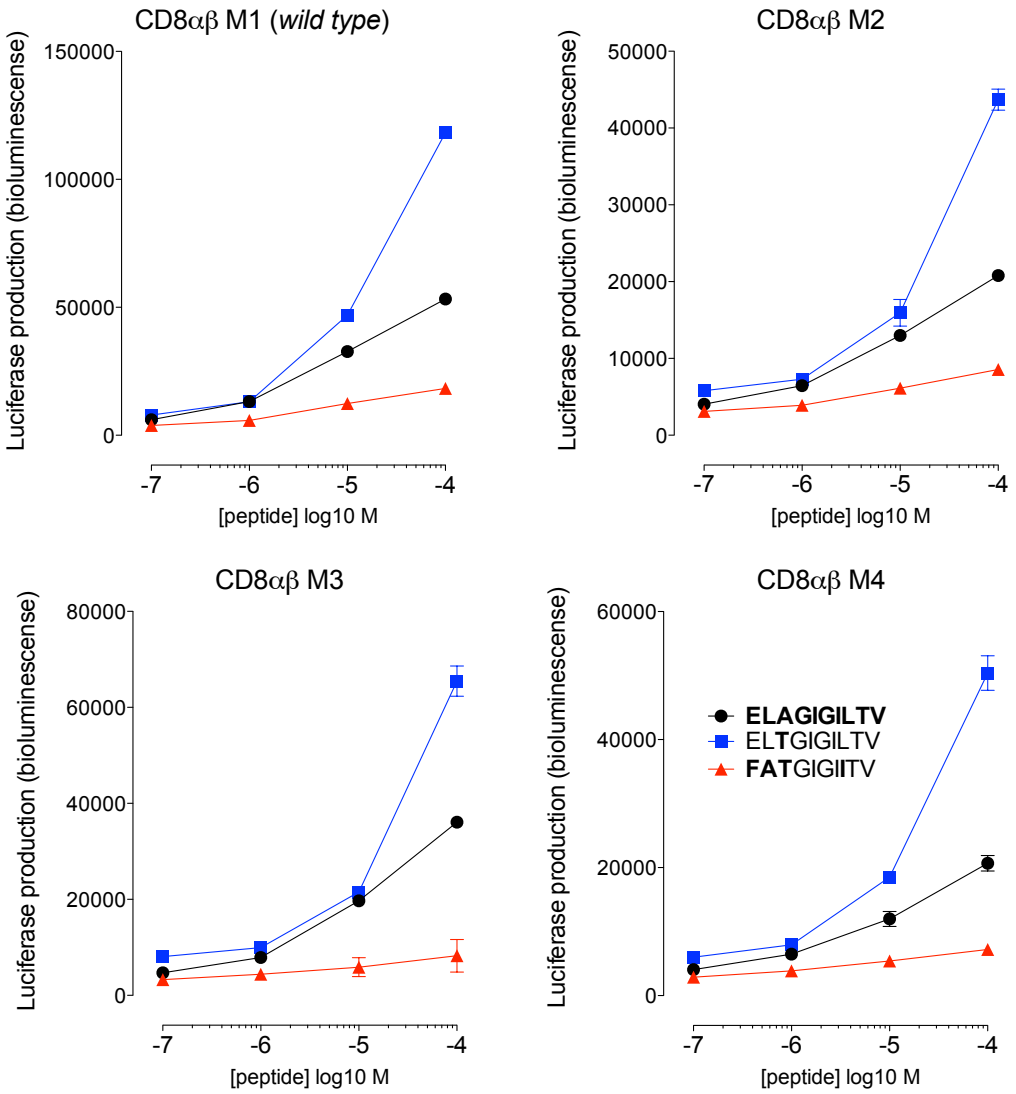

Figure E.3: JRT3-3.5 NFAT GLuc MELTCR rCD2^{+} CD8αβ$^{spl.var.}$ cells are capable of responding to peptide through their TCR.

C1R A2 target cells, pre-pulsed with ELA, 3T, or FAT peptides at a final concentration of 10^{-4} - 10^{-7} M, were incubated together with each of the J.RT3-3.5 NFAT GLuc MELTCR^{+} CD8αβ$^{spl.var.}$ lines, at 37 °C for 24 hours. The supernatant was harvested, and assayed for luciferase protein by bioluminescence as per manufacturer's instructions. The data plotted represent the mean of two replicate assays, and these data are representative of two identical experiments.

These data show that these cell lines are capable of activating through their TCR in response to peptide, moreover that there appear to be differences between different species, however experimental design limits the usefulness of this interpretation.

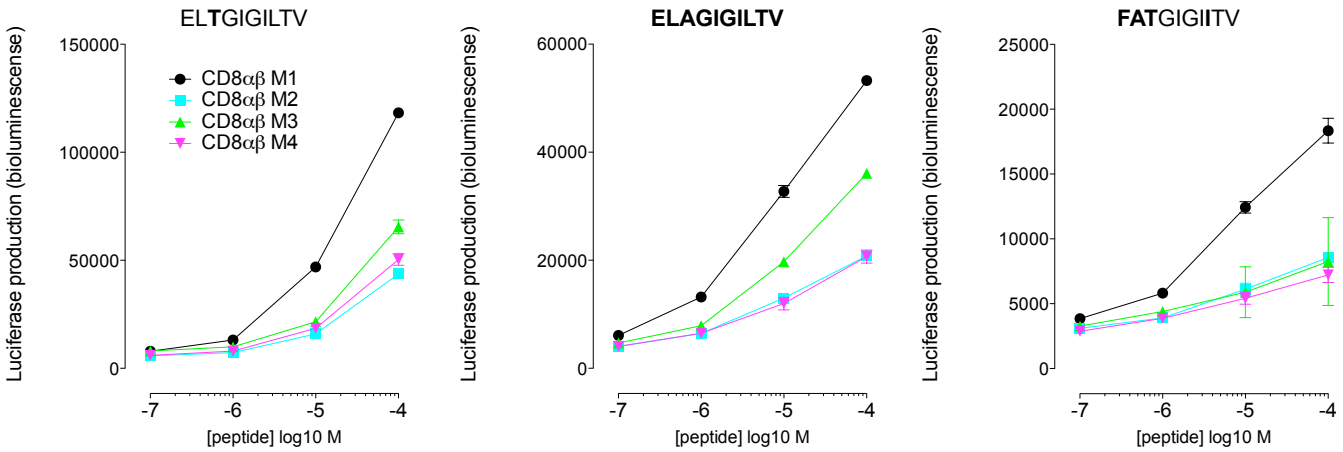

Figure E.4:
The same data shown is figure E.3 is re-plotted in order to examine activation by different affinity TCR agonists, where co-receptor help is provided by each ß-chain splice variant. Differential activation is observed by the M3 variant, suggesting that further exploration of this system is indicated.

Bibleography

2017. Erratum for the Report: "Molecular remission of infant B-ALL after infusion of universal TALEN gene-edited CAR T cells" by W. Qasim, H. Zhan, S. Samarasinghe, S. Adams, P. Amrolia, S. Stafford, K. Butler, C. Rivat, G. Wright, K. Somana, S. Ghorashian, D. Pinner, G. Ahsan, K. Gilmour, G. Lucchini, S. Inglott, W. Mifsud, R. Chiesa, K. S. Peggs, L. Chan, F. Farzeneh, A. J. Thrasher, A. Vora, M. Pule, P. Veys. *Sci Transl Med,* 9.

ABBEY, J. L. & O'NEILL, H. C. 2008. Expression of T-cell receptor genes during early T-cell development. *Immunology and cell biology,* 86**,** 166-74.

ABEDIA. 2017. *Gene Therapy Clinical Trials Worldwide* [Online]. Journal of Gene Medicine: Wiley online. Available: http://www.abedia.com/wiley/.

ACCAPEZZATO, D., VISCO, V., FRANCAVILLA, V., MOLETTE, C., DONATO, T., PAROLI, M., MONDELLI, M. U., DORIA, M., TORRISI, M. R. & BARNABA, V. 2005. Chloroquine enhances human CD8+ T cell responses against soluble antigens in vivo. *J Exp Med,* 202**,** 817-28.

ADAMS, E. J., GU, S. & LUOMA, A. M. 2015. Human gamma delta T cells: Evolution and ligand recognition. *Cell Immunol,* 296**,** 31-40.

ADAMS, J. 2003. The proteasome: structure, function, and role in the cell. *Cancer Treat Rev.,* Volume 29, Supplement 1**,** 3-9.

AIVAZIAN, D. & STERN, L. J. 2000. Phosphorylation of T cell receptor zeta is regulated by a lipid dependent folding transition. *Nat Struct Biol,* 7**,** 1023-6.

ALARCON, B., MESTRE, D. & MARTINEZ-MARTIN, N. 2011. The immunological synapse: a cause or consequence of T-cell receptor triggering? *Immunology,* 133**,** 420-5.

ALTMAN, J. D., MOSS, P. A., GOULDER, P. J., BAROUCH, D. H., MCHEYZER-WILLIAMS, M. G., BELL, J. I., MCMICHAEL, A. J. & DAVIS, M. M. 1996. Phenotypic analysis of antigen-specific T lymphocytes. *Science,* 274**,** 94-6.

AMADOU, C., KUMANOVICS, A., JONES, E. P., LAMBRACHT-WASHINGTON, D., YOSHINO, M. & LINDAHL, K. F. 1999. The mouse major histocompatibility complex: some assembly required. *Immunol Rev,* 167**,** 211-21.

ANDERTON, S. M. & WRAITH, D. C. 2002. Selection and fine-tuning of the autoimmune T-cell repertoire. *Nat Rev Immunol,* 2**,** 487-98.

ANNUNZIATO, F., COSMI, L., SANTARLASCI, V., MAGGI, L., LIOTTA, F., MAZZINGHI, B., PARENTE, E., FILI, L., FERRI, S., FROSALI, F., GIUDICI, F., ROMAGNANI, P., PARRONCHI, P., TONELLI, F., MAGGI, E. & ROMAGNANI, S. 2007. Phenotypic and functional features of human Th17 cells. *J Exp Med,* 204**,** 1849-61.

ANTON VAN DER MERWE, P., DAVIS, S. J., SHAW, A. S. & DUSTIN, M. L. 2000. Cytoskeletal polarization and redistribution of cell-surface molecules during T cell antigen recognition. *Semin Immunol,* 12**,** 5-21.

ANTONY, G. K. & DUDEK, A. Z. 2010. Interleukin 2 in cancer therapy. *Curr Med Chem,* 17**,** 3297-302.

APPLEMAN, L. J. & BOUSSIOTIS, V. A. 2003. T cell anergy and costimulation. *Immunol Rev,* 192**,** 161-80.

APTE, S. H., BAZ, A., GROVES, P., KELSO, A. & KIENZLE, N. 2008. Interferon-gamma and interleukin-4 reciprocally regulate CD8 expression in CD8+ T cells. *Proc Natl Acad Sci U S A,* 105**,** 17475-80.

ARCARO, A., GREGOIRE, C., BAKKER, T. R., BALDI, L., JORDAN, M., GOFFIN, L., BOUCHERON, N., WURM, F., VAN DER MERWE, P. A., MALISSEN, B. & LUESCHER, I. F. 2001. CD8beta endows CD8 with efficient coreceptor function by coupling T cell receptor/CD3 to raft-associated CD8/p56(lck) complexes. *J Exp Med,* 194**,** 1485-95.

ARCARO, A., GREGOIRE, C., BOUCHERON, N., STOTZ, S., PALMER, E., MALISSEN, B. & LUESCHER, I. F. 2000. Essential role of CD8 palmitoylation in CD8 coreceptor function. *J Immunol,* 165**,** 2068-76.

ARCHBOLD, J. K., MACDONALD, W. A., MILES, J. J., BRENNAN, R. M., KJER-NIELSEN, L., MCCLUSKEY, J., BURROWS, S. R. & ROSSJOHN, J. 2006. Alloreactivity between disparate cognate and allogeneic pMHC-I complexes is the result of highly focused, peptide-dependent structural mimicry. *J Biol Chem,* 281**,** 34324-32.

ARDOLINO, M., AZIMI, C. S., IANNELLO, A., TREVINO, T. N., HORAN, L., ZHANG, L., DENG, W., RING, A. M., FISCHER, S., GARCIA, K. C. & RAULET, D. H. 2014. Cytokine therapy reverses NK cell anergy in MHC-deficient tumors. *J Clin Invest,* 124**,** 4781-94.

ARDOLINO, M., HSU, J. & RAULET, D. H. 2015. Cytokine treatment in cancer immunotherapy. *Oncotarget,* 6**,** 19346-7.

ARENS, R. & SCHOENBERGER, S. P. 2010. Plasticity in programming of effector and memory CD8 T-cell formation. *Immunological reviews,* 235**,** 190-205.

ARIOTTI, S., BELTMAN, J. B., CHODACZEK, G., HOEKSTRA, M. E., VAN BEEK, A. E., GOMEZ-EERLAND, R., RITSMA, L., VAN RHEENEN, J., MAREE, A. F., ZAL, T., DE BOER, R. J., HAANEN, J. B. & SCHUMACHER, T. N. 2012. Tissue-resident memory CD8+ T cells continuously patrol skin epithelia to quickly recognize local antigen. *Proc Natl Acad Sci U S A,* 109**,** 19739-44.

ARMANDA CASROUGE, E. B., SOPHIE DALLE, CHRISTOPHE PANNETIER, JEAN KANELLOPOULOS, AND PHILIPPE KOURILSKY 2000. Size Estimate of the αß TCR Repertoire of Naive Mouse Splenocytes. *Journal of Immunology,* vol. 164 5782-5787.

ARSTILA TP, C. A., BARON V, EVEN J, KANELLOPOULOS J, KOURILSKY P. 1999. A direct estimate of the human alphabeta T cell receptor diversity. *Science,* Oct 29; 286**,** 958-61.

ARSTILA, T. P., CASROUGE, A., BARON, V., EVEN, J., KANELLOPOULOS, J. & KOURILSKY, P. 1999. A direct estimate of the human alphabeta T cell receptor diversity. *Science,* 286**,** 958-61.

ARTYOMOV, M. N., LIS, M., DEVADAS, S., DAVIS, M. M. & CHAKRABORTY, A. K. 2010. CD4 and CD8 binding to MHC molecules primarily acts to enhance Lck delivery. *Proc Natl Acad Sci U S A,* 107**,** 16916-21.

ARUM, C. J., ANDERSSEN, E., VISET, T., KODAMA, Y., LUNDGREN, S., CHEN, D. & ZHAO, C. M. 2010. Cancer immunoediting from immunosurveillance to tumor escape in microvillus-formed niche: a study of syngeneic orthotopic rat bladder cancer model in comparison with human bladder cancer. *Neoplasia,* 12**,** 434-42.

ASSAL, A., KANER, J., PENDURTI, G. & ZANG, X. 2015. Emerging targets in cancer immunotherapy: beyond CTLA-4 and PD-1. *Immunotherapy,* 7**,** 1169-86.

ATCC. 2014a. *H9 [derivative of HuT 78] (ATCC® HTB-176™)* [Online]. Available: http://www.lgcstandards-atcc.org/products/all/HTB-176.aspx?geo_country=gb - generalinformation.

ATCC. 2014b. *J.RT3-T3.5 (ATCC® TIB-153™)* [Online]. Available: http://www.lgcstandards-atcc.org/products/all/TIB-153.aspx?geo_country=gb - generalinformation.

ATTAL, J., THERON, M. C. & HOUDEBINE, L. M. 1999. The optimal use of IRES (internal ribosome entry site) in expression vectors. *Genet Anal,* 15**,** 161-5.

AYYAR, B. V., ARORA, S. & O'KENNEDY, R. 2016. Coming-of-Age of Antibodies in Cancer Therapeutics. *Trends Pharmacol Sci,* 37**,** 1009-1028.

BADOVINAC, V. P. & HARTY, J. T. 2006. Programming, demarcating, and manipulating CD8+ T-cell memory. *Immunol Rev,* 211**,** 67-80.

BADOVINAC, V. P., TVINNEREIM, A. R. & HARTY, J. T. 2000. Regulation of antigen-specific CD8+ T cell homeostasis by perforin and interferon-gamma. *Science,* 290**,** 1354-8.

BALAR, A. V. & WEBER, J. S. 2017. PD-1 and PD-L1 antibodies in cancer: current status and future directions. *Cancer Immunol Immunother,* 66**,** 551-564.

BALDO, B. A. 2013. Adverse events to monoclonal antibodies used for cancer therapy: Focus on hypersensitivity responses. *Oncoimmunology,* 2**,** e26333.

BALDWIN, C. L. & TELFER, J. C. 2015. The bovine model for elucidating the role of gammadelta T cells in controlling infectious diseases of importance to cattle and humans. *Mol Immunol,* 66**,** 35-47.

BARRY, M. & BLEACKLEY, R. C. 2002. Cytotoxic T lymphocytes: all roads lead to death. *Nature reviews Immunology,* 2**,** 401-9.

BARRY, S. C., HARDER, B., BRZEZINSKI, M., FLINT, L. Y., SEPPEN, J. & OSBORNE, W. R. 2001. Lentivirus vectors encoding both central polypurine tract and posttranscriptional regulatory element provide enhanced transduction and transgene expression. *Human gene therapy,* 12**,** 1103-8.

BEDDOE, T., CHEN, Z., CLEMENTS, C. S., ELY, L. K., BUSHELL, S. R., VIVIAN, J. P., KJER-NIELSEN, L., PANG, S. S., DUNSTONE, M. A., LIU, Y. C., MACDONALD, W. A., PERUGINI, M. A., WILCE, M. C., BURROWS, S. R., PURCELL, A. W., TIGANIS, T., BOTTOMLEY, S. P., MCCLUSKEY, J. & ROSSJOHN, J. 2009. Antigen ligation triggers a conformational change within the constant domain of the alphabeta T cell receptor. *Immunity,* 30**,** 777-88.

BENNETT, M. S., ROUND, J. L. & LEUNG, D. T. 2015. Innate-like lymphocytes in intestinal infections. *Curr Opin Infect Dis,* 28**,** 457-63.

BERGLUND, P., FINZI, D., BENNINK, J. R. & YEWDELL, J. W. 2007. Viral alteration of cellular translational machinery increases defective ribosomal products. *J Virol,* 81**,** 7220-9.

BESSER, M. J. 2013. Is there a future for adoptive cell transfer in melanoma patients? *Oncoimmunology,* 2**,** e26098.

BESSER, M. J., SHAPIRA-FROMMER, R., TREVES, A. J., ZIPPEL, D., ITZHAKI, O., HERSHKOVITZ, L., LEVY, D., KUBI, A., HOVAV, E., CHERMOSHNIUK, N., SHALMON, B., HARDAN, I., CATANE, R., MARKEL, G., APTER, S., BEN-NUN, A., KUCHUK, I., SHIMONI, A., NAGLER, A. & SCHACHTER, J. 2010. Clinical responses in a phase II study using adoptive transfer of short-term cultured tumor infiltration lymphocytes in metastatic melanoma patients. *Clin Cancer Res,* 16**,** 2646-55.

BESSER, M. J., SHOHAM, T., HARARI-STEINBERG, O., ZABARI, N., ORTENBERG, R., YAKIREVITCH, A., NAGLER, A., LOEWENTHAL, R., SCHACHTER, J. & MARKEL, G. 2013. Development of allogeneic NK cell adoptive transfer therapy in metastatic melanoma patients: in vitro preclinical optimization studies. *PLoS One,* 8**,** e57922.

BEUNEU, H., LEMAITRE, F., DEGUINE, J., MOREAU, H. D., BOUVIER, I., GARCIA, Z., ALBERT, M. L. & BOUSSO, P. 2010. Visualizing the functional diversification of CD8+ T cell responses in lymph nodes. *Immunity,* 33**,** 412-23.

BICKNELL, D. C., ROWAN, A. & BODMER, W. F. 1994. Beta 2-microglobulin gene mutations: a study of established colorectal cell lines and fresh tumors. *Proc Natl Acad Sci U S A,* 91**,** 4751-5.

BILLADEAU, D. D. 2010. T cell activation at the immunological synapse: vesicles emerge for LATer signaling. *Science Signaling,* May 11;3(121).

BJORKMAN, P. J., SAPER, M. A., SAMRAOUI, B., BENNETT, W. S., STROMINGER, J. L. & WILEY, D. C. 1987a. The foreign antigen binding site and T cell recognition regions of class I histocompatibility antigens. *Nature,* 329**,** 512-8.

BJORKMAN, P. J., SAPER, M. A., SAMRAOUI, B., BENNETT, W. S., STROMINGER, J. L. & WILEY, D. C. 1987b. Structure of the human class I histocompatibility antigen, HLA-A2. *Nature,* 329**,** 506-12.

BLUESTONE, J. A., MACKAY, C. R., O'SHEA, J. J. & STOCKINGER, B. 2009. The functional plasticity of T cell subsets. *Nat Rev Immunol,* 9**,** 811-6.

BOEHM, T. 2011. Design principles of adaptive immune systems. *Nat Rev Immunol,* 11, 307-17.

BOON, T. & VAN DER BRUGGEN, P. 1996. Human tumor antigens recognized by T lymphocytes. *J Exp Med,* 183, 725-9.

BORGER, J. G., ZAMOYSKA, R. & GAKAMSKY, D. M. 2014. Proximity of TCR and its CD8 coreceptor controls sensitivity of T cells. *Immunol Lett,* 157, 16-22.

BOSHOFF, C. & WEISS, R. 2002. AIDS-related malignancies. *Nat Rev Cancer,* 2, 373-82.

BOSSELUT, R., KUBO, S., GUINTER, T., KOPACZ, J. L., ALTMAN, J. D., FEIGENBAUM, L. & SINGER, A. 2000. Role of CD8beta domains in CD8 coreceptor function: importance for MHC I binding, signaling, and positive selection of CD8+ T cells in the thymus. *Immunity,* 12, 409-18.

BOSSELUT, R., ZHANG, W., ASHE, J. M., KOPACZ, J. L., SAMELSON, L. E. & SINGER, A. 1999. Association of the adaptor molecule LAT with CD4 and CD8 coreceptors identifies a new coreceptor function in T cell receptor signal transduction. *The Journal of experimental medicine,* 190, 1517-26.

BOTS, M. & MEDEMA, J. P. 2006. Granzymes at a glance. *Journal of cell science,* 119, 5011-4.

BOUABE, H., FASSLER, R. & HEESEMANN, J. 2008. Improvement of reporter activity by IRES-mediated polycistronic reporter system. *Nucleic Acids Res,* 36, e28.

BOVENSCHEN, N. & KUMMER, J. A. 2010. Orphan granzymes find a home. *Immunological reviews,* 235, 117-27.

BOYMAN, O., LETOURNEAU, S., KRIEG, C. & SPRENT, J. 2009. Homeostatic proliferation and survival of naive and memory T cells. *Eur J Immunol,* 39, 2088-94.

BOYMAN, O. & SPRENT, J. 2012. The role of interleukin-2 during homeostasis and activation of the immune system. *Nat Rev Immunol,* 12, 180-90.

BRETSCHER, P. A. 1999. A two-step, two-signal model for the primary activation of precursor helper T cells. *Proc Natl Acad Sci U S A,* 96, 185-90.

BRIDGEMAN, J. S., HAWKINS, R. E., BAGLEY, S., BLAYLOCK, M., HOLLAND, M. & GILHAM, D. E. 2010a. The optimal antigen response of chimeric antigen receptors harboring the CD3zeta transmembrane domain is dependent upon incorporation of the receptor into the endogenous TCR/CD3 complex. *J Immunol,* 184, 6938-49.

BRIDGEMAN, J. S., HAWKINS, R. E., HOMBACH, A. A., ABKEN, H. & GILHAM, D. E. 2010b. Building better chimeric antigen receptors for adoptive T cell therapy. *Curr Gene Ther,* 10, 77-90.

BRIDGEMAN, J. S., SEWELL, A. K., MILES, J. J., PRICE, D. A. & COLE, D. K. 2012. Structural and biophysical determinants of alphabeta T-cell antigen recognition. *Immunology,* 135, 9-18.

BRIGINO, E., HARAGUCHI, S., KOUTSONIKOLIS, A., CIANCIOLO, G. J., OWENS, U., GOOD, R. A. & DAY, N. K. 1997. Interleukin 10 is induced by recombinant HIV-1 Nef protein involving the calcium/calmodulin-dependent phosphodiesterase signal transduction pathway. *Proc Natl Acad Sci U S A,* 94**,** 3178-82.

BRIMNES, M. K., GANG, A. O., DONIA, M., THOR STRATEN, P., SVANE, I. M. & HADRUP, S. R. 2012. Generation of autologous tumor-specific T cells for adoptive transfer based on vaccination, in vitro restimulation and CD3/CD28 dynabead-induced T cell expansion. *Cancer Immunol Immunother,* 61**,** 1221-31.

BRINKMAN, J. A., FAUSCH, S. C., WEBER, J. S. & KAST, W. M. 2004. Peptide-based vaccines for cancer immunotherapy. *Expert Opin Biol Ther,* 4**,** 181-98.

BUBENIK, J. 2004. MHC class I down-regulation: tumour escape from immune surveillance? (review). *Int J Oncol,* 25**,** 487-91.

BURROWS, S. R., KHANNA, R., BURROWS, J. M. & MOSS, D. J. 1994. An alloresponse in humans is dominated by cytotoxic T lymphocytes (CTL) cross-reactive with a single Epstein-Barr virus CTL epitope: implications for graft-versus-host disease. *J Exp Med,* 179**,** 1155-61.

BURROWS, S. R., KIENZLE, N., WINTERHALTER, A., BHARADWAJ, M., ALTMAN, J. D. & BROOKS, A. 2000. Peptide-MHC class I tetrameric complexes display exquisite ligand specificity. *J Immunol,* 165**,** 6229-34.

BURROWS, S. R., SCULLEY, T. B., MISKO, I. S., SCHMIDT, C. & MOSS, D. J. 1990. An Epstein-Barr virus-specific cytotoxic T cell epitope in EBV nuclear antigen 3 (EBNA 3). *J Exp Med,* 171**,** 345-9.

BURROWS, S. R., SILINS, S. L., MOSS, D. J., KHANNA, R., MISKO, I. S. & ARGAET, V. P. 1995. T cell receptor repertoire for a viral epitope in humans is diversified by tolerance to a background major histocompatibility complex antigen. *J Exp Med,* 182**,** 1703-15.

BUSSE, D., DE LA ROSA, M., HOBIGER, K., THURLEY, K., FLOSSDORF, M., SCHEFFOLD, A. & HOFER, T. 2010. Competing feedback loops shape IL-2 signaling between helper and regulatory T lymphocytes in cellular microenvironments. *Proc Natl Acad Sci U S A,* 107**,** 3058-63.

BUTTE, M. J., KEIR, M. E., PHAMDUY, T. B., SHARPE, A. H. & FREEMAN, G. J. 2007. Programmed death-1 ligand 1 interacts specifically with the B7-1 costimulatory molecule to inhibit T cell responses. *Immunity,* 27**,** 111-22.

CAI, Z., KISHIMOTO, H., BRUNMARK, A., JACKSON, M. R., PETERSON, P. A. & SPRENT, J. 1997. Requirements for peptide-induced T cell receptor downregulation on naive CD8+ T cells. *J Exp Med,* 185**,** 641-51.

CAMPANELLI, R., PALERMO, B., GARBELLI, S., MANTOVANI, S., LUCCHI, P., NECKER, A., LANTELME, E. & GIACHINO, C. 2002. Human CD8 co-receptor is strictly involved in MHC-peptide tetramer-TCR binding and T cell activation. *Int Immunol,* 14**,** 39-44.

CAO, H., AGRAWAL, D., KUSHNER, N., TOUZJIAN, N., ESSEX, M. & LU, Y. 2002. Delivery of exogenous protein antigens to major histocompatibility complex class I pathway in cytosol. *J Infect Dis,* 185, 244-51.

CARRENO, L. J., GONZALEZ, P. A. & KALERGIS, A. M. 2006. Modulation of T cell function by TCR/pMHC binding kinetics. *Immunobiology,* 211, 47-64.

CASROUGE, A., BEAUDOING, E., DALLE, S., PANNETIER, C., KANELLOPOULOS, J. & KOURILSKY, P. 2000. Size estimate of the alpha beta TCR repertoire of naive mouse splenocytes. *J Immunol,* 164, 5782-7.

CATALFAMO, M. & HENKART, P. A. 2003. Perforin and the granule exocytosis cytotoxicity pathway. *Curr Opin Immunol,* 15, 522-7.

CAWTHON, A. G., LU, H. & ALEXANDER-MILLER, M. A. 2001. Peptide requirement for CTL activation reflects the sensitivity to CD3 engagement: correlation with CD8alphabeta versus CD8alphaalpha expression. *J Immunol,* 167, 2577-84.

CELLA, M., ENGERING, A., PINET, V., PIETERS, J. & LANZAVECCHIA, A. 1997. Inflammatory stimuli induce accumulation of MHC class II complexes on dendritic cells. *Nature,* 388, 782-7.

CHAKRABORTY, A. K. & WEISS, A. 2014. Insights into the initiation of TCR signaling. *Nat Immunol,* 15, 798-807.

CHANG, H. C., TAN, K. & HSU, Y. M. 2006. CD8alphabeta has two distinct binding modes of interaction with peptide-major histocompatibility complex class I. *J Biol Chem,* 281, 28090-6.

CHANG, H. C., TAN, K., OUYANG, J., PARISINI, E., LIU, J. H., LE, Y., WANG, X., REINHERZ, E. L. & WANG, J. H. 2005. Structural and mutational analyses of a CD8alphabeta heterodimer and comparison with the CD8alphaalpha homodimer. *Immunity,* 23, 661-71.

CHANG, J. T., PALANIVEL, V. R., KINJYO, I., SCHAMBACH, F., INTLEKOFER, A. M., BANERJEE, A., LONGWORTH, S. A., VINUP, K. E., MRASS, P., OLIARO, J., KILLEEN, N., ORANGE, J. S., RUSSELL, S. M., WENINGER, W. & REINER, S. L. 2007. Asymmetric T lymphocyte division in the initiation of adaptive immune responses. *Science,* 315, 1687-91.

CHANG, V. T., FERNANDES, R. A., GANZINGER, K. A., LEE, S. F., SIEBOLD, C., MCCOLL, J., JONSSON, P., PALAYRET, M., HARLOS, K., COLES, C. H., JONES, E. Y., LUI, Y., HUANG, E., GILBERT, R. J. C., KLENERMAN, D., ARICESCU, A. R. & DAVIS, S. J. 2016. Initiation of T cell signaling by CD45 segregation at 'close contacts'. *Nat Immunol,* 17, 574-582.

CHAPMAN, J. R., WEBSTER, A. C. & WONG, G. 2013. Cancer in the transplant recipient. *Cold Spring Harb Perspect Med,* 3.

CHEN, J. L., DUNBAR, P. R., GILEADI, U., JAGER, E., GNJATIC, S., NAGATA, Y., STOCKERT, E., PANICALI, D. L., CHEN, Y. T., KNUTH, A., OLD, L. J. & CERUNDOLO, V. 2000. Identification of NY-ESO-1 peptide analogues capable of improved stimulation of tumor-reactive CTL. *J Immunol,* 165, 948-55.

CHEN, L. & FLIES, D. B. 2013. Molecular mechanisms of T cell co-stimulation and co-inhibition. *Nat Rev Immunol,* 13**,** 227-42.

CHEN, T. R. 1992. Karyotypic derivation of H9 cell line expressing human immunodeficiency virus susceptibility. *J Natl Cancer Inst,* 84**,** 1922-6.

CHEROUTRE, H. & LAMBOLEZ, F. 2008. Doubting the TCR coreceptor function of CD8alphaalpha. *Immunity,* 28**,** 149-59.

CHICHILI, G. R., CAIL, R. C. & RODGERS, W. 2012. Cytoskeletal modulation of lipid interactions regulates Lck kinase activity. *J Biol Chem,* 287**,** 24186-94.

CHINNAIYAN, A. M., O'ROURKE, K., TEWARI, M. & DIXIT, V. M. 1995. FADD, a novel death domain-containing protein, interacts with the death domain of Fas and initiates apoptosis. *Cell,* 81**,** 505-12.

CLEMENT, M., LADELL, K., EKERUCHE-MAKINDE, J., MILES, J. J., EDWARDS, E. S., DOLTON, G., WILLIAMS, T., SCHAUENBURG, A. J., COLE, D. K., LAUDER, S. N., GALLIMORE, A. M., GODKIN, A. J., BURROWS, S. R., PRICE, D. A., SEWELL, A. K. & WOOLDRIDGE, L. 2011. Anti-CD8 antibodies can trigger CD8+ T cell effector function in the absence of TCR engagement and improve peptide-MHCI tetramer staining. *J Immunol,* 187**,** 654-63.

CLEMENT, M., PEARSON, J. A., GRAS, S., VAN DEN BERG, H. A., LISSINA, A., LLEWELLYN-LACEY, S., WILLIS, M. D., DOCKREE, T., MCLAREN, J. E., EKERUCHE-MAKINDE, J., GOSTICK, E., ROBERTSON, N. P., ROSSJOHN, J., BURROWS, S. R., PRICE, D. A., WONG, F. S., PEAKMAN, M., SKOWERA, A. & WOOLDRIDGE, L. 2016. Targeted suppression of autoreactive CD8+ T-cell activation using blocking anti-CD8 antibodies. *Sci Rep,* 6**,** 35332.

CLEVELAND, J. L. & IHLE, J. N. 1995. Contenders in FasL/TNF death signaling. *Cell,* 81**,** 479-82.

COHEN, J. J. 1991. Programmed cell death in the immune system. *Adv Immunol,* 50**,** 55-85.

COHEN, J. J., DUKE, R. C., CHERVENAK, R., SELLINS, K. S. & OLSON, L. K. 1985. DNA fragmentation in targets of CTL: an example of programmed cell death in the immune system. *Adv Exp Med Biol,* 184**,** 493-508.

COLE, D. K., DUNN, S. M., SAMI, M., BOULTER, J. M., JAKOBSEN, B. K. & SEWELL, A. K. 2008. T cell receptor engagement of peptide-major histocompatibility complex class I does not modify CD8 binding. *Mol Immunol,* 45**,** 2700-9.

COLE, D. K., LAUGEL, B., CLEMENT, M., PRICE, D. A., WOOLDRIDGE, L. & SEWELL, A. K. 2012. The molecular determinants of CD8 co-receptor function. *Immunology,* 137**,** 139-48.

COLE, D. K., MILES, K. M., MADURA, F., HOLLAND, C. J., SCHAUENBURG, A. J., GODKIN, A. J., BULEK, A. M., FULLER, A., AKPOVWA, H. J., PYMM, P. G., LIDDY, N., SAMI, M., LI, Y., RIZKALLAH, P. J., JAKOBSEN, B. K. & SEWELL, A. K. 2014. T-cell receptor (TCR)-peptide specificity overrides affinity-enhancing TCR-major histocompatibility complex interactions. *J Biol Chem,* 289**,** 628-38.

COLE, D. K., RIZKALLAH, P. J., BOULTER, J. M., SAMI, M., VUIDEPOT, A. L., GLICK, M., GAO, F., BELL, J. I., JAKOBSEN, B. K. & GAO, G. F. 2007. Computational design and crystal structure of an enhanced affinity mutant human CD8 alphaalpha coreceptor. *Proteins,* 67**,** 65-74.

COLE, D. K., RIZKALLAH, P. J., SAMI, M., LISSIN, N. M., GAO, F., BELL, J. I., BOULTER, J. M., GLICK, M., VUIDEPOT, A. L., JAKOBSEN, B. K. & GAO, G. F. 2005. Crystallization and preliminary X-ray structural studies of a high-affinity CD8alphaalpha co-receptor to pMHC. *Acta Crystallogr Sect F Struct Biol Cryst Commun,* 61**,** 285-7.

COLF, L. A., BANKOVICH, A. J., HANICK, N. A., BOWERMAN, N. A., JONES, L. L., KRANZ, D. M. & GARCIA, K. C. 2007. How a single T cell receptor recognizes both self and foreign MHC. *Cell,* 129**,** 135-46.

COLOMBANI, J. 1990. Conserved and variable structures in HLA class I molecules: a review. *Tissue Antigens,* 35**,** 103-13.

COOPER, G. 2000. *The Cell: A Molecular Approach. ,* Sunderland (MA), Sinauer Associates.

CORRALIZA-GORJON, I., SOMOVILLA-CRESPO, B., SANTAMARIA, S., GARCIA-SANZ, J. A. & KREMER, L. 2017. New Strategies Using Antibody Combinations to Increase Cancer Treatment Effectiveness. *Front Immunol,* 8**,** 1804.

CORRIVEAU, R. A., HUH, G. S. & SHATZ, C. J. 1998. Regulation of class I MHC gene expression in the developing and mature CNS by neural activity. *Neuron,* 21**,** 505-20.

COSTELLO, R. T., GASTAUT, J. A. & OLIVE, D. 1999. Tumor escape from immune surveillance. *Arch Immunol Ther Exp (Warsz),* 47**,** 83-8.

CRESSWELL, P. 1994. Assembly, transport, and function of MHC class II molecules. *Annu Rev Immunol,* 12**,** 259-93.

CROTTY, S. 2014. T follicular helper cell differentiation, function, and roles in disease. *Immunity,* 41**,** 529-42.

CUENCA, A., CHENG, F., WANG, H., BRAYER, J., HORNA, P., GU, L., BIEN, H., BORRELLO, I. M., LEVITSKY, H. I. & SOTOMAYOR, E. M. 2003. Extra-lymphatic solid tumor growth is not immunologically ignored and results in early induction of antigen-specific T-cell anergy: dominant role of cross-tolerance to tumor antigens. *Cancer Res,* 63**,** 9007-15.

CURTSINGER, J. M. & MESCHER, M. F. 2010. Inflammatory cytokines as a third signal for T cell activation. *Curr Opin Immunol,* 22**,** 333-40.

DANIELS, M. A. & JAMESON, S. C. 2000. Critical role for CD8 in T cell receptor binding and activation by peptide/major histocompatibility complex multimers. *J Exp Med,* 191**,** 335-46.

DAS, G., AUGUSTINE, M. M., DAS, J., BOTTOMLY, K., RAY, P. & RAY, A. 2003. An important regulatory role for CD4+CD8 alpha alpha T cells in the intestinal epithelial layer in the prevention of inflammatory bowel disease. *Proc Natl Acad Sci U S A,* 100**,** 5324-9.

DAVIS, A. M. & BERG, J. M. 2009. Homodimerization and heterodimerization of minimal zinc(II)-binding-domain peptides of T-cell proteins CD4, CD8alpha, and Lck. *J Am Chem Soc,* 131**,** 11492-7.

DAVIS, M. M. & BJORKMAN, P. J. 1988. T-cell antigen receptor genes and T-cell recognition. *Nature,* 334**,** 395-402.

DAVIS, M. M., BONIFACE, J. J., REICH, Z., LYONS, D., HAMPL, J., ARDEN, B. & CHIEN, Y. 1998. Ligand recognition by alpha beta T cell receptors. *Annu Rev Immunol,* 16**,** 523-44.

DAVIS, S. J. & VAN DER MERWE, P. A. 2006. The kinetic-segregation model: TCR triggering and beyond. *Nat Immunol,* 7**,** 803-9.

DAVIS, Z. B., FELICES, M., VERNERIS, M. R. & MILLER, J. S. 2015. Natural Killer Cell Adoptive Transfer Therapy: Exploiting the First Line of Defense Against Cancer. *Cancer J,* 21**,** 486-91.

DE CHARETTE, M., MARABELLE, A. & HOUOT, R. 2016. Turning tumour cells into antigen presenting cells: The next step to improve cancer immunotherapy? *Eur J Cancer,* 68**,** 134-147.

DE LA CALLE-MARTIN, O., HERNANDEZ, M., ORDI, J., CASAMITJANA, N., AROSTEGUI, J. I., CARAGOL, I., FERRANDO, M., LABRADOR, M., RODRIGUEZ-SANCHEZ, J. L. & ESPANOL, T. 2001. Familial CD8 deficiency due to a mutation in the CD8 alpha gene. *J Clin Invest,* 108**,** 117-23.

DEDEOGLU, F., HUBBARD, R. A., SCHLUTER, S. F. & MARCHALONIS, J. J. 1992. T-cell receptors of man and mouse studied with antibodies against synthetic peptides. *Exp Clin Immunogenet,* 9**,** 95-108.

DELVES, P. J. & ROITT, I. M. 1998. *Encyclopedia of immunology,* San Diego, Academic Press.

DEMOTTE, N., COLAU, D., OTTAVIANI, S., GODELAINE, D., VAN PEL, A., BOON, T. & VAN DER BRUGGEN, P. 2002. A reversible functional defect of CD8+ T lymphocytes involving loss of tetramer labeling. *Eur J Immunol,* 32**,** 1688-97.

DENIZOT, F., WILSON, A., BATTYE, F., BERKE, G. & SHORTMAN, K. 1986. Clonal expansion of T cells: a cytotoxic T-cell response in vivo that involves precursor cell proliferation. *Proc Natl Acad Sci U S A,* 83**,** 6089-92.

DEVINE, L., KIEFFER, L. J., AITKEN, V. & KAVATHAS, P. B. 2000. Human CD8 beta, but not mouse CD8 beta, can be expressed in the absence of CD8 alpha as a beta beta homodimer. *J Immunol,* 164**,** 833-8.

DEVINE, L., THAKRAL, D., NAG, S., DOBBINS, J., HODSDON, M. E. & KAVATHAS, P. B. 2006. Mapping the binding site on CD8 beta for MHC class I reveals mutants with enhanced binding. *J Immunol,* 177**,** 3930-8.

DISANTO, J. P., KNOWLES, R. W. & FLOMENBERG, N. 1988. The human Lyt-3 molecule requires CD8 for cell surface expression. *EMBO J,* 7**,** 3465-70.

DISANTO, J. P., SMITH, D., DE BRUIN, D., LACY, E. & FLOMENBERG, N. 1993. Transcriptional diversity at the duplicated human CD8 beta loci. *European journal of immunology,* 23**,** 320-6.

DO, M. H. & LI, M. O. 2016. Metabolic control of asyMYCtric division. *Cell Res*.

DOCKREE, T., HOLLAND, C. J., CLEMENT, M., LADELL, K., MCLAREN, J. E., VAN DEN BERG, H. A., GOSTICK, E., K, L. M., LLEWELLYN-LACEY, S., BRIDGEMAN, J. S., MAN, S., BAILEY, M., BURROWS, S. R., PRICE, D. A. & WOOLDRIDGE, L. 2017. CD8+ T-cell specificity is compromised at a defined MHCI/CD8 affinity threshold. *Immunol Cell Biol,* 95**,** 68-76.

DRAKE, D. R., 3RD, REAM, R. M., LAWRENCE, C. W. & BRACIALE, T. J. 2005. Transient loss of MHC class I tetramer binding after CD8+ T cell activation reflects altered T cell effector function. *J Immunol,* 175**,** 1507-15.

DUBRIDGE, R. B., TANG, P., HSIA, H. C., LEONG, P. M., MILLER, J. H. & CALOS, M. P. 1987. Analysis of mutation in human cells by using an Epstein-Barr virus shuttle system. *Mol Cell Biol,* 7**,** 379-87.

DUDLEY, M. E. & ROSENBERG, S. A. 2003. Adoptive-cell-transfer therapy for the treatment of patients with cancer. *Nat Rev Cancer,* 3**,** 666-75.

DUDLEY, M. E., WUNDERLICH, J. R., ROBBINS, P. F., YANG, J. C., HWU, P., SCHWARTZENTRUBER, D. J., TOPALIAN, S. L., SHERRY, R., RESTIFO, N. P., HUBICKI, A. M., ROBINSON, M. R., RAFFELD, M., DURAY, P., SEIPP, C. A., ROGERS-FREEZER, L., MORTON, K. E., MAVROUKAKIS, S. A., WHITE, D. E. & ROSENBERG, S. A. 2002. Cancer regression and autoimmunity in patients after clonal repopulation with antitumor lymphocytes. *Science,* 298**,** 850-4.

DUDLEY, M. E., YANG, J. C., SHERRY, R., HUGHES, M. S., ROYAL, R., KAMMULA, U., ROBBINS, P. F., HUANG, J., CITRIN, D. E., LEITMAN, S. F., WUNDERLICH, J., RESTIFO, N. P., THOMASIAN, A., DOWNEY, S. G., SMITH, F. O., KLAPPER, J., MORTON, K., LAURENCOT, C., WHITE, D. E. & ROSENBERG, S. A. 2008. Adoptive cell therapy for patients with metastatic melanoma: evaluation of intensive myeloablative chemoradiation preparative regimens. *Journal of clinical oncology : official journal of the American Society of Clinical Oncology,* 26**,** 5233-9.

DUNN, G. P., BRUCE, A. T., IKEDA, H., OLD, L. J. & SCHREIBER, R. D. 2002. Cancer immunoediting: from immunosurveillance to tumor escape. *Nat Immunol,* 3**,** 991-8.

EKERUCHE-MAKINDE, J., CLEMENT, M., COLE, D. K., EDWARDS, E. S., LADELL, K., MILES, J. J., MATTHEWS, K. K., FULLER, A., LLOYD, K. A., MADURA, F., DOLTON, G. M., PENTIER, J., LISSINA, A., GOSTICK, E., BAXTER, T. K., BAKER, B. M., RIZKALLAH, P. J., PRICE, D. A., WOOLDRIDGE, L. & SEWELL, A. K. 2012. T-cell receptor-optimized peptide skewing of the T-cell repertoire can enhance antigen targeting. *J Biol Chem,* 287**,** 37269-81.

EYERICH, S., EYERICH, K., PENNINO, D., CARBONE, T., NASORRI, F., PALLOTTA, S., CIANFARANI, F., ODORISIO, T., TRAIDL-HOFFMANN, C., BEHRENDT, H., DURHAM, S. R., SCHMIDT-WEBER, C. B. & CAVANI, A. 2009. Th22 cells represent a distinct human T cell subset involved in epidermal immunity and remodeling. *J Clin Invest,* 119**,** 3573-85.

FEARON, D. T. & LOCKSLEY, R. M. 1996. The instructive role of innate immunity in the acquired immune response. *Science,* 272**,** 50-3.

FEINERMAN, O., VEIGA, J., DORFMAN, J. R., GERMAIN, R. N. & ALTAN-BONNET, G. 2008. Variability and robustness in T cell activation from regulated heterogeneity in protein levels. *Science,* 321**,** 1081-4.

FERBER, M., ZOETE, V. & MICHIELIN, O. 2012. T-cell receptors binding orientation over peptide/MHC class I is driven by long-range interactions. *PLoS One,* 7**,** e51943.

FINN, O. J. 2012. Immuno-oncology: understanding the function and dysfunction of the immune system in cancer. *Ann Oncol,* 23 Suppl 8**,** viii6-9.

FOOKSMAN, D. R., VARDHANA, S., VASILIVER-SHAMIS, G., LIESE, J., BLAIR, D. A., WAITE, J., SACRISTAN, C., VICTORA, G. D., ZANIN-ZHOROV, A. & DUSTIN, M. L. 2010. Functional anatomy of T cell activation and synapse formation. *Annu Rev Immunol,* 28**,** 79-105.

FUJITA, H. 2013. The role of IL-22 and Th22 cells in human skin diseases. *J Dermatol Sci,* 72**,** 3-8.

GACZYNSKA, M., ROCK, K. L. & GOLDBERG, A. L. 1993. Role of proteasomes in antigen presentation. *Enzyme Protein,* 47**,** 354-69.

GAKAMSKY, D. M., LUESCHER, I. F., PRAMANIK, A., KOPITO, R. B., LEMONNIER, F., VOGEL, H., RIGLER, R. & PECHT, I. 2005. CD8 kinetically promotes ligand binding to the T-cell antigen receptor. *Biophys J,* 89**,** 2121-33.

GANGADHARAN, D. & CHEROUTRE, H. 2004. The CD8 isoform CD8alphaalpha is not a functional homologue of the TCR co-receptor CD8alphabeta. *Curr Opin Immunol,* 16**,** 264-70.

GAO, G. F. & JAKOBSEN, B. K. 2000. Molecular interactions of coreceptor CD8 and MHC class I: the molecular basis for functional coordination with the T-cell receptor. *Immunol Today,* 21**,** 630-6.

GAO, G. F., TORMO J FAU - GERTH, U. C., GERTH UC FAU - WYER, J. R., WYER JR FAU - MCMICHAEL, A. J., MCMICHAEL AJ FAU - STUART, D. I., STUART DI FAU - BELL, J. I., BELL JI FAU - JONES, E. Y., JONES EY FAU - JAKOBSEN, B. K. & JAKOBSEN, B. K. 1997a. Crystal structure of the complex between human CD8alpha(alpha) and HLA-A2. *Nature,* 387**,** 630-4.

GAO, G. F., TORMO, J., GERTH, U. C., WYER, J. R., MCMICHAEL, A. J., STUART, D. I., BELL, J. I., JONES, E. Y. & JAKOBSEN, B. K. 1997b. Crystal structure of the complex between human CD8alpha(alpha) and HLA-A2. *Nature,* 387**,** 630-4.

GAO, G. F., WILLCOX, B. E., WYER, J. R., BOULTER, J. M., O'CALLAGHAN, C. A., MAENAKA, K., STUART, D. I., JONES, E. Y., VAN DER MERWE, P. A., BELL, J. I. & JAKOBSEN, B. K. 2000. Classical and nonclassical class I major histocompatibility complex molecules exhibit subtle conformational differences that affect binding to CD8alphaalpha. *J Biol Chem,* 275**,** 15232-8.

GARCIA, K. C., SCOTT, C. A., BRUNMARK, A., CARBONE, F. R., PETERSON, P. A., WILSON, I. A. & TEYTON, L. 1996. CD8 enhances formation of stable T-cell receptor/MHC class I molecule complexes. *Nature,* 384**,** 577-81.

GASCOIGNE, N. R., CASAS, J., BRZOSTEK, J. & RYBAKIN, V. 2011. Initiation of TCR phosphorylation and signal transduction. *Front Immunol,* 2**,** 72.

GERLACH, C., ROHR, J. C., PERIE, L., VAN ROOIJ, N., VAN HEIJST, J. W., VELDS, A., URBANUS, J., NAIK, S. H., JACOBS, H., BELTMAN, J. B., DE BOER, R. J. & SCHUMACHER, T. N. 2013. Heterogeneous differentiation patterns of individual CD8+ T cells. *Science,* 340**,** 635-9.

GERLACH, C., VAN HEIJST, J. W., SWART, E., SIE, D., ARMSTRONG, N., KERKHOVEN, R. M., ZEHN, D., BEVAN, M. J., SCHEPERS, K. & SCHUMACHER, T. N. 2010. One naive T cell, multiple fates in CD8+ T cell differentiation. *J Exp Med,* 207**,** 1235-46.

GERMAIN, R. N. 1994. MHC-dependent antigen processing and peptide presentation: providing ligands for T lymphocyte activation. *Cell,* 76**,** 287-99.

GEUKES FOPPEN, M. H., DONIA, M., SVANE, I. M. & HAANEN, J. B. 2015. Tumor-infiltrating lymphocytes for the treatment of metastatic cancer. *Mol Oncol,* 9**,** 1918-35.

GIBLIN, P., LEDBETTER, J. A. & KAVATHAS, P. 1989. A secreted form of the human lymphocyte cell surface molecule CD8 arises from alternative splicing. *Proc Natl Acad Sci U S A,* 86**,** 998-1002.

GOFF, S. L., SMITH, F. O., KLAPPER, J. A., SHERRY, R., WUNDERLICH, J. R., STEINBERG, S. M., WHITE, D., ROSENBERG, S. A., DUDLEY, M. E. & YANG, J. C. 2010. Tumor infiltrating lymphocyte therapy for metastatic melanoma: analysis of tumors resected for TIL. *J Immunother,* 33**,** 840-7.

GOLDRATH, A. W. & BEVAN, M. J. 1999. Selecting and maintaining a diverse T-cell repertoire. *Nature,* 402**,** 255-62.

GOOTENBERG, J. E., RUSCETTI, F. W., MIER, J. W., GAZDAR, A. & GALLO, R. C. 1981. Human cutaneous T cell lymphoma and leukemia cell lines produce and respond to T cell growth factor. *J Exp Med,* 154**,** 1403-18.

GORMAN, S. D., SUN, Y. H., ZAMOYSKA, R. & PARNES, J. R. 1988. Molecular linkage of the Ly-3 and Ly-2 genes. Requirement of Ly-2 for Ly-3 surface expression. *J Immunol,* 140**,** 3646-53.

GRAHAM, F. L., SMILEY, J., RUSSELL, W. C. & NAIRN, R. 1977. Characteristics of a human cell line transformed by DNA from human adenovirus type 5. *J Gen Virol,* 36**,** 59-74.

GRAKOUI, A., BROMLEY, S. K., SUMEN, C., DAVIS, M. M., SHAW, A. S., ALLEN, P. M. & DUSTIN, M. L. 1999. The immunological synapse: a molecular machine controlling T cell activation. *Science,* 285**,** 221-7.

GREEN, K. J., MILES, J. J., TELLAM, J., VAN ZUYLEN, W. J., CONNOLLY, G. & BURROWS, S. R. 2004. Potent T cell response to a class I-binding 13-mer

viral epitope and the influence of HLA micropolymorphism in controlling epitope length. *Eur J Immunol,* 34**,** 2510-9.

GRIFFIOEN, M., VAN EGMOND, E. H., KESTER, M. G., WILLEMZE, R., FALKENBURG, J. H. & HEEMSKERK, M. H. 2009. Retroviral transfer of human CD20 as a suicide gene for adoptive T-cell therapy. *Haematologica,* 94**,** 1316-20.

GROSSMAN, W. J., REVELL, P. A., LU, Z. H., JOHNSON, H., BREDEMEYER, A. J. & LEY, T. J. 2003. The orphan granzymes of humans and mice. *Curr Opin Immunol,* 15**,** 544-52.

HAHNE, M., RIMOLDI, D., SCHROTER, M., ROMERO, P., SCHREIER, M., FRENCH, L. E., SCHNEIDER, P., BORNAND, T., FONTANA, A., LIENARD, D., CEROTTINI, J. & TSCHOPP, J. 1996. Melanoma cell expression of Fas(Apo-1/CD95) ligand: implications for tumor immune escape. *Science,* 274**,** 1363-6.

HAJI-FATAHALIHA, M., HOSSEINI, M., AKBARIAN, A., SADREDDINI, S., JADIDI-NIARAGH, F. & YOUSEFI, M. 2015. CAR-modified T-cell therapy for cancer: an updated review. *Artif Cells Nanomed Biotechnol***,** 1-11.

HAMPL, J., CHIEN, Y. H. & DAVIS, M. M. 1997. CD4 augments the response of a T cell to agonist but not to antagonist ligands. *Immunity,* 7**,** 379-85.

HANAGIRI, T., SHIGEMATSU, Y., SHINOHARA, S., TAKENAKA, M., OKA, S., CHIKAISHI, Y., NAGATA, Y., BABA, T., URAMOTO, H., SO, T. & YAMADA, S. 2013. Clinical significance of expression of cancer/testis antigen and down-regulation of HLA class-I in patients with stage I non-small cell lung cancer. *Anticancer Res,* 33**,** 2123-8.

HANAHAN, D. 1983. Studies on transformation of Escherichia coli with plasmids. *J Mol Biol,* 166**,** 557-80.

HARDARDOTTIR, F., BARON JL FAU - JANEWAY, C. A., JR. & JANEWAY, C. A., JR. 1995. T cells with two functional antigen-specific receptors. *Proc Natl Acad Sci U S A,* 92(2)**,** 354-8.

HARDING, C. V. & SONG, R. 1994. Phagocytic processing of exogenous particulate antigens by macrophages for presentation by class I MHC molecules. *J Immunol,* 153**,** 4925-33.

HARDY, R. R. & HAYAKAWA, K. 2001. B cell development pathways. *Annu Rev Immunol,* 19**,** 595-621.

HARTY, J. T., TVINNEREIM, A. R. & WHITE, D. W. 2000. CD8+ T cell effector mechanisms in resistance to infection. *Annu Rev Immunol,* 18**,** 275-308.

HE, J.-S., GONG, D.-E. & OSTERGAARD, H. L. 2010. Stored Fas ligand, a mediator of rapid CTL-mediated killing, has a lower threshold for response than degranulation or newly synthesized Fas ligand. *Journal of immunology (Baltimore, Md : 1950),* 184**,** 555-63.

HE, J.-S. & OSTERGAARD, H. L. 2007. CTLs contain and use intracellular stores of FasL distinct from cytolytic granules. *Journal of immunology (Baltimore, Md : 1950),* 179**,** 2339-48.

HEBEISEN, M., OBERLE, S. G., PRESOTTO, D., SPEISER, D. E., ZEHN, D. & RUFER, N. 2013. Molecular insights for optimizing T cell receptor specificity against cancer. *Front Immunol,* 4**,** 154.

HENNECKE, J., CARFI, A. & WILEY, D. C. 2000. Structure of a covalently stabilized complex of a human alphabeta T-cell receptor, influenza HA peptide and MHC class II molecule, HLA-DR1. *EMBO J,* 19**,** 5611-24.

HICKLIN, D. J., MARINCOLA, F. M. & FERRONE, S. 1999. HLA class I antigen downregulation in human cancers: T-cell immunotherapy revives an old story. *Mol Med Today,* 5**,** 178-86.

HIGASHIMOTO, T., URBINATI, F., PERUMBETI, A., JIANG, G., ZARZUELA, A., CHANG, L. J., KOHN, D. B. & MALIK, P. 2007. The woodchuck hepatitis virus post-transcriptional regulatory element reduces readthrough transcription from retroviral vectors. *Gene therapy,* 14**,** 1298-304.

HINRICHS, C. S. & ROSENBERG, S. A. 2014. Exploiting the curative potential of adoptive T-cell therapy for cancer. *Immunol Rev,* 257**,** 56-71.

HIRAHARA, K., POHOLEK, A., VAHEDI, G., LAURENCE, A., KANNO, Y., MILNER, J. D. & O'SHEA, J. J. 2013. Mechanisms underlying helper T-cell plasticity: implications for immune-mediated disease. *J Allergy Clin Immunol,* 131**,** 1276-87.

HOGQUIST, K. A., XING, Y., HSU, F. C. & SHAPIRO, V. S. 2015. T Cell Adolescence: Maturation Events Beyond Positive Selection. *J Immunol,* 195**,** 1351-7.

HOLLER, P. D., CHLEWICKI, L. K. & KRANZ, D. M. 2003. TCRs with high affinity for foreign pMHC show self-reactivity. *Nat Immunol,* 4**,** 55-62.

HOLLER, P. D. & KRANZ, D. M. 2003. Quantitative analysis of the contribution of TCR/pepMHC affinity and CD8 to T cell activation. *Immunity,* 18**,** 255-64.

HOLMBERG, K., MARIATHASAN, S., OHTEKI, T., OHASHI, P. S. & GASCOIGNE, N. R. 2003. TCR binding kinetics measured with MHC class I tetramers reveal a positive selecting peptide with relatively high affinity for TCR. *J Immunol,* 171**,** 2427-34.

HOMET MORENO, B. & RIBAS, A. 2015. Anti-programmed cell death protein-1/ligand-1 therapy in different cancers. *Br J Cancer,* 112**,** 1421-7.

HUANG, J., EDWARDS, L. J., EVAVOLD, B. D. & ZHU, C. 2007. Kinetics of MHC-CD8 interaction at the T cell membrane. *J Immunol,* 179**,** 7653-62.

HUANG, J., ZARNITSYNA, V. I., LIU, B., EDWARDS, L. J., JIANG, N., EVAVOLD, B. D. & ZHU, C. 2010. The kinetics of two-dimensional TCR and pMHC interactions determine T-cell responsiveness. *Nature,* 464**,** 932-6.

HUTCHINSON, S. L., WOOLDRIDGE, L., TAFURO, S., LAUGEL, B., GLICK, M., BOULTER, J. M., JAKOBSEN, B. K., PRICE, D. A. & SEWELL, A. K. 2003. The CD8 T cell coreceptor exhibits disproportionate biological activity at extremely low binding affinities. *J Biol Chem,* 278**,** 24285-93.

IEZZI, G., SCHEIDEGGER, D. & LANZAVECCHIA, A. 2001. Migration and function of antigen-primed nonpolarized T lymphocytes in vivo. *J Exp Med,* 193**,** 987-93.

IGLESIAS, M. C., ALMEIDA, J. R., FASTENACKELS, S., VAN BOCKEL, D. J., HASHIMOTO, M., VENTURI, V., GOSTICK, E., URRUTIA, A., WOOLDRIDGE, L., CLEMENT, M., GRAS, S., WILMANN, P. G., AUTRAN, B., MORIS, A., ROSSJOHN, J., DAVENPORT, M. P., TAKIGUCHI, M., BRANDER, C., DOUEK, D. C., KELLEHER, A. D., PRICE, D. A. & APPAY, V. 2011. Escape from highly effective public CD8+ T-cell clonotypes by HIV. *Blood,* 118**,** 2138-49.

IGNEY, F. H. & KRAMMER, P. H. 2002. Immune escape of tumors: apoptosis resistance and tumor counterattack. *J Leukoc Biol,* 71**,** 907-20.

IOANNIDES, C. G., FREEDMAN, R. S., PLATSOUCAS, C. D., RASHED, S. & KIM, Y. P. 1991. Cytotoxic T cell clones isolated from ovarian tumor-infiltrating lymphocytes recognize multiple antigenic epitopes on autologous tumor cells. *J Immunol,* 146**,** 1700-7.

IRVING, M., ZOETE, V., HEBEISEN, M., SCHMID, D., BAUMGARTNER, P., GUILLAUME, P., ROMERO, P., SPEISER, D., LUESCHER, I., RUFER, N. & MICHIELIN, O. 2012. Interplay between T cell receptor binding kinetics and the level of cognate peptide presented by major histocompatibility complexes governs CD8+ T cell responsiveness. *J Biol Chem,* 287**,** 23068-78.

ITOH, Y., HEMMER, B., MARTIN, R. & GERMAIN, R. N. 1999. Serial TCR engagement and down-modulation by peptide:MHC molecule ligands: relationship to the quality of individual TCR signaling events. *J Immunol,* 162**,** 2073-80.

JACOB, J. & BALTIMORE, D. 1999. Modelling T-cell memory by genetic marking of memory T cells in vivo. *Nature,* 399**,** 593-7.

JAGER, E., CHEN, Y. T., DRIJFHOUT, J. W., KARBACH, J., RINGHOFFER, M., JAGER, D., ARAND, M., WADA, H., NOGUCHI, Y., STOCKERT, E., OLD, L. J. & KNUTH, A. 1998. Simultaneous humoral and cellular immune response against cancer-testis antigen NY-ESO-1: definition of human histocompatibility leukocyte antigen (HLA)-A2-binding peptide epitopes. *J Exp Med,* 187**,** 265-70.

JAKOWLEW, S. B. 2006. Transforming growth factor-beta in cancer and metastasis. *Cancer Metastasis Rev,* 25**,** 435-57.

JANES, P. W., LEY, S. C., MAGEE, A. I. & KABOURIDIS, P. S. 2000. The role of lipid rafts in T cell antigen receptor (TCR) signalling. *Semin Immunol,* 12**,** 23-34.

JANEWAY CA JR, T. P., WALPORT M, ET AL. 2001. *The Immune System in Health and Disease*. , New York, Garland Science.

JANEWAY, C. A., JR. 1992. The T cell receptor as a multicomponent signalling machine: CD4/CD8 coreceptors and CD45 in T cell activation. *Annu Rev Immunol,* 10**,** 645-74.

JEROME, K. R., BARND, D. L., BENDT, K. M., BOYER, C. M., TAYLOR-PAPADIMITRIOU, J., MCKENZIE, I. F., BAST, R. C., JR. & FINN, O. J. 1991. Cytotoxic T-lymphocytes derived from patients with breast adenocarcinoma

recognize an epitope present on the protein core of a mucin molecule preferentially expressed by malignant cells. *Cancer Res,* 51**,** 2908-16.

JIANG, N., HUANG, J., EDWARDS, L. J., LIU, B., ZHANG, Y., BEAL, C. D., EVAVOLD, B. D. & ZHU, C. 2011. Two-stage cooperative T cell receptor-peptide major histocompatibility complex-CD8 trimolecular interactions amplify antigen discrimination. *Immunity,* 34**,** 13-23.

JIN, Y. X., JEON, Y., LEE, S. H., KWON, M. S., KIM, T., CUI, X. S., HYUN, S. H. & KIM, N. H. 2014. Production of pigs expressing a transgene under the control of a tetracycline-inducible system. *PLoS One,* 9**,** e86146.

JOHNSON, H., SCORRANO, L., KORSMEYER, S. J. & LEY, T. J. 2003. Cell death induced by granzyme C. *Blood,* 101**,** 3093-101.

JOLY, E., MUCKE, L. & OLDSTONE, M. B. 1991. Viral persistence in neurons explained by lack of major histocompatibility class I expression. *Science,* 253**,** 1283-5.

JONSSON, P., SOUTHCOMBE, J. H., SANTOS, A. M., HUO, J., FERNANDES, R. A., MCCOLL, J., LEVER, M., EVANS, E. J., HUDSON, A., CHANG, V. T., HANKE, T., GODKIN, A., DUNNE, P. D., HORROCKS, M. H., PALAYRET, M., SCREATON, G. R., PETERSEN, J., ROSSJOHN, J., FUGGER, L., DUSHEK, O., XU, X. N., DAVIS, S. J. & KLENERMAN, D. 2016. Remarkably low affinity of CD4/peptide-major histocompatibility complex class II protein interactions. *Proc Natl Acad Sci U S A,* 113**,** 5682-7.

JUNE, C. H. 2007. Adoptive T cell therapy for cancer in the clinic. *J Clin Invest,* 117**,** 1466-76.

JUNEJA, V. R., MCGUIRE, K. A., MANGUSO, R. T., LAFLEUR, M. W., COLLINS, N., HAINING, W. N., FREEMAN, G. J. & SHARPE, A. H. 2017. PD-L1 on tumor cells is sufficient for immune evasion in immunogenic tumors and inhibits CD8 T cell cytotoxicity. *J Exp Med,* 214**,** 895-904.

KAECH, S. M., WHERRY, E. J. & AHMED, R. 2002. Effector and memory T-cell differentiation: implications for vaccine development. *Nat Rev Immunol,* 2**,** 251-62.

KAHLER, K. C., HASSEL, J. C., HEINZERLING, L., LOQUAI, C., MOSSNER, R., UGUREL, S., ZIMMER, L., GUTZMER, R. & CUTANEOUS SIDE EFFECTS" COMMITTEE OF THE WORK GROUP DERMATOLOGICAL, O. 2016. Management of side effects of immune checkpoint blockade by anti-CTLA-4 and anti-PD-1 antibodies in metastatic melanoma. *J Dtsch Dermatol Ges,* 14**,** 662-81.

KAO, C., DANIELS, M. A. & JAMESON, S. C. 2005. Loss of CD8 and TCR binding to Class I MHC ligands following T cell activation. *Int Immunol,* 17**,** 1607-17.

KAPLAN, D. H., SHANKARAN, V., DIGHE, A. S., STOCKERT, E., AGUET, M., OLD, L. J. & SCHREIBER, R. D. 1998. Demonstration of an interferon gamma-dependent tumor surveillance system in immunocompetent mice. *Proc Natl Acad Sci U S A,* 95**,** 7556-61.

KAPLAN, M. H. 2013. Th9 cells: differentiation and disease. *Immunol Rev,* 252**,** 104-15.

KAPPES, D. J. 2007a. CD4 and CD8: Hogging All the Lck. *Immunity,* 27**,** 691-693.

KAPPES, D. J. 2007b. CD4 and CD8: hogging all the Lck. *Immunity,* 27**,** 691-3.

KATAOKA, T., SCHROTER, M., HAHNE, M., SCHNEIDER, P., IRMLER, M., THOME, M., FROELICH, C. J. & TSCHOPP, J. 1998. FLIP prevents apoptosis induced by death receptors but not by perforin/granzyme B, chemotherapeutic drugs, and gamma irradiation. *J Immunol,* 161**,** 3936-42.

KAWAKAMI, Y., ELIYAHU, S., SAKAGUCHI, K., ROBBINS, P. F., RIVOLTINI, L., YANNELLI, J. R., APPELLA, E. & ROSENBERG, S. A. 1994. Identification of the immunodominant peptides of the MART-1 human melanoma antigen recognized by the majority of HLA-A2-restricted tumor infiltrating lymphocytes. *J Exp Med,* 180**,** 347-52.

KELLY, J. M., WATERHOUSE, N. J., CRETNEY, E., BROWNE, K. A., ELLIS, S., TRAPANI, J. A. & SMYTH, M. J. 2004. Granzyme M mediates a novel form of perforin-dependent cell death. *The Journal of biological chemistry,* 279**,** 22236-42.

KERN, P., HUSSEY, R. E., SPOERL, R., REINHERZ, E. L. & CHANG, H. C. 1999. Expression, purification, and functional analysis of murine ectodomain fragments of CD8alphaalpha and CD8alphabeta dimers. *J Biol Chem,* 274**,** 27237-43.

KERN, P. S., TENG, M. K., SMOLYAR, A., LIU, J. H., LIU, J., HUSSEY, R. E., SPOERL, R., CHANG, H. C., REINHERZ, E. L. & WANG, J. H. 1998. Structural basis of CD8 coreceptor function revealed by crystallographic analysis of a murine CD8alphaalpha ectodomain fragment in complex with H-2Kb. *Immunity,* 9**,** 519-30.

KERR, J. F., WYLLIE, A. H. & CURRIE, A. R. 1972. Apoptosis: a basic biological phenomenon with wide-ranging implications in tissue kinetics. *Br J Cancer,* 26**,** 239-57.

KESSLER, J. H., KHAN, S., SEIFERT, U., LE GALL, S., CHOW, K. M., PASCHEN, A., BRES-VLOEMANS, S. A., DE RU, A., VAN MONTFOORT, N., FRANKEN, K. L., BENCKHUIJSEN, W. E., BROOKS, J. M., VAN HALL, T., RAY, K., MULDER, A., DOXIADIS, II, VAN SWIETEN, P. F., OVERKLEEFT, H. S., PRAT, A., TOMKINSON, B., NEEFJES, J., KLOETZEL, P. M., RODGERS, D. W., HERSH, L. B., DRIJFHOUT, J. W., VAN VEELEN, P. A., OSSENDORP, F. & MELIEF, C. J. 2011. Antigen processing by nardilysin and thimet oligopeptidase generates cytotoxic T cell epitopes. *Nat Immunol,* 12**,** 45-53.

KHAMMARI, A., LABARRIERE, N., VIGNARD, V., NGUYEN, J. M., PANDOLFINO, M. C., KNOL, A. C., QUEREUX, G., SAIAGH, S., BROCARD, A., JOTEREAU, F. & DRENO, B. 2009. Treatment of metastatic melanoma with autologous Melan-A/MART-1-specific cytotoxic T lymphocyte clones. *J Invest Dermatol,* 129**,** 2835-42.

KIENZLE, N., BAZ, A. & KELSO, A. 2004. Profiling the CD8low phenotype, an alternative career choice for CD8 T cells during primary differentiation. *Immunol Cell Biol,* 82**,** 75-83.

KIENZLE, N., BUTTIGIEG, K., GROVES, P., KAWULA, T. & KELSO, A. 2002. A clonal culture system demonstrates that IL-4 induces a subpopulation of noncytolytic T cells with low CD8, perforin, and granzyme expression. *J Immunol,* 168**,** 1672-81.

KINNUNEN, R. E., TALLBERG, T., STENBACK, H. & SARNA, S. 1999. Equine sarcoid tumour treated by autogenous tumour vaccine. *Anticancer Res,* 19**,** 3367-74.

KISHIMOTO, H. & SPRENT, J. 1997. Negative selection in the thymus includes semimature T cells. *J Exp Med,* 185**,** 263-71.

KJER-NIELSEN, L., CLEMENTS, C. S., PURCELL, A. W., BROOKS, A. G., WHISSTOCK, J. C., BURROWS, S. R., MCCLUSKEY, J. & ROSSJOHN, J. 2003. A structural basis for the selection of dominant alphabeta T cell receptors in antiviral immunity. *Immunity,* 18**,** 53-64.

KLAUS, G. G. 1978. The generation of memory cells. II. Generation of B memory cells with preformed antigen-antibody complexes. *Immunology,* 34**,** 643-52.

KLEBANOFF, C. A., YAMAMOTO, T. N. & RESTIFO, N. P. 2014. Immunotherapy: Treatment of aggressive lymphomas with anti-CD19 CAR T cells. *Nat Rev Clin Oncol,* 11**,** 685-6.

KLIMATCHEVA, E., ROSENBLATT, J. D. & PLANELLES, V. 1999. Lentiviral vectors and gene therapy. *Frontiers in bioscience : a journal and virtual library,* 4**,** D481-96.

KNALL, C., SMITH, P. A. & POTTER, T. A. 1995. CD8-dependent CTL require co-engagement of CD8 and the TCR for phosphatidylinositol hydrolysis, but CD8-independent CTL do not and can kill in the absence of phosphatidylinositol hydrolysis. *Int Immunol,* 7**,** 995-1004.

KONKEL, J. E., MARUYAMA, T., CARPENTER, A. C., XIONG, Y., ZAMARRON, B. F., HALL, B. E., KULKARNI, A. B., ZHANG, P., BOSSELUT, R. & CHEN, W. 2011. Control of the development of CD8alphaalpha+ intestinal intraepithelial lymphocytes by TGF-beta. *Nat Immunol,* 12**,** 312-9.

KONNO, A., OKADA, K., MIZUNO, K., NISHIDA, M., NAGAOKI, S., TOMA, T., UEHARA, T., OHTA, K., KASAHARA, Y., SEKI, H., YACHIE, A. & KOIZUMI, S. 2002. CD8alpha alpha memory effector T cells descend directly from clonally expanded CD8alpha +beta high TCRalpha beta T cells in vivo. *Blood,* 100**,** 4090-7.

KUBICA, A. W. & BREWER, J. D. 2012. Melanoma in immunosuppressed patients. *Mayo Clin Proc,* 87**,** 991-1003.

KVISTBORG, P., SHU, C. J., HEEMSKERK, B., FANKHAUSER, M., THRUE, C. A., TOEBES, M., VAN ROOIJ, N., LINNEMANN, C., VAN BUUREN, M. M., URBANUS, J. H., BELTMAN, J. B., THOR STRATEN, P., LI, Y. F., ROBBINS, P. F., BESSER, M. J., SCHACHTER, J., KENTER, G. G., DUDLEY, M. E., ROSENBERG, S. A., HAANEN, J. B., HADRUP, S. R. & SCHUMACHER, T. N. 2012. TIL therapy broadens the tumor-reactive CD8(+) T cell compartment in melanoma patients. *Oncoimmunology,* 1**,** 409-418.

LA ROCCA, R., TALLERICO, R., TALIB HASSAN, A., DAS, G., LAKSHMIKANTH, T., MATTEUCCI, M., LIBERALE, C., MESURACA, M., SCUMACI, D., GENTILE, F., COJOC, G., PEROZZIELLO, G., AMMENDOLIA, A., GALLO, A., KARRE, K., CUDA, G., CANDELORO, P., DI FABRIZIO, E. & CARBONE, E. 2014. Mechanical stress downregulates MHC class I expression on human cancer cell membrane. *PLoS One,* 9**,** e111758.

LAUGEL, B., COLE, D. K., CLEMENT, M., WOOLDRIDGE, L., PRICE, D. A. & SEWELL, A. K. 2011. The multiple roles of the CD8 coreceptor in T cell biology: opportunities for the selective modulation of self-reactive cytotoxic T cells. *J Leukoc Biol,* 90**,** 1089-99.

LAUGEL, B., PRICE, D. A., MILICIC, A. & SEWELL, A. K. 2007a. CD8 exerts differential effects on the deployment of cytotoxic T lymphocyte effector functions. *Eur J Immunol,* 37**,** 905-13.

LAUGEL, B., VAN DEN BERG, H. A., GOSTICK, E., COLE, D. K., WOOLDRIDGE, L., BOULTER, J., MILICIC, A., PRICE, D. A. & SEWELL, A. K. 2007b. Different T cell receptor affinity thresholds and CD8 coreceptor dependence govern cytotoxic T lymphocyte activation and tetramer binding properties. *J Biol Chem,* 282**,** 23799-810.

LEAHY, D. J. 1995. A structural view of CD4 and CD8. *FASEB J,* 9**,** 17-25.

LEAHY, D. J., AXEL, R. & HENDRICKSON, W. A. 1992. Crystal structure of a soluble form of the human T cell coreceptor CD8 at 2.6 A resolution. *Cell,* 68**,** 1145-62.

LEISHMAN, A. J., NAIDENKO, O. V., ATTINGER, A., KONING, F., LENA, C. J., XIONG, Y., CHANG, H. C., REINHERZ, E., KRONENBERG, M. & CHEROUTRE, H. 2001. T cell responses modulated through interaction between CD8alphaalpha and the nonclassical MHC class I molecule, TL. *Science,* 294**,** 1936-9.

LI, Y., YIN, Y. & MARIUZZA, R. A. 2013. Structural and biophysical insights into the role of CD4 and CD8 in T cell activation. *Front Immunol,* 4**,** 206.

LICHTENFELS, R., RAPPL, G., HOMBACH, A. A., RECKTENWALD, C. V., DRESSLER, S. P., ABKEN, H. & SELIGER, B. 2012. A proteomic view at T cell costimulation. *PLoS One,* 7**,** e32994.

LINETTE, G. P., STADTMAUER, E. A., MAUS, M. V., RAPOPORT, A. P., LEVINE, B. L., EMERY, L., LITZKY, L., BAGG, A., CARRENO, B. M., CIMINO, P. J., BINDER-SCHOLL, G. K., SMETHURST, D. P., GERRY, A. B., PUMPHREY, N. J., BENNETT, A. D., BREWER, J. E., DUKES, J., HARPER, J., TAYTON-MARTIN, H. K., JAKOBSEN, B. K., HASSAN, N. J., KALOS, M. & JUNE, C. H. 2013. Cardiovascular toxicity and titin cross-reactivity of affinity-enhanced T cells in myeloma and melanoma. *Blood,* 122**,** 863-71.

LIPOWSKA-BHALLA, G., GILHAM, D. E., HAWKINS, R. E. & ROTHWELL, D. G. 2012. Targeted immunotherapy of cancer with CAR T cells: achievements and challenges. *Cancer Immunol Immunother,* 61**,** 953-62.

LIU, H., RHODES, M., WIEST, D. L. & VIGNALI, D. A. 2000. On the dynamics of TCR:CD3 complex cell surface expression and downmodulation. *Immunity,* 13**,** 665-75.

LOPEZ, D., BARBER, D. F., VILLADANGOS, J. A. & LOPEZ DE CASTRO, J. A. 1993. Cross-reactive T cell clones from unrelated individuals reveal similarities in peptide presentation between HLA-B27 and HLA-DR2. *J Immunol,* 150**,** 2675-86.

LOWIN, B., PEITSCH, M. C. & TSCHOPP, J. 1995. Perforin and granzymes: crucial effector molecules in cytolytic T lymphocyte and natural killer cell-mediated cytotoxicity. *Curr Top Microbiol Immunol,* 198**,** 1-24.

LUESCHER, I. F., VIVIER, E., LAYER, A., MAHIOU, J., GODEAU, F., MALISSEN, B. & ROMERO, P. 1995. CD8 modulation of T-cell antigen receptor-ligand interactions on living cytotoxic T lymphocytes. *Nature,* 373**,** 353-6.

MACDONALD, W. A., CHEN, Z., GRAS, S., ARCHBOLD, J. K., TYNAN, F. E., CLEMENTS, C. S., BHARADWAJ, M., KJER-NIELSEN, L., SAUNDERS, P. M., WILCE, M. C., CRAWFORD, F., STADINSKY, B., JACKSON, D., BROOKS, A. G., PURCELL, A. W., KAPPLER, J. W., BURROWS, S. R., ROSSJOHN, J. & MCCLUSKEY, J. 2009. T cell allorecognition via molecular mimicry. *Immunity,* 31**,** 897-908.

MACKAY, L. K. & GEBHARDT, T. 2013. Tissue-resident memory T cells: local guards of the thymus. *Eur J Immunol,* 43**,** 2259-62.

MAENAKA, K. & JONES, E. Y. 1999. MHC superfamily structure and the immune system. *Curr Opin Struct Biol,* 9**,** 745-53.

MAHONEY, K. M., FREEMAN, G. J. & MCDERMOTT, D. F. 2015. The Next Immune-Checkpoint Inhibitors: PD-1/PD-L1 Blockade in Melanoma. *Clin Ther,* 37**,** 764-82.

MALDONADO-LOPEZ, R., DE SMEDT, T., PAJAK, B., HEIRMAN, C., THIELEMANS, K., LEO, O., URBAIN, J., MALISZEWSKI, C. R. & MOSER, M. 1999. Role of CD8alpha+ and CD8alpha- dendritic cells in the induction of primary immune responses in vivo. *J Leukoc Biol,* 66**,** 242-6.

MANN, D. L., O'BRIEN, S. J., GILBERT, D. A., REID, Y., POPOVIC, M., READ-CONNOLE, E., GALLO, R. C. & GAZDAR, A. F. 1989. Origin of the HIV-susceptible human CD4+ cell line H9. *AIDS Res Hum Retroviruses,* 5**,** 253-5.

MARINCOLA, F. M., JAFFEE, E. M., HICKLIN, D. J. & FERRONE, S. 2000. Escape of human solid tumors from T-cell recognition: molecular mechanisms and functional significance. *Adv Immunol,* 74**,** 181-273.

MARTINEZ, C. D. A. G. J. 2010. T cells: the usual subsets. *Nature Reviews; Immunology,* 10.

MASON, D. 1998. A very high level of crossreactivity is an essential feature of the T-cell receptor. *Immunol Today,* 19**,** 395-404.

MASSAGUE, J. 2008. TGFbeta in Cancer. *Cell,* 134**,** 215-30.

MASSON, D. & TSCHOPP, J. 1987. A family of serine esterases in lytic granules of cytolytic T lymphocytes. *Cell,* 49**,** 679-85.

MATECHAK, E. O., KILLEEN, N., HEDRICK, S. M. & FOWLKES, B. J. 1996. MHC class II-specific T cells can develop in the CD8 lineage when CD4 is absent. *Immunity,* 4, 337-47.

MATIS, L. A., EZQUERRA A FAU - COLIGAN, J. E. & COLIGAN, J. E. 1988. Expression of two distinct T cell receptor alpha/beta heterodimers by an antigen-specific T cell clone. *J Exp Med,* 168(6), 2379-84.

MATRAI, J., CHUAH, M. K. L. & VANDENDRIESSCHE, T. 2010. Recent advances in lentiviral vector development and applications. *Molecular therapy : the journal of the American Society of Gene Therapy,* 18, 477-90.

MAYOR, P. C., ENG, K. H., SINGEL, K. L., ABRAMS, S. I., ODUNSI, K., MOYSICH, K. B., FULEIHAN, R., GARABEDIAN, E., LUGAR, P., OCHS, H. D., BONILLA, F. A., BUCKLEY, R. H., SULLIVAN, K. E., BALLAS, Z. K., CUNNINGHAM-RUNDLES, C. & SEGAL, B. H. 2017. Cancer in primary immunodeficiency diseases: Cancer incidence in the United States Immune Deficiency Network Registry. *J Allergy Clin Immunol*.

MCHEYZER-WILLIAMS, M. G. & AHMED, R. 1999. B cell memory and the long-lived plasma cell. *Curr Opin Immunol,* 11, 172-9.

MCNICOL, A. M., BENDLE, G., HOLLER, A., MATJEKA, T., DALTON, E., RETTIG, L., ZAMOYSKA, R., UCKERT, W., XUE, S. A. & STAUSS, H. J. 2007. CD8alpha/alpha homodimers fail to function as co-receptor for a CD8-dependent TCR. *Eur J Immunol,* 37, 1634-41.

MEDZHITOV, R. & JANEWAY, C. A., JR. 1998. Innate immune recognition and control of adaptive immune responses. *Semin Immunol,* 10, 351-3.

MELENHORST, J. J., SCHEINBERG, P., CHATTOPADHYAY, P. K., LISSINA, A., GOSTICK, E., COLE, D. K., WOOLDRIDGE, L., VAN DEN BERG, H. A., BORNSTEIN, E., HENSEL, N. F., DOUEK, D. C., ROEDERER, M., SEWELL, A. K., BARRETT, A. J. & PRICE, D. A. 2008. Detection of low avidity CD8(+) T cell populations with coreceptor-enhanced peptide-major histocompatibility complex class I tetramers. *J Immunol Methods,* 338, 31-9.

MESCHER, M. F., CURTSINGER, J. M., AGARWAL, P., CASEY, K. A., GERNER, M., HAMMERBECK, C. D., POPESCU, F. & XIAO, Z. 2006. Signals required for programming effector and memory development by CD8+ T cells. *Immunol Rev,* 211, 81-92.

MEUER, S. C., HUSSEY, R. E., HODGDON, J. C., HERCEND, T., SCHLOSSMAN, S. F. & REINHERZ, E. L. 1982. Surface structures involved in target recognition by human cytotoxic T lymphocytes. *Science,* 218, 471-3.

MICELI, M. C. & PARNES, J. R. 1991. The roles of CD4 and CD8 in T cell activation. *Semin Immunol,* 3, 133-41.

MICELI, M. C. & PARNES, J. R. 1993. Role of CD4 and CD8 in T cell activation and differentiation. *Adv Immunol,* 53, 59-122.

MICELI, M. C., VON HOEGEN, P. & PARNES, J. R. 1991. Adhesion versus coreceptor function of CD4 and CD8: role of the cytoplasmic tail in coreceptor activity. *Proc Natl Acad Sci U S A,* 88, 2623-7.

MITCHELL, D. M., RAVKOV, E. V. & WILLIAMS, M. A. 2010. Distinct roles for IL-2 and IL-15 in the differentiation and survival of CD8+ effector and memory T cells. *J Immunol,* 184**,** 6719-30.

MOCELLIN, S. & NITTI, D. 2013. CTLA-4 blockade and the renaissance of cancer immunotherapy. *Biochim Biophys Acta,* 1836**,** 187-96.

MONKS, C. R., FREIBERG, B. A., KUPFER, H., SCIAKY, N. & KUPFER, A. 1998. Three-dimensional segregation of supramolecular activation clusters in T cells. *Nature,* 395**,** 82-6.

MOON, Y. W., HAJJAR, J., HWU, P. & NAING, A. 2015. Targeting the indoleamine 2,3-dioxygenase pathway in cancer. *J Immunother Cancer,* 3**,** 51.

MORGAN, R. A., COUTURE, L., ELROY-STEIN, O., RAGHEB, J., MOSS, B. & ANDERSON, W. F. 1992. Retroviral vectors containing putative internal ribosome entry sites: development of a polycistronic gene transfer system and applications to human gene therapy. *Nucleic Acids Res,* 20**,** 1293-9.

MORGAN, R. A., DUDLEY, M. E., WUNDERLICH, J. R., HUGHES, M. S., YANG, J. C., SHERRY, R. M., ROYAL, R. E., TOPALIAN, S. L., KAMMULA, U. S., RESTIFO, N. P., ZHENG, Z., NAHVI, A., DE VRIES, C. R., ROGERS-FREEZER, L. J., MAVROUKAKIS, S. A. & ROSENBERG, S. A. 2006. Cancer regression in patients after transfer of genetically engineered lymphocytes. *Science,* 314**,** 126-9.

MOSER, M. & LEO, O. 2010. Key concepts in immunology. *Vaccine,* 28 Suppl 3**,** C2-13.

MOSMANN, T. R. & SAD, S. 1996. The expanding universe of T-cell subsets: Th1, Th2 and more. *Immunol Today,* 17**,** 138-46.

MUENST, S., SCHAERLI, A. R., GAO, F., DASTER, S., TRELLA, E., DROESER, R. A., MURARO, M. G., ZAJAC, P., ZANETTI, R., GILLANDERS, W. E., WEBER, W. P. & SOYSAL, S. D. 2014. Expression of programmed death ligand 1 (PD-L1) is associated with poor prognosis in human breast cancer. *Breast Cancer Res Treat,* 146**,** 15-24.

MULLER, C. & TSCHOPP, J. 1994. Resistance of CTL to perforin-mediated lysis. Evidence for a lymphocyte membrane protein interacting with perforin. *J Immunol,* 153**,** 2470-8.

MURPHY, K. M. & STOCKINGER, B. 2010. Effector T cell plasticity: flexibility in the face of changing circumstances. *Nat Immunol,* 11**,** 674-80.

NAIDOO, J., PAGE, D. B., LI, B. T., CONNELL, L. C., SCHINDLER, K., LACOUTURE, M. E., POSTOW, M. A. & WOLCHOK, J. D. 2015. Toxicities of the anti-PD-1 and anti-PD-L1 immune checkpoint antibodies. *Ann Oncol,* 26**,** 2375-91.

NAIDOO, J., PAGE, D. B., LI, B. T., CONNELL, L. C., SCHINDLER, K., LACOUTURE, M. E., POSTOW, M. A. & WOLCHOK, J. D. 2016. Toxicities of the anti-PD-1 and anti-PD-L1 immune checkpoint antibodies. *Ann Oncol,* 27**,** 1362.

NAKAYAMA, K., KAWACHI, Y., TOKITO, S., MINAMI, N., YAMAMOTO, R., IMAI, T., GACHELIN, G. & NAKAUCHI, H. 1992. Recent duplication of the two human CD8 beta-chain genes. *J Immunol,* 148**,** 1919-27.

NEEFJES, J., JONGSMA, M. L., PAUL, P. & BAKKE, O. 2011. Towards a systems understanding of MHC class I and MHC class II antigen presentation. *Nat Rev Immunol,* 11**,** 823-36.

NI, L. & DONG, C. 2017. New checkpoints in cancer immunotherapy. *Immunol Rev,* 276**,** 52-65.

NICOLSON, G. L. 1976. Transmembrane control of the receptors on normal and tumor cells. I. Cytoplasmic influence over surface components. *Biochim Biophys Acta,* 457**,** 57-108.

NICOLSON, G. L. 2014. The Fluid-Mosaic Model of Membrane Structure: still relevant to understanding the structure, function and dynamics of biological membranes after more than 40 years. *Biochim Biophys Acta,* 1838**,** 1451-66.

NIKOLICH-ZUGICH, J., SLIFKA, M. K. & MESSAOUDI, I. 2004. The many important facets of T-cell repertoire diversity. *Nat Rev Immunol,* 4**,** 123-32.

NORMENT, A. M. & LITTMAN, D. R. 1988. A second subunit of CD8 is expressed in human T cells. *EMBO J,* 7**,** 3433-9.

NORMENT, A. M., LONBERG, N., LACY, E. & LITTMAN, D. R. 1989. Alternatively spliced mRNA encodes a secreted form of human CD8 alpha. Characterization of the human CD8 alpha gene. *J Immunol,* 142**,** 3312-9.

NUTTON, V. 2005. The fatal embrace: Galen and the history of ancient medicine. *Science in Context,* 18**,** 111-121.

O'SHANNESSY, D. J., BRIGHAM-BURKE, M. & PECK, K. 1992. Immobilization chemistries suitable for use in the BIAcore surface plasmon resonance detector. *Anal Biochem,* 205**,** 132-6.

O'SHEA, J. J. & PAUL, W. E. 2010. Mechanisms underlying lineage commitment and plasticity of helper CD4+ T cells. *Science,* 327**,** 1098-102.

OBAR, J. J. & LEFRANCOIS, L. 2010. Early events governing memory CD8+ T-cell differentiation. *Int Immunol,* 22**,** 619-25.

OHASHI, P. S., MAK, T. W., VAN DEN ELSEN, P., YANAGI, Y., YOSHIKAI, Y., CALMAN, A. F., TERHORST, C., STOBO, J. D. & WEISS, A. 1985. Reconstitution of an active surface T3/T-cell antigen receptor by DNA transfer. *Nature,* 316**,** 606-9.

OKAMURA, K., OTOTAKE, M., NAKANISHI, T., KUROSAWA, Y. & HASHIMOTO, K. 1997. The most primitive vertebrates with jaws possess highly polymorphic MHC class I genes comparable to those of humans. *Immunity,* 7**,** 777-90.

OLVER, S., APTE, S. H., BAZ, A., KELSO, A. & KIENZLE, N. 2013. Interleukin-4-induced loss of CD8 expression and cytolytic function in effector CD8 T cells persists long term in vivo. *Immunology,* 139**,** 187-96.

OPFERMAN, J. T., OBER, B. T., NARAYANAN, R. & ASHTON-RICKARDT, P. G. 2001. Suicide induced by cytolytic activity controls the differentiation of memory CD8(+) T lymphocytes. *Int Immunol,* 13**,** 411-9.

ORRU, V., STERI, M., SOLE, G., SIDORE, C., VIRDIS, F., DEI, M., LAI, S., ZOLEDZIEWSKA, M., BUSONERO, F., MULAS, A., FLORIS, M., MENTZEN, W. I., URRU, S. A., OLLA, S., MARONGIU, M., PIRAS, M. G., LOBINA, M., MASCHIO, A., PITZALIS, M., URRU, M. F., MARCELLI, M., CUSANO, R., DEIDDA, F., SERRA, V., OPPO, M., PILU, R., REINIER, F., BERUTTI, R., PIREDDU, L., ZARA, I., PORCU, E., KWONG, A., BRENNAN, C., TARRIER, B., LYONS, R., KANG, H. M., UZZAU, S., ATZENI, R., VALENTINI, M., FIRINU, D., LEONI, L., ROTTA, G., NAITZA, S., ANGIUS, A., CONGIA, M., WHALEN, M. B., JONES, C. M., SCHLESSINGER, D., ABECASIS, G. R., FIORILLO, E., SANNA, S. & CUCCA, F. 2013. Genetic variants regulating immune cell levels in health and disease. *Cell,* 155**,** 242-56.

OTTEN, N., VON TSCHARNER, C., LAZARY, S., ANTCZAK, D. F. & GERBER, H. 1993. DNA of bovine papillomavirus type 1 and 2 in equine sarcoids: PCR detection and direct sequencing. *Arch Virol,* 132**,** 121-31.

PAILLARD, F., STERKERS, G. & VAQUERO, C. 1990. Transcriptional and post-transcriptional regulation of TcR, CD4 and CD8 gene expression during activation of normal human T lymphocytes. *EMBO J,* 9**,** 1867-72.

PANDEY, K. N. 2009. Functional roles of short sequence motifs in the endocytosis of membrane receptors. *Front Biosci (Landmark Ed),* 14**,** 5339-60.

PANG, D. J., HAYDAY, A. C. & BIJLMAKERS, M. J. 2007. CD8 Raft localization is induced by its assembly into CD8alpha beta heterodimers, Not CD8alpha alpha homodimers. *J Biol Chem,* 282**,** 13884-94.

PARDIGON, N., BERCOVICI, N., CALBO, S., SANTOS-LIMA, E. C., LIBLAU, R., KOURILSKY, P. & ABASTADO, J. P. 1998. Role of co-stimulation in CD8+ T cell activation. *Int Immunol,* 10**,** 619-30.

PARK, H., LI, Z., YANG, X. O., CHANG, S. H., NURIEVA, R., WANG, Y. H., WANG, Y., HOOD, L., ZHU, Z., TIAN, Q. & DONG, C. 2005. A distinct lineage of CD4 T cells regulates tissue inflammation by producing interleukin 17. *Nat Immunol,* 6**,** 1133-41.

PARK, J. H., ADORO, S., LUCAS, P. J., SARAFOVA, S. D., ALAG, A. S., DOAN, L. L., ERMAN, B., LIU, X., ELLMEIER, W., BOSSELUT, R., FEIGENBAUM, L. & SINGER, A. 2007. 'Coreceptor tuning': cytokine signals transcriptionally tailor CD8 coreceptor expression to the self-specificity of the TCR. *Nat Immunol,* 8**,** 1049-59.

PARKER, B. S., RAUTELA, J. & HERTZOG, P. J. 2016. Antitumour actions of interferons: implications for cancer therapy. *Nat Rev Cancer,* 16**,** 131-44.

PARMIANI, G., CASTELLI, C., DALERBA, P., MORTARINI, R., RIVOLTINI, L., MARINCOLA, F. M. & ANICHINI, A. 2002. Cancer immunotherapy with peptide-based vaccines: what have we achieved? Where are we going? *J Natl Cancer Inst,* 94**,** 805-18.

PEARCE, E. L., SHEDLOCK, D. J. & SHEN, H. 2004. Functional characterization of MHC class II-restricted CD8+CD4- and CD8-CD4- T cell responses to infection in CD4-/- mice. *J Immunol,* 173**,** 2494-9.

PELLICCI, D. G., ULDRICH, A. P., LE NOURS, J., ROSS, F., CHABROL, E., ECKLE, S. B., DE BOER, R., LIM, R. T., MCPHERSON, K., BESRA, G., HOWELL, A. R., MORETTA, L., MCCLUSKEY, J., HEEMSKERK, M. H., GRAS, S., ROSSJOHN, J. & GODFREY, D. I. 2014. The molecular bases of delta/alphabeta T cell-mediated antigen recognition. *J Exp Med,* 211**,** 2599-615.

PENN, I. & STARZL, T. E. 1973. Immunosuppression and cancer. *Transplant Proc,* 5**,** 943-7.

PENNOCK, N. D., WHITE, J. T., CROSS, E. W., CHENEY, E. E., TAMBURINI, B. A. & KEDL, R. M. 2013. T cell responses: naive to memory and everything in between. *Adv Physiol Educ,* 37**,** 273-83.

PERICA, K., VARELA, J. C., OELKE, M. & SCHNECK, J. 2015. Adoptive T cell immunotherapy for cancer. *Rambam Maimonides Med J,* 6**,** e0004.

PETERS, P. J., BORST, J., OORSCHOT, V., FUKUDA, M., KRAHENBUHL, O., TSCHOPP, J., SLOT, J. W. & GEUZE, H. J. 1991. Cytotoxic T lymphocyte granules are secretory lysosomes, containing both perforin and granzymes. *J Exp Med,* 173**,** 1099-109.

PITCHER, C., HONING, S., FINGERHUT, A., BOWERS, K. & MARSH, M. 1999. Cluster of differentiation antigen 4 (CD4) endocytosis and adaptor complex binding require activation of the CD4 endocytosis signal by serine phosphorylation. *Mol Biol Cell,* 10**,** 677-91.

PODACK, E. R., YOUNG, J. D. & COHN, Z. A. 1985. Isolation and biochemical and functional characterization of perforin 1 from cytolytic T-cell granules. *Proc Natl Acad Sci U S A,* 82**,** 8629-33.

POPMIHAJLOV, Z. & SMITH, K. A. 2008. Negative feedback regulation of T cells via interleukin-2 and FOXP3 reciprocity. *PLoS One,* 3**,** e1581.

PRAVEEN, P. V. K., YANEVA, R., KALBACHER, H. & SPRINGER, S. 2010. Tapasin edits peptides on MHC class I molecules by accelerating peptide exchange. *European Journal of Immunology,* 40**,** 214-224.

PURBHOO, M. A., BOULTER, J. M., PRICE, D. A., VUIDEPOT, A. L., HOURIGAN, C. S., DUNBAR, P. R., OLSON, K., DAWSON, S. J., PHILLIPS, R. E., JAKOBSEN, B. K., BELL, J. I. & SEWELL, A. K. 2001. The human CD8 coreceptor effects cytotoxic T cell activation and antigen sensitivity primarily by mediating complete phosphorylation of the T cell receptor zeta chain. *J Biol Chem,* 276**,** 32786-92.

PURBHOO, M. A., IRVINE, D. J., HUPPA, J. B. & DAVIS, M. M. 2004. T cell killing does not require the formation of a stable mature immunological synapse. *Nat Immunol,* 5**,** 524-30.

PURBHOO, M. A., LI, Y., SUTTON, D. H., BREWER, J. E., GOSTICK, E., BOSSI, G., LAUGEL, B., MOYSEY, R., BASTON, E., LIDDY, N., CAMERON, B., BENNETT, A. D., ASHFIELD, R., MILICIC, A., PRICE, D. A., CLASSON, B. J., SEWELL, A.

K. & JAKOBSEN, B. K. 2007. The HLA A*0201-restricted hTERT(540-548) peptide is not detected on tumor cells by a CTL clone or a high-affinity T-cell receptor. *Mol Cancer Ther,* 6**,** 2081-91.

QASIM, W., ZHAN, H., SAMARASINGHE, S., ADAMS, S., AMROLIA, P., STAFFORD, S., BUTLER, K., RIVAT, C., WRIGHT, G., SOMANA, K., GHORASHIAN, S., PINNER, D., AHSAN, G., GILMOUR, K., LUCCHINI, G., INGLOTT, S., MIFSUD, W., CHIESA, R., PEGGS, K. S., CHAN, L., FARZENEH, F., THRASHER, A. J., VORA, A., PULE, M. & VEYS, P. 2017. Molecular remission of infant B-ALL after infusion of universal TALEN gene-edited CAR T cells. *Sci Transl Med,* 9.

RAMOS, C. A., SAVOLDO, B. & DOTTI, G. 2014. CD19-CAR trials. *Cancer J,* 20**,** 112-8.

RAY, A. & COHN, L. 1999. Th2 cells and GATA-3 in asthma: new insights into the regulation of airway inflammation. *J Clin Invest,* 104**,** 985-93.

RENARD, V., ROMERO, P., VIVIER, E., MALISSEN, B. & LUESCHER, I. F. 1996. CD8 beta increases CD8 coreceptor function and participation in TCR-ligand binding. *J Exp Med,* 184**,** 2439-44.

REZVANI, K. & ROUCE, R. H. 2015. The Application of Natural Killer Cell Immunotherapy for the Treatment of Cancer. *Front Immunol,* 6**,** 578.

RIELLA, L. V., PATERSON, A. M., SHARPE, A. H. & CHANDRAKER, A. 2012. Role of the PD-1 pathway in the immune response. *Am J Transplant,* 12**,** 2575-87.

RILEY, J. L. 2009. PD-1 signaling in primary T cells. *Immunol Rev,* 229**,** 114-25.

ROBBINS, P. F., EL-GAMIL, M., LI, Y. F., KAWAKAMI, Y., LOFTUS, D., APPELLA, E. & ROSENBERG, S. A. 1996. A mutated beta-catenin gene encodes a melanoma-specific antigen recognized by tumor infiltrating lymphocytes. *J Exp Med,* 183**,** 1185-92.

ROBBINS, P. F., LI, Y. F., EL-GAMIL, M., ZHAO, Y., WARGO, J. A., ZHENG, Z., XU, H., MORGAN, R. A., FELDMAN, S. A., JOHNSON, L. A., BENNETT, A. D., DUNN, S. M., MAHON, T. M., JAKOBSEN, B. K. & ROSENBERG, S. A. 2008. Single and dual amino acid substitutions in TCR CDRs can enhance antigen-specific T cell functions. *J Immunol,* 180**,** 6116-31.

ROBERT, V., TRIFFAUX, E., SAVIGNAC, M. & PELLETIER, L. 2011. Calcium signalling in T-lymphocytes. *Biochimie,* 93**,** 2087-94.

ROBINSON, J., HALLIWELL, J. A., HAYHURST, J. D., FLICEK, P., PARHAM, P. & MARSH, S. G. 2015. The IPD and IMGT/HLA database: allele variant databases. *Nucleic Acids Res,* 43**,** D423-31.

ROCK, K. L., GRAMM, C., ROTHSTEIN, L., CLARK, K., STEIN, R., DICK, L., HWANG, D. & GOLDBERG, A. L. 1994. Inhibitors of the proteasome block the degradation of most cell proteins and the generation of peptides presented on MHC class I molecules. *Cell,* 78**,** 761-771.

ROSENBERG, S. A. & DUDLEY, M. E. 2009. Adoptive cell therapy for the treatment of patients with metastatic melanoma. *Current opinion in immunology,* 21**,** 233-40.

ROSENBERG, S. A., PACKARD, B. S., AEBERSOLD, P. M., SOLOMON, D., TOPALIAN, S. L., TOY, S. T., SIMON, P., LOTZE, M. T., YANG, J. C., SEIPP, C. A. & ET AL. 1988. Use of tumor-infiltrating lymphocytes and interleukin-2 in the immunotherapy of patients with metastatic melanoma. A preliminary report. *N Engl J Med,* 319**,** 1676-80.

ROSENBERG, S. A., RESTIFO, N. P., YANG, J. C., MORGAN, R. A. & DUDLEY, M. E. 2008. Adoptive cell transfer: a clinical path to effective cancer immunotherapy. *Nat Rev Cancer,* 8**,** 299-308.

ROSENBERG, S. A., SPIESS, P. & LAFRENIERE, R. 1986. A new approach to the adoptive immunotherapy of cancer with tumor-infiltrating lymphocytes. *Science,* 233**,** 1318-21.

RUDOLPH, M. G., STANFIELD, R. L. & WILSON, I. A. 2006. How TCRs bind MHCs, peptides, and coreceptors. *Annual review of immunology,* 24**,** 419-66.

RYBAKIN, V., CLAMME, J. P., AMPUDIA, J., YACHI, P. P. & GASCOIGNE, N. R. 2011. CD8alphaalpha and -alphabeta isotypes are equally recruited to the immunological synapse through their ability to bind to MHC class I. *EMBO Rep,* 12**,** 1251-6.

SAD, S. & MOSMANN, T. R. 1994. Single IL-2-secreting precursor CD4 T cell can develop into either Th1 or Th2 cytokine secretion phenotype. *J Immunol,* 153**,** 3514-22.

SAITO, T. & YAMASAKI, S. 2003. Negative feedback of T cell activation through inhibitory adapters and costimulatory receptors. *Immunol Rev,* 192**,** 143-60.

SALMAGGI, A., GELATI, M., POLLO, B., FRIGERIO, S., EOLI, M., SILVANI, A., BROGGI, G., CIUSANI, E., CROCI, D., BOIARDI, A. & DE ROSSI, M. 2004. CXCL12 in malignant glial tumors: a possible role in angiogenesis and cross-talk between endothelial and tumoral cells. *J Neurooncol,* 67**,** 305-17.

SAN JOSE, E., BORROTO, A., NIEDERGANG, F., ALCOVER, A. & ALARCON, B. 2000. Triggering the TCR complex causes the downregulation of nonengaged receptors by a signal transduction-dependent mechanism. *Immunity,* 12**,** 161-70.

SANDERS, S. K., FOX, R. O. & KAVATHAS, P. 1991. Mutations in CD8 that affect interactions with HLA class I and monoclonal anti-CD8 antibodies. *J Exp Med,* 174**,** 371-9.

SATO, K., OHTSUKA, K., WATANABE, H., ASAKURA, H. & ABO, T. 1993. Detailed characterization of gamma delta T cells within the organs in mice: classification into three groups. *Immunology,* 80**,** 380-7.

SAVILL, J., FADOK, V., HENSON, P. & HASLETT, C. 1993. Phagocyte recognition of cells undergoing apoptosis. *Immunol Today,* 14**,** 131-6.

SCHAMBACH, A., BOHNE, J., BAUM, C., HERMANN, F. G., EGERER, L., VON LAER, D. & GIROGLOU, T. 2006. Woodchuck hepatitis virus post-transcriptional regulatory element deleted from X protein and promoter sequences enhances retroviral vector titer and expression. *Gene therapy,* 13**,** 641-5.

SCHATZ, D. G. & JI, Y. 2011. Recombination centres and the orchestration of V(D)J recombination. *Nat Rev Immunol,* 11, 251-63.

SCHLUNS, K. S. & LEFRANCOIS, L. 2003. Cytokine control of memory T-cell development and survival. *Nat Rev Immunol,* 3, 269-79.

SCHNEIDER, U., SCHWENK, H. U. & BORNKAMM, G. 1977. Characterization of EBV-genome negative "null" and "T" cell lines derived from children with acute lymphoblastic leukemia and leukemic transformed non-Hodgkin lymphoma. *Int J Cancer,* 19, 621-6.

SCHUBERT, U., ANTON, L. C., GIBBS, J., NORBURY, C. C., YEWDELL, J. W. & BENNINK, J. R. 2000. Rapid degradation of a large fraction of newly synthesized proteins by proteasomes. *Nature,* 404, 770-4.

SCHULZ, T. F. 2009. Cancer and viral infections in immunocompromised individuals. *Int J Cancer,* 125, 1755-63.

SCHUMACHER, T. N. & SCHREIBER, R. D. 2015. Neoantigens in cancer immunotherapy. *Science,* 348, 69-74.

SCHWARZ, T. F., SPACZYNSKI, M., SCHNEIDER, A., WYSOCKI, J., GALAJ, A., PERONA, P., PONCELET, S., ZAHAF, T., HARDT, K., DESCAMPS, D., DUBIN, G. & WOMEN, H. P. V. S. G. F. A. 2009. Immunogenicity and tolerability of an HPV-16/18 AS04-adjuvanted prophylactic cervical cancer vaccine in women aged 15-55 years. *Vaccine,* 27, 581-7.

SELIGER, B. 2005. Strategies of tumor immune evasion. *BioDrugs,* 19, 347-54.

SEWELL, A. K. 2012. Why must T cells be cross-reactive? *Nat Rev Immunol,* 12, 669-77.

SHANKARAN, V., IKEDA, H., BRUCE, A. T., WHITE, J. M., SWANSON, P. E., OLD, L. J. & SCHREIBER, R. D. 2001. IFNgamma and lymphocytes prevent primary tumour development and shape tumour immunogenicity. *Nature,* 410, 1107-11.

SHAPIRO-SHELEF, M. & CALAME, K. 2005. Regulation of plasma-cell development. *Nat Rev Immunol,* 5, 230-42.

SHARMA, P., HU-LIESKOVAN, S., WARGO, J. A. & RIBAS, A. 2017. Primary, Adaptive, and Acquired Resistance to Cancer Immunotherapy. *Cell,* 168, 707-723.

SHARPE, A. H. & FREEMAN, G. J. 2002. The B7-CD28 superfamily. *Nat Rev Immunol,* 2, 116-26.

SHATZ, C. J. 2009. MHC class I: an unexpected role in neuronal plasticity. *Neuron,* 64, 40-5.

SHERIDAN, B. S. & LEFRANCOIS, L. 2010. Intraepithelial lymphocytes: to serve and protect. *Curr Gastroenterol Rep,* 12, 513-21.

SHERIDAN, B. S. & LEFRANCOIS, L. 2011. Regional and mucosal memory T cells. *Nat Immunol,* 12, 485-91.

SHORE, D. A., ISSAFRAS, H., LANDAIS, E., TEYTON, L. & WILSON, I. A. 2008. The crystal structure of CD8 in complex with YTS156.7.7 Fab and interaction with other CD8 antibodies define the binding mode of CD8 alphabeta to MHC class I. *J Mol Biol,* 384**,** 1190-202.

SHRESTHA, D., JENEI, A., NAGY, P., VEREB, G. & SZOLLOSI, J. 2015. Understanding FRET as a research tool for cellular studies. *Int J Mol Sci,* 16**,** 6718-56.

SINGER, S. J. & NICOLSON, G. L. 1972. The fluid mosaic model of the structure of cell membranes. *Science,* 175**,** 720-31.

SMEETON, P. S. N. C. 2007. *Applied Nonparametric Statistical Methods,* Chapman & Hall/CRC London.

SMITH-GARVIN, J. E., KORETZKY, G. A. & JORDAN, M. S. 2009. T cell activation. *Annu Rev Immunol,* 27**,** 591-619.

SMYTH, M. J., THIA, K. Y., STREET, S. E., MACGREGOR, D., GODFREY, D. I. & TRAPANI, J. A. 2000. Perforin-mediated cytotoxicity is critical for surveillance of spontaneous lymphoma. *J Exp Med,* 192**,** 755-60.

SORIANO, C., MUKARO, V., HODGE, G., AHERN, J., HOLMES, M., JERSMANN, H., MOFFAT, D., MEREDITH, D., JURISEVIC, C., REYNOLDS, P. N. & HODGE, S. 2012. Increased proteinase inhibitor-9 (PI-9) and reduced granzyme B in lung cancer: mechanism for immune evasion? *Lung Cancer,* 77**,** 38-45.

SPRENT, J. & SURH, C. D. 2011. Normal T cell homeostasis: the conversion of naive cells into memory-phenotype cells. *Nat Immunol,* 12**,** 478-84.

STEMBERGER, C., HUSTER, K. M., KOFFLER, M., ANDERL, F., SCHIEMANN, M., WAGNER, H. & BUSCH, D. H. 2007. A single naive CD8+ T cell precursor can develop into diverse effector and memory subsets. *Immunity,* 27**,** 985-97.

STIEGER, K., BELBELLAA, B., LE GUINER, C., MOULLIER, P. & ROLLING, F. 2009. In vivo gene regulation using tetracycline-regulatable systems. *Adv Drug Deliv Rev,* 61**,** 527-41.

STORKUS, W. J., HOWELL, D. N., SALTER, R. D., DAWSON, J. R. & CRESSWELL, P. 1987. NK susceptibility varies inversely with target cell class I HLA antigen expression. *J Immunol,* 138**,** 1657-9.

STRAATHOF, K. C., SPENCER, D. M., SUTTON, R. E. & ROONEY, C. M. 2003. Suicide genes as safety switches in T lymphocytes. *Cytotherapy,* 5**,** 227-30.

STREET, S. E., TRAPANI, J. A., MACGREGOR, D. & SMYTH, M. J. 2002. Suppression of lymphoma and epithelial malignancies effected by interferon gamma. *J Exp Med,* 196**,** 129-34.

SUN, J. & KAVATHAS, P. B. 1997. Comparison of the roles of CD8 alpha alpha and CD8 alpha beta in interaction with MHC class I. *J Immunol,* 159**,** 6077-82.

SUN, J., LEAHY, D. J. & KAVATHAS, P. B. 1995. Interaction between CD8 and major histocompatibility complex (MHC) class I mediated by multiple contact surfaces that include the alpha 2 and alpha 3 domains of MHC class I. *J Exp Med,* 182**,** 1275-80.

SUNDER-PLASSMANN, R., LIALIOS, F., MADSEN, M., KOYASU, S. & REINHERZ, E. L. 1997. Functional analysis of immunoreceptor tyrosine-based activation motif (ITAM)-mediated signal transduction: the two YxxL segments within a single CD3zeta-ITAM are functionally distinct. *Eur J Immunol,* 27**,** 2001-9.

SUNSHINE, J. & TAUBE, J. M. 2015. PD-1/PD-L1 inhibitors. *Curr Opin Pharmacol,* 23**,** 32-8.

SURH, C. D. & SPRENT, J. 2008. Homeostasis of naive and memory T cells. *Immunity,* 29**,** 848-62.

SUSSMAN, J. J., MERCEP, M., SAITO, T., GERMAIN, R. N., BONVINI, E. & ASHWELL, J. D. 1988. Dissociation of phosphoinositide hydrolysis and Ca2+ fluxes from the biological responses of a T-cell hybridoma. *Nature,* 334**,** 625-8.

SWANN, J. B. & SMYTH, M. J. 2007. Immune surveillance of tumors. *J Clin Invest,* 117**,** 1137-46.

SZOMOLAY, B. & VAN DEN BERG, H. A. 2014. Modulation of T-cell receptor functional sensitivity via the opposing actions of protein tyrosine kinases and phosphatases: a mathematical model. *Integr Biol (Camb),* 6**,** 1183-95.

SZOMOLAY, B., WILLIAMS, T., WOOLDRIDGE, L. & VAN DEN BERG, H. A. 2013. Co-Receptor CD8-Mediated Modulation of T-Cell Receptor Functional Sensitivity and Epitope Recognition Degeneracy. *Front Immunol,* 4**,** 329.

SZYMCZAK, A. L., WORKMAN, C. J., WANG, Y., VIGNALI, K. M., DILIOGLOU, S., VANIN, E. F. & VIGNALI, D. A. A. 2004. Correction of multi-gene deficiency in vivo using a single 'self-cleaving' 2A peptide-based retroviral vector. *Nature biotechnology,* 22**,** 589-94.

TAKADA, K. & JAMESON, S. C. 2009a. Naive T cell homeostasis: from awareness of space to a sense of place. *Nat Rev Immunol,* 9**,** 823-32.

TAKADA, K. & JAMESON, S. C. 2009b. Self-class I MHC molecules support survival of naive CD8 T cells, but depress their functional sensitivity through regulation of CD8 expression levels. *J Exp Med,* 206**,** 2253-69.

TAN, M. P., GERRY, A. B., BREWER, J. E., MELCHIORI, L., BRIDGEMAN, J. S., BENNETT, A. D., PUMPHREY, N. J., JAKOBSEN, B. K., PRICE, D. A., LADELL, K. & SEWELL, A. K. 2015. T cell receptor binding affinity governs the functional profile of cancer-specific CD8+ T cells. *Clin Exp Immunol,* 180**,** 255-70.

TERTIPIS, N., HAEGGBLOM, L., GRUN, N., NORDFORS, C., NASMAN, A., DALIANIS, T. & RAMQVIST, T. 2015. Reduced Expression of the Antigen Processing Machinery Components TAP2, LMP2, and LMP7 in Tonsillar and Base of Tongue Cancer and Implications for Clinical Outcome. *Transl Oncol,* 8**,** 10-7.

THAKRAL, D., COMAN, M. M., BANDYOPADHYAY, A., MARTIN, S., RILEY, J. L. & KAVATHAS, P. B. 2013. The human CD8beta M-4 isoform dominant in effector memory T cells has distinct cytoplasmic motifs that confer unique properties. *PLoS One,* 8**,** e59374.

THAKRAL, D., DOBBINS, J., DEVINE, L. & KAVATHAS, P. B. 2008. Differential expression of the human CD8beta splice variants and regulation of the M-2 isoform by ubiquitination. *J Immunol,* 180**,** 7431-42.

TOPALIAN, S. L., MUUL, L. M., SOLOMON, D. & ROSENBERG, S. A. 1987. Expansion of human tumor infiltrating lymphocytes for use in immunotherapy trials. *J Immunol Methods,* 102**,** 127-41.

TOPFER, K., KEMPE, S., MULLER, N., SCHMITZ, M., BACHMANN, M., CARTELLIERI, M., SCHACKERT, G. & TEMME, A. 2011. Tumor evasion from T cell surveillance. *J Biomed Biotechnol,* 2011**,** 918471.

TRAPANI, J. A. 2012. Granzymes, cytotoxic granules and cell death: the early work of Dr. Jurg Tschopp. *Cell Death Differ,* 19**,** 21-7.

TRAPANI, J. A. & SMYTH, M. J. 2002. Functional significance of the perforin/granzyme cell death pathway. *Nat Rev Immunol,* 2**,** 735-47.

TRICKETT, A. & KWAN, Y. L. 2003. T cell stimulation and expansion using anti-CD3/CD28 beads. *J Immunol Methods,* 275**,** 251-5.

TRIFARI, S., PIPKIN, M. E., BANDUKWALA, H. S., AIJO, T., BASSEIN, J., CHEN, R., MARTINEZ, G. J. & RAO, A. 2013. MicroRNA-directed program of cytotoxic CD8+ T-cell differentiation. *Proc Natl Acad Sci U S A,* 110**,** 18608-13.

TROBRIDGE, P. A., FORBUSH, K. A. & LEVIN, S. D. 2001. Positive and negative selection of thymocytes depends on Lck interaction with the CD4 and CD8 coreceptors. *J Immunol,* 166**,** 809-18.

TYNAN, F. E., BURROWS, S. R., BUCKLE, A. M., CLEMENTS, C. S., BORG, N. A., MILES, J. J., BEDDOE, T., WHISSTOCK, J. C., WILCE, M. C., SILINS, S. L., BURROWS, J. M., KJER-NIELSEN, L., KOSTENKO, L., PURCELL, A. W., MCCLUSKEY, J. & ROSSJOHN, J. 2005. T cell receptor recognition of a 'super-bulged' major histocompatibility complex class I-bound peptide. *Nat Immunol,* 6**,** 1114-22.

ULDRICH, A. P., LE NOURS, J., PELLICCI, D. G., GHERARDIN, N. A., MCPHERSON, K. G., LIM, R. T., PATEL, O., BEDDOE, T., GRAS, S., ROSSJOHN, J. & GODFREY, D. I. 2013. CD1d-lipid antigen recognition by the gammadelta TCR. *Nat Immunol,* 14**,** 1137-45.

UYTTENHOVE, C., PILOTTE, L., THEATE, I., STROOBANT, V., COLAU, D., PARMENTIER, N., BOON, T. & VAN DEN EYNDE, B. J. 2003. Evidence for a tumoral immune resistance mechanism based on tryptophan degradation by indoleamine 2,3-dioxygenase. *Nat Med,* 9**,** 1269-74.

VALITUTTI, S., MULLER, S., CELLA, M., PADOVAN, E. & LANZAVECCHIA, A. 1995. Serial triggering of many T-cell receptors by a few peptide-MHC complexes. *Nature,* 375**,** 148-51.

VALITUTTI, S., MULLER, S., DESSING, M. & LANZAVECCHIA, A. 1996a. Different responses are elicited in cytotoxic T lymphocytes by different levels of T cell receptor occupancy. *J Exp Med,* 183**,** 1917-21.

VALITUTTI, S., MULLER, S., DESSING, M. & LANZAVECCHIA, A. 1996b. Signal extinction and T cell repolarization in T helper cell-antigen-presenting cell conjugates. *Eur J Immunol,* 26**,** 2012-6.

VALITUTTI, S., MULLER, S., SALIO, M. & LANZAVECCHIA, A. 1997. Degradation of T cell receptor (TCR)-CD3-zeta complexes after antigenic stimulation. *J Exp Med,* 185**,** 1859-64.

VAN DEN BERG, H. A., LADELL, K., MINERS, K., LAUGEL, B., LLEWELLYN-LACEY, S., CLEMENT, M., COLE, D. K., GOSTICK, E., WOOLDRIDGE, L., SEWELL, A. K., BRIDGEMAN, J. S. & PRICE, D. A. 2013. Cellular-level versus receptor-level response threshold hierarchies in T-cell activation. *Front Immunol,* 4**,** 250.

VAN DEN BERG, H. A., WOOLDRIDGE, L., LAUGEL, B. & SEWELL, A. K. 2007. Coreceptor CD8-driven modulation of T cell antigen receptor specificity. *J Theor Biol,* 249**,** 395-408.

VAN DER MERWE, P. A. & CORDOBA, S. P. 2011. Late arrival: recruiting coreceptors to the T cell receptor complex. *Immunity,* 34**,** 1-3.

VAN DER MERWE, P. A. & DAVIS, S. J. 2003. Molecular interactions mediating T cell antigen recognition. *Annu Rev Immunol,* 21**,** 659-84.

VAN LAETHEM, F., SARAFOVA, S. D., PARK, J. H., TAI, X., POBEZINSKY, L., GUINTER, T. I., ADORO, S., ADAMS, A., SHARROW, S. O., FEIGENBAUM, L. & SINGER, A. 2007. Deletion of CD4 and CD8 coreceptors permits generation of alphabetaT cells that recognize antigens independently of the MHC. *Immunity,* 27**,** 735-50.

VAN LAETHEM, F., TIKHONOVA, A. N. & SINGER, A. 2012. MHC restriction is imposed on a diverse T cell receptor repertoire by CD4 and CD8 co-receptors during thymic selection. *Trends Immunol,* 33**,** 437-41.

VAN MAELE, B., DE RIJCK, J., DE CLERCQ, E. & DEBYSER, Z. 2003. Impact of the central polypurine tract on the kinetics of human immunodeficiency virus type 1 vector transduction. *Journal of virology,* 77**,** 4685-94.

VAN OERS, N. S., TAO, W., WATTS, J. D., JOHNSON, P., AEBERSOLD, R. & TEH, H. S. 1993. Constitutive tyrosine phosphorylation of the T-cell receptor (TCR) zeta subunit: regulation of TCR-associated protein tyrosine kinase activity by TCR zeta. *Mol Cell Biol,* 13**,** 5771-80.

VAN STIPDONK, M. J., LEMMENS, E. E. & SCHOENBERGER, S. P. 2001. Naive CTLs require a single brief period of antigenic stimulation for clonal expansion and differentiation. *Nat Immunol,* 2**,** 423-9.

VANTOUROUT, P. & HAYDAY, A. 2013. Six-of-the-best: unique contributions of gammadelta T cells to immunology. *Nat Rev Immunol,* 13**,** 88-100.

VEILLETTE, A., BOOKMAN, M. A., HORAK, E. M. & BOLEN, J. B. 1988. The CD4 and CD8 T cell surface antigens are associated with the internal membrane tyrosine-protein kinase p56lck. *Cell,* 55**,** 301-8.

VELLA, L. A., YU, M., FUHRMANN, S. R., EL-AMINE, M., EPPERSON, D. E. & FINN, O. J. 2009. Healthy individuals have T-cell and antibody responses to the

tumor antigen cyclin B1 that when elicited in mice protect from cancer. *Proc Natl Acad Sci U S A,* 106**,** 14010-5.

VEUGELERS, K., MOTYKA, B., GOPING, I. S., SHOSTAK, I., SAWCHUK, T. & BLEACKLEY, R. C. 2006. Granule-mediated killing by granzyme B and perforin requires a mannose 6-phosphate receptor and is augmented by cell surface heparan sulfate. *Mol Biol Cell,* 17**,** 623-33.

VISCHER, T. L., STASTNY, P. & ZIFF, M. 1967. Development of immunological memory during the primary immune response. *Nature,* 213**,** 923-5.

VYAS, J. M., VAN DER VEEN, A. G. & PLOEGH, H. L. 2008. The known unknowns of antigen processing and presentation. *Nat Rev Immunol,* 8**,** 607-18.

WANG, J. H., MEIJERS, R., XIONG, Y., LIU, J. H., SAKIHAMA, T., ZHANG, R., JOACHIMIAK, A. & REINHERZ, E. L. 2001. Crystal structure of the human CD4 N-terminal two-domain fragment complexed to a class II MHC molecule. *Proc Natl Acad Sci U S A,* 98**,** 10799-804.

WANG, Q., LIU, F. & LIU, L. 2017. Prognostic significance of PD-L1 in solid tumor: An updated meta-analysis. *Medicine (Baltimore),* 96**,** e6369.

WANG, Q. & WU, X. 2017. Primary and acquired resistance to PD-1/PD-L1 blockade in cancer treatment. *Int Immunopharmacol,* 46**,** 210-219.

WANG, R., NATARAJAN, K. & MARGULIES, D. H. 2009. Structural basis of the CD8 alpha beta/MHC class I interaction: focused recognition orients CD8 beta to a T cell proximal position. *J Immunol,* 183**,** 2554-64.

WANG, R. F. & WANG, H. Y. 2017. Immune targets and neoantigens for cancer immunotherapy and precision medicine. *Cell Res,* 27**,** 11-37.

WANISCH, K. & YANEZ-MUNOZ, R. J. 2009. Integration-deficient lentiviral vectors: a slow coming of age. *Molecular therapy : the journal of the American Society of Gene Therapy,* 17**,** 1316-32.

WARING, P. & MULLBACHER, A. 1999. Cell death induced by the Fas/Fas ligand pathway and its role in pathology. *Immunology and cell biology,* 77**,** 312-7.

WEISS, A. & STOBO, J. D. 1984. Requirement for the coexpression of T3 and the T cell antigen receptor on a malignant human T cell line. *J Exp Med,* 160**,** 1284-99.

WENCKER, M., TURCHINOVICH, G., DI MARCO BARROS, R., DEBAN, L., JANDKE, A., COPE, A. & HAYDAY, A. C. 2014. Innate-like T cells straddle innate and adaptive immunity by altering antigen-receptor responsiveness. *Nat Immunol,* 15**,** 80-7.

WHITMIRE, J. K. & AHMED, R. 2000. Costimulation in antiviral immunity: differential requirements for CD4(+) and CD8(+) T cell responses. *Curr Opin Immunol,* 12**,** 448-55.

WILLCOX, B. E., GAO, G. F., WYER, J. R., O'CALLAGHAN, C. A., BOULTER, J. M., JONES, E. Y., VAN DER MERWE, P. A., BELL, J. I. & JAKOBSEN, B. K. 1999.

Production of soluble alphabeta T-cell receptor heterodimers suitable for biophysical analysis of ligand binding. *Protein Sci,* 8**,** 2418-23.

WOLCHOK, J. D. & SAENGER, Y. 2008. The mechanism of anti-CTLA-4 activity and the negative regulation of T-cell activation. *Oncologist,* 13 Suppl 4**,** 2-9.

WOOLDRIDGE, L., CLEMENT, M., LISSINA, A., EDWARDS, E. S., LADELL, K., EKERUCHE, J., HEWITT, R. E., LAUGEL, B., GOSTICK, E., COLE, D. K., DEBETS, R., BERREVOETS, C., MILES, J. J., BURROWS, S. R., PRICE, D. A. & SEWELL, A. K. 2010a. MHC class I molecules with Superenhanced CD8 binding properties bypass the requirement for cognate TCR recognition and nonspecifically activate CTLs. *J Immunol,* 184**,** 3357-66.

WOOLDRIDGE, L., EKERUCHE-MAKINDE, J., VAN DEN BERG, H. A., SKOWERA, A., MILES, J. J., TAN, M. P., DOLTON, G., CLEMENT, M., LLEWELLYN-LACEY, S., PRICE, D. A., PEAKMAN, M. & SEWELL, A. K. 2012. A single autoimmune T cell receptor recognizes more than a million different peptides. *J Biol Chem,* 287**,** 1168-77.

WOOLDRIDGE, L., HUTCHINSON, S. L., CHOI, E. M., LISSINA, A., JONES, E., MIRZA, F., DUNBAR, P. R., PRICE, D. A., CERUNDOLO, V. & SEWELL, A. K. 2003. Anti-CD8 antibodies can inhibit or enhance peptide-MHC class I (pMHCI) multimer binding: this is paralleled by their effects on CTL activation and occurs in the absence of an interaction between pMHCI and CD8 on the cell surface. *J Immunol,* 171**,** 6650-60.

WOOLDRIDGE, L., LAUGEL, B., EKERUCHE, J., CLEMENT, M., VAN DEN BERG, H. A., PRICE, D. A. & SEWELL, A. K. 2010b. CD8 controls T cell cross-reactivity. *J Immunol,* 185**,** 4625-32.

WOOLDRIDGE, L., LISSINA, A., COLE, D. K., VAN DEN BERG, H. A., PRICE, D. A. & SEWELL, A. K. 2009. Tricks with tetramers: how to get the most from multimeric peptide-MHC. *Immunology,* 126**,** 147-64.

WOOLDRIDGE, L., LISSINA, A., VERNAZZA, J., GOSTICK, E., LAUGEL, B., HUTCHINSON, S. L., MIRZA, F., DUNBAR, P. R., BOULTER, J. M., GLICK, M., CERUNDOLO, V., VAN DEN BERG, H. A., PRICE, D. A. & SEWELL, A. K. 2007. Enhanced immunogenicity of CTL antigens through mutation of the CD8 binding MHC class I invariant region. *Eur J Immunol,* 37**,** 1323-33.

WOOLDRIDGE, L., VAN DEN BERG, H. A., GLICK, M., GOSTICK, E., LAUGEL, B., HUTCHINSON, S. L., MILICIC, A., BRENCHLEY, J. M., DOUEK, D. C., PRICE, D. A. & SEWELL, A. K. 2005. Interaction between the CD8 coreceptor and major histocompatibility complex class I stabilizes T cell receptor-antigen complexes at the cell surface. *J Biol Chem,* 280**,** 27491-501.

WORLD HEALTH ORGANIZATION. ELECTRONIC ADDRESS, S. W. I. 2017. Human papillomavirus vaccines: WHO position paper, May 2017-Recommendations. *Vaccine,* 35**,** 5753-5755.

WRAITH, D. C., BRUUN, B. & FAIRCHILD, P. J. 1992. Cross-reactive antigen recognition by an encephalitogenic T cell receptor. Implications for T cell biology and autoimmunity. *J Immunol,* 149**,** 3765-70.

WUCHERPFENNIG, K. W., GAGNON, E., CALL, M. J., HUSEBY, E. S. & CALL, M. E. 2010. Structural biology of the T-cell receptor: insights into receptor assembly, ligand recognition, and initiation of signaling. *Cold Spring Harb Perspect Biol,* 2**,** a005140.

WYER, J. R., WILLCOX, B. E., GAO, G. F., GERTH, U. C., DAVIS, S. J., BELL, J. I., VAN DER MERWE, P. A. & JAKOBSEN, B. K. 1999. T cell receptor and coreceptor CD8 alphaalpha bind peptide-MHC independently and with distinct kinetics. *Immunity,* 10**,** 219-25.

XIAO, Z., MESCHER, M. F. & JAMESON, S. C. 2007. Detuning CD8 T cells: down-regulation of CD8 expression, tetramer binding, and response during CTL activation. *J Exp Med,* 204**,** 2667-77.

XIONG, Y., KERN, P., CHANG, H. & REINHERZ, E. 2001. T Cell Receptor Binding to a pMHCII Ligand Is Kinetically Distinct from and Independent of CD4. *J Biol Chem,* 276**,** 5659-67.

XU, X. N., PURBHOO, M. A., CHEN, N., MONGKOLSAPAYA, J., COX, J. H., MEIER, U. C., TAFURO, S., DUNBAR, P. R., SEWELL, A. K., HOURIGAN, C. S., APPAY, V., CERUNDOLO, V., BURROWS, S. R., MCMICHAEL, A. J. & SCREATON, G. R. 2001. A novel approach to antigen-specific deletion of CTL with minimal cellular activation using alpha3 domain mutants of MHC class I/peptide complex. *Immunity,* 14**,** 591-602.

YACHI, P. P., AMPUDIA, J., GASCOIGNE, N. R. & ZAL, T. 2005. Nonstimulatory peptides contribute to antigen-induced CD8-T cell receptor interaction at the immunological synapse. *Nat Immunol,* 6**,** 785-92.

YAMAMOTO, T., HATTORI, M. & YOSHIDA, T. 2007. Induction of T-cell activation or anergy determined by the combination of intensity and duration of T-cell receptor stimulation, and sequential induction in an individual cell. *Immunology,* 121**,** 383-91.

YEE, C. & GREENBERG, P. 2002. Modulating T-cell immunity to tumours: new strategies for monitoring T-cell responses. *Nat Rev Cancer,* 2**,** 409-19.

YEWDELL, J. W., REITS, E. & NEEFJES, J. 2003. Making sense of mass destruction: quantitating MHC class I antigen presentation. *Nature reviews Immunology,* 3**,** 952-61.

YOKOSUKA, T., KOBAYASHI, W., SAKATA-SOGAWA, K., TAKAMATSU, M., HASHIMOTO-TANE, A., DUSTIN, M. L., TOKUNAGA, M. & SAITO, T. 2008. Spatiotemporal regulation of T cell costimulation by TCR-CD28 microclusters and protein kinase C theta translocation. *Immunity,* 29**,** 589-601.

YOKOSUKA, T., KOBAYASHI, W., TAKAMATSU, M., SAKATA-SOGAWA, K., ZENG, H., HASHIMOTO-TANE, A., YAGITA, H., TOKUNAGA, M. & SAITO, T. 2010. Spatiotemporal basis of CTLA-4 costimulatory molecule-mediated negative regulation of T cell activation. *Immunity,* 33**,** 326-39.

ZAMOYSKA, R. 1994. The CD8 coreceptor revisited: one chain good, two chains better. *Immunity,* 1**,** 243-6.

ZHAO, T., LI, C., WU, Y., LI, B. & ZHANG, B. 2017. Prognostic value of PD-L1 expression in tumor infiltrating immune cells in cancers: A meta-analysis. *PLoS One,* 12**,** e0176822.

ZHONG, S., MALECEK, K., JOHNSON, L. A., YU, Z., VEGA-SAENZ DE MIERA, E., DARVISHIAN, F., MCGARY, K., HUANG, K., BOYER, J., CORSE, E., SHAO, Y., ROSENBERG, S. A., RESTIFO, N. P., OSMAN, I. & KROGSGAARD, M. 2013. T-cell receptor affinity and avidity defines antitumor response and autoimmunity in T-cell immunotherapy. *Proc Natl Acad Sci U S A,* 110**,** 6973-8.

ZHOU, L., CHONG, M. M. & LITTMAN, D. R. 2009. Plasticity of CD4+ T cell lineage differentiation. *Immunity,* 30**,** 646-55.

ZIMMERMANN, C., RAWIEL, M., BLASER, C., KAUFMANN, M. & PIRCHER, H. 1996. Homeostatic regulation of CD8+ T cells after antigen challenge in the absence of Fas (CD95). *Eur J Immunol,* 26**,** 2903-10.